DISTRIBUTION AND DISPERSION OF METALS AND THEIR ECONOMIC POTENTIAL: A CASE STUDY OF THE FUMANI TAILINGS DAMS, LIMPOPO PROVINCE, SOUTH AFRICA

BY

SHAVHANI TSHEDZA
STUDENT NO:11616229

DISSERTATION SUBMITTED TO THE DEPARTMENTOF EARTH SCIENCES, FACULTY OF SCIENCE, ENGINEERING AND AGRICULTURE, UNIVERSITY OF VENDA, IN FULFILMENTOF MASTER OF EARTH SCIENCES IN MINING AND ENVIRONMENTAL GEOLOGY

SUPERVISOR : EMERITUS PROF. J.S. OGOLA
CO-SUPERVISOR : DR. H.R. MUNDALAMO

August 2023

DECLARATION

I, Shavhani Tshedza, declare that this dissertation submitted for a Master's degree in Mining and Environmental Geology at the University of Venda, is my own work and that it has not been submitted for any degree by me or anyone in this or any other University.

Student's signature  Date…..17 August 2023

DEDICATION

This work is dedicated to:

My day ones (Ntakadzeni Nkhangweleni Shavhani and Eric Ailwei Shavhani), my beloved husband Masala Ntshavheni Victor Ramaphosa and our beautiful kids, Watshilidzi Rotakala Ramaphosa and Nditshilidzi Masana Ramaphosa.

ACKNOWLEDGEMENTS

First of all, I would like to acknowledge my mother Ntakadzeni Nkhangweleni Shavhani who has been a great inspiration to me from the beginning of this dissertation. She always gave me strength and advice during this journey, though we did not finish the dissertation together, I'm grateful she was part of the journey. I would like to thank my family members who have always sacrificed, given me patient, support and understood the struggles of this journey, their encouragement kept me going even though it seemed impossible to go further. I feel more than blessed to have you guys as my family and would never trade you for anything in this world. A great thank you to my father Eric Ailwei Shavhani, my grandmothers; Tshinakaho Matamela and Emelinah Nemasiwana, my brothers; Thabelo, Mukundi and Gundo Shavhani. I can never thank you enough for helping me through out.

A great and special acknowledgement to my husband, Masala Ntshavheni Victor Ramaphosa, and our beautiful kids, Wawa and Masana, whom I love whole heartedly; I am thankful for all the support you have shown to me throughout this project. You were always ready to help in whatever way you could. Words can never describe how grateful I am. Love you always.

To my mother-in-law, Marema Tshililo Mary, you have been nothing but a great mother to me, thank you for taking care of my kids so that I could conduct this work. I am grateful.

A special thank you to my Supervisor, Prof. J.S. Ogola as well as Co-supervisor Dr. H.R. Mundalamo for helping me throughout this project both financially and academically. Your efforts are very much appreciated. To CIMERA for sponsoring this project. It wouldn't have been easy without the sponsorship as this project required funding.

To the community of Mtititi as well as LIEDA for allowing me and my team to conduct sample collection within the tailings dams. It was not an easy task, however, with your assistance it was much easier. A special thank you to Mr. T. Tshishonge who went an extra mile to ensure that this project is as it is today.

To my team of helpers, Mukwevho Thudzelani, Mbadaliga Hulisani, Mashimbye Revonia, Mpho Mudau, Baloyi Muvhuso and Nemapate Ndivhuwo thank you for helping me throughout the field work. You had to leave the comfort of your homes to come help collect samples for this project, I am very grateful. To my friends who helped keep my sanity by providing fun and laughter when the work got more than serious, you helped me escape the reality for a while. I'm more than grateful for that.

Abstract

The study was conducted at the Fumani Tailings Dams 1 and 2 located in Malamulele, Mtititi village and the area surrounding it to investigate the distribution and dispersion of gold and metals such as Pb, Zn, Cu, As, Co, Cd, Cr and Ni, and also to determine their pollution status, whilst looking at possibilities of reprocessing the tailings as well as using tailings for brick production.

A total of 84 and 63 tailings samples were collected from tailings dams 1 and 2 respectively. 3 profiles were set on each tailings dams, with 4 and 3 boreholes set on each profile of Fumani Tailings Dams 1 and 2 respectively. All boreholes were drilled by a hand auger up to a depth of 7 m, collecting samples of approximately 5 kg at each 1 m interval.

The samples were prepared at the University of Venda MEG laboratory where they were analysed for pH using pH meter, metals and major elements using X-ray Spectrometry, Gold using AAS as well as geotechnical tests using sieve analysis.

Profile logs as well as pH logs revealed that the tailings dams were highly oxidized at the surface of the tailings dams to about 2 m. The average pH revealed that the entire tailings is slightly acidic to neutral. X-ray fluorescence spectrometry confirmed the presence of Pb, Zn, Cu, As, Co, Cd, Cr and Ni. The pollution status conducted revealed that As and Ni pollutes the tailings dams whilst the remaining metals are within the required standard.

Gold values within the tailings dams showed a very erratic trend with depth, with an average concentration of 1.34 ppm and 1.44 ppm at tailings dams 1 and 2 respectively. The study ascertained that there is about 299.1 kg and 225.5 kg of gold within Fumani Tailings Dams 1 and 2 respectively.

Soil samples were collected in four directions from the Fumani tailings Dams at an interval of 200 m. The samples were prepared and analysed using XRF for Pb, Zn, Cu, As, Co, Cd, Cr and Ni at the university of Venda. The Study showed that Zn and Cd do not contaminate the soil whilst Pb, As, Cu, Cr and Co highly pollutes the soil. These might be from a different source since they are low within the tailings dams.

The Major oxides, sieve analysis, liquid limit test and the plastic limit test were used to classify the tailings using USCS and AASHTO Classification system. The USCS revealed that the tailings were ML and/or CL fine grained silty clay, whilst AASHTO Classification system

revealed that the Fumani Tailings Dams 1 and 2 were in class A-4(3) and A-4(1) respectively. The tailings had low LL, low PI, and low alumina content required for brick production. The tailings, therefore, had a low compressibility, slight to low plasticity, and no cohesion, and therefore were not suitable for brick production on their own.

Clay and cement bricks of different tailings to soil and cement ratios were made at Tshidino Bricks. All bricks were tested for dimension tolerance test, water absorption test, compressive strength test, hardness test as well as the impact test. All clay bricks failed these tests. The cement bricks passed the hardness test, water absorption test, and hardness test. This was not enough to make them suitable for brick production as they failed the dimension tolerance test and compressive strength test.

TABLE OF CONTENT

LIST OF FIGURES

LIST OF TABLES

ACRONYMS AND ABBREVIATIONS

AAS	Atomic absorption spectrometry
AASHTO	American association of state highway and transportation official system
ALS	Australian laboratory services
AMD	Acid mine drainage
BIF	Banded iron formation
CIP	Carbon in pulp
CP	Cumulative passing
FRD	Fine residue dump
GDP	Gross domestic product
GGB	Giyani greenstone belt
GIS	Geographic information system
GPS	Global positioning system
IDW	Inverse distance weighting
IS	Indian standard
LL	Liquid limit
PP	Percentage passing
PI	Plasticity index
PL	Plastic limit
SGB	Sutherland greenstone belt
SSV	Soil screening values
TMF	Tailings management facility
TMR	Total mass retained
TSF	Tailings storage facility
USCS	Unified soil classification system
XRF	X-ray fluorescence

CHAPTER 1: INTRODUCTION

1.1 Background

A variety of useful materials are produced from minerals that are extracted from the earth's crust as a result of various mining methods and various beneficiation techniques. These products make our lives easier and provide citizens with economic benefits as well as job opportunities. However, these benefits come at an expense to both the environment and human health. This is because the safety of areas affected by mining and mineral processing is compromised by waste produced during and after mining as well as mineral processing.

Amongst the waste produced during mineral processing are tailings. Tailings are fine materials left after the valuable mineral has been separated from gangue. Tailings are stored in tailings facilities referred to as tailings dams. Unrehabilitated tailings dams pose environmental and health problems. According to McMillan (2020), they can either be blown by the wind, dispersing metals into nearby water sources or leached by rainwater, contaminating both surface and groundwater resources. The dispersion of these metals to the environment may enter humans through dust inhalation, water resources, dermal contact as well as food chain (Nengovhela *et al*., 2006; Matshusa *et al*., 2012; Harvey *et al*., 2015; Oladejo, *et al*., 2021).

The composition of tailings is directly dependent on the composition of the ore, host rock and the type of mineral beneficiation process used. Fumani was a gold mine, hence, metals such as lead (Pb), zinc (Zn), copper (Cu), arsenic (As), cobalt (Co), cadmium (Cd), gold (Au), chromium (Cr) and nickel (Ni) are expected in the tailings.

Metals occurring in high concentrations can be toxic to living species (Oladejo, *et al*., 2021). The effects can be alleviated through rehabilitation. The challenge encountered is that tailings dams' rehabilitation on its own is quite costly and does not bring any profit to the mining companies. However, recent technological advancements, continuous studies and an increase in commodity prices have led to an era whereby tailings can be reprocessed for valuable minerals, for example, gold, while rehabilitating the site (Matshusa *et al*., 2012; Rosner, 2001; Nummi, 2015; Nemapate, 2017; Ogola *et al*., 2018; Intellidex, 2018).

The study, therefore, focused on establishing the distribution and quantity of gold and other metals within and around the Fumani tailings dams to ascertain the environmental impacts, reprocessing of gold and explore the alternative use of tailings as a construction material.

1.2 Study Area

1.2.1 Location

The Fumani Mine is situated in the Malamulele area sandwiched between the Mtititi, Plange and Altein villages (Fig. 1.1). The area lies about 40 km away from the Punda Maria gate of the Kruger National Park. The tailings dams are situated about 45 km from Thohoyandou town and about 21 km from Malamulele town in the south-eastern direction from both Thohoyandou and Malamulele town. The mine has two tailings dams that occur at geographic coordinates of 23°6'35''S and 30°53'40''E. This area is positioned in the north-eastern part of the Kaapvaal Craton within the Giyani Greenstone Belt (GGB), which is well known for its gold sulphide mineralisation.

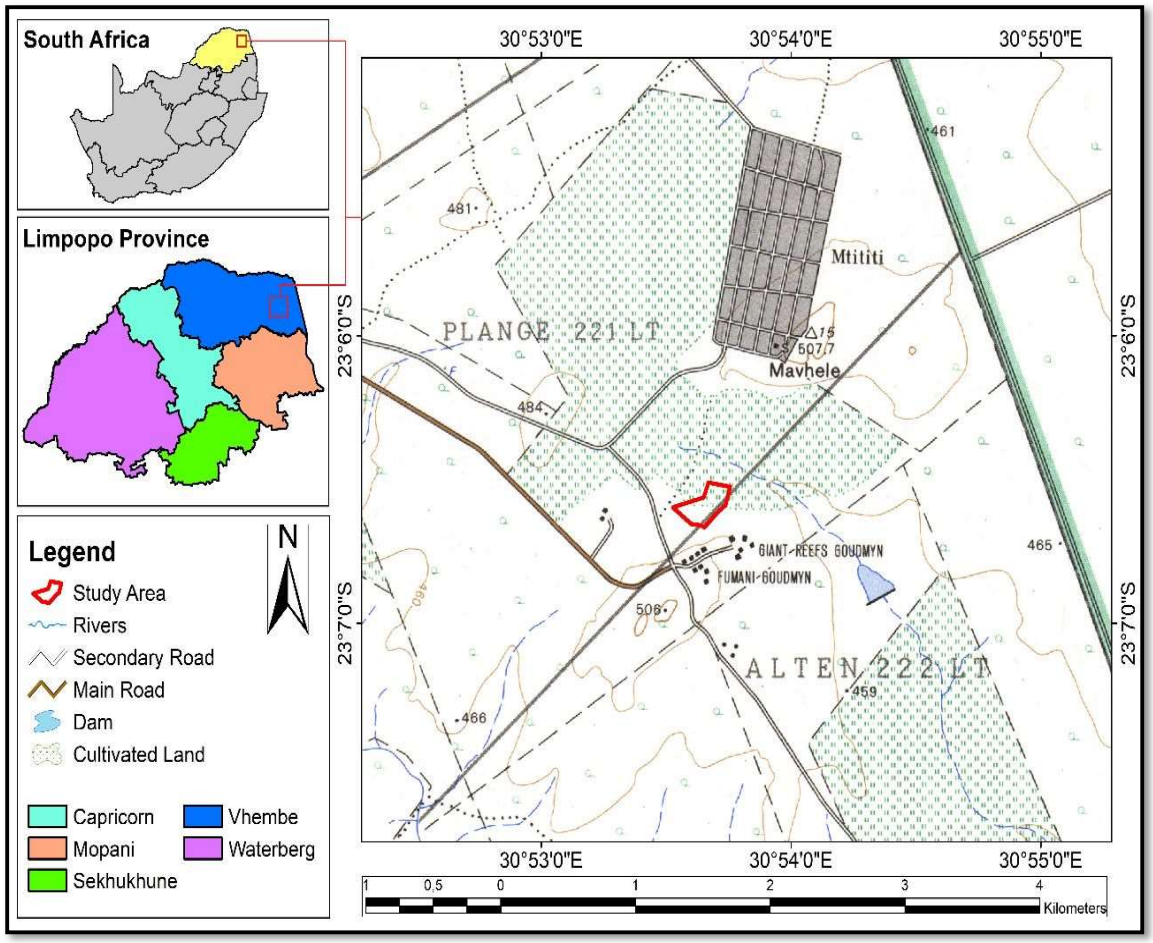

Figure 1. 1: Location map of the study area (ArcGIS 10.8, 2022).

1.2.2 Climate

The area is characterised by a dry subtropical climate. The summer seasons (between September and March) are long, hot and rainy, with the average midday temperatures reaching more than 30.5°C during this season. The average midday and night-time temperatures are 31°C and 19°C respectively during the hottest month (Fig. 1.2). The winter season (between April and August) is cool and dry with very short days. During this season, the average day and night-time temperatures drop to about 23°C and 8°C respectively (Fig. 1.2).

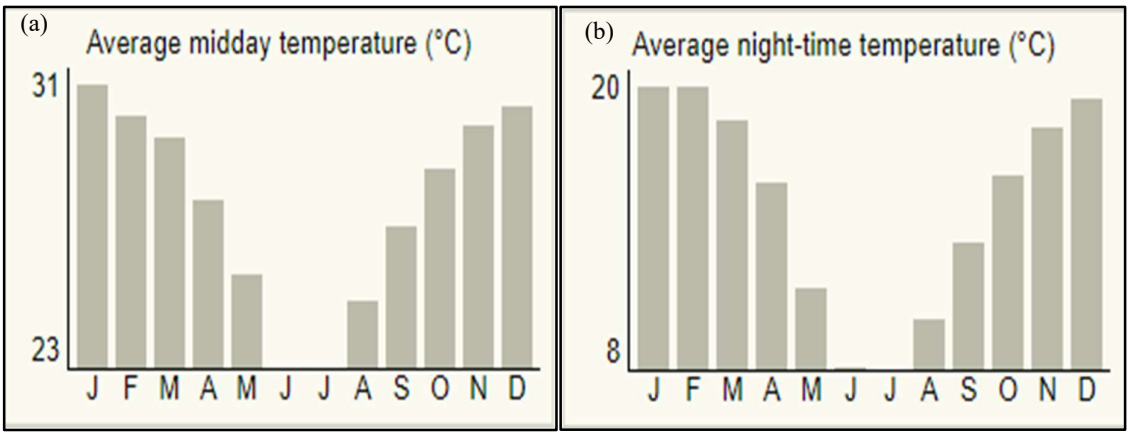

Figure 1. 2: Monthly distribution of temperature in Malamulele area: (a) average midday temperature ; and (b) average night-time temperature (Saexplorer, 2016).

About 691 mm of rain is typically received in Malamulele per year (Saexplorer, 2016). Most rainfall is received in November, December, January, February and March. The lowest and highest rainfall received is 3 mm in July and 139 mm in January respectively (Fig. 1.3).

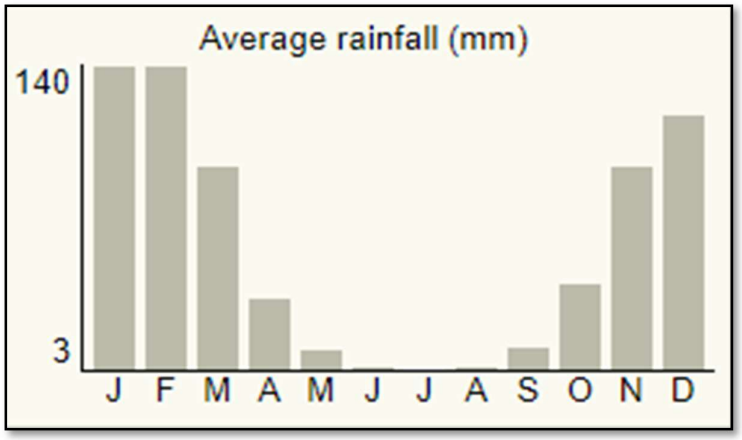

Figure 1. 3: Average monthly rainfall in the Malamulele area (Saexplorer, 2016).

1.2.3 Topography and Drainage

The Malamulele area is characterised by flat-lying land with a few discontinuous hills. This area is surrounded by steep slopes and hills that form boundaries around the flat-lying central parts. No known mountains exist in the area, except further South in the Giyani area.

The Klein Letaba, Nsami, Molototsi as well as Shingwisi rivers are the four major perennial rivers that form part of the Giyani Greenstone Belt drainage system. These rivers are seasonal and flow to their full capacities during the rainy season which is between September and March. The Klein Letaba River has tributaries that include the Soeketse River and the Koedoes River. The Nsami River, Nsami Dam, Middle Letaba River, Middle Letaba Dam, Koedoes River, Brandboontjies, Klein Letaba River and other minor tributaries produce major surface water resources within the Malamulele area.

1.2.4 Soil and Vegetation

The area is characterised by different types of soil, with the loamy reddish soil as the dominant soil type. The soil is produced from the weathering of the parent rocks, with the red colour indicating the presence of iron oxides in the soil.

The area is characterised by dense vegetation. The Giyani Greenstone Belt comprises alien invasions such as the lantana and triffid weeds. The indigenous vegetation includes the large cocklebur, castor-oil plant, mopani trees, acacia, commiphora, maroela, baobab trees as well as the thistle.

1.2.5 Land-use

The area has been home to mines such as the Fumani Mine, though the mine is not in operation as of the present, the area is still used for small-scale mining by illegal miners. Sand mining also exists in the nearby rivers and streams. The greater part of the area is used for settlement with villages located in the whole area. Subsistence farming exists in the area.

1.3 Problem Statement

The Fumani Mine tailings dams remain a potential threat to both the environment and the inhabitants around the area as they have not been rehabilitated. This leaves the area exposed to metals such as Pb, Zn, Cu, As, Co, Cd, Cr and Ni. Previous studies conducted by Ogola (2010); Matshusa *et al*. (2012); and Nemapate (2017), on gold tailings dams within the GGB, confirmed the occurrence of these metals. However, the studies conducted at the Fumani tailings dams did not ascertain the extent of these metals dispersion in and around the area and the economic potential or alternative uses of the Fumani tailings.

1.4 Justification

The longer the tailings dams remain without being rehabilitated, the greater the impacts would be on the environment as a result of wind and water erosion, and the possible generation of acid mine drainage. However, rehabilitation is costly and does not bring any form of profit to the mining companies, thus, reprocessing the tailings for gold and finding alternative uses of tailings becomes more lucrative and acceptable.

During gold processing, not all gold is recovered as some is left behind with some metals as waste and stored in tailings dams. The rise of new technologies has improved the recovery rates and hence high potential for the reprocessing of old tailings dams. The general trend of gold prices in the world market has been increasing significantly since the start of this project. The price of gold was about R17 000 per ounce in 2015 and has risen to R30 893.67 in March 2020 (Kitco, 2020). With reduced cost and complexity of recovery methods, tight environmental regulations, public outcries relating to the effects of tailings dams, and the price of gold in the increase, the recovery of gold tailings has become a viable business (Fleming, 2003; Loots, 2020).

Tailings can also be used in the production of construction material. Previous studies on the production of construction material from tailings have been conducted by researchers such as Koumal (1994); Yang *et al*. (2011); Saeed and Zhang (2012); Manoharan (2012); Zhang (2013) and Malatse and Ndlovu (2015). Consequently, converting tailings into a commercial product is the best way of rehabilitating the abandoned tailings dams.

1.5 Research Questions

- Which metals are occurring within the Fumani tailings dams?
- To what extent is the distribution and dispersion of such metals within the tailings dams and the surrounding area?
- What are the environmental impacts associated with the Fumani tailings dams?
- To what extent is the oxidation of tailings within the dams?
- Can the Fumani Tailings Dams be reprocessed for gold?
- What are the economic benefits of the metals within the tailings?
- What characteristics of tailings are important for brick production?

1.6 Objectives

The main objective of this research was to establish the values, distribution and dispersion of gold and other metals within and around the Fumani tailings dams, with a view to determine the pollution status of the tailings dams and their surrounding area, reprocess the tailings for gold and find alternative uses of tailings.

The specific objectives of the study were to:

- characterie Fumani Tailings Dams 1 and 2 into different zones (oxidised, transition and unoxidised zone) through borehole logging and pH analysis;
- determine metal values within and around the Fumani Tailings Dams 1 and 2 using X-ray Fluorescence spectrometry;
- determine the distribution and dispersion of metals within and around the Fumani Tailings Dams through vertical distribution logs and prediction maps produced through kriging;
- determine the pollution status within and around Fumani Tailings Dams 1 and 2 using Dutch Guideline of Concentrations in Soil, Single Factor Index Method as well as the South African Guideline of Standards;
- determine gold values within the tailings dams through fire assaying and evaluate its potential for re-processing;
- investigate the suitability of tailings for brick production through major oxide and sieve analysis as well as Atterberg limits; and
- investigate the qualities of bricks through production of bricks of different tailings to soil ratios and testing them against the control bricks.

CHAPTER 2: LITERATURE REVIEW

2.1 Giyani Greenstone Belt

The Giyani Greenstone Belt (GGB) previously referred to as the Sutherland Greenstone Belt (SGB) is located on the north-eastern edge of the Kaapvaal Craton and south of the regional Hout River shear zone (Brandal *et al*., 2006). The Giyani Greenstone Belt is a NE-trending feature that is about 15 km wide and 70 km long (Johnson *et al*., 2006). Towards the southwest, the GGB bifurcates into two arms known as the northern Khavagari arm and the southern Lwaji arm (Brandal *et al*., 2006). These two arms are separated by granite and granitoid gneiss.

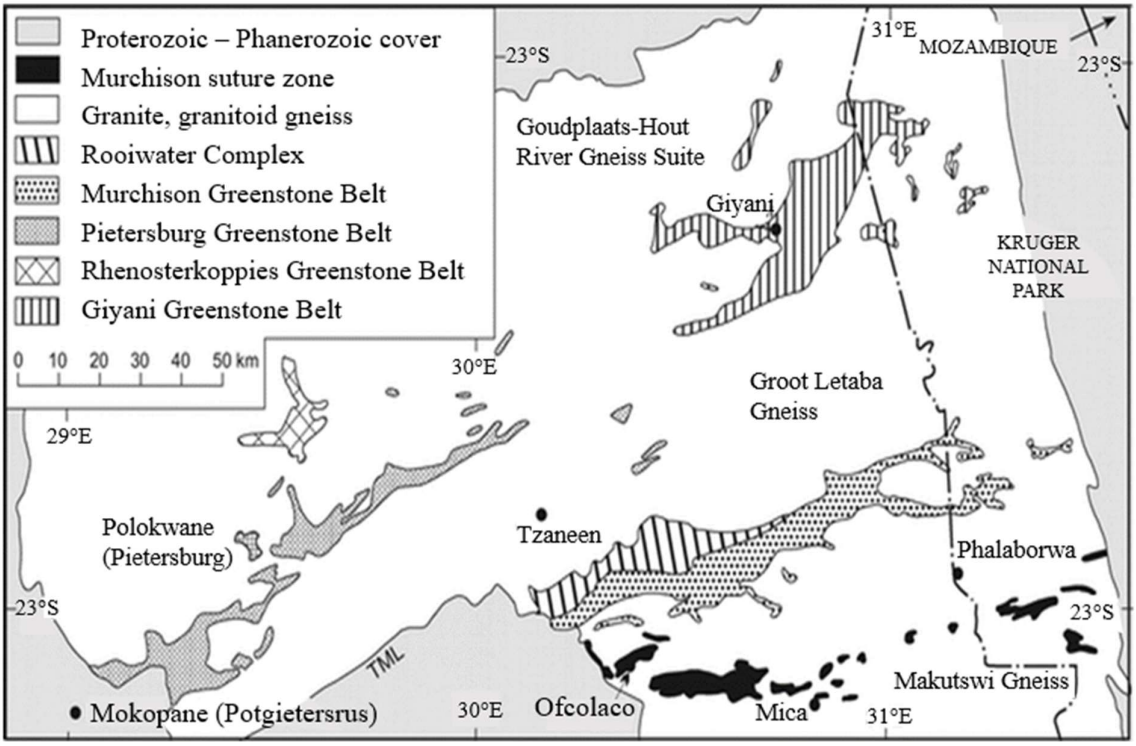

Figure 2. 1: Map of the Giyani Greenstone Belt (Department of Land Affairs, 2006).

The Giyani Greenstone Belt is dominated by ultramafic schists composed of tremolite, talc, chlorite or hornblende. Thin beds of mafic volcanic rocks and iron formations occur within the schists. It also includes a thin unit made up of felsic volcanic and sedimentary rocks including quartz-sericite schist, rhyolite, ferruginous quartzite and iron-formation (Brandal *et al*., 2006). The belt includes mafic and ultramafic units in repeated cycles capped by iron formations, these include; massive and pillowed amphibolites, and banded iron formation (BIF) capped by dolomite (Brandal *et al*., 2006).

2.2 History of Gold Mining in the Giyani Greenstone Belt

Like all other Greenstone Belts, the GGB was and still is a known prospect area for gold mineralisation. The belt has been home to more than 44 small-scale mines and a few that managed to be fully developed such as; New Union, Fumani, Gemsbok, West-59, Louis Moore, Birthday, Black Mountain and Klein Letaba Mines (Fig. 2.2). It is these mines that contributed more than 97% of the total declared gold within the Giyani Greenstone Belt which is over 10 tons of gold recovered (Ward and Wilson, 1998; Smit *et al*, 2019).

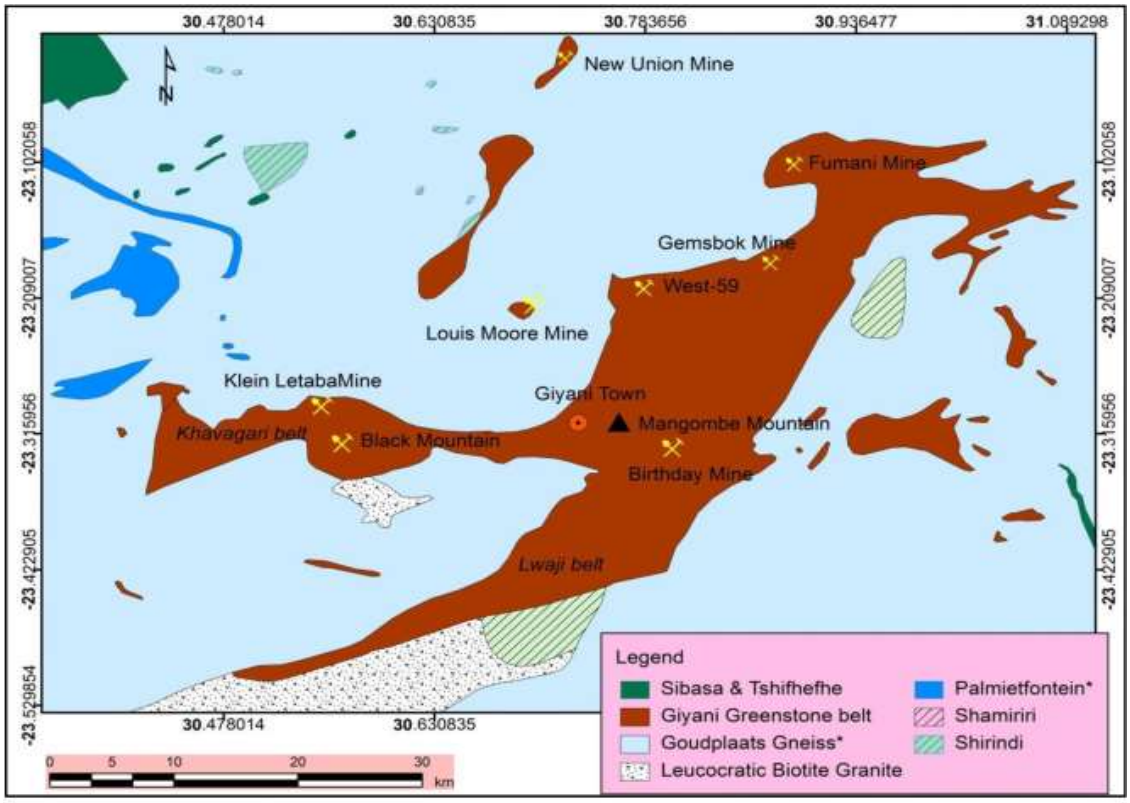

Figure 2. 2: Fully developed mines within the Giyani Greenstone Belt (Ward and Wilson, 1998).

Prospectors Button and Sutherland discovered the Murchison and Sutherland Greenstone Belt goldfields in 1870. The first gold to be discovered here was within the Letaba and Shingwezi rivers. Although gold was discovered in 1870, it was only in 1886 that gold rush started in the area, and the then Zuid Afrikaansche Republic declared the area as a public digging area. This gold rush later resulted in the founding of the Leydrop town. The Second Anglo-Boer War disrupted mining operations, and by 1928 most of the mines in the area had ceased operations (Steenkamp and Clark-Mostert, 2012).

Most of the gold deposits within the GGB were found either in quartz veins with sulphide mineralisation, BIF, quartz and sulphide replacement veins or carbonate veins (Lombaard, 1956, Smit *et al*., 2019). Steenkamp and Clark-Mosteret (2012) observed that all the preserved historic workings were focused on outcrops of quartz veins, with trenches dug either in the quartz vein outcrop or parallel to the outcrop.

As compared to the other Greenstone Belts in South Africa, the GGB was a relatively small producer of gold, however, slightly above ten tonnes of gold were recovered (Ward and Wilson, 1998, Smit *et al*., 2019). The biggest producer of gold within the Giyani Greenstone Belt was the Klein Letaba Mine during the 1960s (Bullen *et al*., 1995) followed by the Louis Moore mine which yielded grades up to 6 g/t Au (Collins, 1991).

Mining History of Fumani Deposit

Mining operations within the Giant Reefs Mine started in 1934 and continued up to 1963. Illegal miners, however, continued to try their luck after the mine ceased operations. This led to further exploration that indicated that the ore reserve still existed and extended to a depth of about 600 m (Ward and Wilson, 1998; Smit *et al*., 2019). This led to the mine reopening again under the name Fumani Mine in 1977. Even though the mine reopened in 1977, it only started operating again in 1980 and remained in operation until 1991 when it was forced to shut down after the mine went into liquidation (Ward and Wilson, 1998).

Gold mineralisation within the Fumani Mine occurs in clear association with sulphide minerals, often in association with BIF. Gold occurs in quartz, amphibole, biotite as well as arsenopyrite as an inclusion in these minerals. The difference in competence during BIF and micaceous quartzite shearing possibly created appropriate channels for mineralizing fluids (Pretorius et al.,1988).

During the life of mine, a total of 289 257 metric tonnes of ore was milled, of which 11 709 metric tonnes of ore was milled when the mine was known as Giant Reefs and 277 548 metric tonnes was milled and treated when the mine was known as Fumani Mine. A total of 150 tons of ore could be processed daily in the mine's commination and reduction plant. The ore was then extracted using the carbon-in-pulp (CIP) method. In total, over 1.1 tonnes of gold were mined over the mine-life span. The average grade of the ore was over 4g/t (Ward and Wilson, 1998; Smit *et al*., 2019).

2.3 Tailings Dams and their Impacts

When the desired product is extracted from a mined-out ore using either mechanical or chemical processes, a waste stream known as tailings is produced. Tailings.info (2017) has adequately summarised the definition and processes in which tailings are handled. Tailings are fine-grained materials that are in powder form when dry. They contain unrecoverable and uneconomic metals (due to the technology of the time and demand), minerals, chemicals, organics as well as processing water. Since all these may be toxic and harmful to the environment, they are discharged in a form of a slurry to a storage area known as a Tailings Management Facility (TMF) or Tailings Storage Facility (TSF) in an attempt to protect the natural environment from damage (Zongjie, 2019).

Tailings Storage Facilities are usually developed on the surface either within retaining structures or simply in the form of piles. However, tailings can also be stored underground by the process of backfilling previously mined-out areas (Todorova, *et al*., 2017).

An increase in commodity prices and technological advancement in mining and processing plants allows for low-grade ore to be mined at a profit. This means that less concentrate is obtained whilst large amounts of waste are produced which will require bigger TSF.

In most cases, tailings dams are left without adequate continuous treatment or proper rehabilitation as it is costly to maintain them both during and after mining (Zongjie, 2019; Loots, 2020). This can lead to TSF failure. Poor construction of TSF, inadequate regulations on design standards of TSF, high cost of maintenance after mining closure coupled with poor understanding of the impacts of TSF failure are the main reasons for TSF failures (Rico *et al*., 2008; Zongjie, 2019).

Due to the impacts of tailings on the environment, the environmental regulations are also advancing, requiring proper planning and execution of tailings management facilities or tailings storage facilities (Tailings.info, 2017).

Tailings are therefore viewed as waste that is harmful to the environment and has no financial gain to the operator at some point, however, they should be stored in the most cost-effective way possible to meet regulations and site-specific factors (Tailings.info, 2017). The construction of TMF is site-specific and may not be identical to another.

Tailings usually cause high mobility of elements because their exposure makes them vulnerable to weathering. This increases the possibility of higher environmental impacts. The single most significant source of environmental impact for many mining operations has been recognised as the disposal of tailings (Vick, 1990; Khobragade, 2020). The environmental impacts of tailings namely; acid mine drainage and metal pollution are detailed below.

2.3.1 Acid Mine Drainage

Poor control of tailings dams leads to a hysterical release of acid mine drainage (AMD) into the environment, causing AMD to be recognised globally as a significant pollution hazard to the environment from the mining sector.

Acid mine drainage is formed when sulphide minerals such as pyrite, chalcopyrite and arsenopyrite get exposed to moisture and oxygen, then oxidise to form acidic water referred to as acid mine drainage. Acid mine drainage in turn generates sulphates, metals and acid that pose environmental risks (Nengovhela *et al*., 2006).

The major sources of AMD are tailings, waste rock dumps, low-grade ore, overburden as well as run-off mill stockpiles that contain sulphide minerals. When the rate at which acid is being generated is faster than the rate at which it can be neutralised by any alkaline material, AMD occurs. This acidic water is generated from the oxidation of sulphides, usually pyrite (FeS_2), pyrrhotite (FeS), marcasite (FeS_2), arsenopyrite (FeAsS), sphalerite (ZnS), galena (PbS) and chalcopyrite (Cu,FeS_2) (Ogola *et al*., 2002). According to Nengovhela *et al*. (2006), FeS_2 is oxidised in the following four ways indicated below to produce AMD:

$$2FeS_2 + 7O_2 + 2H_2O = 2Fe^{2+} + 4SO_4^{2-} + 4H^+ \quad \text{.....Equation 2.1}$$

$$4Fe^{2+} + 10H_2O + O_2 = 4Fe(OH)_3 + 8H^+ \quad \text{.....Equation 2.2}$$

$$3Fe^{2+} + O_2 + 2H^+ = 2Fe^{3+} + H_2O \quad \text{.....Equation 2.3}$$

$$FeS_2 + 14Fe^{3+} + 8H_2O = 15Fe^{2+} + 2SO_4^{2-} + 16H^+ \quad \text{.....Equation 2.4}$$

Nengovhela *et al*. (2006) further explained that the chemical parameters that define the intensity of the acid generated are pH, temperature, oxygen, water and surface area of the exposed metal sulphides. Of these, the primary requirements needed for sulphide oxidation to befall are water and oxygen. Oxygen concentration inside a tailings dam differs depending on the degree of water saturation, temperature, rate of water infiltration and the rate of oxygen intake. If the tailings are porous, it makes way for oxygen to enter, hence oxidation usually

takes place in the first three meters of the tailings where there is enough oxygen for oxidation, thus the rest of the tailings that are compacted and lack oxygen is not prone seriously to AMD. Since different tailings dams have these parameters in different proportions, the amount of acid mine water generated is thus site-specific.

Impacts of Acid Mine Drainage

The impacts of AMD continue to affect the environment long after mining operations have ceased. Several studies on the impacts of AMD have been conducted (Ogola *et al*., 2002; McCathy, 2011; Ramontja *et al*., 2011; Matandare, *et al*., 2019). The acidic water infiltrates the ground to contaminate groundwater while the run-off contaminates surface water. Once the acid water has been generated, it is washed to nearby surface water resources to form a yellow or orange colour that covers the rivers, dams and ponds, polluting the water and attacking aquatic life. Acid mine drainage also has the corroding effect of acid on parts of infrastructure such as bridges.

As a result of AMD, sulphide minerals are broken down mainly into Pb, Zn, Cu, As, Co and Cd that are released to the environment and may end up in surface or groundwater, soil and plants, thus entering the food chain and attack humans. The metals become more soluble in water as the acid solution becomes stronger, thus decreasing the water pH (Ogola *et al*., 2002).

2.3.2 Metal Pollution

Metals investigated are those elements that exhibit metallic properties characterised by relatively high density and high atomic weight (greater than 20) (Oladejo, *et al*., 2021; Chibuike and Obiora, 2014). These metals are naturally present in soils, and some are essential in small quantities in organisms diets (Banfalvi, 2011; Chibuike and Obiora, 2014). Anthropogenic activities, usually mining, increase concentrations of these metals to undesired levels that contaminate soil (Howell *et al*., 2012; Oladejo, *et al*., 2021) and affects human health.

Metals reach the human body through ingestion of contaminated foods, inhalation of contaminated air and absorption through skin contact (Qu *et al*., 2014). The metals thus bioaccumulate as they are hard to metabolize (Pezzarossa *et al*., 2011).

Plants on contaminated soils have been found to exhibit growth complications, more especially reduction, as a consequence of alterations in physiological and biological processes (Chibuike and Obiora, 2014; Asati, *et al*., 2016). Soil properties such as moister content and water

capacity reduce with increases in metal pollution (Sharma and Raju, 2013). Symptoms and effects of metal poisoning can vary according to the quantity and nature of the metal (Neilen and Marvin, 2008). A discussion of the nature and effects of these minerals is presented.

- **Lead**

Lead (Pb) is one of the sulphide minerals commonly associated with gold mineralisation. It usually occurs in the form of galena (PbS). It is released into the environment through the processing of sulphide ores or associated minerals. It ends in the tailings dams with other metals after mineral processing.

Lead limits plant chlorophyll synthesis and when plants take up high levels of lead it negatively influences plant growth, reduces plant biomass and reduces plant protein content (Hussain *et al*., 2013; Asati, *et al*., 2016). Overexposure to humans has the following symptoms: colic, skin pigmentation and paralysis. It has no benefits for humans.

The general effects of lead are neurological or tetratogenic. Organic lead affects the neurons by causing necrosis, whereas inorganic lead causes axonal degeneration and demyelination (Lenntech, 2017). Both organic and inorganic lead may cause cerebral oedema and congestion. Chronic exposure may lead to anaemia, encephalopathy, kidney diseases as well as palsy and it is also carcinogenic. A combination of drinking water infrastructures such as lead joined pipelines and other household plumbing elevates lead values and worsens the effects (Harvey *et al*., 2015).

- **Zinc**

Zinc (Zn) is of great importance in the human diet as it helps in DNA replication as well as enzymatic processes, however, intake in excess amounts can have negative impacts in both humans and the environment. The most common zinc ore is sphalerite [(Zn.Fe)S].

Intake of 2 g of zinc sulphate at once causes acute toxicity leading to stomach aches and vomiting. Overexposure includes mucous membrane infection from zinc chloride. If intake exceeds a dose of 3-5 g, then it becomes lethal. Zinc also causes zinc vitriol poisoning which is fatal if consumed in quantities greater than 5 g (Lenntech, 2017).

Plants such as cluster beans that grow on zinc-contaminated soil reduce germination, plant growth, plant biomass, chlorophyll, carotenoid, sugar, starch and amino acid content.

- **Copper**

Lenntech (2017) described Copper (Cu) as a common metal that occurs naturally in the environment as chalcopyrite ($CuFeS_2$), Azurite [$Cu_3(Co_3)_2(OH)_2$] and malachite [$Cu_2CO_3(OH)_2$]. Lenntech (2017) further alluded that the production of Cu has increased over the last decades, causing elevated quantities of Cu in the environment. Lenntech (2017) further explained that the effects of Cu in high concentrations are devastating to the well-being of humans and the environment at large.

Copper is a trace element that is essential for human health, however, large quantities in the body causes devastating health problems. In a working environment, Cu contamination can lead to metal fever which is a flu-like condition. This may pass after some days.

Long-term exposure to Cu leads to irritation of the nose, mouth and eyes. It can also cause headaches, stomach-aches, dizziness, vomiting and diarrhoea. High uptake of Cu can cause liver and kidney damage and even death. Chronic Cu poisoning results in Wilson's disease.

In soils, Cu attaches to organic matter and minerals and as a result, it does not travel far but accumulates. A limited number of plants have a chance of survival on Cu-contaminated soils. It also affects soil activity as it negatively affects microorganisms and earthworms in the contaminated soil, causing the decomposition of organic matter to slowdown (Manivasagaperumal *et al*., 2011).

- **Arsenic**

Arsenic (As) compounds are abundant in the earth's crust. The particles are usually released during mining and spread throughout the environment. Inorganic As is derived from rocks in the form of arsenopyrite (FeAsS), orpiment (As_2S_3), realgar (As_4S_4) and arsenic trioxide (As_2O_3) (Lenntech, 2017). Lenntech (2017) explains that overexposure to As has a negative effect on humans.

Overexposure to As in humans can damage the organs and cause skin pigmentation, hair loss and nail growth may stop. Symptoms of acute arsenic poisoning are nausea, vomiting, diarrhoea, cyanosis, cardiac arrhythmia, confusion and hallucinations. Symptoms of chronic As are less specific and can lead to cancer (mainly skin cancer), diabetes as well as hypopigmentation.

- **Cobalt**

Cobalt (Co) occurs in the earth's crust in relatively low quantities and is released into the environment during mining. The main sources of cobalt are cobaltite (CoAsS), erythrite [$Co_3(AsO_4)_2.8H_2O$] as well as glaucodot [(Co, Fe)AsS].

Cobalt is essential for human health and can be used to treat anaemia in pregnant women. The total daily intake of Co is variable and may be as much as 1 mg. However, high concentrations of Co may damage human health as it affects the lungs and causes illnesses such as asthma and pneumonia. This is predominant in areas within the vicinity of mines.

Increased amounts of Co in the soil cause a reduction in plant nutrient content, especially in tomatoes (Jayakumar *et al*., 2013). Fruits, seeds and leaves of contaminated plants are the fastest pathways of Co into the human body as ingestion of these fruits, seeds and leaves of cause nausea, vomiting, vision problems, heart problems as well as thyroid damage. Radiation from radioactive Cobalt isotopes causes sterility, hair loss, vomiting, bleeding, diarrhoea, coma and death (Lenntech, 2017).

- **Cadmium**

Cadmium (Cd) is released into the environment due to mining activities. It occurs in a form of cadmium sulphide (CdS) in trace quantities in sphalerite (ZnS), hence it is released into tailings during mineral processing.

Consumption of Cd causes softening of the bones of humans and other organisms, and it also causes kidney failure (Vallero and Letcher, 2013). Acute exposure causes pneumonitis which is lung inflammation. Chronic exposure, however, causes lung cancer, osteomalacia (softening of bones) as well as proteinuria which is excess protein in the urine that can damage the kidneys (Lenntech, 2017).

- **Chromium**

Chromium (Cr) is mainly from the mineral chromite ($FeCr_2O_2$). Chromium exposure can be through ingestion, breathing or dermal contact. chromium (III) is essential in the human diet as shortage of it can cause heart problems, disruptions of metabolism and diabetes. Too much uptake of chromium (III), however, causes negative impacts on human health and one symptom of this includes skin rushes (Lenntech, 2017).

Acute exposure to chromium causes acute renal failure, destruction of red blood cells and gastrointestinal haemorrhage which is bleeding. Chronic exposure causes lung cancer as well as pulmonary fibrosis which is lung scarring (Lenntech, 2017). Chromium (VI) causes skin rushes, upsets the stomach, and causes ulcers, respiratory problems, alteration of genetic material, lung cancer and even death (Lenntech, 2017). Nematshahi *et al*. (2012) mentioned that a high Cr content in onions inhibits the germination process and reduces its biomass.

- **Nickel**

Nickel (Ni) may be found in slate, sandstone, clay minerals and basalt. The main source of nickel is pentlandite [$(Fe,Ni)_9S_8$]. Nickel is a dietary requirement for many organisms, but may be toxic in larger doses. Metallic nickel and some other nickel compounds are teratogenic and carcinogenic to mammals. Nickel inhalation can cause lung cancer or nasal tumours. Dermal contact causes dermatitis upon contact with nickel (Lenntech, 2017).

2.4 Soil Assessment for Metal Pollution

2.4.1 Dutch Guideline

To assess soil for heavy metal pollution, the Dutch Guideline of concentration can be used to classify the soil as either contaminated or not contaminated and to determine if the soil requires a clean-up or not. Table 2.1 gives the Dutch ABC concentration standards which categorise concentrations of metals in soils as A, B or C. The A values are those concentrations of metals below which the soil is probably not contaminated, B values are those concentrations of metals that require more investigation and C values are those concentrations of metals that require site-cleaning (Steyn *et al*., 1996).

Table 2.1: Dutch guideline of concentrations in soil (mg/kg) (Steyn *et al*., 1996)

Category	**Pb**	**Zn**	**Cu**	**As**	**Co**	**Cd**	**Cr**	**Ni**
A	50	200	50	20	20	1	100	50
B	150	500	100	30	50	5	250	100
C	600	3000	500	50	300	20	800	500

2.4.2 Single Factor Index Method

The concentration of metals in soils can be used to determine the pollution status of soils using other known soil pollution standards to confirm the pollution status of that area (Gouzhan *et al*., 2005). For this work, the Single Factor Index Method (SFIM) was used to determine the pollution status of the soil. The assessment standards used in this dissertation are those of the Dutch Guideline (Table 2.1).

The pollution status of tailings and soil using SFIM is then calculated using the following formula as detailed by Gouzhan *et al* (2005):

$P_i = C_i / S_i$ ……...…….. Equation 2.5

Where:
P_i – is the quality index of the pollutant in the environment
C_i – is the concentration of the pollutant in the soil
S_i – is the assessment standard (Dutch Guideline of concentrations)

If P_i is equal to or less than 0.7, the site is most likely uncontaminated with the metals. When P_i lies between 0.7 and 1, the metal concentrations are still within the environmental quality standards, that is no harm to human health or the environment, however, special care must be taken not to exceed these values as they are approaching contamination concentrations.

When P_i is greater than 1, the metal concentration in soils is beyond the environmental quality standard and begins to become a threat to the environment and human health.

If P_i lies between 1 and 2, it indicates light pollution. Moderate pollution occurs when P_i is between 2 and 3, but the area or site is said to be heavily polluted when P_i is greater than 3 (Guozhang *et al*., 2005).

2.4.3 South African Constitution on Contaminated Sites

The constitution of the Republic of South Africa, 1996 enforces sustainable use of the land by providing laws that protect the environment (Government Gazette, 2014). The government Gazzete of 2nd May 2014 states that any contaminated site must be remedied to the soil screening values (SSV) (Table 2.2). Any site with concentrations greater than this is considered polluted and requires clean-up.

Table 2.2: Soil screening values for metals (Government Gazette, 2014)

Metals and metalloids	All land uses protective of the water resources (ppm)	Informal Residential areas (ppm)	Standard residential areas (ppm)	Commercial industrial (ppm)	Protection of ecosystem and health (ppm)
Arsenic	5.8	23	48	150	580
Cadmium	7.5	15	32	260	37
Cobalt	300	300	630	5000	22000
Copper	16	1100	2300	19000	16
Lead	20	110	230	1900	100
Zinc	240	9200	19000	150 000	240
Nickel	91	620	1200	10 000	1 400
Chromium	6.5	6.5	13	40	260

2.5 Geo-Environmental Modelling

Geo-environmental modelling refers to the simplified and less complex representation of the environment, representing a particular phenomenon in order to understand the real-life environment. This can also be used to determine the concentration of an ore body, its location in the real environment as well as the distribution of metals and trace elements associated with that ore. It can also be used to predict the toxicity of tailings through interpolation. This is quite important especially with respect to the dispersion of heavy metals within the environs of tailings dams and their potential impacts on the environment and human health.

Interpolation

When sampling a large area, the distance between two sampling points becomes greater. This is mainly due to lack of time, resources, or inaccessibility to the study area. Interpolation techniques may be used to understand the values in the area not sampled.

Interpolation refers to any estimation of surface values in the area that was not sampled. This estimation is based on or generated from the known surface values (obtained from the sampled points) surrounding the unknown points. Interpolation can be used to estimate unknown values of elevation, rainfall, temperature, chemical dispersion, or any other spatially based phenomena (Childs, 2004).

Kriging

Kriging is one of the well-known interpolation techniques (Altaany and Jassim, 2013) that can be used to produce geo-environmental models. It is a powerful interpolation method used for diverse applications. Kriging is often used for applications in soil sciences and geology (Childs, 2004). Kriging assumes that spatial correlation reflects the distance or 20 direction between known sample points and can be used to describe surface deviations (Childs, 2004).

The relationship between sampling points is weighed using sophisticated weighed average technique to predict values of the non-sampled points. The search radius used in kriging can either be variable or fixed. The value range of the known areas can be less or lower than that obtained from the sampled areas (Childs, 2004).

The most common kriging method is referred to as ordinary kriging. This technique assumes that from the known sampled areas there is no trend that exists, hence no constant mean for the data over an area mean (Childs, 2004). Another type of kriging that is not common assumes that a trend does exist in the data collected, and that this trend can be modelled. This type of kriging is known or referred to as universal kriging (Childs, 2004).

Another interpolation technique is referred to as inverse distance weighted (IDW). When the set of samples collected is dense enough to capture the extent of local surface variations needed for analysis, then the IDW technique becomes the most appropriate one. In the IDW, a linear-weighted combination set of sample points is used to determine unknown cells. This means that the greater the distance between two sampling points, the less influence the cell has on the output value (Childs, 2004).

2.6 Economic Potential of Tailings

2.6.1 Gold Reprocessing

Recent technological advancements and an increase in the price of gold has led to an era where the recovery of gold and other metals from tailings is possible at a profit (Ogola, *et al*., 2018). Ogola *et al* (2018) further alluded that the mining industry's impact on the South African gross domestic product (GDP) is about 8.3% and this can be increased by reprocessing gold and uranium that occur within the tailings dams. This is particularly practical in a country like South Africa which has a long history of gold mining and a subsequent high volume of tailing dams,

about 1.7 billion and from which approximately 470 000 kg of gold can be recovered (Ogola, *et al*., 2018).

South Africa has been one of the largest gold producers worldwide for more than 120 years ever since the beginning of advanced large-scale gold mining, with over 50% of all gold reserves found in South Africa (Matshusa, 2012; Pistilli, 2022). The gold reef deposits in the Witwatersrand Basin have been identified as the largest gold producer in South Africa and most widespread gold deposit in the world (Frimmel, 2019).

Rosner (2001) mentioned that prior to 1999, it was estimated that over 18000 hectares of land were covered in tailings dams, amounting to over 400 million tons of waste produced in South Africa. This in turn was responsible for 81% of the total mine waste produced in South Africa at that time.

Antony Turton, a professor at the University of the Free State and trustee of the Water Stewardship Council concluded that minerals within tailings dams and closed mines can keep illegal and small-scale miners going for more than a century (Turton, 2016). He further noted that these materials can be mined for a decade or so by larger mining companies.

Gold tailings dams in South Africa remain a potential risk to both the environment and the inhabitants around such facilities as most of these tailings dams have not been rehabilitated. This leaves the area exposed to metals such as Pb, Zn, Cu, As, Co, Cd, Cr and Ni. Previous studies conducted on various tailings dams confirm the occurrence of these metals in high concentrations, placing emphasis on the need to rehabilitate the tailings dams. These metals are toxic and can have short or long-term devastating impacts such as acid mine generation, water pollution, as well as soil degradation and subsequently enter the food chain.

One best way of remedial action against potential tailings hazards is through tailings reprocessing to recover economic minerals that were left behind during ore processing. Reprocessing is gaining more attention from different companies as well as positive press (Calam, 2020). This is because not only does the company benefit economically from this, but the environment and the inhabitants also benefit by having a safer environment and more land to use for other activities.

Tailings Reprocessing

All processes and activities conducted in a bid to extract the valuable minerals from the tailings dams are known as reprocessing, re-mining or tailings dams beneficiation. Tailings reprocessing is a relatively new approach to mining in South Africa with the potential of sparking a new gold rush as more companies are looking into reprocessing previously abandoned tailings that were viewed as waste and a threat to the environment as well as freshly produced tailings. For active and future mines, reprocessing can be planned for as the mine progresses and operate simultaneously with the original mining. The benefits which necessitate reprocessing of gold tailings are detailed below:

- **Increase in the Price of Gold**

  The price of gold has been on the increase over the years (Fig. 2.3). From 2003 to 2022, it has increased by over 580% thus increasing the likelihood of recovering low grade ore at a profit. This in turn can lead to reprocessing of gold from tailings to be economically viable.

Figure 2. 3: 20-year gold unit price (US dollar/ounce) (Gold Price, 2022).

- **Advances in Technology**

  During mineral processing, not all required mineral or commodity is recovered, however, some amount is left behind with gangue minerals and stored in tailings dams. Continuous research and recent technological advancement have made it possible to recover 98% of gold within the tailings dams in particular the carbon-in-column method (Dehghani, *et al*., 2009). This breakthrough in technology makes reprocessing of metals from tailings viable.

- **Shortage of Gold Reserves**

With mining companies growing, mineral resources are becoming more and more depleted, leading to a scarcity of reserves. Gold reserves in the Witwatersrand are now being found at ultra-deep levels. The subsequent increase in costs such as ventilation (25-50% of electrical operating cost), geotechnical designs, and amelioration of seismic activities dwindle the profit margins and hence increase the cost of mining – reducing the reserves (Costa and Silva, 2020). Mining companies are now focusing on previously mined and processed ore tailings to recover previously missed metals.

- **Low Capital Required**

Traditional mining requires a relatively large amount of capital and operating costs. It also takes much time to make a profit as developing a mine is time and resource consuming without any immediate return. On the other hand, reprocessing of tailings requires limited equipment, development work as well as fewer employees, hence it requires relatively low capital.

- **Environmental Benefits**

Reprocessing of tailings does not further increase the mine's footprint. This is because no additional damage or disturbance is done on land. However, reprocessing can be viewed as a rehabilitation strategy and can be coupled with other beneficial tailings remedial techniques such as using tailings as a construction material as metal recovery takes place (Calam, 2020). Reprocessing also removes large hips of tailings covering large amounts of land, allowing the aesthetic beauty of the area to be restored as well as the ability to reuse that area for a particular activity, for example, the creation of parks or simply using the area for farming.

- **Permit Requirements**

Since reprocessing takes place in a previous mine site, no additional permit may be required to conduct reprocessing. This makes it easier to start reprocessing operations once other technical issues, such as metal valuations and machinery are sorted out.

Reprocessing Techniques

Merging of Tailings

For better management of tailings reprocessing and rehabilitation, smaller tailings dams are merged into one big tailings facility. This is made possible through hydraulic mining or self-propelled cyclonic units (Blake, 2013). This is possible where there are several tailings dams within a given mine site, for example, at the Fumani Mine.

Dry Tailings

Dry tailings are mined using hydraulic mining monitors. These monitors use high pressure water to erode the tailings in sections. The tailings are then eroded downstream along a channel, pass through a screen and collected in a sump. Large objects are prohibited from entering the sump by the screen. The tailings, now in slurry form, are pumped into a thickener where the underflow is reprocessed at the plant (Groenheide, 2021).

Wet Tailings

A dredge is used to mine wet tailings dams. The dredge extracts the tailings and pumps the material into a reprocessing plant. During mining, the dam is divided into smaller sections known as holding ponds. This is important for better management of the material and water within the tailings dam. To maintain the dams' footprint and prevent more environmental issues, the void created in a holding pond is refilled up with the tailings from the reprocessing plant. To save and use water sustainably, the dredged water is re-circulated back to the pond and reused for the same purpose (Tailings.info, 2017).

Current Gold Reprocessing

Many gold mines in South Africa are looking into reprocessing gold from tailings as it is much more economical and beneficial to both the company and the environment. Ergo mining and Brakpan have a joint venture to facilitate the reprocessing of 1.7 billion tonnes of gold tailings dams believed to have the capacity and possibility to refine 15 million ounces of gold (Test, 2008). This is due to the ability of modern gold beneficiation techniques that can produce gold with a purity of 99% (Dehghani *et al.*, 2009). Cooke tailings have a capacity of 83 million tons (Blake, 2013). This attracted Chinese investors who then recently bought these tailings intending to reprocess for gold, uranium as well as sulphur. It is estimated that 0.8 million ounces and 544 million ounces of Gold and Uranium respectively will be recovered over a period of 12 years (Blake, 2013).

2.6.2 Brick Production

Bricks are used worldwide and are always in demand as construction never ceases to take place. Though bricks are made internationally and the process of brick making looks like an easy job, there are a lot of considerations that are taken into account to ensure the quality of bricks produced is of great quality. The primary brick-making raw material comprises clay soil and water.

Clay Soil

The major constituent of almost all bricks is clay. Clay is a term that is generally used to describe; natural materials that exhibit plastic properties, very fine particle sizes of soil, finer than 2 micrometres, mineral particles that are mostly composed of hydrous layered silicates of aluminium and occasionally containing magnesium and iron (Grim and Kodama, 2013).

Clay soil is composed of silica, alumina, magnesia and iron. Good bricks, tiles, stoneware glazed products and ceramics are produced from a clay mixture in which illite is most abundant (Grim and Kodama, 2013). Calcareous clay contains calcium carbonate, which results in a yellow or cream colour after the bricks have been burnt. Non-calcareous clay on the other hand contains feldspars as well as iron oxides and turns to either red, pink or brown after burning.

When silica is heated at high temperatures, it turns to a glassy phase in a process known as vitrification. In brick making, it is thus important to have silica as it converts the clay to a crystalline structure. Consequently, the clay used for brick making should have the right amount of silica (50-60%), alumina (20-30%), iron oxide (4-6%), Lime (1-4%) and magnesia (4-5%) (Civilseek, 2022). It should be plastic when mixed with the right amount of water. Such clay should have enough tensile strength so that the brick can keep its shape. Clay particles should be able to fuse to form a pulp. It would take approximately 3 m^3 of clay soil to make 1000 bricks.

Water

To produce approximately a thousand bricks, about 600 litres of water is required. It is therefore important to ensure that the source of water is always available for brick making. Water is used to mix the clay soil to produce clay pulp that is moulded to produce bricks.

Sand

Sand is used to adjust the quality of the clay soil. Sand is added to the pulp when drying to prevent the clay soil from becoming too brittle. Sand can also be used to stabilise the mixture, thus preventing the pulp from sticking to the moulds. In the absence of sand during the brick making process, sawdust, ash as well as fine dry silicon can be used to prevent the soil from sticking to the mould.

Energy

The most common energy sources for brick burning are coal and firewood. The easiest coal source to use is the coal waste from a power plant if available in the area. The bricks need to be burnt for them to be vitrified enough to give enough strength to the brick. The bricks, however, do not have to be completely vitrified. The temperature thus must be controlled. If the bricks are under-fired, the clay particles will have a poor bond, resulting in weak bricks (Maskell, *et al*., 2016). If the bricks are over-burnt at a very high temperature they will either melt or slump. It is therefore important to regulate the temperature as it can affect the quality of the bricks produced.

Earth masonry is not "fired" like the conventional bricks. The masonry units are therefore air-dried after being moulded. This is done to reduce shrinkage and to improve the strength of the brick. These types of bricks are ideal as they do not require energy to dry beside the air (Maskell, *et al*., 2016).

Soil Classification Systems

To use tailings as a construction material, it is crucial to know the geochemical and physical quality of the tailings. Clay is a very important constituent in the production of bricks; hence, it is crucial to know the amount of clay within the tailings. To determine the ability of tailings to be used for construction purposes, multiple geotechnical tests and the data analysed using various classification systems.

Unified Soil Classification System

The Unified Soil Classification System (USCS) is a system used in engineering and geology to describe the texture as well as the grain size of soil, and to classify and identify soils for general engineering purposes. Symbols are used to classify soil into different categories. This system is used mostly in natural and unconsolidated materials (Evett and Cheng, 2007).

The USCS broadly divides soils into coarse-grained soils, fine-grained soils, organic soils and peat (Mishra, 2017). In order to use the USCS, sieve analysis, as well as Atterberg tests, are undertaken prior to the classification.

Coarse-grained Soil

If 50% or more of the total material by weight is greater than the 0.075 mm after sieve tests, then the material is said to be coarse-grained. Since coarse grained is a broad reference, the soils in this category can further be classified as either gravel or sand.

Gravel (G) is defined as the soil that allows less than 50% of the total material by weight to pass through the 4.75 mm sieve. The soils in this category are denoted by a G. These include gravels as well as gravelly soil.

Sand (S) is defined as the soil that allows more than 50% of the total material by weight to pass through the 4.75 mm sieve. The soils in this category are denoted by an S. These include sands as well as sandy soil.

Fine-grained Soil

If 50% or more of the total material by weight passes through the 0.075 mm sieve during sieve tests, then the material is said to be fine-grained. Since fine-grained is a broad term, the soils in this category can further be classified as either inorganic silts and very fine sands, inorganic clay, or organic silts and clays and organic matter.

Organic Soil

Organic clay is a term used to define clay that its' liquid limit after drying in the oven, is less than 75% of its liquid limit before oven drying.

Organic silt is a term used to define silt that its liquid limit after drying in the oven, is less than 75% of its liquid limit before oven drying.

Peat

Peat is a dark brown to black soil, usually found at the top layer of soil containing a spongy consistency and a textural range of fibrous to amorphous. Peat contains remains of organic material and sometimes non-organic in various stages of decomposition.

The USCS is summarised in Table 2.3, indicating the major division, group symbols, typical names for soils as well as the classification criteria.

Table 2.3: Unified soil classification system chart (Mishra, 2017)

<table>
<tr><th colspan="3">Major Divisions</th><th>Group Symbols</th><th>Typical Name</th><th colspan="2">Classification Criteria</th></tr>
<tr><td rowspan="7">Coarse Grained Soils [More than 50% retained on No. 200 (0. 075 mm)</td><td rowspan="3">Gravel [50% or more of coarse fraction retained on No. 4 sieve (4.75 mm)]</td><td>Clean Gravels</td><td>GW</td><td>Well graded gravels</td><td colspan="2">Cu>4
Cc = 1 to 3</td></tr>
<tr><td></td><td>GP</td><td>Poorly graded gravels</td><td colspan="2">Not meeting both criteria for GW</td></tr>
<tr><td>Gravels with fines</td><td>GM</td><td>Silty gravels</td><td>Atterberg Limit below A-line or plasticity index less than 4</td><td rowspan="2">Atterberg Limits in hatched GM-GC</td></tr>
<tr><td></td><td>GC</td><td>Clayey gravels</td><td>Atterberg Limit above A-line or plasticity index greater than 7</td></tr>
<tr><td rowspan="3">Sand [50% or more of coarse fraction passing through No. 4 sieve (4.75 mm)]</td><td>Clean Sands</td><td>SW</td><td>Well graded Sands</td><td colspan="2">Cu>6
Cc= 1 to 3</td></tr>
<tr><td></td><td>SP</td><td>Poorly graded Sands</td><td colspan="2">Not meeting both criteria for GW</td></tr>
<tr><td>Sands with fines</td><td>SM</td><td>Silty Sands</td><td>Atterberg Limit below A-line or plasticity index less than 4</td><td rowspan="2">Atterberg Limits in hatched SM-SC</td></tr>
<tr><td rowspan="6">Fine Grained Soils [50% or more passing No. 200 (0. 075 mm)</td><td colspan="2" rowspan="3">Silts and clays Liquid Limit 50% or less</td><td></td><td>SC</td><td>Clayey Sands</td><td>Atterberg Limit above A-line or plasticity index greater than 7</td></tr>
<tr><td>ML</td><td>Inorganic silts of low plasticity</td><td colspan="2" rowspan="6"> 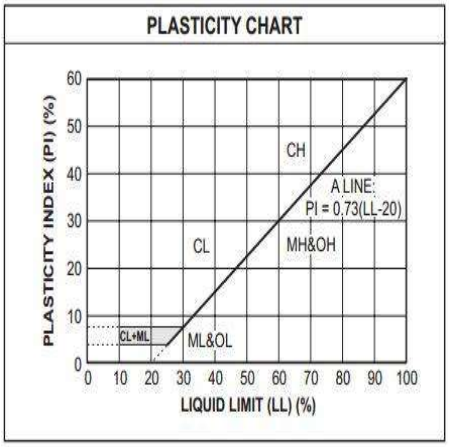

Visual-manual identification</td></tr>
<tr><td></td><td>CL</td><td>Inorganic clays of high plasticity</td></tr>
<tr><td></td><td>OL</td><td>Organic silts of low plasticity</td></tr>
<tr><td colspan="2" rowspan="3">Silts and clays Liquid Limit greater than 50%</td><td>MH</td><td>Inorganic silts of high plasticity</td></tr>
<tr><td>CH</td><td>Inorganic clays of high plasticity</td></tr>
<tr><td>OH</td><td>Organic silts of high plasticity</td></tr>
<tr><td colspan="3">Highly organic Soils</td><td>Pt</td><td>Peat, muck and other highly organic soils</td></tr>
</table>

American Association of State Highway and Transportation Officials System (AASHTO)

AASHTO classification system was developed originally by the Bureau of Public Roads for classification of soils for highway subgrade use in 1920 (Mishra, 2017). It was later proposed by the Highway Research Boards Committee on Classification of Materials for Subgrades and Granular Type Roads in 1945.

Presently, AASHTO classifies soils into seven major groups A-1 to A-7 as indicated in Table 2.4 based on the distribution of grain size within the soil, the liquid limit as well as the plasticity index of the soil (Das, 2006).

Table 2.4: The AASHTO material classification system (Das, 2006)

General Classification	**Granular Materials (35% or less passing the 0.075 mm sieve)**							**Silt-Clay Materials (>35% passing the 0.075 mm sieve)**			
Group Classification	A-1		A-3	A-2				A-4	A-5	A-6	A-7
	A-1-a	A-1-b		A-2-4	A-2-5	A-2-6	A-2-7				A-7-5 A-7-6
Sieve Analysis (% passing)											
2 mm	50 max										
0.425 mm	30 max	50 max	51 min								
0.075 mm	15 max	25 max	10 max	35 max	35 max	35 max	35 max	36 min	36 min	36 min	36 min
Characteristics of fraction passing 0.425 mm											
Liquid Limit				40 max	41 min	40 max	41 min	40 max	41 min	40 max	41 min
Plasticity Index	6 max		NP	10 max	10 max	11 min	11 min	10 max	19 max	11 min	11 min
Significant constituent materials	Stone fragments gravel sand		Fine sand	Silty or clayey gravel sand				Silty soils	Clayey soils		
General rating as a subgrade	excellent to good							fair to poor			

CHAPTER 3: MATERIALS AND METHODS

To accomplish the objectives of this study, the following field, laboratory methods and procedures as well as data analysis were adopted (Fig. 3.1).

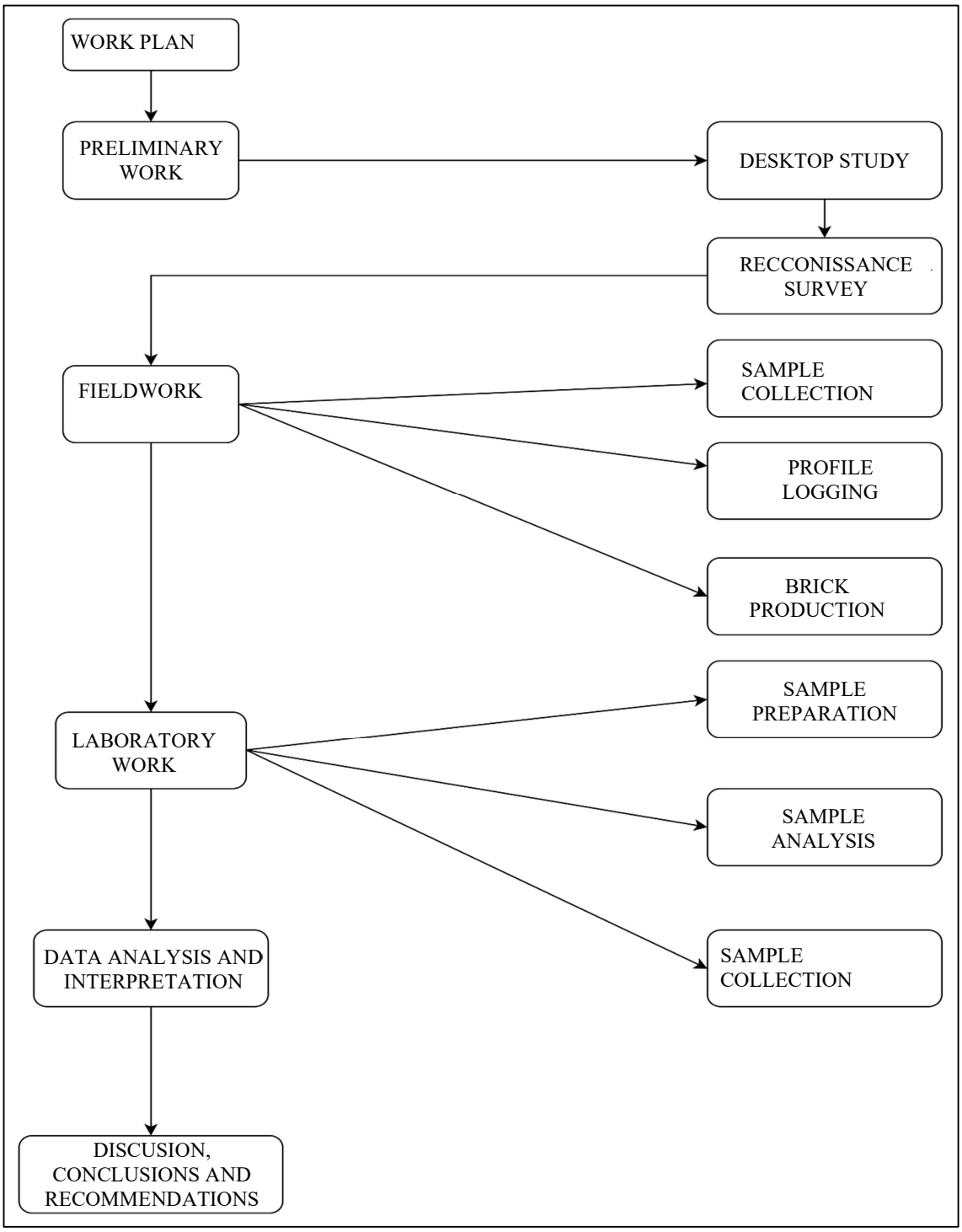

Figure 3. 1: Flow chart indicating methods and procedures applied in the study.

3.1 Preliminary Work

3.1.1 Desktop Study

Desktop study was done to acquire first-hand information about the location, characteristics, and accessibility to the study area. It provided information on how to best conduct the fieldwork. Various sources of information used included: review of books, unpublished technical reports, previous geological reports, topographical maps, journals, and internet sources.

3.1.2 Reconnaissance Survey

Reconnaissance was done prior to the actual fieldwork. It was during this stage that the residence of the Mtititi area, the relevant stake holders of the Fumani Mine as well as the owners of Tshidino brick manufacturing company were informed about the work to be conducted and asked for permission to conduct the fieldwork at the respective study areas.

Once permission was granted, observations such as accessibility, topography and drainage of the area were made. Observations of the type of samples to be collected as well as the sampling patterns were made. It was after these observations that it was decided that the soil samples were to be collected in four directions of the tailings dams, tailings samples were to be collected on two tailings dams, and that bricks were to be manufactured from tailings samples collected. It was crucial to conduct reconnaissance as it made the actual fieldwork to commence with ease. The methods, equipment, and tools used were identified and tested at this stage (Fig. 3.2).

Figure 3. 2: Equipment and tools used for fieldwork: hand auger, shovel, notebook, pen, marker, sampling tags, sampling bags, string and hammer.

3.2 Fieldwork

The fieldwork comprised sample collection, profile logging as well as brick production. The work was carried out on the Fumani Tailings Dams 1 and 2, the surrounding area as well as on a small-scale brick manufacturing company called Tshidino bricks located in Hamakhuvha Village.

3.2.1 Sample Collection

Soil Sampling

Soil samples were collected in four directions; east, west, north and south of the Fumani Tailings Dams (Fig. 3.3). Samples were collected at an interval of 200 m in each direction along traverses T1 to T4 for a distance of 2.2 km, 4 km, 5 km and 4.2 km respectively. Traverse1 was in the direction of Kruger National Park, thus making more than half the traverse inaccessible. A total of 11, 20, 25 and 21 samples were collected from Traverses 1, 2, 3 and 4 respectively, amounting to a total of 77 soil samples.

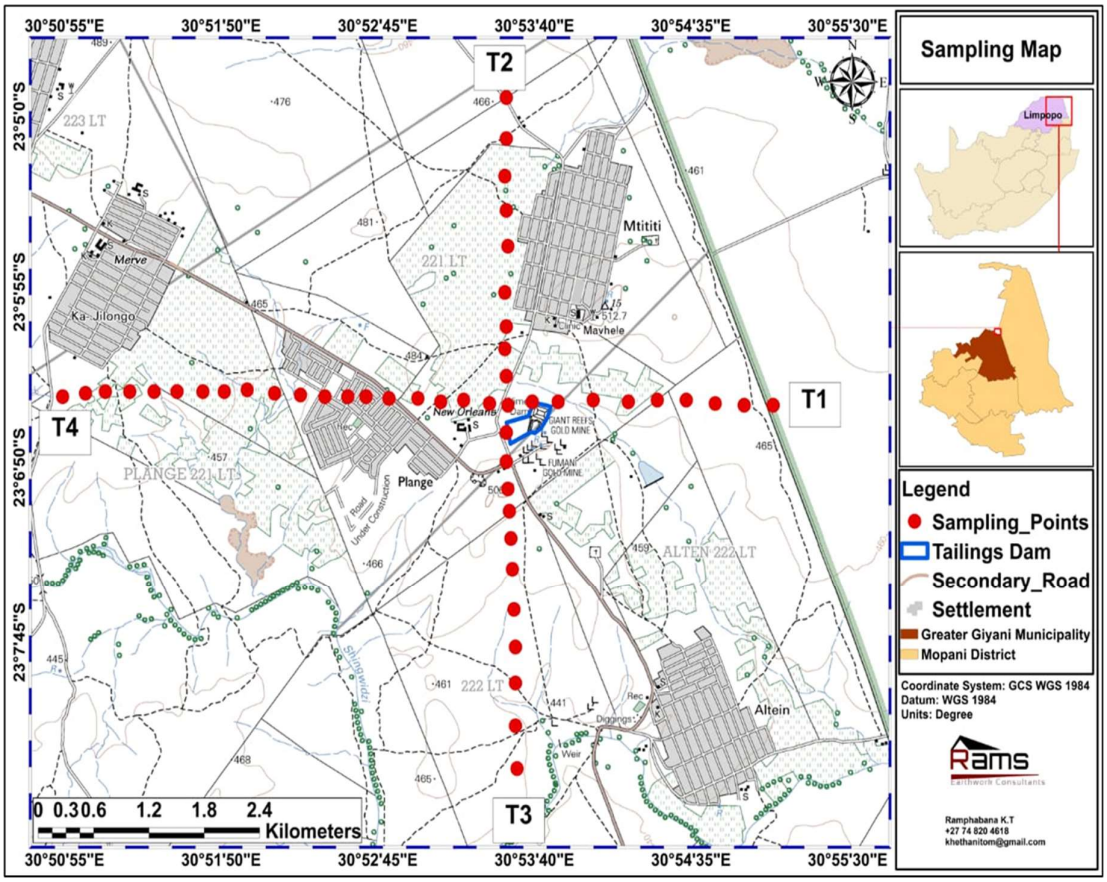

Figure 3. 3: Location of traverses and sampling points around the Fumani Tailings Dams.

A compas was used to ensure sampling was conducted within the intended study area on the correct location. A global positioning system (GPS) was then used to confirm the location of the sampling point. Once it was established that the sampling point corresponds to the map, GPS co-ordinates were recorded in the field notebook.

A shovel was then used to clear the identified sampling point as well as to collect the soil samples (Fig. 3.4). Soil samples of approximately 2 kg each were collected up to a depth of 30 cm. All samples were stored in marked and labeled sample bags. To avoid contamination, the sample bags were tied tightly with a string. During sampling, the coordinates were recorded in the field notebook and summerised (Appendix C1).

Figure 3. 4: Soil sampling using a spade.

Tailings sampling

Three profiles were set on the surface of the two tailings dams. Fumani Tailings Dam 1 had 4 sampling points along each profile, whilst Fumani Tailings Dam 2 had 3 (Fig. 3.5) due to the different sizes and shapes of the tailings dams.

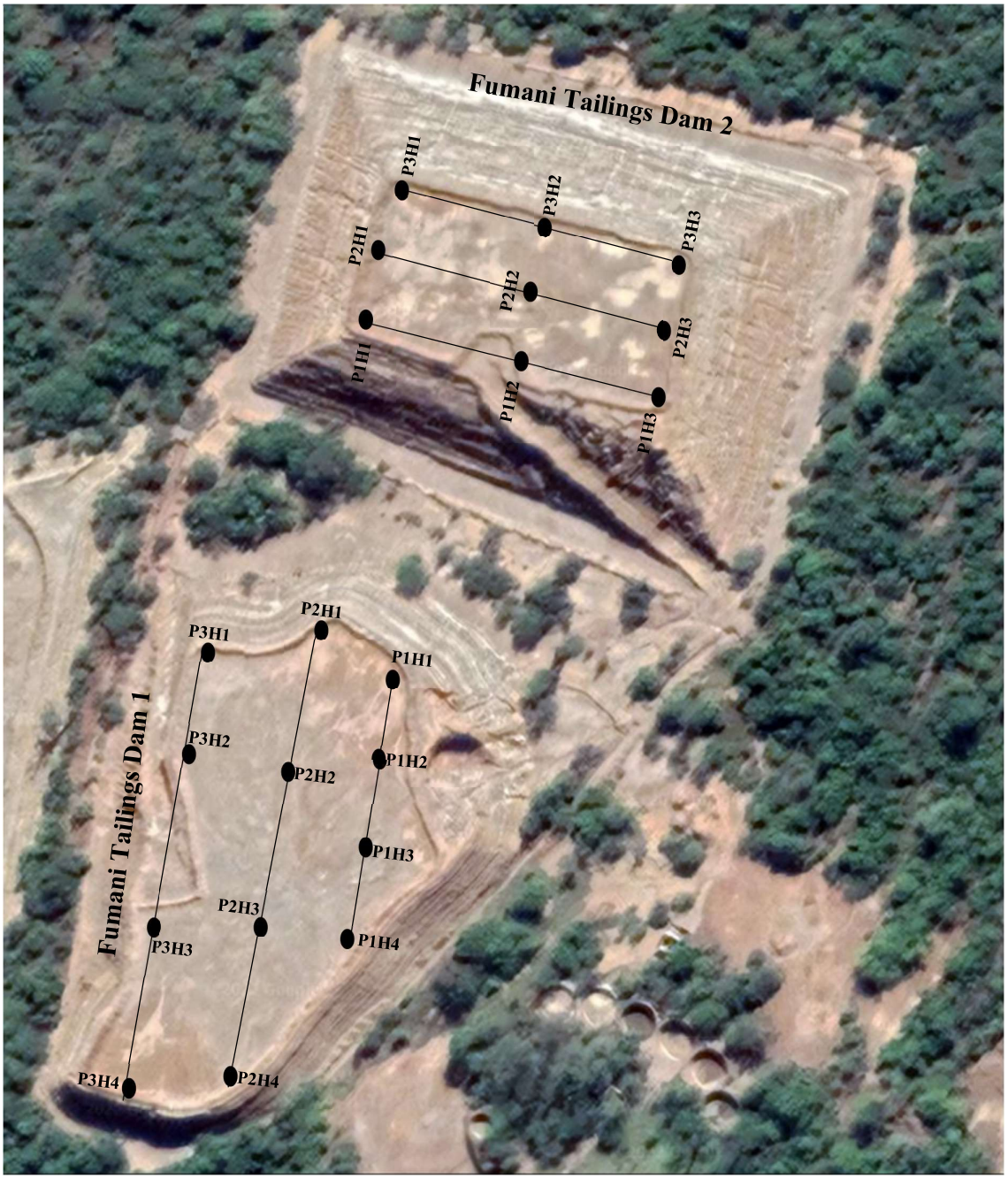

Figure 3. 5: Location of profiles and boreholes on Fumani Tailings Dams (Google earth, 2022).

At each sampling point, a shovel was used to clean the area prior to sampling. An auger drill was then used for sampling (Fig. 3.6). Samples of approximately 5 kg were collected at 1m interval from the top of the tailings dam to a depth of 7 m. a total of 84 and 63 tailings samples were collected from Fumani Tailings Dams 1 and 2 respectively. The samples were stored in sample bags that were marked and labeled. To avoid any contamination, the sample bags were tied with a string. The area was rehabilitated by backfilling tailings into the boreholes.

Figure 3. 6: Tailings sample collection: (a) hand auger drilling; (b) collected sample in labeled sample bag.

3.2.2 Profile Logging

Tailings sampling and profile logging were conducted simultaneously. During sampling, physical characteristics such as: colour, texture, hardness and moisture content of the material from the auger bucket were carefully assessed with depth and recorded in the field book (Table 3.1) and summarised in Appendix A1 and B1. A total of 12 and 9 boreholes were sampled and logged at the Fumani Tailings Dam 1 and 2 respectively. Profile logging was crucial as it helped to identify the oxidation zone (OZ), transition zone (TZ) as well as the un-oxidized zone (UZ) of the tailings dams to get a clear understanding of the processes taking place within the tailings dams and to determine the extent of acid mine water generation.

Table 3.1: Physical characteristics of tailings from P1H1 of Tailings Dam 1 and 2

	Interval (m)		Physical characteristics					Illustration
	From	To	Colour	Texture	Hardness	Moisture	Other	
Fumani Tailings Dam 1 P1H1	0	0.1	orange	gritty	Mixed	dry dusty	loose, dusty with hard pebbles	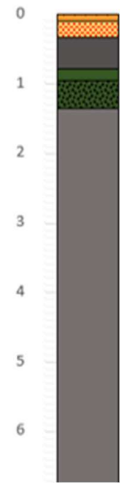
	0.1	0.33	light orange	gritty	very hard	dry	gritty feel	
	0.33	0.78	grey	smooth	Soft	moist	soft and sticky	
	0.78	0.95	green	gritty	Hard	dry	compacted and feels gritty	
	0.95	1.35	dark grey	smooth	soft	wet	very sticky	
	1.35	7	light grey	smooth	Soft	moist	easy to drill	
Fumani Tailings Dam 2 P1H1	0	0.25	orange	smooth	very hard	dry dusty	flaky, highly oxidised	
	0.25	0.75	light orange	gritty	Hard	dry	compacted, oxidised with pebbled	
	0.75	0.92	orange brown	gritty	very hard	dry	compacted and crust like	
	0.92	0.98	orange brown	smooth	Soft	wet	muddy and shinny	
	0.98	7	light grey	smooth	Soft	moist	muddy and shinny	

3.2.3 Brick Production

It was decided that both clay and cement bricks will be made using different soil to tailings ratios and different cement to tailings ratios to produce the optimum high-quality brick suitable for construction. Both clay and cement bricks were produced at Tshidino Bricks.

3.2.3.1 Clay Bricks

An attempt had was made to make bricks using tailings as the main material. The materials used for brick production were soil, tailings, water, brick mould, and a measuring container (Fig. 3.7). Ten different soil to tailings ratios were used to produce bricks of different qualities as shown on Table 3.2 below. This was done to determine the optimum tailings to soil ratio for production of suitable bricks. Three bricks were made from each tailings to soil ratio, with an additional 3 bricks made of soil without any tailings that was used as control, this gave a total of 33 bricks produced.

Figure 3. 7: Equipment and tools used for brick production: mould, shovel, water, and measuring container.

Table 3.2: Tailings to soil ratios used in the brick production of clay bricks

Sample name	Tailings (%)	soil (%)	No. of bricks	Comments
A	100	0	3	Grey and dusty with loose edges
B	90	10	3	Grey and dusty with loose edges
C	80	20	3	Grey and dusty with loose edges
D	70	30	3	Grey and dusty with loose edges
E	60	40	3	Brown
F	50	50	3	Brown
G	40	60	3	Brown
H	30	70	3	Red
I	20	80	3	Red
J	10	90	3	Red
K	7.5	92.5	3	Red
L	5	95	3	Red and competent
M	2.5	97.5	3	Red and competent
N	0	100	3	Control bricks, red and competent

Procedure

A measuring cup was used as a scale to measure the tailings and the soil. A spade was used to mix the measured material. A depression was created in the center of the mixture and water was added at the center. The material was mixed to create a mortar. The mortar was manually placed in the brick mold. The bricks were removed, labeled, and allowed to air dry for 14 days (Fig. 3.8) before being burnt. The bricks were burnt in a kiln oven made from bricks and soil. Wood and charcoal were used to create a fire in the oven. Soil was then used to close and insulate the oven. The bricks produced as well as their descriptions are shown in appendix D1.

Figure 3. 8: Photograph illustrating brick making process: (a) soil, tailings, and water; (b) brick mould with mortar; and (c) bricks.

3.2.3.2 Cement Bricks

Materials used for brick production were water, tailings, cement and sand mixture, manual brick molding machine, measuring container and a spade. Four different ratios of tailings to cement mixture were used to create bricks (Fig. 3.9). Four bricks were made from each tailings to cement mixture, giving a total of 20 bricks produced. This was done to analyse and compare all bricks to produce the optimum strength of the bricks to be recommended for use. Table 3.3 illustrates the different ratios of tailings to cement mixture, and water used to produce different bricks. Some bricks already made at Tshidino, and ready to be sold, were used as control bricks.

Table 3.3: Different ratios of tailings to cement, soil, and water

Name	Cement mixture	Tailings	% Tailings	Water
A	2 kg	2 kg	50	2 L
B	2 kg	1 kg	33.33	1.5 L
C	2 kg	0.5 kg	20	1.25 L
D	1 kg	2 kg	66.66	1 L

Procedure

A scale was used to accurately measure the cement mixture and tailings. A spade was used to mix the measured material. A depression was created in the center of the mixture and water was added into it. The material was mixed to create a mortar. The mortar was manually placed in the brick mold. The bricks were removed, labelled, and allowed to air dry for 14 days (Fig. 3.9). After drying, the bricks were sent for testing at the Soillab in Pretoria. The bricks produced as well as their descriptions are shown in appendix D2.

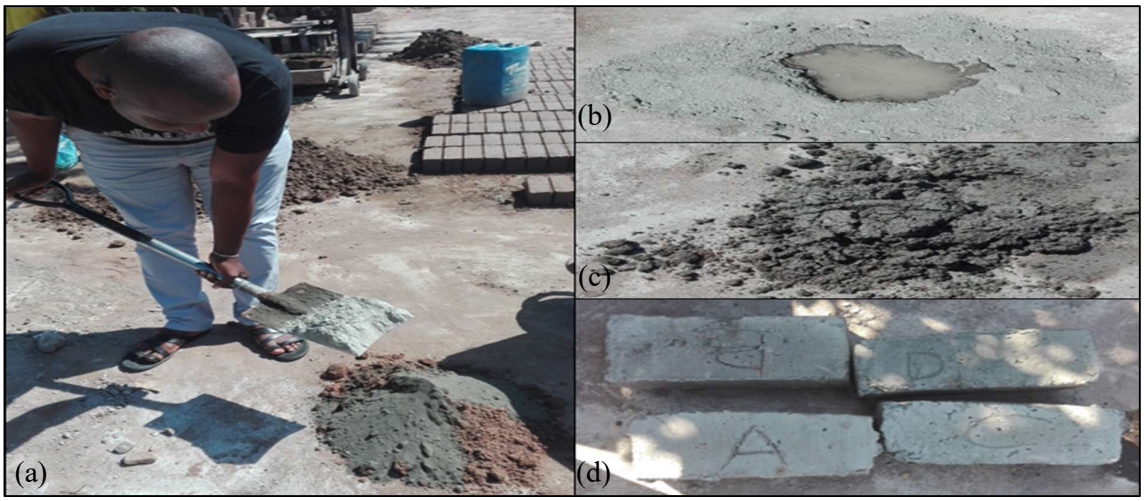

Figure 3. 9: Photograph illustrating brick making process: (a) mixing the dry measured material; (b) well created and water added; (c) mortar; (d) bricks.

3.3 Laboratory Work

The following laboratory methods and procedures were adopted to accomplish the objectives of this study (Fig. 3.10)

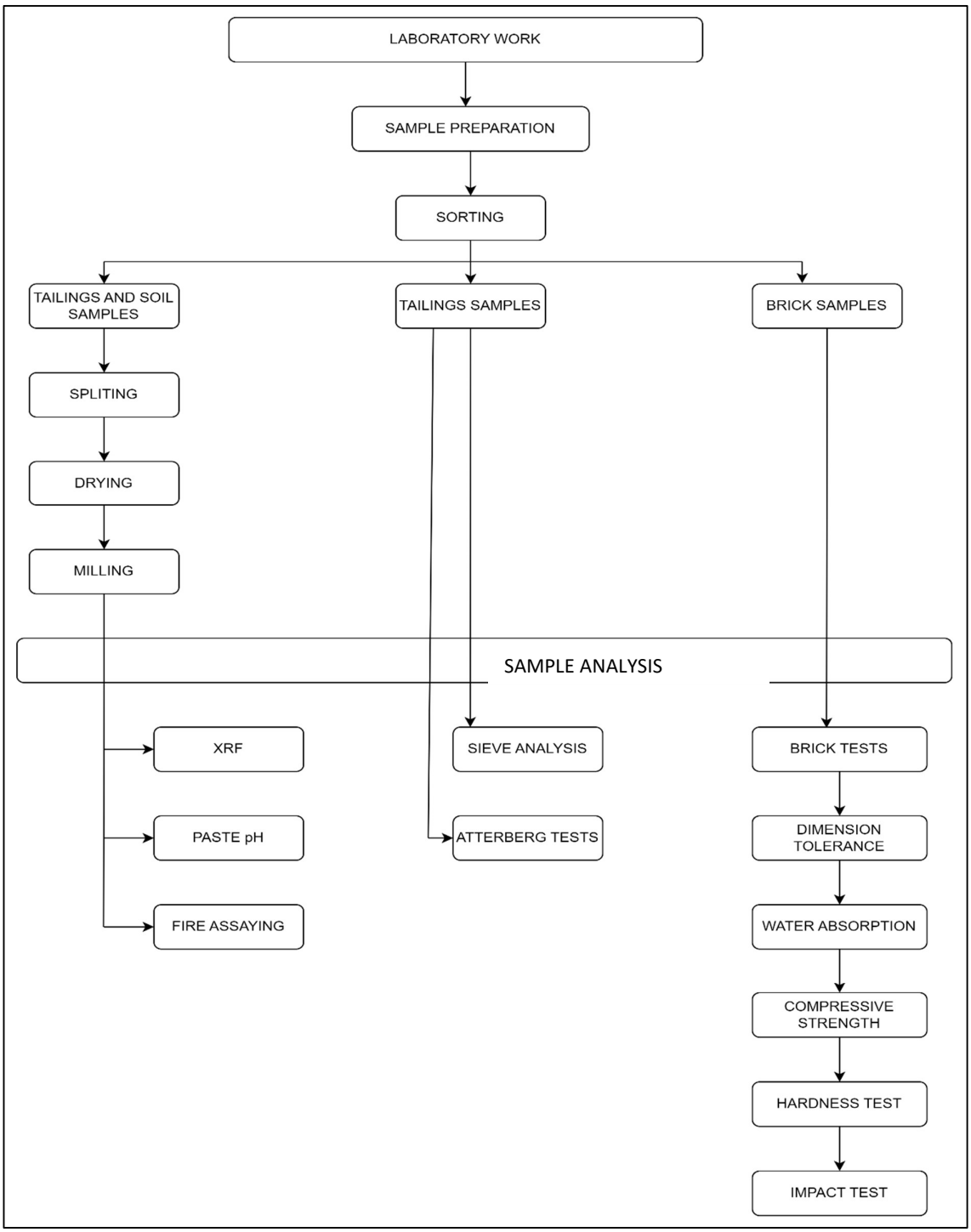

Figure 3. 10: Flow chart indicating laboratory methods and procedures applied in this study.

3.3.1 Sample Preparation

Sorting

Once the samples got to the University of Venda, they were sorted according to their type (tailings, soil and bricks) at the Mining and Environmental Geology laboratory. The samples were then arranged according to sample tags and labels to ensure that all samples were present. After sorting, only tailings and soil samples underwent splitting, drying, and milling whilst brick samples underwent sample analysis directly after sorting.

Splitting

Tailings and soil samples were split using a riffle splitter (Fig. 3.11). A total of 147 tailings samples and 77 soil samples were prepared. This was done to obtain smaller manageable samples that were representatives of the whole samples. The smaller samples of about 2 kg were placed in drying bags before placing them into the drying oven. The drying bags were labelled to prevent sample mix up and allow for easy identification. The remaining samples were then stored carefully as duplicate samples at the Mining and Environmental Geology laboratory.

Figure 3. 11: Riffle splitter used to homogenize the samples.

Drying

The selected samples for analysis were dried using a Bench Vacute laboratory oven (Fig. 3.12). The samples were dried overnight for over 10 hours at a temperature of 110°C. These samples were later allowed to cool to room temperature before the milling process could take place.

Figure 3. 12: Bench Vacute laboratory oven used for drying samples.

Milling

The samples were placed into a milling pot for the milling process by the Retsch model RS 200 milling machine (Fig. 3.13). For quality control measures, the milling pots were thoroughly cleaned using quarts to avoid cross-contamination before milling each sample. To obtain approximately 85% of 75 micro-meter samples, each sample was milled for at least 5 minutes and placed in labelled sample bags.

Figure 3. 13: Retsch model RS 200 milling machine used for milling samples.

3.3.2 Sample Analysis

Metals and Major Oxides Analysis using XRF

Approximately 10 g of the milled tailings and soil samples were weighed and pressed in aluminum cups on a bed of approximately 2.5 g of boric acid. A compressor was then used to apply a pressure of about 40 tons for about 1 minute to create pellets (Fig. 3.14).

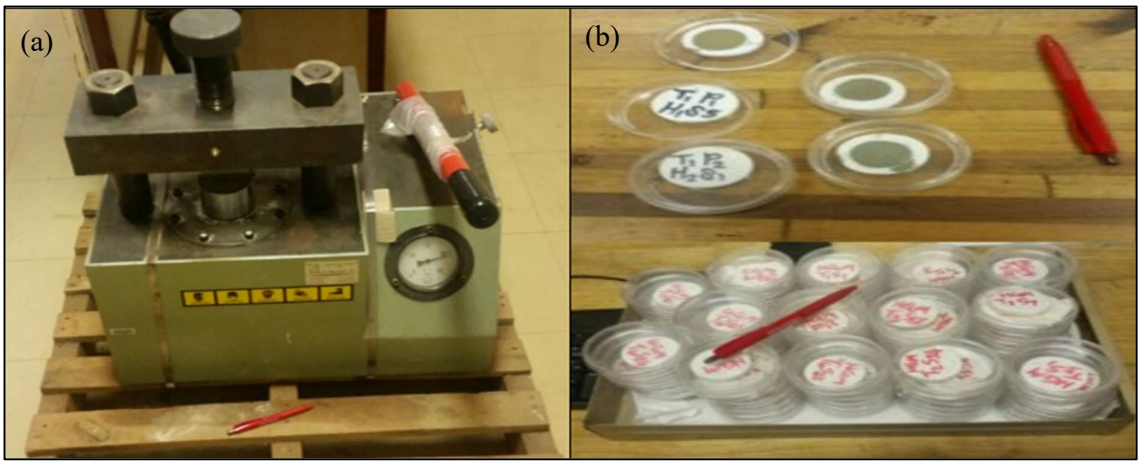

Figure 3. 14: Photograph of (a) compressor; (b) pellets ready for XRF analysis.

Prior to analysis, a set of 5 reference standards purchased from Mintek (SARM 1, 2, 3, 42 and 52) were used to calibrate the S2 Ranger XRF (Fig. 3.14). 147 tailings and 77 soil samples were analysed for the following metals: Cu, Pb, Zn, Co, As, Cr and Ni. This was done to identify the extent of metal pollution within and around the Fumani Tailings Dams. The XRF results obtained for the Fumani Tailings Dam 1 and 2 as well as soil samples are represented in Appendix A2, B2 and C2 respectively.

Figure 3. 15: Photograph of S2 Ranger XRF equipment used for metals analysis.

Paste pH Analysis

Approximately 100 g of the milled tailings samples were accurately weighed and transferred to a beaker containing 100 ml of deionized water. The mixture was then stirred for an hour using a spatula. The pH meter was then calibrated using buffers with a pH of 4, 7 and 14. This was done to ensure the accuracy of the equipment.

A total of 147 tailings samples were then analysed at the Department of Mining and Environmental Geology laboratory, using a pH meter. This helped to identify the possibility of acid mine generation and the identification of the oxidation, transitional and un-oxidised zones within the dams. The results obtained from the Fumani Tailings Dam 1 and Fumani Tailings Dam 2 were recorded and presented in Table 3.4 and Table 3.5 respectively.

Table 3.4: Paste pH values of Fumani Tailings Dam 1

Depth	P1H1	P1H2	P1H3	P1H4	P2H1	P2H2	P2H3	P2H4	P3H1	P3H2	P3H3	P3H4
0-1m	3.273	3.221	3.185	3.375	3.269	3.29	3.74	3.854	3.74	3.38	3.251	3.358
1-2m	4.6	4.652	4.307	4.307	4.598	4.325	4.864	4.815	4.662	4.258	3.725	4.075
2-3m	6.114	6.165	5.33	5.596	6.847	5.264	5.957	6.169	5.958	5.169	4.336	4.958
3-4m	7.219	7.365	6.182	6.503	7.265	6.148	6.754	7.269	7.716	6.698	4.958	6.38
4-5m	7.369	7.601	7.691	8.035	7.985	7.365	7.385	7.695	7.862	7.685	6.004	7.599
5-6m	7.658	7.745	7.745	7.98	8.012	7.264	7.698	7.985	8.199	8.01	7.264	8.045
6-7m	7.804	7.862	7.86	8.025	8.215	7.62	7.932	8.084	8.654	8.22	7.65	8.321

Table 3.5: Paste pH values of Fumani Tailings Dam 2

Depth	P1H1	P1H2	P1H3	P2H1	P2H2	P2H3	P3H1	P3H2	P3H3
0-1m	3.495	3.395	3.395	3.856	3.623	3.562	3.495	3.355	3.215
1-2m	4.665	4.465	4.399	4.015	3.94	3.692	4.365	3.698	3.492
2-3m	5.987	5.892	5.725	5.698	5.325	4.685	5.987	5.392	4.225
3-4m	6.394	6.487	6.334	6.952	6.652	5.964	6.894	6.987	4.984
4-5m	7.362	7.422	6.952	6.984	7.041	6.254	7.362	7.422	6.952
5-6m	7.985	7.985	7.625	7.684	7.652	6.785	7.985	7.985	7.625
6-7m	8.265	8.692	8.003	8.621	7.958	7.985	8.365	8.102	8.003

Gold Analysis using Fire Assay

After the process of splitting, drying and milling at the University of Venda Laboratory, a total of 84 and 63 tailings samples from Fumani Tailings Dams 1 and 2 respectively milled samples of approximately 300 g each were sent to Australian Laboratory Services (ALS) in Johannesburg for Au analysis using fire assaying technique. The Au values for Tailings Dams 1 and 2 are presented in Table 3.6 and Table 3.7 respectively.

Table 3.6: Gold fire assaying results of Fumani Tailings Dam 1 (ppm)

Depth	P1H1	P1H2	P1H3	P1H4	P2H1	P2H2	P2H3	P2H4	P3H1	P3H2	P3H3	P3H4
1 m	1.26	1,98	1,82	1,59	0,48	1,27	1,63	2,33	1,87	1,33	0,58	1,54
2 m	1.52	1,35	1,29	1,23	0,99	0,84	2,02	1,22	1,31	1,06	2,03	1,7
3 m	1.39	1,81	1,28	1,47	1,42	0,84	1,1	1,07	0,99	0,97	1,94	1,08
4 m	2.36	1,98	1,9	0,44	1,2	1,16	2,09	0,51	1,55	1,34	0,99	0,92
5 m	2.67	0,62	1,27	0,36	0,84	1,11	1,44	0,65	1,28	0,89	1,35	1,01
6 m	2.31	0,74	1,44	1,39	0,45	1,27	1,99	1,09	0,31	1,69	1,98	0,95
7 m	2.79	0,92	0,85	1,2	1,19	2,08	1,85	1,34	2,1	0,36	1,21	1,19

Table 3.7: Gold fire assaying results of Fumani Tailings Dam 2 (ppm)

Depth	P1H1	P1H2	P1H3	P2H1	P2H2	P2H3	P3H1	P3H2	P3H3
1 m	1,45	2,25	1,06	1,281	1,27	4,44	1,19	1,44	1,99
2 m	1,82	0,38	1,5	1,983	1,84	1,34	2,03	1,21	1,87
3 m	1,64	1,29	1,47	1,74	0,99	0,48	1,9	0,89	0,45
4 m	1,2	1,1	2,02	2,09	1,27	1,16	0,84	0,92	2,1
5 m	0,84	1,31	1,94	1,98	1,69	1,27	0,62	1,98	1,44
6 m	1,33	0,99	1,85	1,35	1,55	0,36	1,44	1,11	1,31
7 m	1,42	0,84	1,35	1,81	1,63	0,58	2,08	1,28	1,2

Geotechnical Tests

Geotechnical tests allow for the classification of tailings in order to investigate their suitability for brick production. For this study, a total of 8 tailings samples were randomly selected, 4 from Fumani Tailings Dam 1 and 4 from Fumani Tailings Dam 2. The tailings samples for these analysis were only sorted and no other sample preparation was conducted.

Sieve Analysis of Tailings Material

Grain size distribution is an important factor in determining the characteristics and behaviour of soil in order to classify the soil. A total of 4 samples were randomly selected for sieve analysis for Tailings Dams 1. Two of the 4 samples were mixed to form one sample, the remaining two were also mixed together. The same was also done for Fumani Tailings Dams 2, resulting in a total of 4 samples labelled A, B, C and D analysed for sieve analysis.

Prior the analysis, seven sieves of different hole sizes, thus 4, 2, 1, 0.5, 0.25, 0.125, 0.75, as well as a pan were thoroughly cleaned using a brush. The cleaned sieves were then weighed individually and their masses were recorded in grams. The empty sieves were then stacked together in a descending order with the pan at the bottom. The sample was then placed at the top sieve and closed with a lid (Fig. 3.16). The stacked sieves and pan were then placed onto the mechanical sieve shaker and tightly secured with the screws. The shaker was used to mechanically shake the material for an hour at an amplitude of 60 rpm. When the sieving was complete, each sieve with the amount of material retained was weighed again to determine the amount of material passing through the sieve.

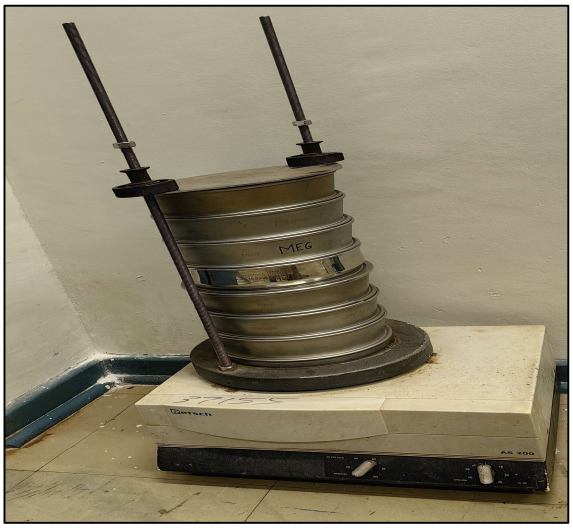

Figure 3.16: Sieve stacks on mechanical shaker.

The following calculations were used to determine the percentage of material passing through each sieve (Table 3.8):

- The mass of the material retained was obtained from subtracting the mass of empty sieve from the mass of sieve with the material. Once the mass retained was determined for each sieve, the total mass retained was recorded.
- To determine the cumulative passing, the mass of the material retained at the top sieve (sieve 4) was subtracted from the total mass retained (TMR). This was done for the top sieve only. For the remaining sieves, the total mass of material retained for that sieve was subtracted from the cumulative passing of the sieve above it. The pan should give a cumulative passing of zero since no material passes through the pan.
- To obtain the percentage passing for each sieve, simply divide the cumulative passing of that sieve by the total mass retained then multiply it by a hundred. This can be mathematically represented as:

PP=(CP/TMR)*100

Where; PP is the percentage passing, CP is the cumulative passing and TMR is the total mass retained. The sieve analysis results for sample A were recorded and represented in Table 3.8, whilst those for sample B are represented in appendix A4, and C and D in appendix B4.

Table 3.8: Sieve analysis results of sample A of Fumani Tailings Dam 1

Sample A					
sieve size (mm)	Mass of sieve (g)	Mass of sieve and material (g)	Mass of material (g)	cumulative passing (g)	percentage passing
4	388.5	389.58	1.02	505.45	100
2	326.98	328.2	1.21	505.26	100
1	295.88	298.5	2.92	503.55	99
0.5	290.32	295.56	5.33	501.14	99
0.25	246	267.75	22.01	484.46	96
0.125	236.35	369.93	123.42	383.05	76
0.075	263.86	386.03	138.46	368.01	73
Pan	527.02	743.69	232.1		
TMR			506.47		

Atterberg Tests

The liquid limit, plastic limit as well as shrinkage tests are collectively known as Atterberg tests. These tests were conducted to determine the moisture content of the material under different moisture conditions. This was essential to classify tailings material and determine if the tailings are suitable for brick production.

A total of two samples (A and B) from Fumani Tailings Dam 1, and two samples (C and D) from Fumani Tailings Dam 2 were randomly selected for the Atterberg tests. Only tailings that pass through the 0.075 mm sieve were used for these tests.

Liquid Limit (LL)

The LL is the minimum moisture content in soil, at which the soil begins to move from plastic state to liquid state, where it flows like a liquid. It is important to determine the LL as it classifies soils based on the minimum amount of water required to make it flow or slide.

The tools used for this test included cleaned mixing dish, water bottle, deionised water, spatula, Casagrande, grooving tool, weighing tray, balance scale and a drying oven. The Casagrande was calibrated before conducting the test. This was done by setting the Casagrande cup to be at a height of 10 mm each time before it dropped. The sample was placed in the mixing dish where a small amount of water was added to the sample and mixed to create a smooth, uniform paste. The mixture was then placed on the Casagrande and smoothened to a depth of 8 mm. A groove was then used to cut the paste into two equal halves (Fig. 3.17). The device was cranked at 2 revolutions per second until the halves of the paste join each other again. The number of blows required for the paste to come together were recorded.

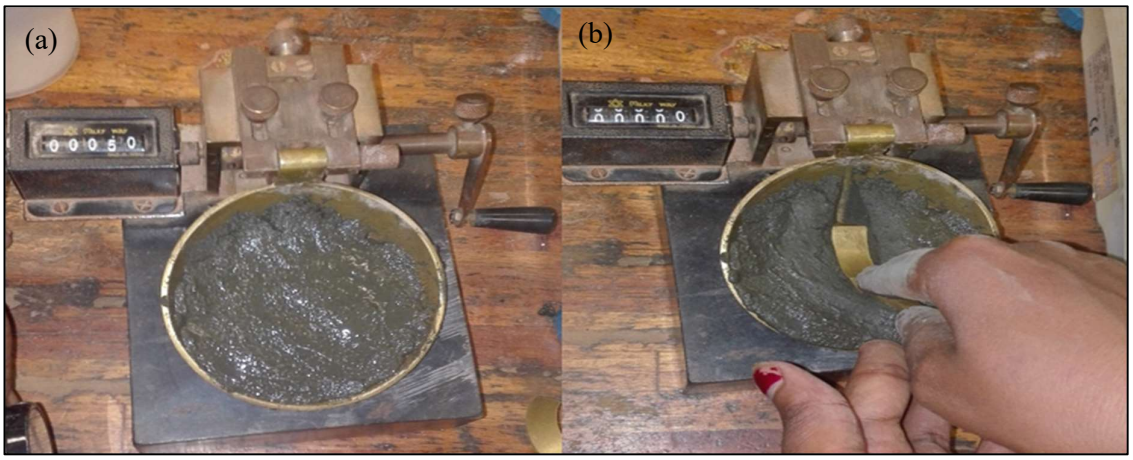

Figure 3. 17: Photograph of (a) paste on the Casagrande and (b) groove cutting paste in halve.

The sample was removed from the Casagrande, placed on a labelled weighing tray, weighed with the balance scale and dried in a Bench Vacute Laboratory Oven for 24 hours at 110℃. This was repeated three times for each sample, changing the amount of water and recording the different number of blows at each trial. After drying, the samples were allowed to cool to room temperature so they could be weighed again and recorded in Table 3.9. The weights of wet samples and that of the dry samples were used to calculate the moisture content using the following formula:

Moisture Content = $\left(\frac{W_W - W_D}{W_D}\right)$ x 100%

Where w_w is weight of wet sample and W_D is the weight of the dried sample.

The liquid limit was then calculated using the following formula:

LL= W (N/25) $^{0.121}$

Where; LL is the liquid limit, W is the moisture content and N is the number of blows.

Table 3.9: Liquid limit of Fumani Tailings Dams 1 and 2

	Sample ID	Trials	No of Blows	Weight before drying (g)	Weight after drying (g)	Moisture content (%)	Liquid Limit (%)	LL (%)
Fumani Tailings	A	Trial 1	15	128,12	100,48	27,51	25,89	26
		Trial 2	18	135,62	108,35	25,17	24,19	24
		Trial 3	24	121,81	98,16	24,09	23,97	24
		Average					**24,68**	**25**
	B	Trial 1	15	140,61	111,64	25,95	25,95	26
		Trial 2	25	132,59	105,51	25,67	25,8	26
		Trial 3	26	141,96	112,29	26,42	24,86	25
		Average					**25,54**	**26**
Fumani Tailings	C	Trial 1	19	130,98	105,2	24,51	23,7	24
		Trial 2	24	121,99	98,74	23,55	23,43	23
		Trial 3	28	139,85	114,82	21,8	22,11	22
		Average					**23,08**	**23**
	D	Trial 1	25	137,43	109,99	24,95	24,95	25
		Trial 2	26	137,47	111,51	23,28	23,4	23
		Trial 3	28	148,6	120,84	22,97	23,18	23
		Average					**23,84**	**24**

Plastic Limit (PL)

The water content at which clay can be rolled to a 3 mm diameter thread is known as the PL. This is the moisture content at which soil changes from its plastic state to solid state.

The tools used for this test included cleaned mixing dish, water bottle, deionized water, ground glass plate, weighing tray, balance scale, 3 mm diameter rod that is 100 m long and a drying oven. About 20 g of the sample was placed on the cleaned mixing dish where a small amount of water was added and mixed together to create a smooth, uniform paste.

About 8 g of the paste was rolled onto the ground glass plate using the palm of hand and fingers, maintaining constant pressure. If the sample crumbled when the diameter was greater than 3 mm, more water had to be added to it. If the sample could be rolled to less than 3 mm diameter without breaking, water had to be evaporated through rolling. A wet sample was rolled by hand on the ground glass to 3 mm diameter thread, the thread was molded into a ball by hand and the process was repeated until the thread started to crumble just above 3 mm diameter. This was the satisfactory result; provided, the sample was rolled to 3 mm diameter before. The thread was then weighed and the results recorded before placing it in oven for 24 hours at 110°C. The dried sample was cooled down before measuring it again.

The plastic limit was calculated using the formular: Plastic Limit= $(\frac{W_W - W_D}{W_D}) \times 100\%$

Where W_W is the weight of wet sample and W_D is the weight of dried sample.

Table 3.10: Plastic limit test results

	Trials	Weight before drying (g)	Weight after drying (g)	Weight of water (g)	PL (%)
A	Trial 1	10,13	8,43	1,7	20
	Trial 2	10,14	8,42	1,72	20
	Trial 3	10,11	8,42	1,69	20
	Average				**20**
B	Trial 1	10,09	8,38	1,71	20
	Trial 2	10,1	8,29	1,81	22
	Trial 3	10,12	8,48	1,64	19
	Average				**20**
C	Trial 1	10,13	8,59	1,54	18
	Trial 2	10,12	8,43	1,69	20
	Trial 3	10,13	8,53	1,6	19
	Average				**19**
D	Trial 1	10,11	8,39	1,72	21
	Trial 2	10,09	8,4	1,69	20
	Trial 3	10,13	8,49	1,64	19
	Average				**20**

Plasticity Index

The Plasticity Index (PI) is a measure of the plasticity of a soil. The plasticity index is the size of the range of water content where the soil exhibits plastic properties. The PI is determined by subtracting the plastic limit from the liquid limit. A high PI in soil indicates high clay content. Classification of the soil Plasticity Index is presented in Table 3.11. the calculations were used to create Table 3.12. indicating the Plastic limit within the Fumani Tailings Dams.

Table 3.11: Classification of the Plasticity Index (Burmister, 1949)

Plasticity Index	0	1-5	5-10	10-20	20-40	>40
Description	Non-plastic	Slightly Plastic	Low plasticity	Medium plasticity	High plasticity	Very high plasticity

Table 3.12: Liquid limit, plastic limit, and plasticity index of Fumani Tailings Dams

Tailings Dam	Sample ID	LL	PL	PI
1	A	25	20	5
	B	26	20	6
2	C	23	19	4
	D	24	20	4

3.3.3 Brick Tests

After the bricks were produced, it was crucial for them to undergo a series of tests to determine if the quality of the produced bricks is suitable for construction. The bricks were then sent to Soil lab in Pretoria where they underwent Dimension tolerance test, water absorption test, efflorescence test and compressive strength tests as these are the required tests per ISS 1077 (1992).

Dimension Tolerance Test

All the bricks were placed on a straight line in a way that the adjacent bricks are in contact with each other. The bricks were lined three different times to observe the three dimensions. The bricks were laid length side down, width side down and height side down for the length, width, and height tests as per Indian Standard 1077 of 1992. Further, to observe if there were any variances in the shape, size and colour of the bricks as compared to the control brick. All observations for both clay and cement bricks were recorded in Table 3.13 below.

Table 3.13: Dimension test results of bricks produced from different tailings to soil ratios.

	Brick ID	Tailings (%)	Dimensions		
			Length (mm)	Width (mm)	height (mm)
CLAY BRICKS	A	10	50.39	49.83	38.76
	B	20	50.44	50.36	38.53
	C	30	50.19	50.49	40.13
	D	40	50.31	50.04	39.82
	E	50	50.23	50.60	38.16
	F	60	50.39	49.83	38.76
	G	70	50.43	50.60	38.72
	H	80	50.32	51.01	39.41
	I	90	50.39	50.52	39.80
	J	100	50.49	50.13	38.77
	K	0	50.92	49.86	38.76
CEMENT BRICKS	A	50	241.77	100.22	79.29
	B	33.33	249.40	114.64	76.39
	C	20	240.24	103.36	84.65
	D	66.66	242.25	106.53	82.95
	Control	0	242.25	106.53	82.95

Water Absorption Test

This test was carried out at the Soillab according to the SABS 227. A balance scale was used to weigh all the bricks and their measurements were recorded as W1. After all the measurements, the bricks were then each individually submerged in a deionized water container for 24 hours. After 24 hours had passed, the bricks were then removed of excess water using paper towels in the lab. The bricks were then measured when still wet and the measurements were recorded as W2. The water absorption was then calculated from the recorded measurements using the following calculations:

Water absorption (%) = [(W2-W1)/W1] x 100.

From the 33 clay bricks produced, only 10 bricks from different tailings to soil ratios as well as one control brick underwent the water absorption tests of which all bricks with different tailings to clay ratios could not be tested as they dissolved in water. From the 20 cement bricks,

only 12 bricks of different cement to tailings ratio underwent this test. The results obtained from this test are represented in Table 3.4 below.

Table 3.14: Water absorption test results of bricks produced.

Brick ID	Brick ID	Tailings (%)	W1 (kg)	W2 (kg)	Water absorption (%)
CEMENT BRICKS	A	50	4.172	4.563	9.4
	B	33.33	3.969	4.390	10.6
	C	20	3.858	4.295	11.3
	D	66.66	3.787	4.359	15.1
	Control	0	3.787	4.359	15.1

Compressive Strength Test

To determine the crushing strength or compressive strength of the bricks, bricks were sent to the Soillab where they had to undergo the compressive strength test in accordance with SABS 227. In this test, the brick was prepared by submerging it in water for 24 hours, removed from water and allowed to drain water, the openings or cracks were filled with mortar of cement and sand. The bricks were then placed in water again for seven days, allowed to dry and then tested by having the brick placed on a compressor which applied pressure on the brick until the brick broke. When the brick started to crack, the pressure was then noted and recorded as the crushing strength of the brick, represented in Table 3.15 below. Since the clay bricks dissolved in water, only cement bricks were tested.

Table 3.15: Crushing strength of bricks produced using different tailings to soil ratios

Brick Type	Brick ID	Tailings (%)	Brick mass (kg)	Crushing strength (MPa)
CEMENT BRICKS	A	50	4.563	3.5
	B	33.33	4.390	6.5
	C	20	4.295	3.5
	D	66.66	4.359	3.6
	Control	0	4.259	6.5

Hardness Test

To know the hardness of the bricks, a fingernail was used to scratch the surface of the brick. The brick was considered poor and weak if an impression was left on it after scratching, However, if no impression was left behind from the scratch, the brick was considered hard and of good quality. The results obtained from the hardness test are represented in Table 3.16.

Table 3.16: Hardness test results of bricks produced using different tailings to soil ratios

	Brick ID	Tailings (%)	Observation	Hardness
CLAY BRICKS	A to J	10 to 100	easily scratchable, leaving noticeable marking on bricks. Dust could be blown off from sample after scratching	Not hard
	Control	0	brick was difficult to scratch with a nail.	Hard
CEMENT BRICKS	A	50	Bricks could not be scratched by nail	Hard
	B	33.33	Bricks could not be scratched by nail	Hard
	C	20	Bricks could not be scratched by nail	Hard
	D	66.66	Bricks could not be scratched by nail	Hard
	Control	0	Bricks could not be scratched by nail	Hard

Impact test

Bricks were dropped from a height of 1 m onto the ground. After the bricks were dropped, they were assessed, and the observations were recorded and represented on Table 3.17 below. If the brick did not break and remained intact during this process, then the brick was classified as having a high impact value and thus suitable for construction. If the brick broke, it meant they were not suitable for construction as they had a low impact value.

Table 3.17: Impact test results of bricks produced using different tailings to soil ratios

	Brick ID	Tailings Ratio (%)	Observation
Clay Bricks	A-J	10-100	All bricks broke
	Control	0	Brick did not break
CEMENT BRICKS	A	50	Brick did not break
	B	33.33	Brick did not break
	C	20	Brick did not break
	D	66.66	Brick did not break
	Control	0	Brick did not break

3.4 Quality Control and Quality Assurance

Whilst collecting the data, it was always important to ensure that the data was accurate, and that contamination and mistakes were avoided, if not minimised. This was achieved by observing quality assurance at every stage of the work. During the collection of soil and tailings samples, it was important to observe the following:

- GPS readings taken accurately at an accuracy of 5 m or less;
- Sampling points cleaned before collecting the samples;
- Clean sample bag used for collecting samples;
- Sample numbers entered correctly, and each sample tied to avoid any contamination;
- Recording data as it happens and not postponing it for a later time; and
- Keeping all samples under the same conditions.

The following were done to ensure accuracy while producing bricks:

- the area where bricks produced was cleaned;
- use the same measuring cups for all samples;
- ensure the brick mould was clean before using it for each sample; and
- produce all bricks in one day and subject them to the same conditions.

The following were done to ensure the accuracy of the results in the laboratory:

- conduct laboratory work in a neat environment;
- every instrument such as the beakers, volumetric flasks, and balance cleaned thoroughly before they are used;
- all instruments calibrated prior to use;
- deionised water used in preparing the standards;
- all samples kept under the same conditions;
- quarts used to clean the milling pots before any sample was milled;
- during sample analysis, reference material of known concentration used and checked to ensure the accuracy of machine, few samples known as “checks” analysed twice and results compared to check the accuracy of the equipment;
- 3 results were obtained from each analysis and their average was taken as the final;
- bricks of the same tailings to soil ratios were backed together; and
- bricks were each submerged in different water containers.

CHAPTER4: DATA ANALYSIS AND INTERPRETATION

The data obtained from the previous chapter of this study was analysed, presented, and interpreted.

4.1 Fumani Tailings Dams

4.1.1 Characterisation of Fumani Tailings Dams into Different Zones

The characterisation of the Fumani Tailings Dams into oxidation zone (OZ), transition zone (TZ) as well as un-oxidised zone (UZ) was based on the correlation of the physical characteristics of profile logs as well as pH of the tailings at different depths.

4.1.1.1 Profile Logs Correlation

The physical characteristics of the profile logs used to characterise the tailings were colour, texture, hardness as well as moisture content. The contact at the different zones were rather gradual as opposed to the sharp contacts indicated in the figures that follow (Fig. 4.1 – 4.6).

The oxidation zone occurred at the surface of the tailings dam and extended to a few meters below the dam. At the surface of the tailings dam, the material was generally dusty and had an orangish colour indicating oxidation. Where the tailings were not dusty, it was hard and crust like, with blueish (Azurite) and greenish minerals (Malachite) indicating oxidation of sulphides in the tailings dam. The oxidation zone contained ochre colours (yellowish-brown to reddish). This zone was the hardest zone to penetrate using the hand auger, it contained alternating layers of hard and soft material that had a gritty feel.

The transitional zone occurred between the oxidation zone and the un-oxidised zone. The transitional zone was not always visible in all the profiles. The transitional zone of tailings was identified as a thin layer consisting of a mixture of soft grey with green hard material in Fumani Tailings Dam 1, whilst it contained a mixture of soft grey with either green, red or orange-brown hard material in Fumani Tailings Dam 2. In most of the profiles, the transitional zone was not clearly visible.

The un-oxidised zone was soft and contained moist, shiny grey material. It was the easiest zone to penetrate in both tailings dams with the hand auger as it offered no resistance. This was because the material had not hardened as no oxidation had taken place within the zone.

Fumani Tailings Dam 1

Profile 1 (Western Section)

The OZ within the western section of Fumani Tailings Dam 1 extended from the surface of the dam to a depth of 1.35 m, 1.04 m, 1.82 m and 1.82 m as recorded at boreholes H1, H2, H3 and H4 respectively. The deepest part of the oxidation was observed at P1H3 and P1H4, where it reached a depth of 1.82 m below the surface in both boreholes. The shallowest OZ was observed at P1H2 were it only extended from the surface to a depth of 1.04 m (Fig. 4.1).

The Transitional zone was visible at P1H3 at a depth of 1.82-2.08 m, making it 0.13 m thick. It was characterised by a mixture of soft grey and hard green material. The transitional zone was not clearly visible in the other boreholes.

The unoxidized zone in profile 1 was visible from 1.35 m, 1.04 m, 2.08 m, and 1.82 m in P1H1, P1H2, P1H3 and P1H4 respectively and continued below 7 m.

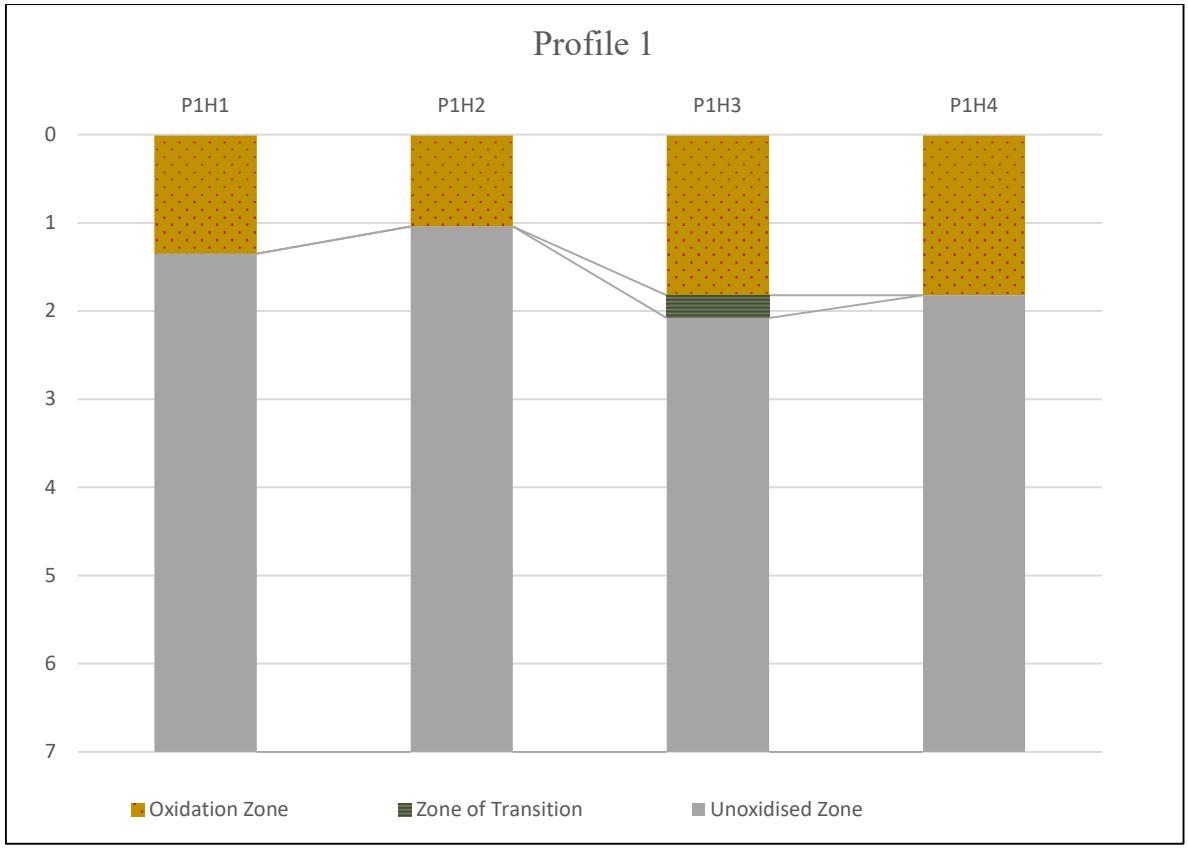

Figure 4.1: Borehole correlation in the western section of Fumani Tailings Dam 1.

Profile 2 (Middle Section)

The OZ within the middle section of Fumani Tailings Dam 1 extended from the surface of the dam to a depth of 1.08 m, 2.4 m, 1.88 m and 1.12 m as recorded at boreholes H1, H2, H3 and H4 respectively. The deepest part of the oxidation was observed at P2H2, where it reached a depth of 2.4 m below the surface. The shallowest OZ was observed at P2H1 where it only extended from the surface to a depth of 1.08 m (Fig. 4.2).

The Transitional zone was visible at P2H3 and P2H4 at a depth of 1.88-2 m and 1.12-1.28 m, making it 0.12 and 0.16 m thick respectively. The transitional zone was not clearly visible in the other boreholes. The unoxidized zone in profile 1 was visible from 1.08 m, 2.4 m, 2 m, and 1.28 m in P2H1, P2H2, P2H3 and P2H4 respectively. The unoxidized zone started from the end of the zone of transition and it extended to a depth below 7 m.

Figure 4.2: Borehole correlation in the middle section of Fumani Tailings Dam 1.

Profile 3 (Eastern Section)

Oz within the eastern section of Fumani Tailings Dam 1 (profile 3) extended from the surface of the tailings dam to depths of 0.64 m, 1.17 m, 2.39 m and 1.22 m as observed from boreholes H1, H2, H3 and H4 respectively (Fig. 4.3). The deepest OZ was observed at P3H2 at a depth of 2.39 m, whilst the shallowest OZ was observed at P3H1 at a depth of 0.64 m.

The transitional zone was observed at P3H1, P3H2 and P3H4 where it extended from 0.64-0.98 m, 1.17-1.24 m and 1.22-1.44m respectively. The unoxidized zone continued from 0.98 m, 1.24 m, 2.39 m and 1.44 m at P3H1, P3H2, P3H3 and P3H4 respectively. The UZ continued from the end of the TZ to below 7 m.

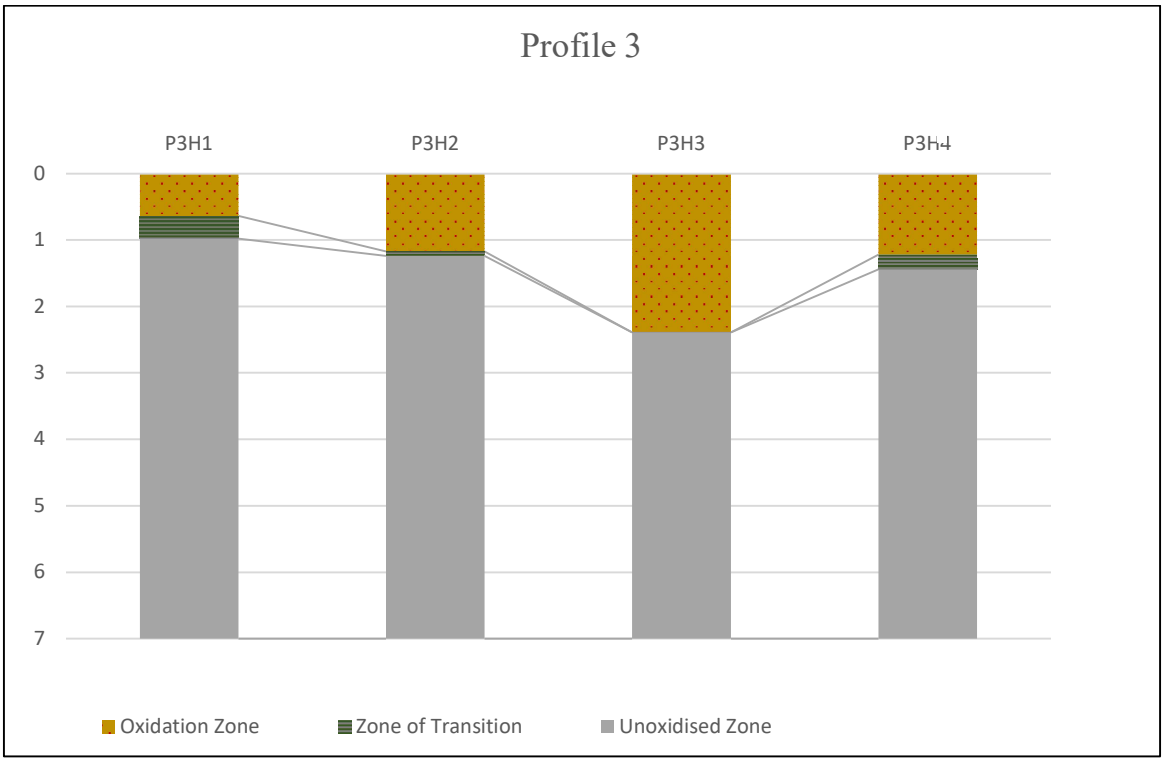

Figure 4.3: Borehole correlation in the eastern section of Fumani Tailings Dam 1.

The OZ was observed from the surface of the Fumani Tailings Dam 1 to a depth of 2.4 m at P2H2. The average thickness of the OZ was 1.25 m below the surface of the tailings dam. Out of the 12 boreholes sampled, only half of them had a clear zone of transition. The thickness of the TZ ranged from 0 m to a thickness of 0.34 m at P3H1. The average TZ thickness in the Fumani Tailings Dam 1 was 0.09 m thick. Making it a very thin layer compared to the Oxidised and unoxidized zones. The Unoxidized zone was the thickest zone where it continued to the base of the tailings dam.

Fumani Tailings Dam 2

Profile 1

The OZ within the Northern section of Fumani Tailings Dam 2 extended from the surface of the dam to a depth of 0.5 m, 0.6 m, and 0.66 m as recorded at boreholes H1, H2, and H3 of profile 1 respectively. The deepest part of the oxidation was observed at P1H3, where it reached a depth of 0.66 m below the surface of the tailings dam. The shallowest OZ was observed at P1H1 were it only extended from the surface to a depth of 0.5 m (Fig. 4.4).

The Transitional zone was visible at P1H2 at a depth of 0.6-0.75 m, making it 0.15 m thick. It was characterised by a mixture of soft grey with green hard material. The transitional zone was also observed at P1H3 at depth of 0.66-1.15 m, this TZ was characterised by dark grey with hard red material. Transitional zone was not clearly visible in borehole P1H1. The unoxidized zone in profile 1 was visible from 0.5 m, 0.75 m, and 1.15 m in P1H1, P1H2, and P1H3 respectively and continued below 7 m.

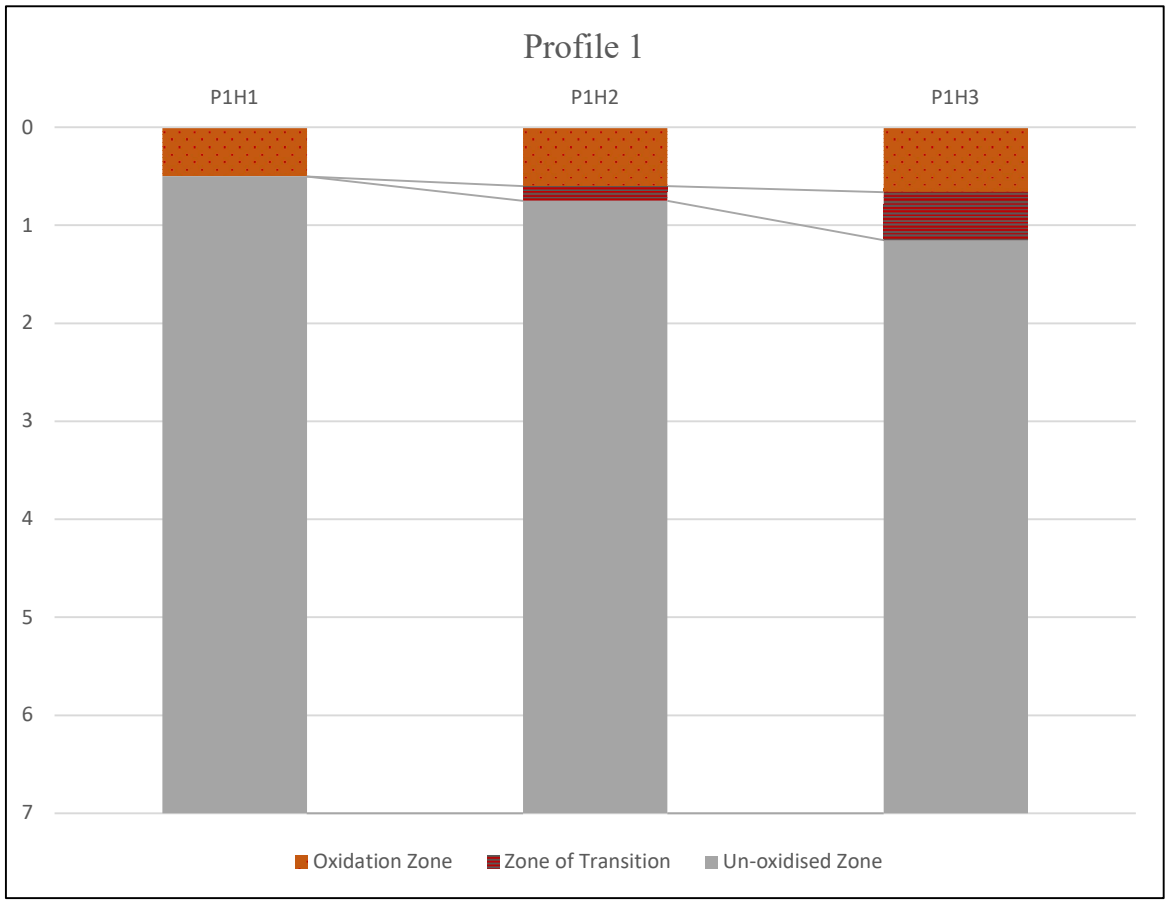

Figure 4.4: Borehole correlation in the northern section of Fumani Tailings Dam 2.

Profile 2

The OZ within the middle section of Fumani Tailings Dam 2 extended from the surface of the dam to a depth of 0.83 m, 0.7 m, and 1.12 m as recorded at boreholes H1, H2, and H3 respectively. The deepest part of the oxidation was observed at P2H3, where it reached a depth of 1.12 m below the surface of the tailings dam. The shallowest OZ was observed at P2H2 were it only extended from the surface to a depth of 0.17 m (Fig. 4.5).

The Transitional zone was visible at a depth of 0.83-1 m, 0,7-1.05 m and 1.12-1.67 m making it 0,17 m, 0.35 m and 0.55 m thick at HI, H2 and H3 respectively. It was characterised by a mixture of soft grey with brown and greenish hard material. The unoxidized zone in profile 2 was visible from 1 m, 1.05 m, and 1.67 m in P2H1, P2H2, and P2H3 respectively and continued below 7 m.

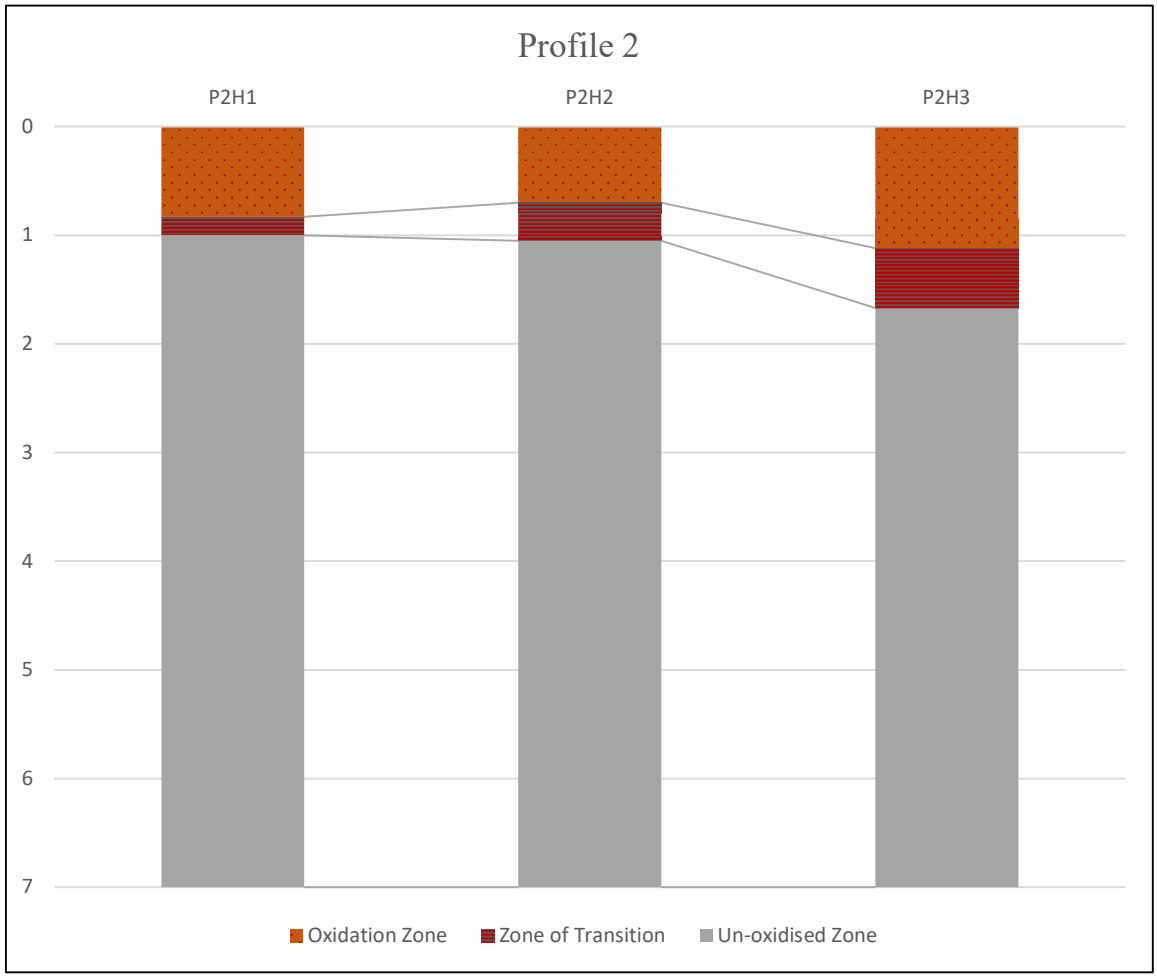

Figure 4.5: Borehole correlation in the middle section of Fumani Tailings Dam 2.

Profile 3

The OZ within the Southern section of Fumani Tailings Dam 2 extended from the surface of the dam to a depth of 0.7 m, 1.61 m, and 2.8 m as recorded at boreholes H1, H2, and H3 of profile 3 respectively. The deepest part of the oxidation was observed at P3H3, where it reached a depth of 2.8 m below the surface of the tailings dam. The shallowest OZ was observed at P1H1 were it only extended from the surface to a depth of 0.7 m (Fig. 4.6).

The Transitional zone was visible at P3H1 at a depth of 0.7-0.91 m, making it 0.21 m thick. It was characterised by a mixture of soft grey with red orange-brown hard material. The transitional zone was not clearly visible in the other boreholes. The unoxidized zone in profile 3 was visible from 0.91 m, 1.61 m, and 2.8 m in P3H1, P3H2, and P3H3 respectively and continued below 7 m.

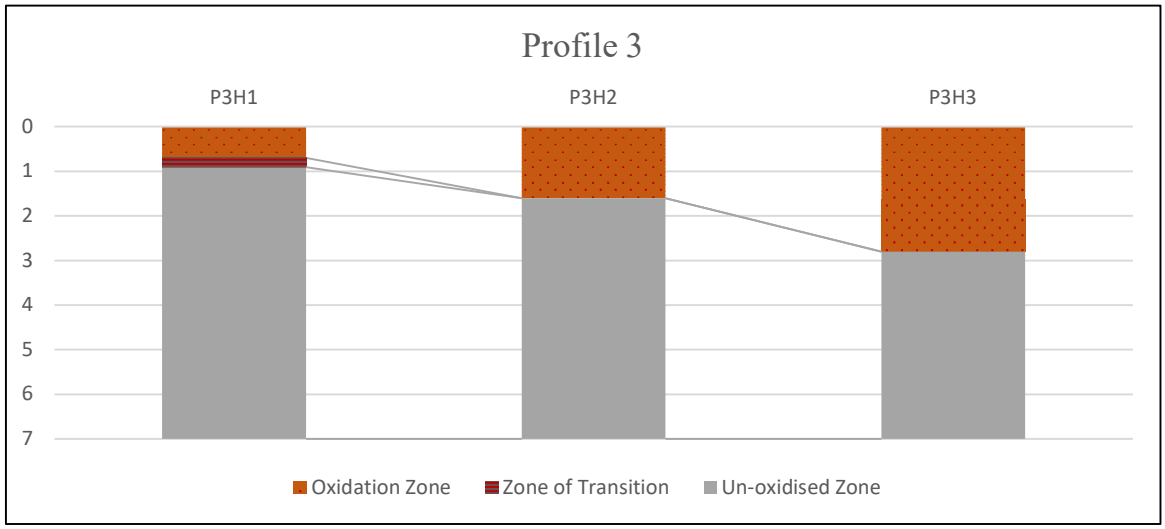

Figure 4.6: Borehole correlation in the southern section of Fumani Tailings Dam 2.

The oxidation zone at the Fumani Tailings Dam 2 appeared to be increasing from profile 1 to profile 3 in all the boreholes with exception to borehole P2H1 and P3H2. The thickest oxidation zone observed within the Fumani Tailings Dam 2 was 2.8 m thick, observed at P3H3. The average thickness of the OZ was 1.06 m below the surface of the tailings dam.

The Zone of transition increased from H1 to H3 in profile 1 and 2. Profile 3 only had a visible TZ in P3H1. The average TZ thickness in the Fumani Tailings Dam 2 was 0.21 m thick. Making it a very thin layer compared to the Oxidised and unoxidized zones. The Unoxidized zone was the thickest zone; it continued to the base of the tailings dam.

4.1.1.2 pH Correlation

Fumani Tailings Dam 1

Profile 1

The pH in the western section (profile 1) of Fumani Tailings Dam 1 increased with depth, ranging from acidic to slightly alkaline (Fig. 4.7). The lowest pH recorded was 3.188 at P1H3S1 and the highest recorded pH was 8.025 at P1H4S7. The pH was acidic from the surface of the dam to a depth of 1 m in all the profiles. The values of pH were slightly acid between 1-3 m. The tailings were neutral between 3-4 m with exception to P1H3 which was still slightly acidic at this depth. This could be since the zone of oxidation was deeper in this borehole as indicated by the profile logs. The tailings was slightly alkaline from 5-7 m, where the change seemed to be constant.

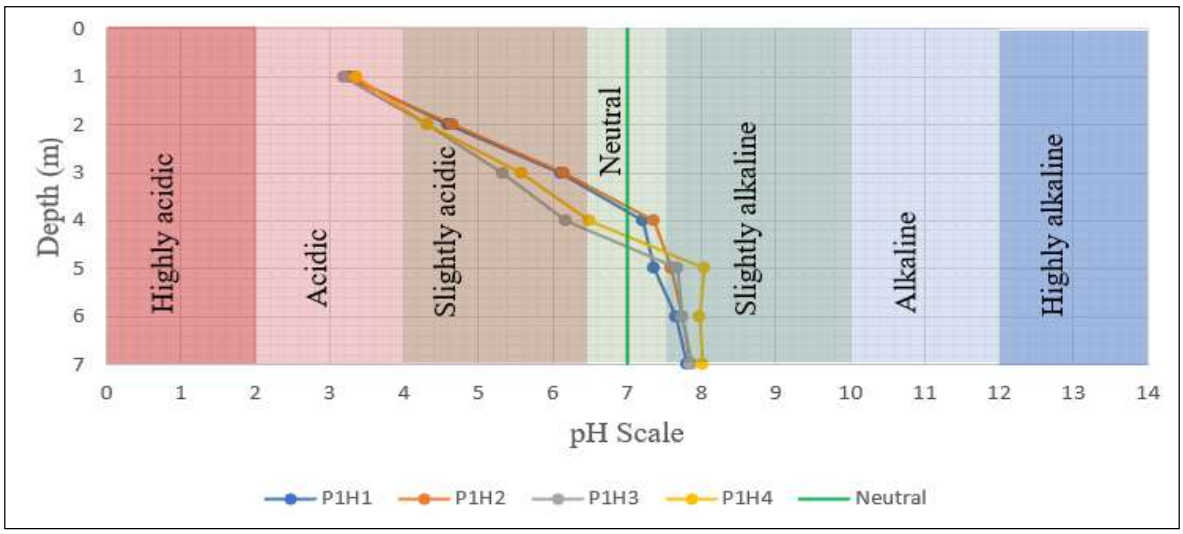

Figure 4.7: Correlation of pH in the western section of Fumani Tailings Dam 1.

Profile 2

The pH in the middle section (profile 2) of Fumani Tailings Dam 1 increased with depth, ranging from acidic to slightly alkaline (Fig. 4.8). The lowest pH recorded was 3.215 at P1H1S1 and the highest recorded pH was 8.215 at P1H1S7. The pH was acidic from the surface of the dam to a depth of 1 m. The values of pH were slightly acid between 1-3 m except P2H1 that was neutral at this depth. The tailings were neutral between 3-4 m with exception to P2H2 which was still slightly acidic, this could have been since OZ at this borehole extended deeper compared to others. The tailings were slightly alkaline from 5-7 m, where the change seemed to be almost constant.

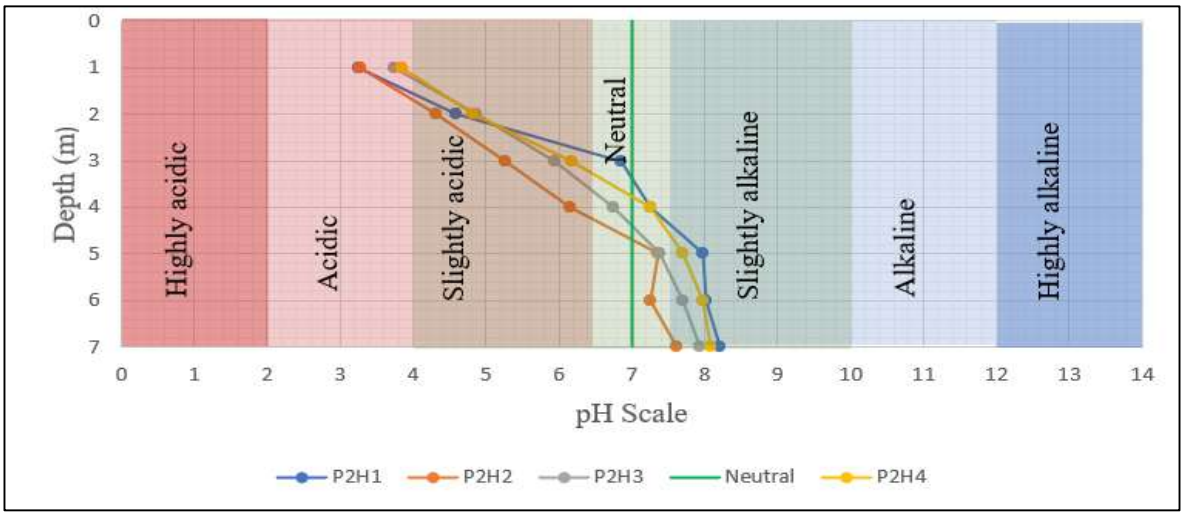

Figure 4.8: Correlation of pH in the middle section of Fumani Tailings Dam 1.

Profile 3

The pH in the eastern section (profile 3) of Fumani Tailings Dam 1 increased with depth, ranging from acidic to slightly alkaline (Fig. 4.9). The lowest pH recorded was 3.215 at P3H3S1 and the highest recorded pH was 8.654 at P3H1S7. The pH was acidic from the surface of the dam to a depth of 1 m in all profiles, with exception to P3H3 which was still acidic at 2 m. The values of pH were slightly acid between 1-3 m. The tailings were neutral between 3-4 m, with P3H3 still slightly acidic at this depth and P3H1 already slightly alkaline at this depth. This could be due to the OZ being shallow at P3H1 and deepest at P3H3 as indicated by the profile logs.

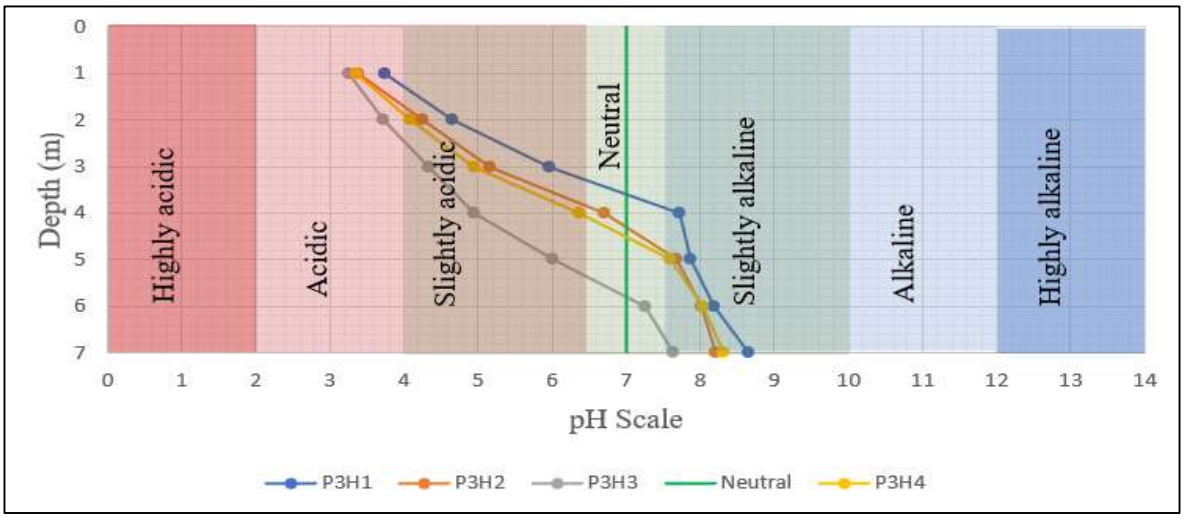

Figure 4.9: Correlation of pH in the eastern section of Fumani Tailings Dam 1.

The pH on the tailings dam increased with depth on all profiles. The surface of the tailings dam was acidic to about 3-4 m on all profiles of the dam. The deepest oxidation was observed at H2 and H3 of all profiles. These boreholes were located at the centre of the Fumani Tailings Dams 1. The average pH of the Fumani Tailings Dam 1 from the surface to 7m depth was 6.412. This means that the tailings dam was slightly acidic at this depth.

Fumani Tailings Dam 2

Profile 1

The pH in the northern section (profile 1) of the Fumani Tailings Dam 2 increases with depth, with the lowest pH of 3,562 recorded at PIH2S1, and highest pH of 8.395 recorded at P1H2S7 and P1H3S7. The pH was acidic in the first meter from the surface, slightly acidic on the 2nd, 3rd and 4th meter, it then becomes neutral on the 5th m. The pH on 6th and 7th m becomes slightly alkaline and consistent. The pH in profile one seems to be increasing from H1 to H3 with depth (Fig. 4.10).

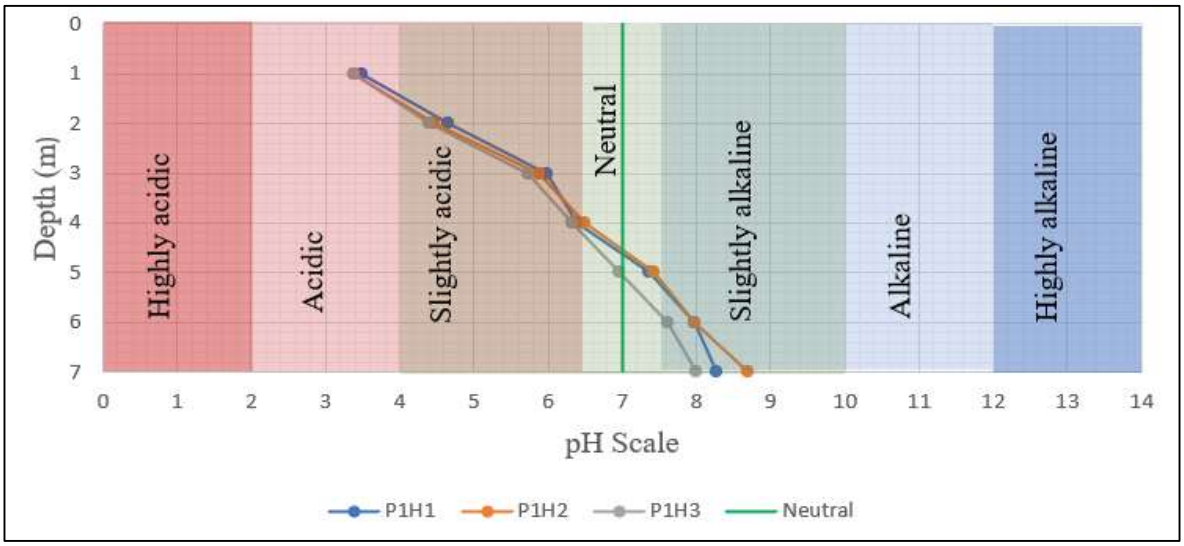

Figure 4.10: Correlation of pH in the northern section of Fumani Tailings Dam 2.

Profile 2

The pH in the middle section (profile 2) of the Fumani Tailings Dam 2 increased with depth, with lowest pH of 3,562 recorded at P2H1S7 and the highest pH of 8,621 recorded at P2H3S7 (Fig. 4.11). The pH at P2H1 and P2H3 was acidic in the first meter from the surface, slightly acidic at 1-3 m, neutral at 3-5 m and slightly alkaline at 5-7 m. The pH at P2H3 was acidic at 0-1 m, slightly acidic at 2-5 m, neutral at 5-6 m and slightly alkaline at 5-6 m. The pH was lower at H3 than H1.

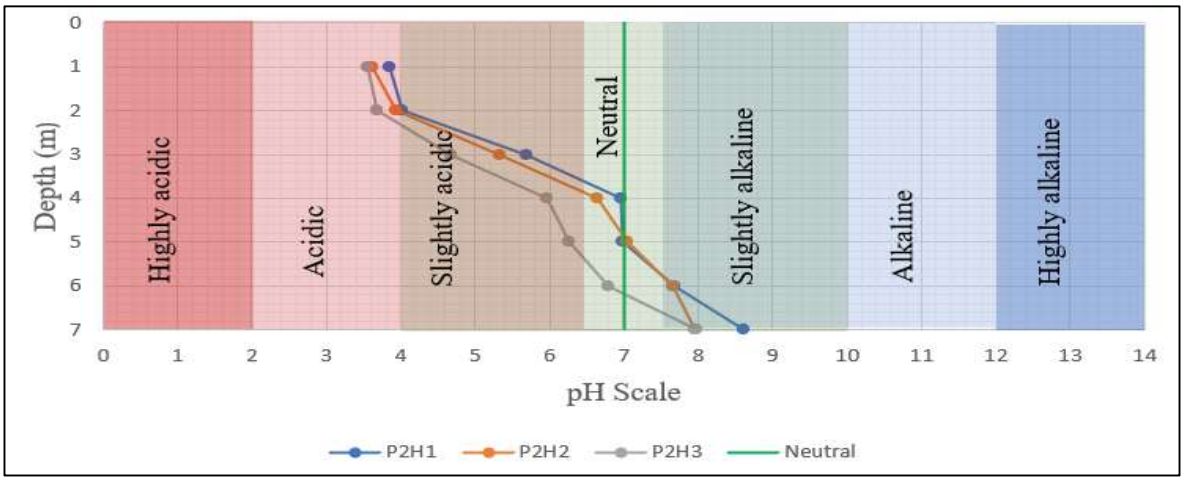

Figure 4.11: Correlation of pH in the middle section of Fumani Tailings Dam 2.

Profile 3

The pH in the southern section (profile 3) of the Fumani Tailings Dam 2 increased with depth, with lowest pH of 3.215 at P3H3S1 and the highest pH of 8,365 at P3H1S7 (Fig. 4.12). The pH was acidic at 0-1 m at P3H1, and 0-2 m at P3H2 and P3H3. The tailings were slightly acidic at 1-3 m, 2-3 m, and 2-4 m at P3H1, P3H2 and P3H3 respectively. The pH was neutral at 3-5 m (P3H1 and P3H2) and 4-5m (P3H3). The tailings were slightly alkaline and constant at 5-7 m.

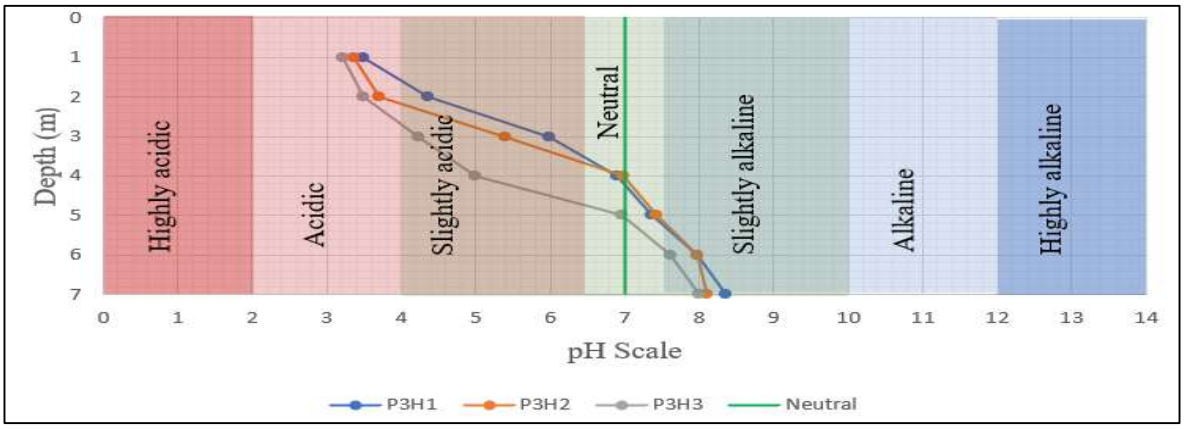

Figure 4.12: Correlation of pH in the southern section of Fumani Tailings Dam 2.

The pH graphs at all profiles in the Fumani Tailings Dam 2 indicate a low pH at the first meter that increased with depth. The pH seemed to be decreasing from H1 to H3 in all profiles. The tailings dams appeared to be acidic from the surface to a depth of about 3-4 m. The average pH of the Fumani Tailings Dam 2 was 6.10. This means that the tailings dam is slightly acidic.

Where the profile logs showed a deeper oxidised Zone, the pH graph showed lower pH values. This indicated that both profile logs and pH graphs interpreted similar findings. The profile logs indicated that the OZ was at 0-3 m within the tailings dams, whilst the pH indicates that the OZ is at 0-4 m; this could be due to 3-4 m not yet visible through profile logs as oxidation is in process.

4.1.2 Distribution of Metals within the Tailings Dams

4.1.2.1 Statistical Analysis and Calculations of Metals

The data presented in Table 4.1 and 4.2 is a summary of the metal data of tailings samples collected from the Fumani Tailings Dam 1 and 2 respectively, obtained from XRF analysis. The following parameters were calculated:

Range

This is the difference between the maximum and the minimum value of an element and is mathematically represented as:

Range (r) = maximum value – minimum value …….…… Equation 4.1

Mean

Also known as the average is obtained through summing all the sample values divided by the total number of samples. This is mathematically represented as:

$$\text{Mean } (\bar{x}) = \frac{\sum (x1 + x2 + x3 \ldots + xn)}{n} \quad \text{Equation 4.2}$$

Where; $\sum$ = sum of all values, x = sample values and n = number of samples

Variance

variance determines how much the values in the data set are likely to differ from the mean of the values. It is the average of the squares of the deviations from the mean. This can be represented mathematically as:

$$\text{variance (v)} = \frac{\sum(x-\bar{x})2}{n-1} \quad \text{Equation 4.3}$$

Where; $\sum$ = sum of all values, x = sample values, n = number of samples and $\bar{x}$ = mean

Standard Deviation

The Standard deviation is a measure of how spread out numbers are. It is the square root of the Variance and can therefore be represented as:

$$\text{Standard deviation } (\sigma) = \sqrt[2]{v} \quad \text{Equation 4.4}$$

Were; v is the variance

Threshold

The threshold concentration is the concentration at which all concentrations greater than it are considered anomalous whilst those below it are considered to be background values. In this study, the threshold concentration was defined as the mean value multiplied by the product of 1.5 standard deviation, which can be represented mathematically as:

Threshold (Th) = $\bar{x}$ + (1.5 σ) …….. Equation 4.5

Where; $\bar{x}$ = mean and σ = standard deviation.

Table 4.1: Statistical summary of metals concentrations within the tailings dams (ppm)

		Pb	Zn	Cu	As	Co	Cd	Cr	Ni
Total samples	T1	84	84	84	84	84	84	84	84
	T2	63	63	63	63	63	63	63	63
Max	T1	49,80	180,70	82,30	9732,60	43,70	1,10	107,00	147,90
	T2	64.31	182.5	85	8789.51	27.42	1	115.32	148.2
Min	T1	8,30	19,50	11,80	1819,00	11,00	0,00	16,30	43,80
	T2	20	43.46	42.98	2850.89	7.5	0.2	23.9	8.17
Range	T1	41,50	161,20	70,50	7913,60	32,70	1,10	90,70	104,10
	T2	44.31	139.04	42.02	5938.62	19.92	0.8	91.42	140.03
Mean	T1	20,22	101,95	60,49	6383,08	24,75	0,67	71,71	99,35
	T2	36.39	96.85	64.48	4989.1	20.77	0.81	72.15	93.25
Variance	T1	66,66	654,33	170,88	4814865,59	35,58	0,06	321,87	574,49
	T2	119.46	696.17	56.65	1199588	19.61	0.03	769.2	669.42
Standard deviation	T1	8,16	25,58	13,07	2194,28	5,96	0,25	17,94	23,97
	T2	10.93	26.38	7.53	1095.26	4.43	0.17	27.73	25.87
Threshold	T1	32,47	140,32	80,10	9674,50	33,69	1,04	98,62	135,30
	T2	52,78	136,4	75,77	6631,98	27,42	1.06	113,74	132,06

T1 and T2 denotes Fumani Tailings Dams 1 and 2 respectively. From the statistical summary, it can be said that the data set within the tailings dams could either be spread out or have a few areas that are highly anomalous as the range and variance is quite high for all the metals with exception of Cd. This indicates that some areas have very low values whilst other areas have very high values of the Metals. Cadmium values seem to be relatively constant within the Fumani Tailings Dams.

4.1.2.2 Correlation Matrix of Metals within Fumani Tailings Dams

Correlation was used in this study in order to determine how one element depends on the other element, thus, to distinguish if any relationship exists between the elements. Correlation is defined as the statistical measure of the relationship formed between two entities. The Pearson correlation coefficient is used to measure the strength of a linear relationship between two entities. It ranges between – 1 and +1, where -1 is considered a perfect negative correlation, this means that the two elements are inversely proportional and thus move in opposite directions, when one increases the other decreases. A positive one (+1) indicates a perfect positive correlation, where both elements are directly proportional to each other and hence move in the same direction. Zero represents no correlation between the elements, hence no relationship exists between the two. The correlation coefficient was calculated using the following mathematical equation:

$$r = \frac{v(xy)}{\sigma x\, \sigma y} \quad \text{.....Equation 4.6}$$

Where: r is the correlation coefficient, v is the variance, and σ is the standard deviation.

The correlation relationship rule of thumb states that if the correlation coefficient is greater than $2/\sqrt{n}$, then the relationship exists between the two elements. Where n is the number of samples. Since Fumani Tailings Dam 1 had 84 samples, $2/\sqrt{84} = 0.218$. For every r greater than 0.218 and less than -0.218, there is a relationship that exists. Out of the 28 correlation coefficients generated, only 14 relationships exist (Table 4.2). A fair to negative correlation of -0.289 between (Cd-Pb). A fair to strong correlation exists between the following pairs respectively: 0.231(Zn-Cu), 0.247 (Zn-Ni), 0.252 (As-Zn), 0.268 (Co-Pb), 0,269 (Cr-Cu), 0.279 (Co-Cu), 0.320 (As-Cu), 0.370 (As-Pb), 0.371 (Cu-Pb), 0.439 (Cr-Pb), 0.477 (Zn-Pb), 0.548 (Cr-As) and 0.604 (Co-Ni). No relationship existed between the remaining pairs.

Table 4.2: Correlation matrix of metals within Fumani Tailings Dam 1 (ppm)

ppm	Pb	Zn	Cu	As	Co	Cd	Cr	Ni
Pb	1							
Zn	0,477	1						
Cu	0,371	0,231	1					
As	0,37	0,252	0,32	1				
Co	0,268	0,181	0,279	0,005	1			
Cd	-0,289	-0,153	0,105	-0,211	0,009	1		
Cr	0,439	0,144	0,269	0,548	0,06	-0,011	1	
Ni	0,036	0,247	0,131	0,038	0,604	0,081	0,065	1

The strongest relationship occurred between Co and Ni, at a correlation coefficient of 0.604, followed by correlation coefficient of 0.548 between Cr and As. The lowest correlation coefficient of 0.005 was found between Co and As. This means that no relationship seems to exist between As and Co within the Fumani Tailings Dam 2.

Since Fumani Tailings Dam 2 had a total of 63 samples, $2/\sqrt{63} = 0.251$, hence, for every r greater than 0.251 and less than -0.251, there is a relationship that exists. Of the 28 correlation coefficients generated, only 14 relationships exist (Table 4.3). A negative relationship exists between the following elements: -0.275 (Cd-Zn), -0.352 (Cd-As) and -0.397 (As-Pb). A strong to fair correlation exists between the following pairs respectively: 0.621 (Cr-Zn), 0.502 (Cd-Pb), 0.492 (Cu-Zn), 0.465 (Co-Cu), 0.419 (Co-Zn), 0.379 (Zn-Ni), 0.350 (Co-Ni), 0.344 (Cu-Ni and Cu-Cr), 0.341 (Pb-Cr), and 0.253 (Zn-As). No relationship was found to exist between the remaining 20 pairs of elements.

Table 4.3: Correlation matrix of metals within Fumani Tailings Dam 2 (ppm)

ppm	Pb	Zn	Cu	As	Co	Cd	Cr	Ni
Pb	1							
Zn	-0,014	1						
Cu	-0,057	0,492	1					
As	-0,397	0,253	0,23	1				
Co	-0,158	0,419	0,465	0,103	1			
Cd	0,502	-0,275	-0,198	-0,352	-0,094	1		
Cr	0,341	0,621	0,344	0,136	0,198	0,048	1	
Ni	0,195	0,379	0,344	0,063	0,35	0,005	0,242	1

The strongest relationship occurred between Cr and Zn, at a correlation coefficient of 0.621, this was followed by a correlation coefficient of 0.502 between Cd and Pb. The lowest correlation coefficient of 0.005 was found between Ni and Cd. This means that no relationship seems to exist between Ni and Cd within the Fumani Tailings Dam 2.

The relationship between the elements seems to change from one tailings dam to another. This may be due to different factors such as the time the tailings were created and other processes that might have taken place on the tailings dams.

4.1.2.3 Vertical and Lateral Distribution of Metals

The vertical and lateral distribution of metals within the Fumani Tailings Dams 1 and 2 are represented using borehole logs for vertical distribution and prediction maps for lateral distribution. The prediction maps were modelled using ordinary kriging method.

Lead

Vertical Distribution of Pb

The lead distribution within Fumani Tailing Dam 1 was characterised by a positively skewed distribution as depicted by the probability density function (Fig. 4.13a). This distribution suggested that lead concentration within the tailings dam was relatively low with a few anomalous values. The lead values ranged from 8.3 ppm to 49.8 ppm, with most of the observed values occurring between 8.3 and 20.3 ppm.

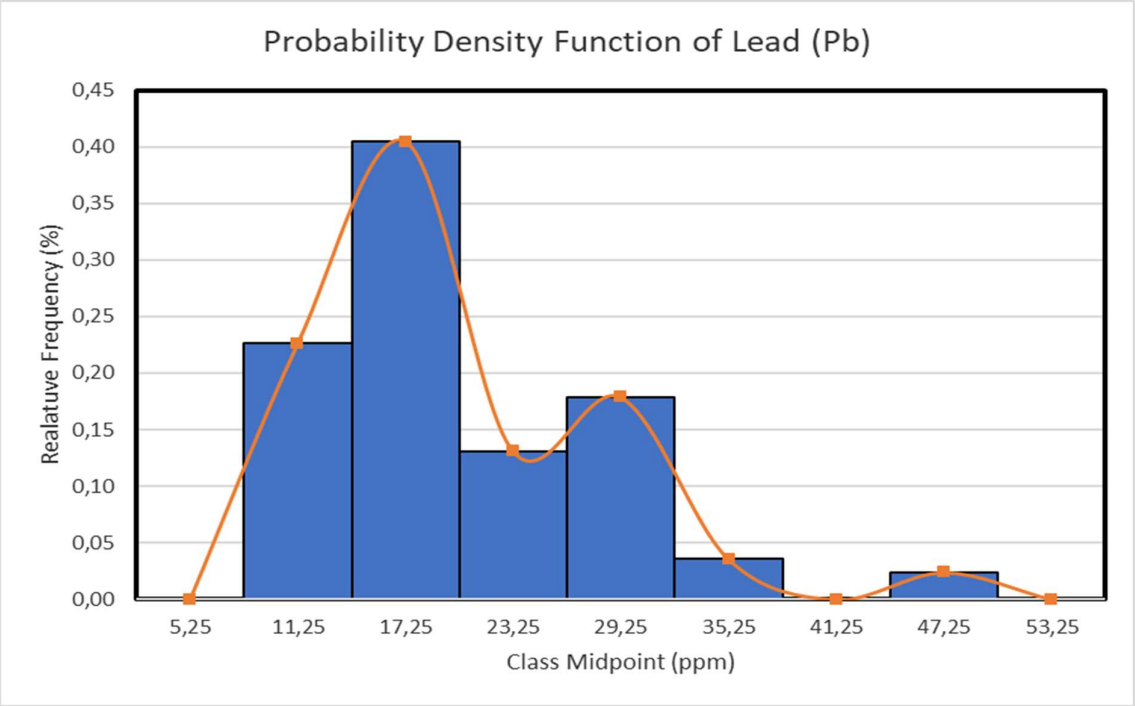

Figure 4.13a: Probability density function of lead within Fumani Tailings Dam 1.

The recorded threshold value of lead was 32.47 with all values above it considered as anomalous. There were 5 Pb anomalous values recorded, that were located at sampling points P3H1S2(33 ppm), P3H3S4 (33.3 ppm), P1H3S6 (37.3 ppm), P1H2S7 (48.8 ppm) and P1H2S4 (49.8 ppm).

An assessment of the borehole logs indicated an overall erratic trend with depth of Pb values within the Fumani Tailings Dam 1. The lowest Pb values were observed in all boreholes of profile 2 located in the centre of the tailings dam (Fig. 4.13b). High Pb values were located in boreholes of the first and last profiles with exception to P1H4. The highest values were located below 3 m at all boreholes of P1 excluding P1H4.

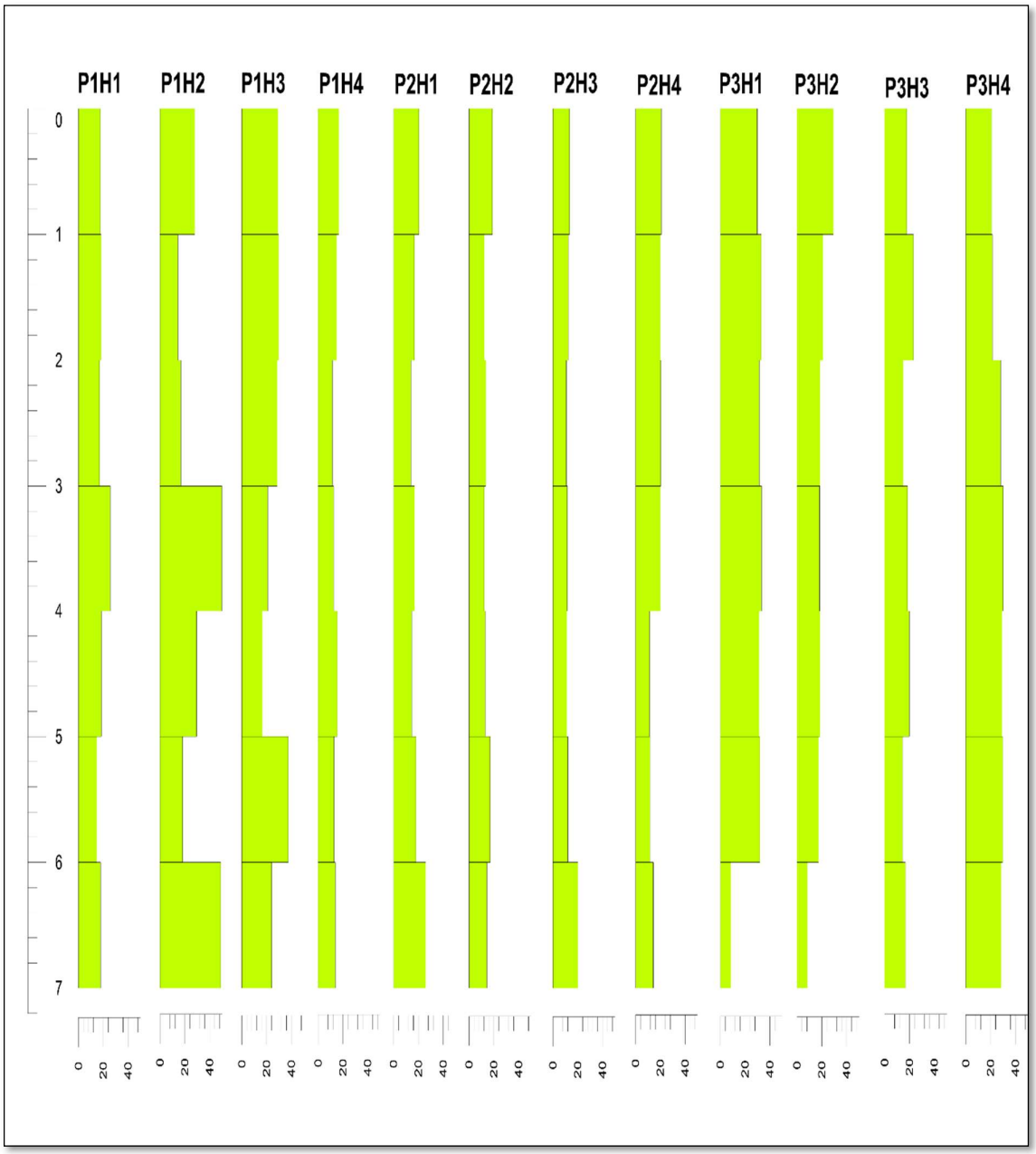

Figure 4.13b: Vertical distribution of Pb within Fumani Tailings Dam 1.

Lateral Distribution of Pb

The prediction map of Pb indicated that the distribution of Pb was low at the centre of Fumani Tailings Dam1 (Fig. 4.13c). The map revealed that the highest Pb values were located along profile 1, with exception to P1H4. These observations align with those already revealed by the borehole logs.

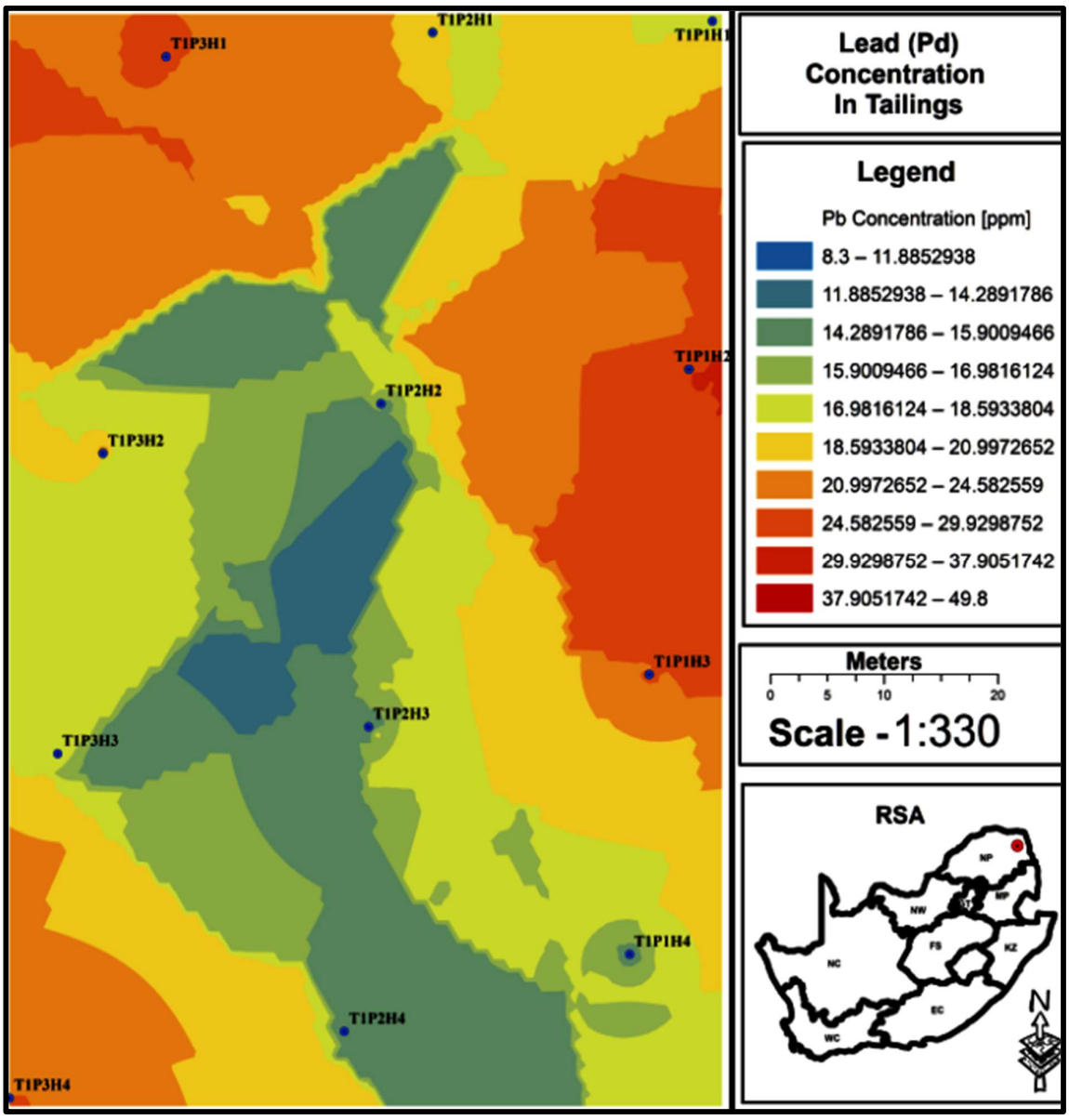

Figure 4.13c: Prediction map of Pb within Fumani Tailings Dam 1.

Zinc

Vertical Distribution of Zn

The zinc distribution within Fumani Tailings Dam 1 was characterised by a normal distribution with a mean of 101.95 ppm (Fig. 4.14a). The distribution was fairly symmetrical which meant that the proportion of high and low values were equal. The zinc values ranged from 19.5 ppm and 180.7 ppm, with most observed values occurring within one standard deviation of the mean, occurring between 63,5 and129,5 ppm. The values of Zn had a threshold concentration of 140.32 ppm, which presented 6 anomalous values out of the 84 values recorded.

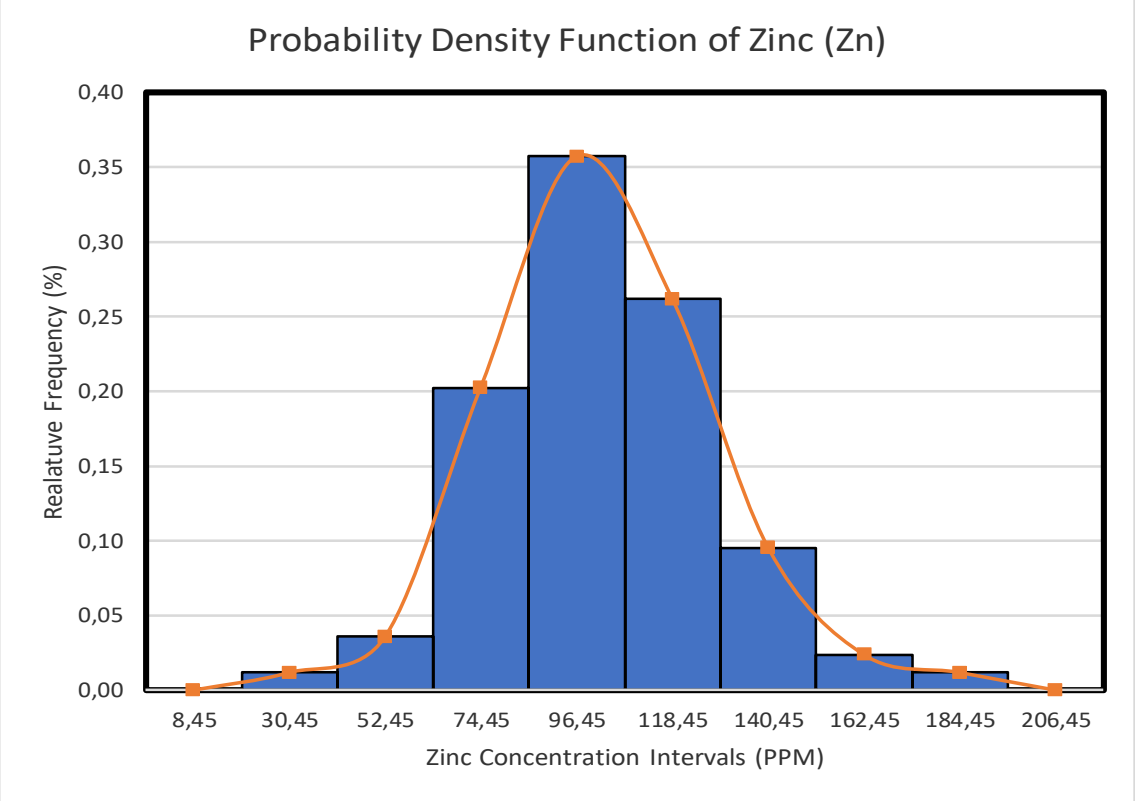

Figure 4.14a: Probability density function of zinc within Fumani Tailings Dam 1.

The values of Zn had a threshold concentration of 140.32 ppm, of which 6 anomalous values were recorded. These anomalous values were recorded at sampling points P1H1S6 (180.7 ppm), P1H1S6 (160.7 ppm), P3H1S2 (152.4 ppm), P3H4S3 (151.1), P1H2S7 (150.3 ppm), P3H3S3 (150.3 ppm) and P2H1S7 (144.4 ppm). The location of the anomalous points revealed no readily apparent trend.

When assessing the vertical distribution through borehole logs (Fig. 4.14b), it was evident that the concentration of Pb appeared to be high within the first 2 m of the tailing dam, then it gradually tapered out between 2 to 5 m of depth and then increased again between 6 and 7 m. There were, however, exceptions as observed in borehole P3H4S4, where the Pb concentration appeared not to decrease between 2 and 5 m depth. The overall Zn distribution was erratic with depth as well as along the profiles.

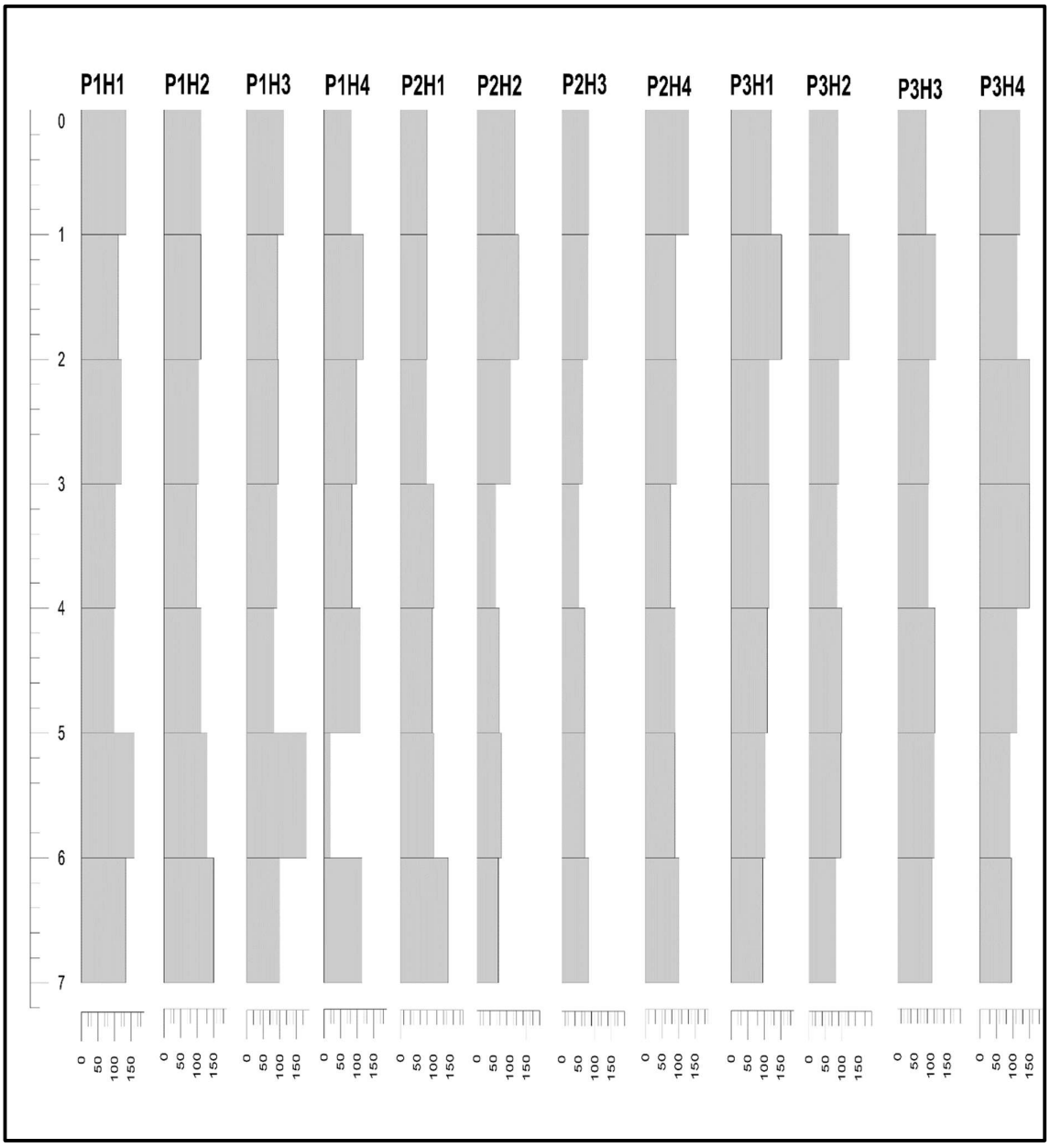

Figure 4.14b: Vertical distribution of Zn within Fumani Tailings Dam 1.

Lateral Distribution of Zn

The distribution of Zn showed low concentration towards the center of the tailings dam with higher concentrations at the edges of the tailings dams (Fig. 4.14c). These low concentrations ran in a Southeast to northwest direction. In the northeast to southwest direction, Pb concentration gradually increased from the center of the tailing dam and peaked towards the edges of the dam. This was evidenced by high zinc concentrations recorded at boreholes P3H4 and P1H1 which were collected at the fringes of the dam.

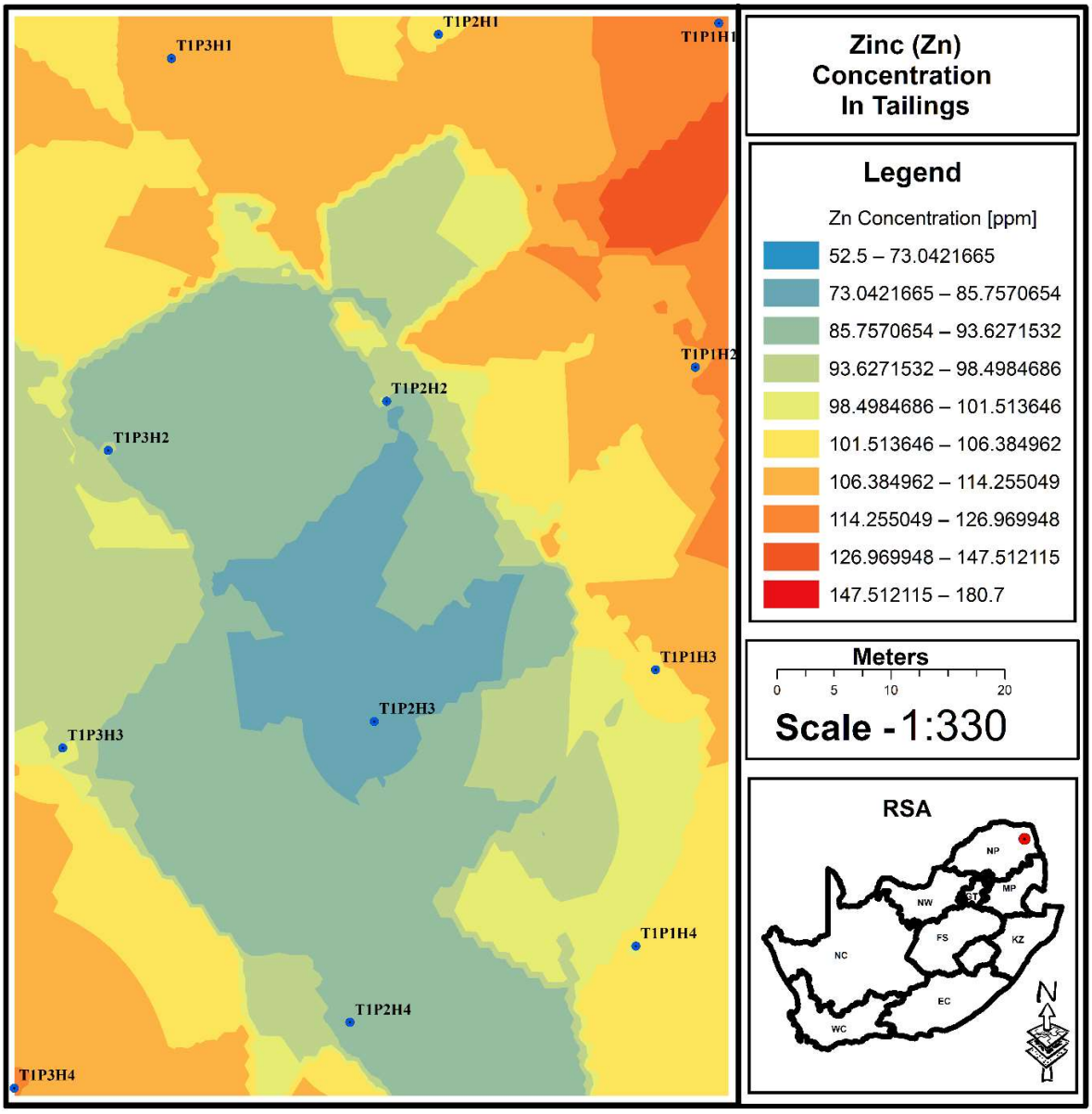

Figure 4.14c: Prediction map of Zn within Fumani Tailings Dam 1.

Copper

Vertical Distribution of Cu

The distribution of copper within Fumani Tailing Dam 1 was characterised by a negatively skewed distribution with a mean of 60.49 ppm, as depicted by the probability density function (Fig. 4.15a). The distribution of copper was highly skewed, which indicated that the majority of values were high, with a small proportion of values being low. based on the aforesaid, one would expect to see significant anomalous values, however at a threshold concentration value of 80.1 ppm, the copper distribution only had 3 recorded anomalous values of 80.1, 80.3 and 80.4 ppm, recorded at boreholes P1H1S2, P3H1S4 and P3H4S4 respectively. The location of the anomalous values did not reveal any readily apparent trend as they were too few to make any conclusion.

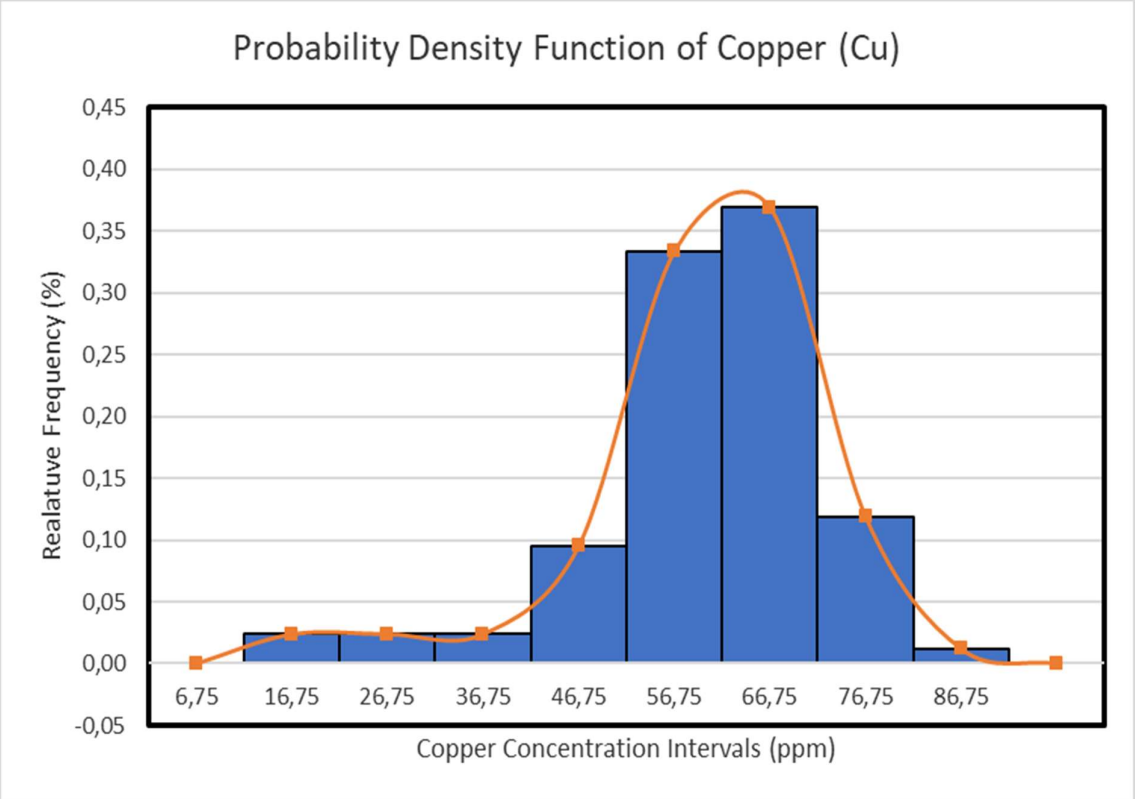

Figure 4.15a: Probability density function of copper within Fumani Tailings Dam 1.

Analysis of the vertical distribution through boreholes logs indicated that copper distribution was evenly distributed from the top to the bottom of the tailings dam (Fig. 4.15b). This is evidenced by 7 of the 12 sampled boreholes, which had fairly consistent copper concentration from the top to the bottom. These boreholes were P1H4, P2H1, P2H2, P2H3, P2H4, P3H1, P3H4. There were exceptions where the remaining 5 of the 12 boreholes had low concentration. These low concentration values randomly occurred at any depth within the boreholes, although it can be said that they were confined within the 2 – 5 m depth of the tailings dam. The overall trend of Cu within the Fumani Tailings Dam 1 was erratic with depth.

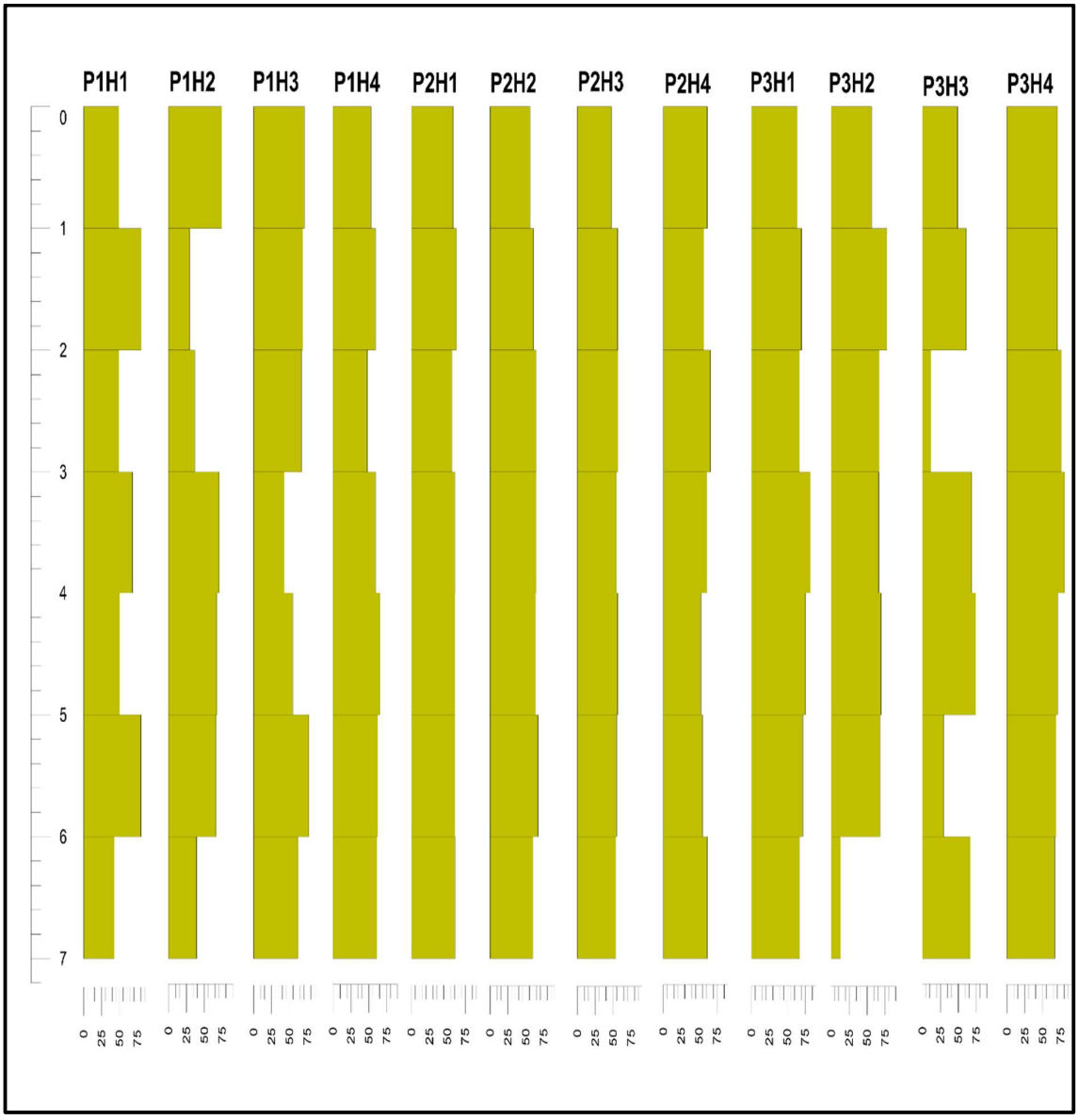

Figure 4.15b: Vertical distribution of Cu within Fumani Tailings Dam 1.

Lateral Distribution of Cu

The spatial behaviour of copper was characterised by high spatial correlation. This meant that the Cu distribution had a high spatial continuity. When this spatial continuity was observed on a geochemical map, it gave the impression of uniformity of concentration within the tailings dam (Fig. 4.15c). Copper appeared to have low concentration values within the centre of the tailings dam. These low concentration values radiated outward and gradually increased in towards the edges of the tailings dam. The peak values at the edges of the tailing dam were characterised by an intermediate concentration.

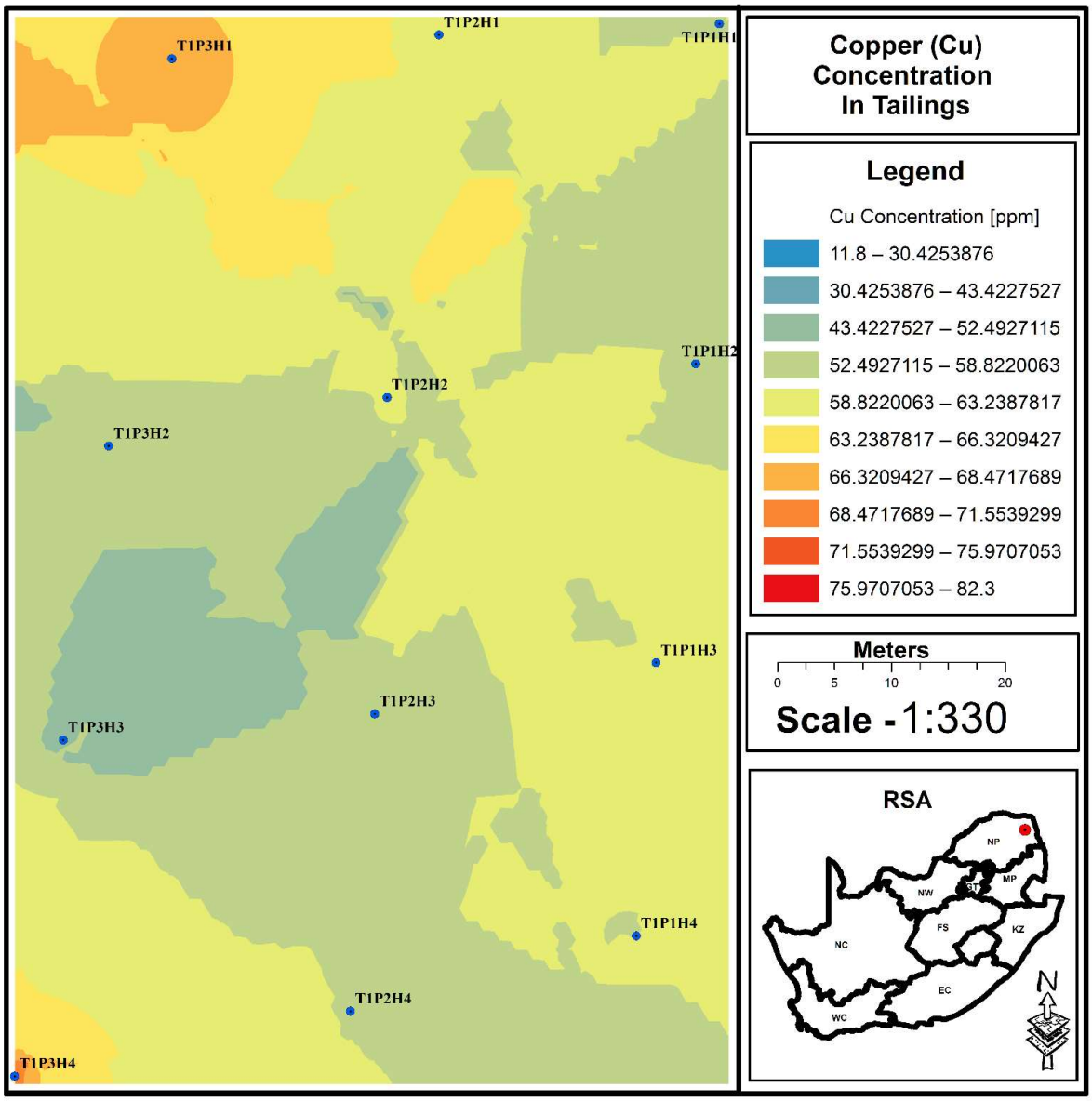

Figure 4.15c: Prediction map of lateral distribution of Cu within the Fumani Tailings Dam 1.

Arsenic

Vertical Distribution of As

Arsenic within Fumani Tailings Dam 1 was characterised by a negatively skewed distribution with a mean of 6383.081 ppm, as depicted by the probability density function (Fig. 4.16a). The skewed distribution indicated that most values were high, with a small proportion of the values being low. Arsenic values ranged from 1819 to 9732.6 ppm with most observed values occurring between 5049.95 to 9357 ppm.

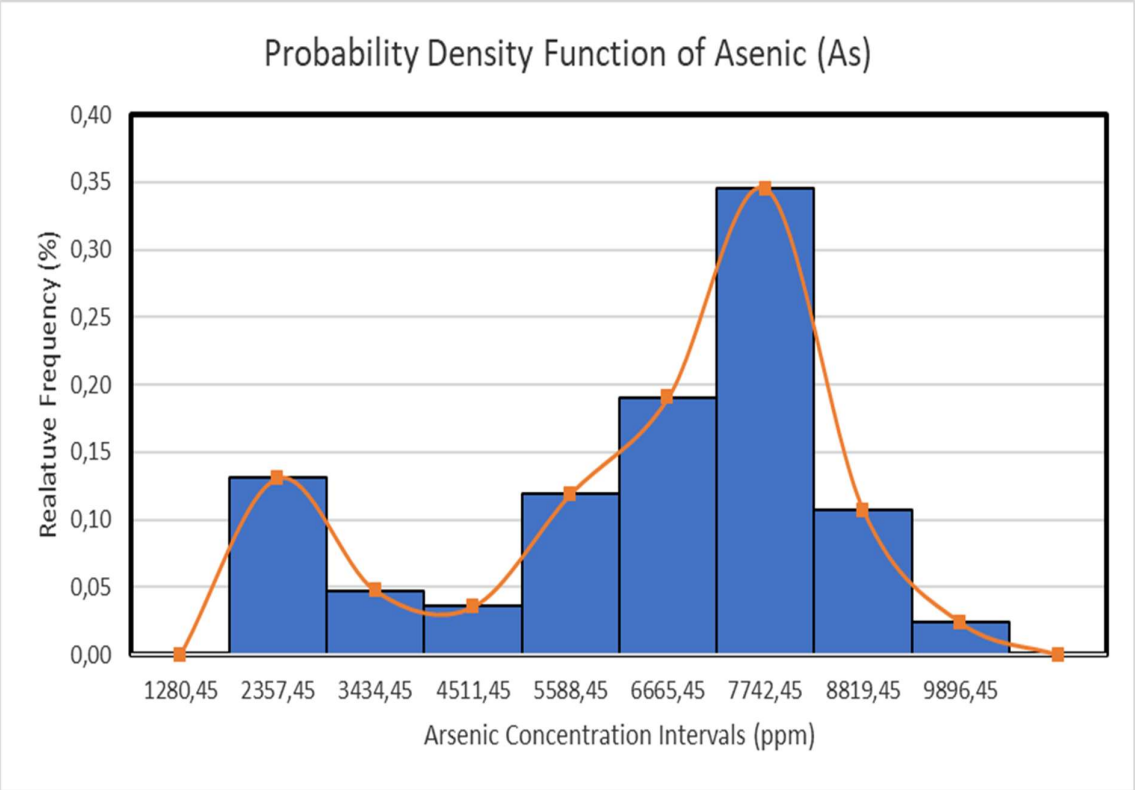

Figure 4.16a: Probability density function of arsenic within Fumani Tailings Dam 1.

The threshold value of As was 9674.501 ppm within the Fumani Tailings Dam 1. Only one anomalous value of 9674.5 located at P2H1S7 was identified in this tailings dam. The lack of the anomalous values shed no light on vertical distribution of As within the tailings dam.

An analysis of borehole logs (Fig. 4.16b) revealed that arsenic was higher within the first 2 m of the dam, at 3 m, the concentration slightly decreased, and it remain at the same level throughout 3 to 5 m and then slightly increased at a depth of 6 m. This trend was observed in boreholes P1H1, P1H2, P1H3, P2H2, P3H2, and P3H3. Notable exceptions to this trend were borehole P1H4 where the concentration was low from the top of the tailing dam up to a depth of 4 m. Borehole P2H4 was also out of place with a fairly low and consistent concentration from the top of the tailing dam all the way to the bottom. The overall As trend within the Fumani Tailings Dam 1 was erratic.

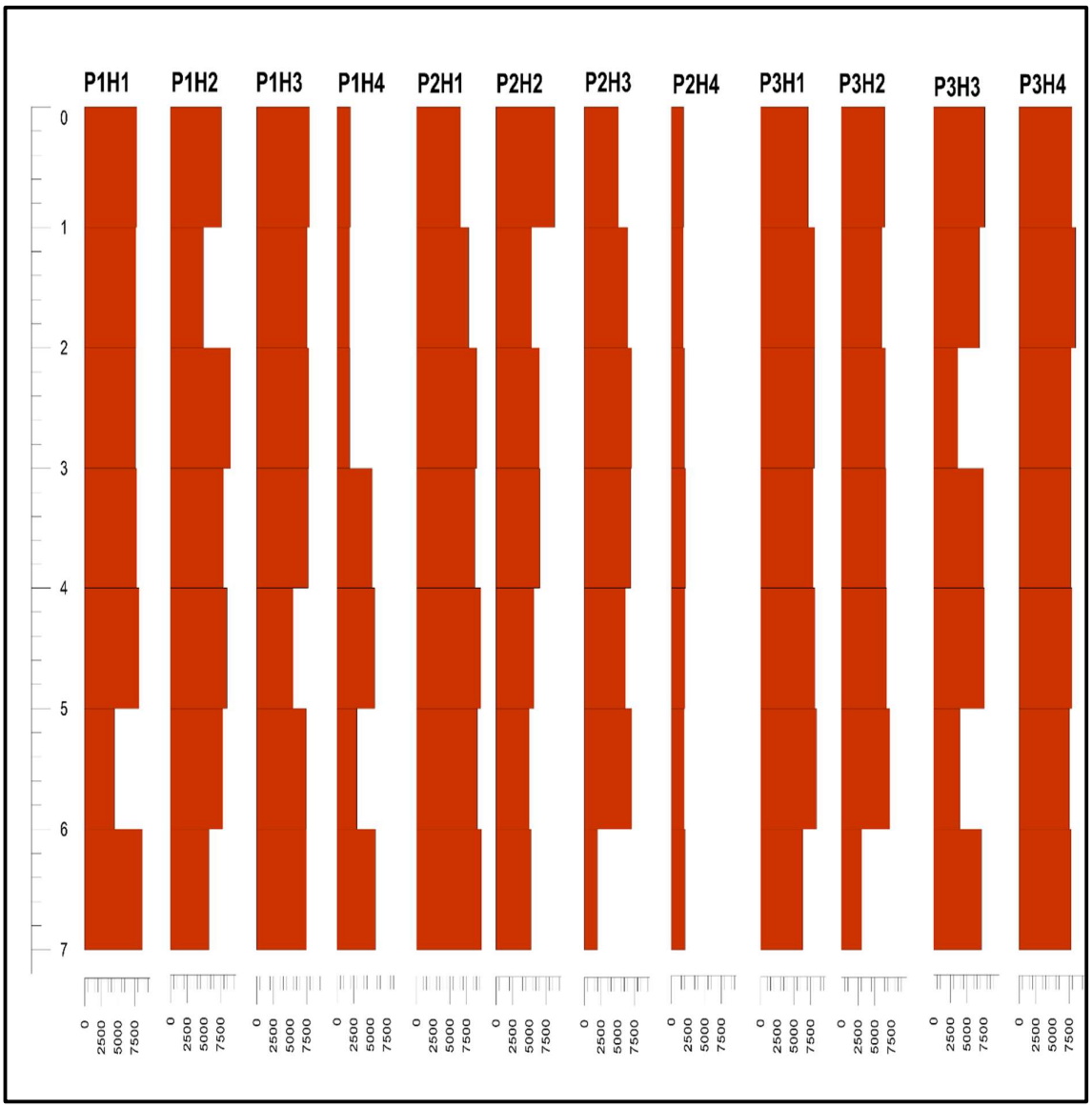

Figure 4.16b: Vertical distribution of As within Fumani Tailings Dam 1.

Lateral Distribution of As

The geochemical map indicated low As concentrations on the southern side of the Fumani Tailings Dam 1 (Fig. 4.16 c). The concentrations then increased from south to north, making high concentrations observed at points P3H1, P2H1 and P1H1 which are located on the northern part of the tailings dam.

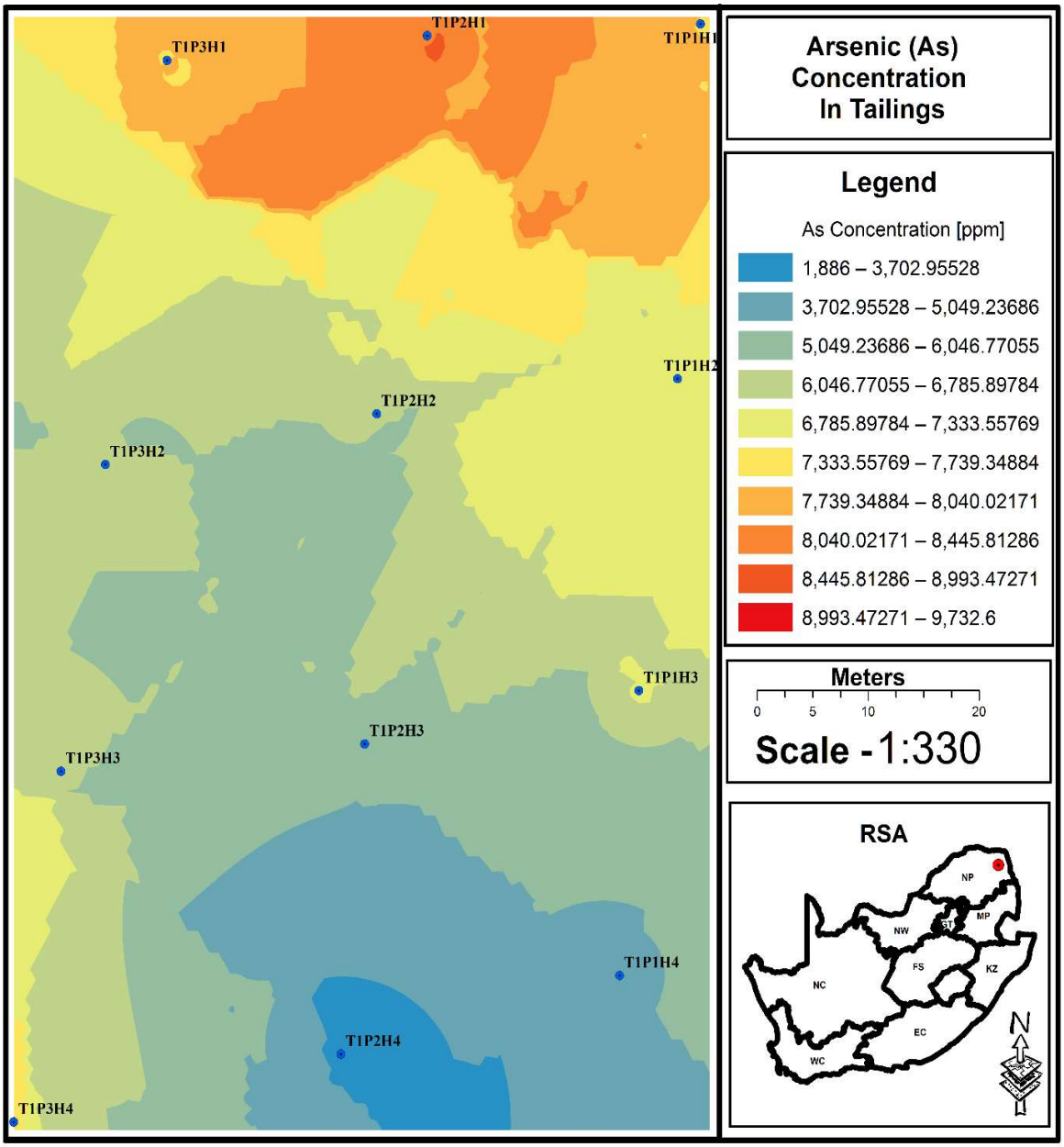

Figure 4.16c: Prediction map of As within Fumani Tailings Dam 1.

Cobalt

Vertical Distribution of Co

Cobalt within Fumani Tailings Dam 1 was characterised by a normal distribution with a mean of 24,75 ppm depicted by the probability density function (Fig. 4.17a). The distribution was almost symmetrical, which indicated that the proportion of high and low values within the data were equal. Observed cobalt values ranged from 11 ppm to 43.7 ppm, with most of the values occurring between 21 to 36 ppm.

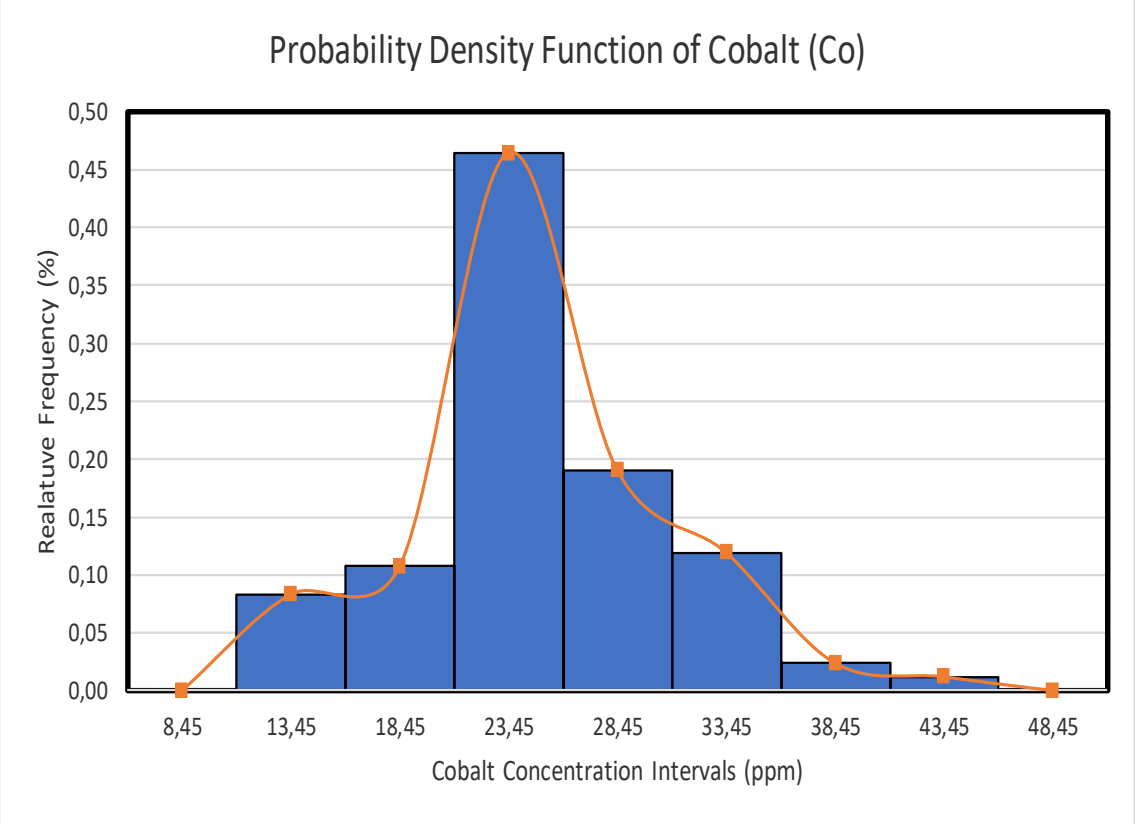

Figure 4.17a: Probability density function of cobalt within Fumani Tailings Dam 1.

The threshold concentration of Cobalt was 33.69 ppm, with 5 anomalous values. The anomalous values were, 34.7 ppm at P1H4S2, 35 ppm at P2H2S2, 36.7 ppm at P3H4S1, 39.1 ppm at P1H2S3 and 43.7 ppm at P1H2S4 (Fig. 4.17a). The locations of the anomalous values were above 4 m, indicating that Co concentrations may be higher at the top of the tailings dams.

An analysis of borehole logs indicated that the concentrations of cobalt were higher above 4 m (fig. 4.17b) as indicated previously. The distribution was slightly constant within the tailings dam. The overall Co trend was erratic with depth.

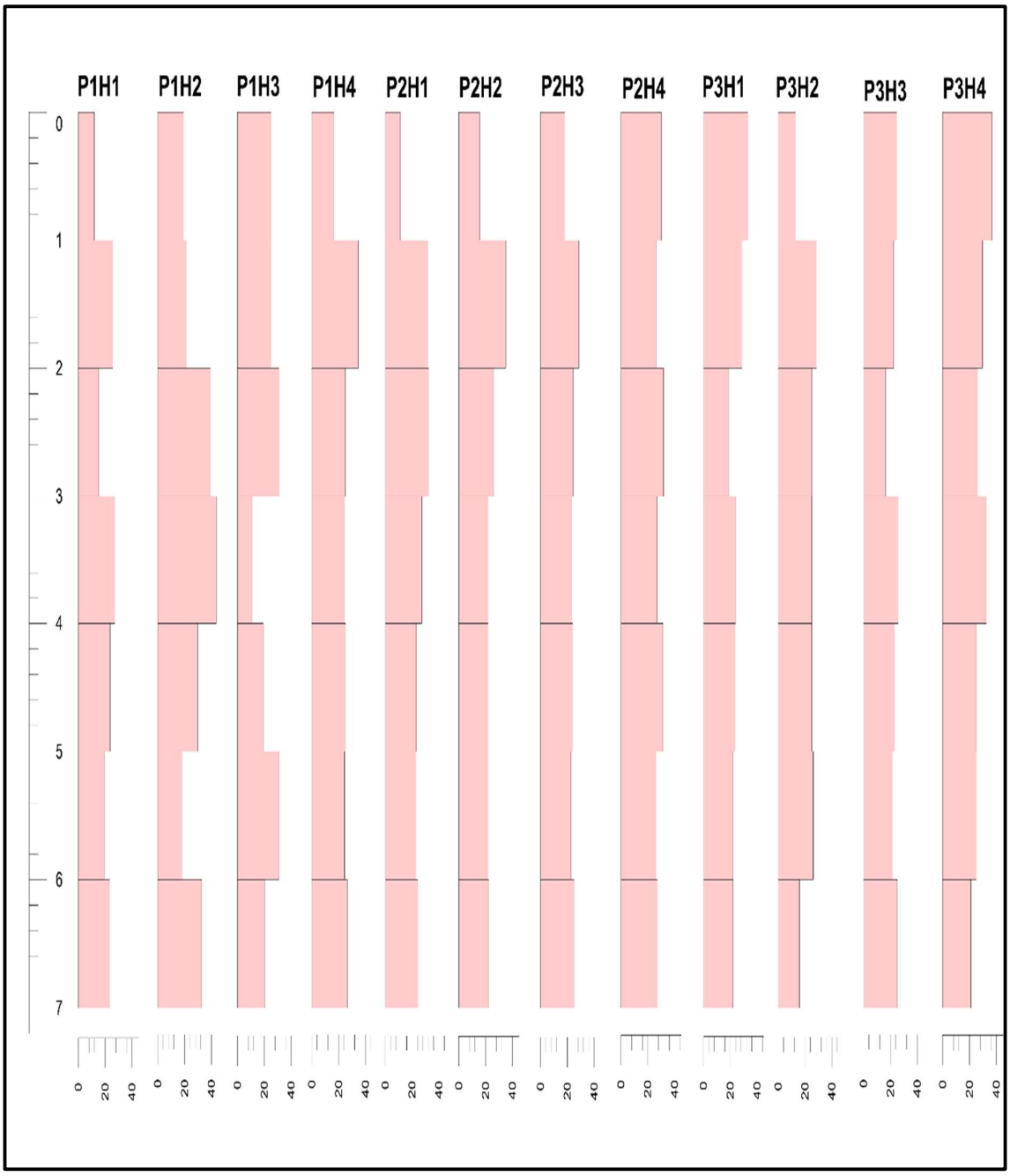

Figure 4.17b: Vertical distribution of Co within Fumani Tailings Dam 1.

Lateral Distribution of Co

Observations of the geochemical map indicate that the concentration of cobalt seemed to be lower at the top left edge of the tailings dam and increased towards the bottom edge of the dam (Fig. 4.17c). The lowest concentration of cobalt was observed at P1H1 that is at the top edge of the first profile and the highest concentration observed at the bottom edge of the second profile.

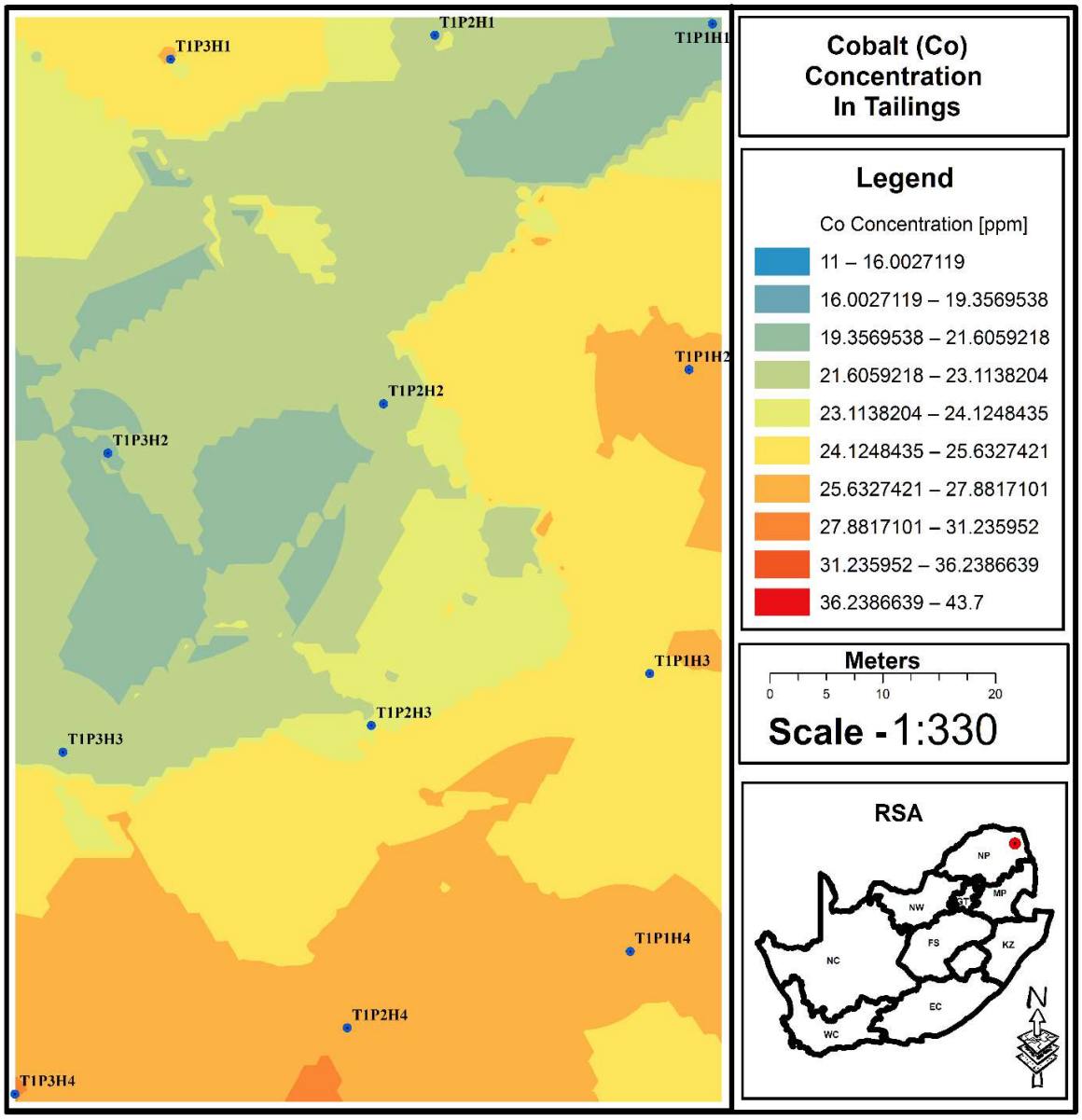

Figure 4.17c: Prediction map of Co within Fumani Tailings Dam 1.

Cadmium

Vertical Distribution of Cd

Cadmium within Fumani Tailings Dam 1 was characterised by a negatively skewed distribution with a mean of 0.67 ppm as depicted by the probability density function (Fig. 4.18a). The Cd distribution indicated that most observed values were high, with a small proportion of low values. The values of cadmium observed ranged from 0 to 1.1 ppm, with most of these values recorded between 0.55 to 1.15 ppm.

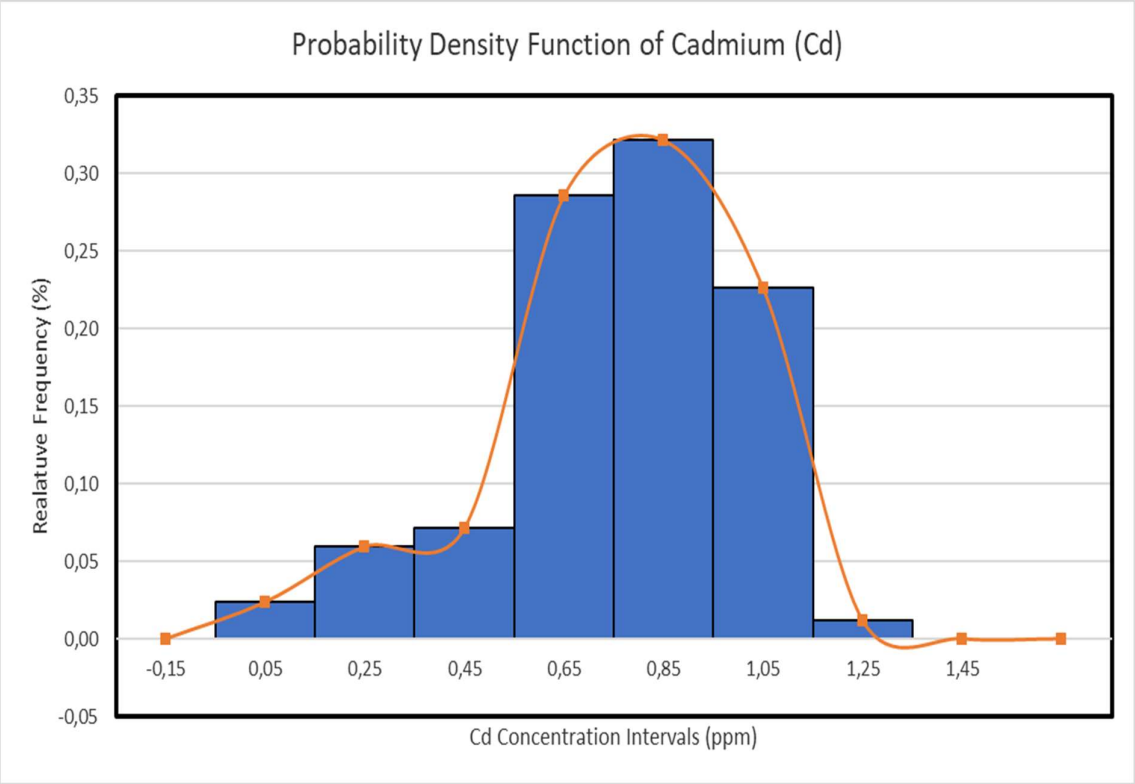

Figure 4.18a: Probability density function of cadmium within Fumani Tailings Dam 1.

The highest value Cd was 1.1 ppm collected from P1H4S7. The concentration of Cd was not detected at P3H3S3 and P2H1S3. At a threshold concentration value of 1.03 ppm, the cadmium distribution was characterised by one anomalous value of 1.1 recorded at borehole P1H4S7. This did not provide any insight into the distribution of Cd within the tailings dam.

Further vertical distribution analysis of Cd was done using borehole logs (Fig. 4.18b). The logs indicated that the vertical distribution of cadmium was rather erratic with no apparent trend. 5 of the 12 boreholes were characterised by an alternating pattern of low and high concentration. The low concentration occurred between 0 – 1, 3 – 4 and 5 – 6 m of depth. The boreholes that were not characterised by this trend exhibited a rather consistent level of concentration values from the top of the tailing dam to the bottom. These boreholes included, P1H4. P2H2, P2H3, P2H4, P3H1, P3H1, and P3H4. The overall distribution was rather uniform with very small changes in values. This can be seen by the scale used in the creation of this borehole log (Fig. 4.18b).

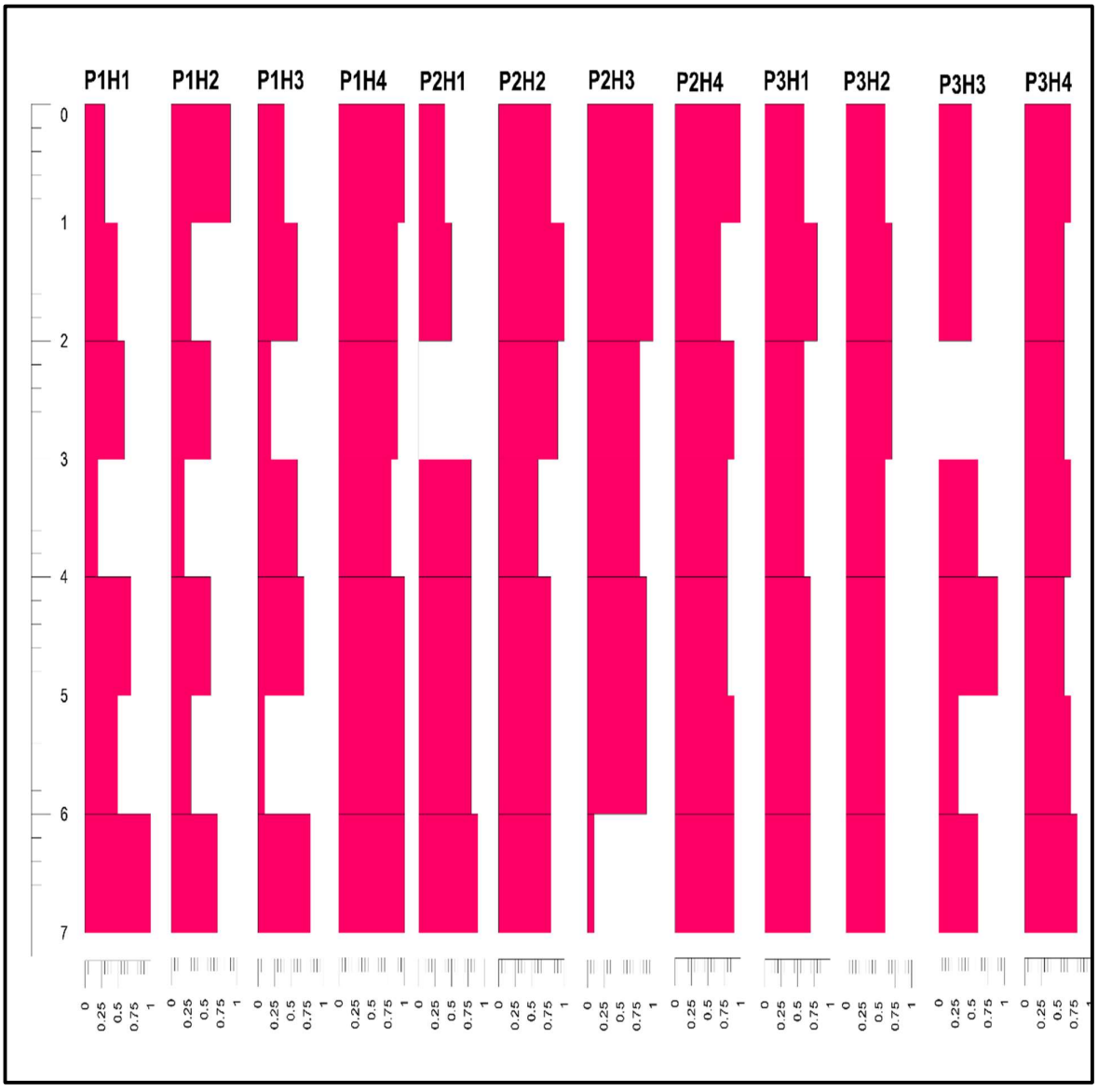

Figure 4.18b: Vertical distribution of Cd within Fumani Tailings Dam 1.

Lateral Distribution of Cd

The geochemical map of Cd within the Fumani Tailings Dam 1 showed a uniform distribution (Fig. 4.18c). Slightly high concentrations of cadmium ran in a southeast to northwest direction and gradually decreased in concentration in the northeast to southwest direction towards the edges of the tailings dam, where the concentration became moderate. The exception however is the cadmium concentration within the south-eastern edge of the tailings dam. Instead of decreasing to a moderate concentration, cadmium concentration within the south-eastern section of the tailings dam increased drastically to a high concentration.

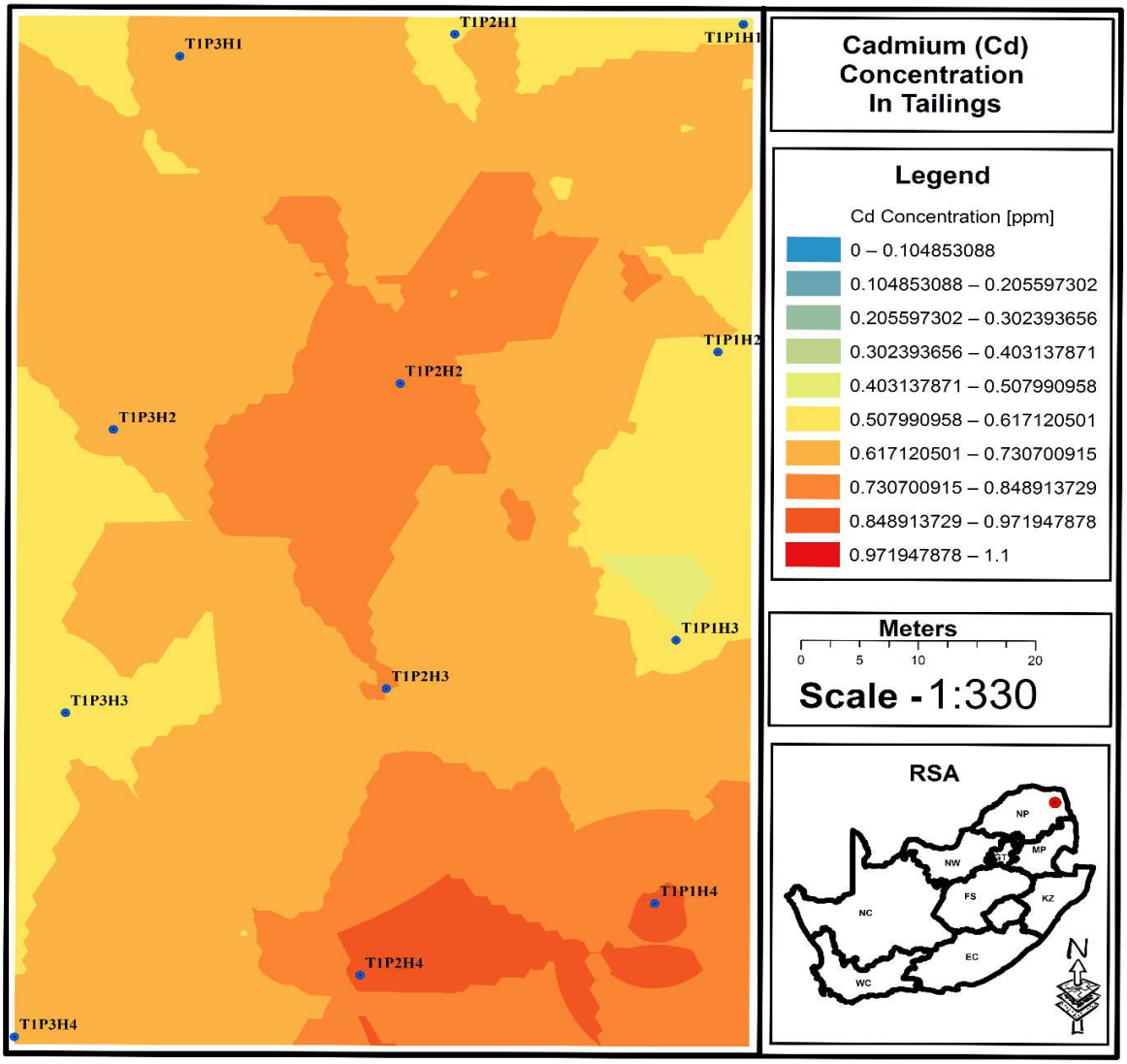

Figure 4.18c: Prediction map of Cd within Fumani Tailings Dam 1.

Chromium

Vertical Distribution of Cr

Chromium within Fumani Tailings Dam 1 was characterised by negatively skewed distribution with a mean of 71.71 ppm as depicted by the probability density function (Fig. 4.19a). Chromium values indicated that most observed values were high, with a small proportion of low values. Observed values ranged from 16.3 to 107 ppm, with most of the values occurring between 40.25 to 88.25 ppm.

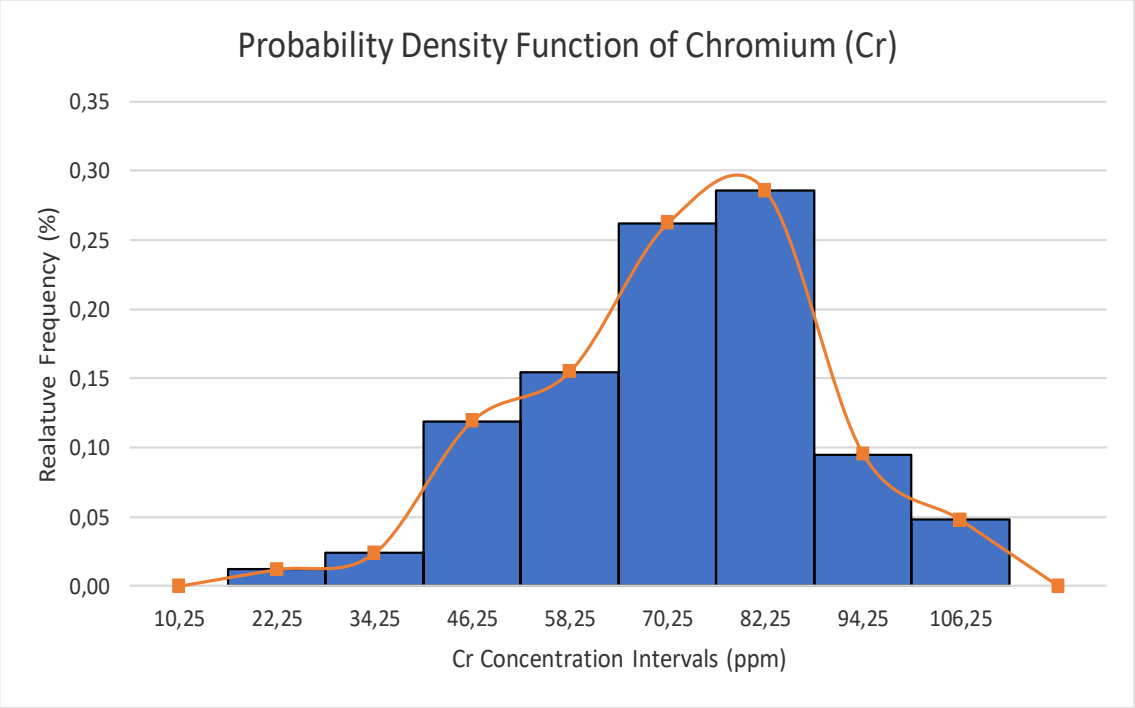

Figure 4.19a: Probability Density Function of chromium within Fumani Tailings Dam 1.

The highest value of Cr was 107 ppm recorded at P3H1S4, and the lowest Cr value of 16.3 ppm was recovered from P1H1S6.Chromium had a threshold value of 98.62 ppm, which resulted in 4 anomalous values. The anomalous values were 106.3 ppm at P3H3S5 and P1H2S1, 106.5 ppm at P3H1S2 and 107 at P3H1S4. The four anomalous values were located in various depth, indicating that the trend could be erratic within the tailings dams.

The results of a borehole analysis indicated that chromium values were indeed erratic with depth (Fig. 4.19b). The values were characterised by erratic alternating bands of low and high concentration. This erratic behaviour occurred between 2 to 6 m of depth. Between 6 and 7 m depth, the concentration increased. This observed trend was similar to that observed for zinc and lead distribution and can be best observed in borehole P1H3.

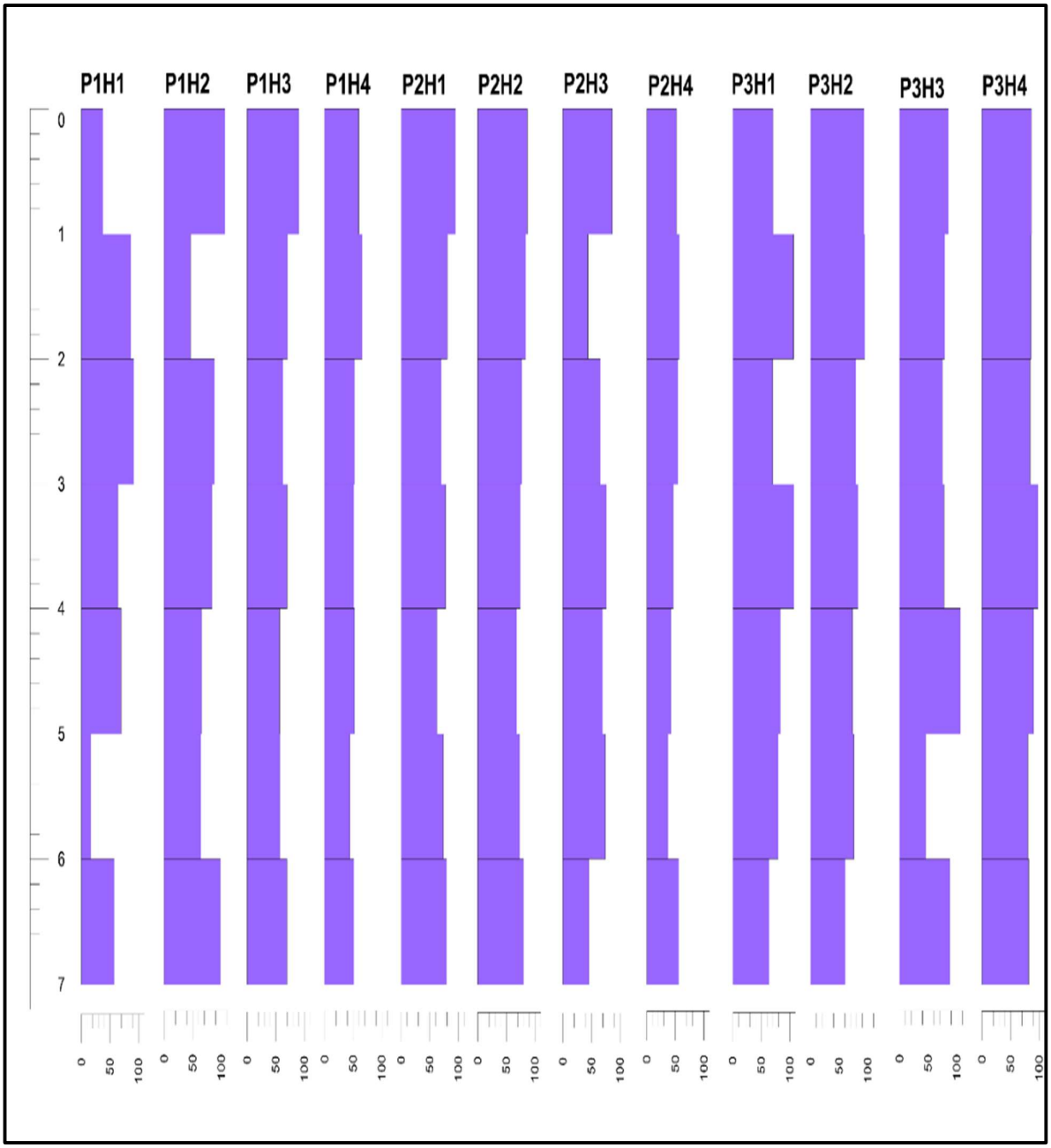

Figure 4.19b: Vertical distribution of Cr within Fumani Tailings Dam 1.

Lateral Distribution of Cr

The geochemical map indicated that chromium values appeared to be concentrated at the western edges of the tailings dam (Fig. 4.19c). The concentration reduced to the southern edge of the tailings dam where it was characterised by patchy areas of moderately low to low concentration. The lowest concentration was observed at the southern edge of the tailings dam (Fig. 4.19c).

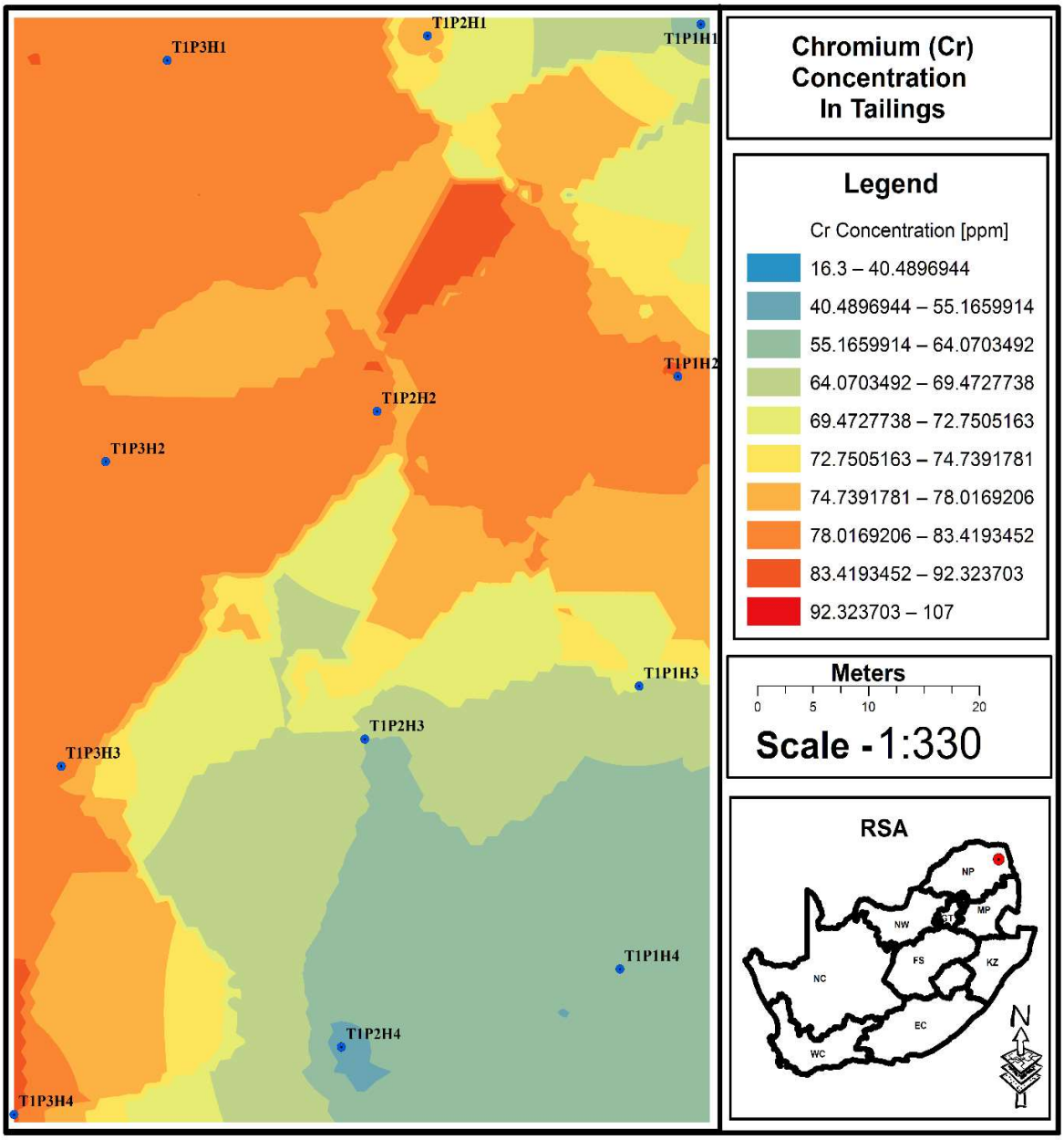

Figure 4.19c: Prediction map of Cr within Fumani Tailings Dam 1.

Nickel

Vertical Distribution of Ni

Nickel within Fumani Tailing Dam 1 was characterised by a slightly negatively skewed distribution with a mean of 99.35 ppm, as depicted by the probability density function (Fig. 4.20a). The distribution indicated that most observed values were high, with a small proportion of low values. Observed nickel values ranged from 43.3 to 147.9 ppm, with most of the observed values occurring between 71.75 to 127.75. The highest observed nickel value of 147.9 ppm was collected in P3H1S1. The lowest value was found in sampling point P2H1S1.

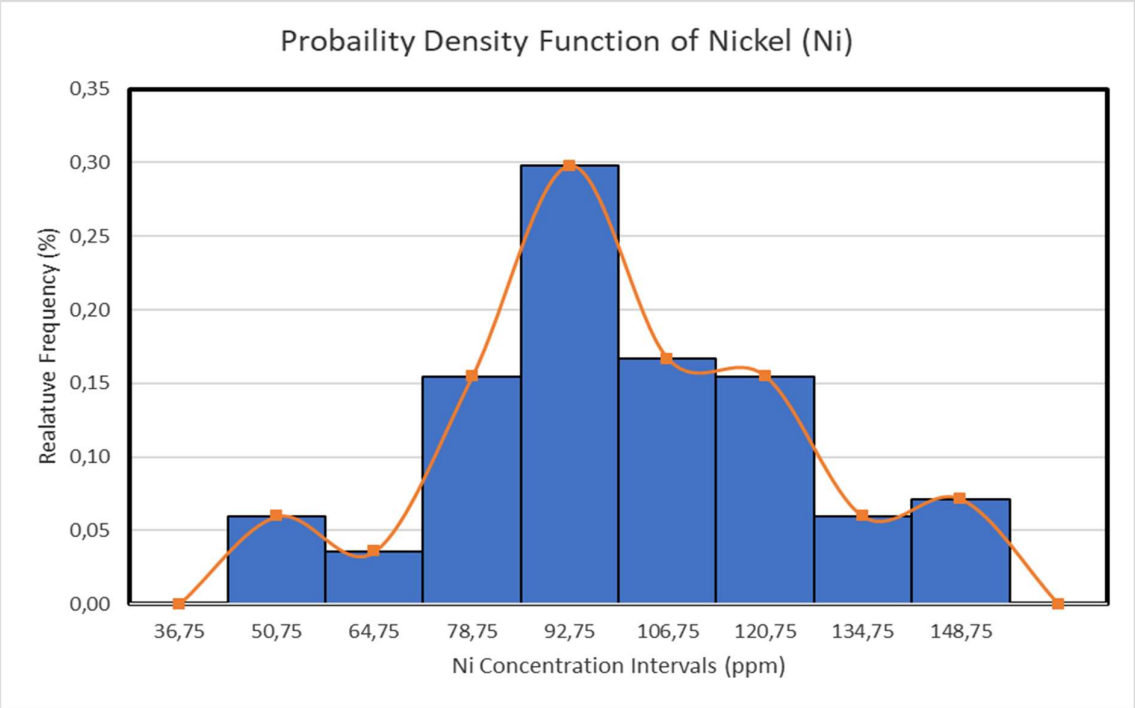

Figure 4.20a: Probability density function of nickel within Fumani Tailings Dam 1.

Nickel had a threshold value of 135.3 ppm with 8 anomalous values. The anomalous values were 136.7 ppm (P1H1S7), 140.2 ppm (P2H2S2), 141.8 ppm (P3H3S2), 143.8 ppm (P1H4S2), 144.1 ppm (P3H2S2), 145.7 ppm (P1H1S4), 147.6 ppm (P3H1S2) and 147.9 ppm (P3H1S1). Five of the eight values were sampled at a depth of 2 m. This indicated that Ni concentration may have been higher at between 1-2 m of the tailing dam.

To further analyse the vertical distribution of nickel, borehole logs were created and evaluated (Fig. 4.20b). The borehole logs indicated that nickel concentration was low within the first meter. The concentration then increased between 1 to 2 m as anticipated from anomalous points, particularly within the first and third profile. Thereafter, the concentration remained consistent with an occasional increase or decrease in concentration. This trend occurred between 2 and 6 m depth. Between the 6 and 7 m mark, the concentration increased, although in some cases this increase was not readily apparent from the borehole logs.

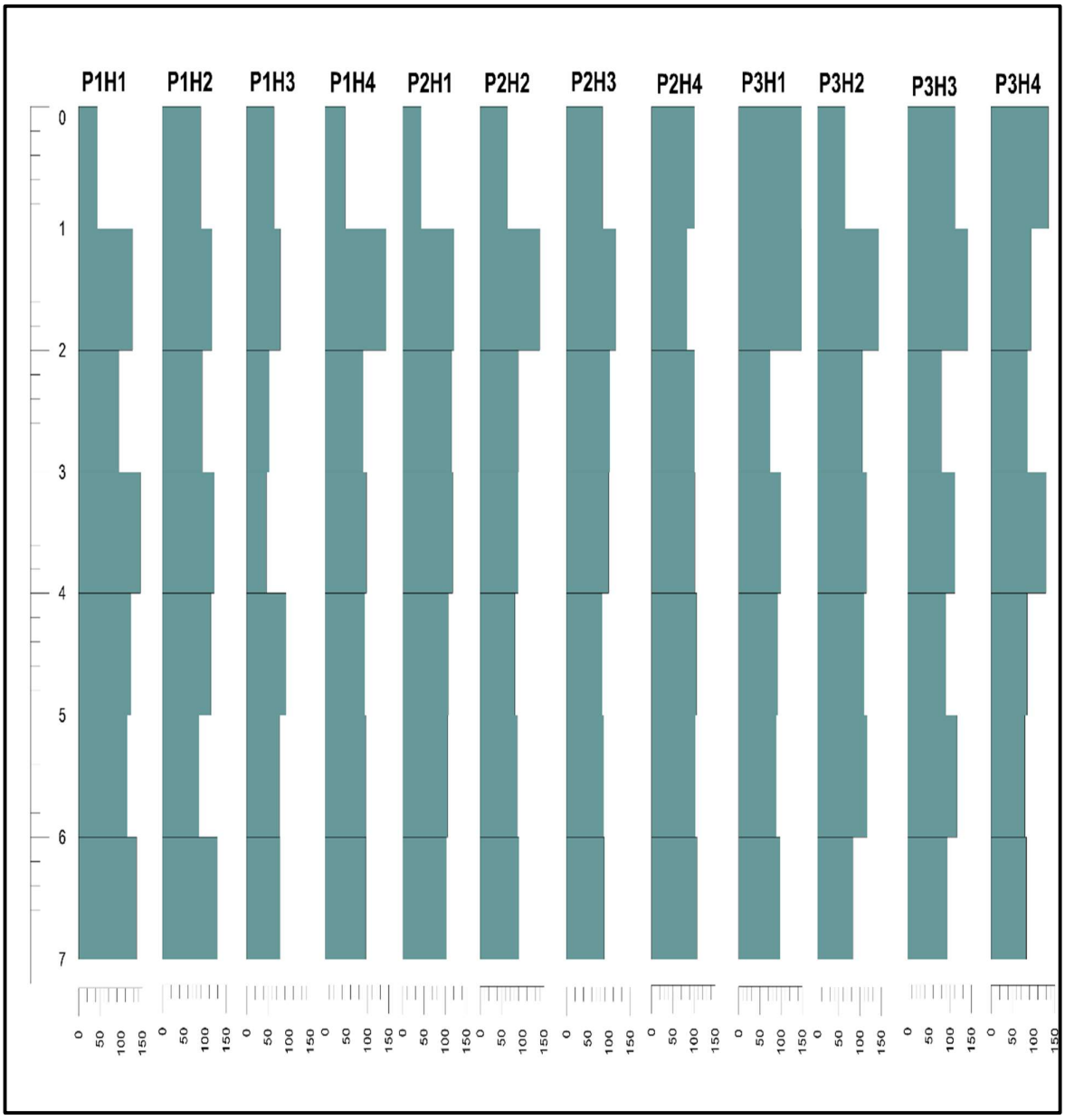

Figure 4.20b: Vertical distribution of Ni within Fumani Tailings Dam 1.

Lateral Distribution of Ni

The geochemical map revealed that the distribution of nickel originated at the center on the eastern edge of the tailings dam (Fig. 4.20c). The concentration started out low then it radiated outward in an omni directional manner. As it radiated it gradually increased in concentration until it peaked in the northwestern and southwestern edges of the tailing dam. The peak in concentration was characterised by a moderately high concentration. The general distribution was almost uniform, with gradual changes.

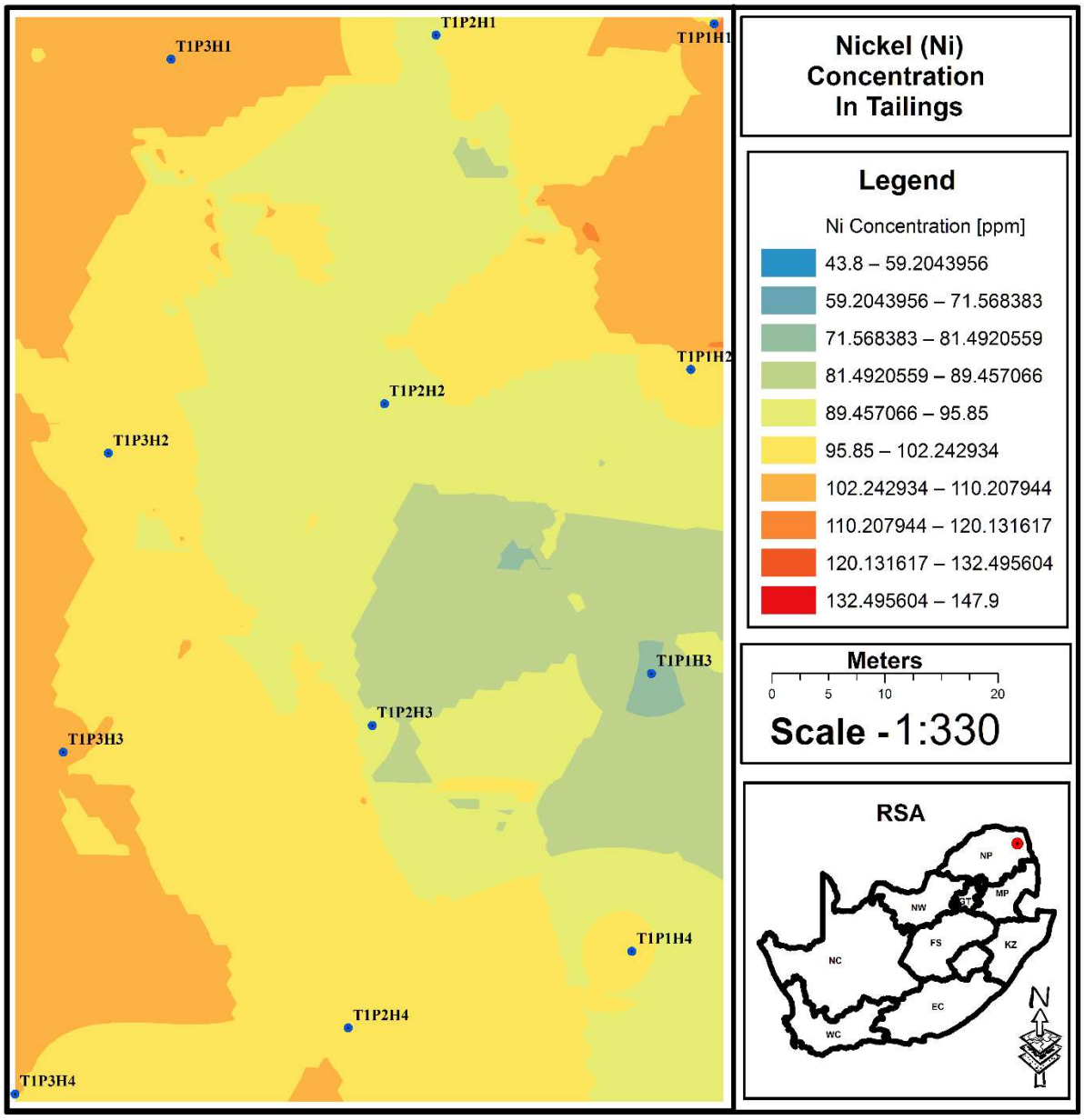

Figure 4.20c: Prediction map of Ni within Fumani Tailings Dam 1.

Fumani Tailings Dam 2

Lead

Vertical Distribution of Pb

Lead concentration within the Fumani Tailings Dam 2 was characterised by a negatively skewed distribution with a mean of 36.39 ppm (Fig. 4.21a). The distribution indicated that most observed lead values were low with a small proportion of high values. The lead concentration values ranged from 20.00 ppm (P3H3S7) to 64.31 ppm (P1H3S2). Most of the observed values were recorded between 20 to 38 ppm.

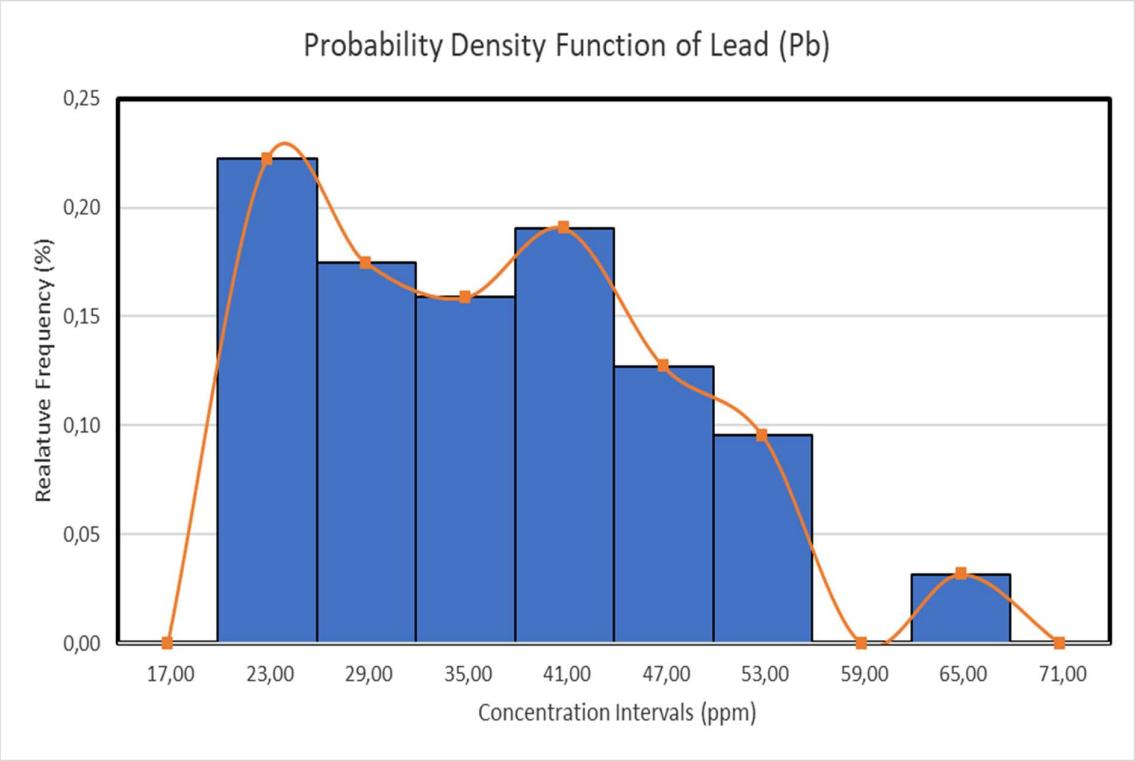

Figure 4.21a: Probability density function of lead within Fumani Tailings Dam 2.

The lead distribution was characterised by a threshold value of 52.78. This led to the identification of 4 anomalous values. These values were 53.01, 54.15, 62.4 and 64.31 ppm located at P2H3S3, P2H3S2, P1H3S1and P1H3S2 respectively. The anomalous values were located above the 3 m and suggested that lead concentration may be higher at the top of the tailings dam.

Borehole analysis (Fig. 4.21b) indicated that lead values were indeed high within the first 3 m of the tailings dam, with the highest concentrations observed between 1-3 m in all boreholes. Thereafter the concentration gradually declined. This trend was observed in boreholes P1H1, P1H2, P1H3, P2H3, P3H1, P3H2 and P3H3. There were two exceptions to the observed trend on boreholes P2H1 and P2H2. These boreholes had low concentrations at the top of the tailings dam. The low concentration continued from the top of the tailings dam to a depth of 6 m. Thereafter, the concentration increased drastically. The overall Pb trend was erratic with depth within the Fumani Tailings Dam 2.

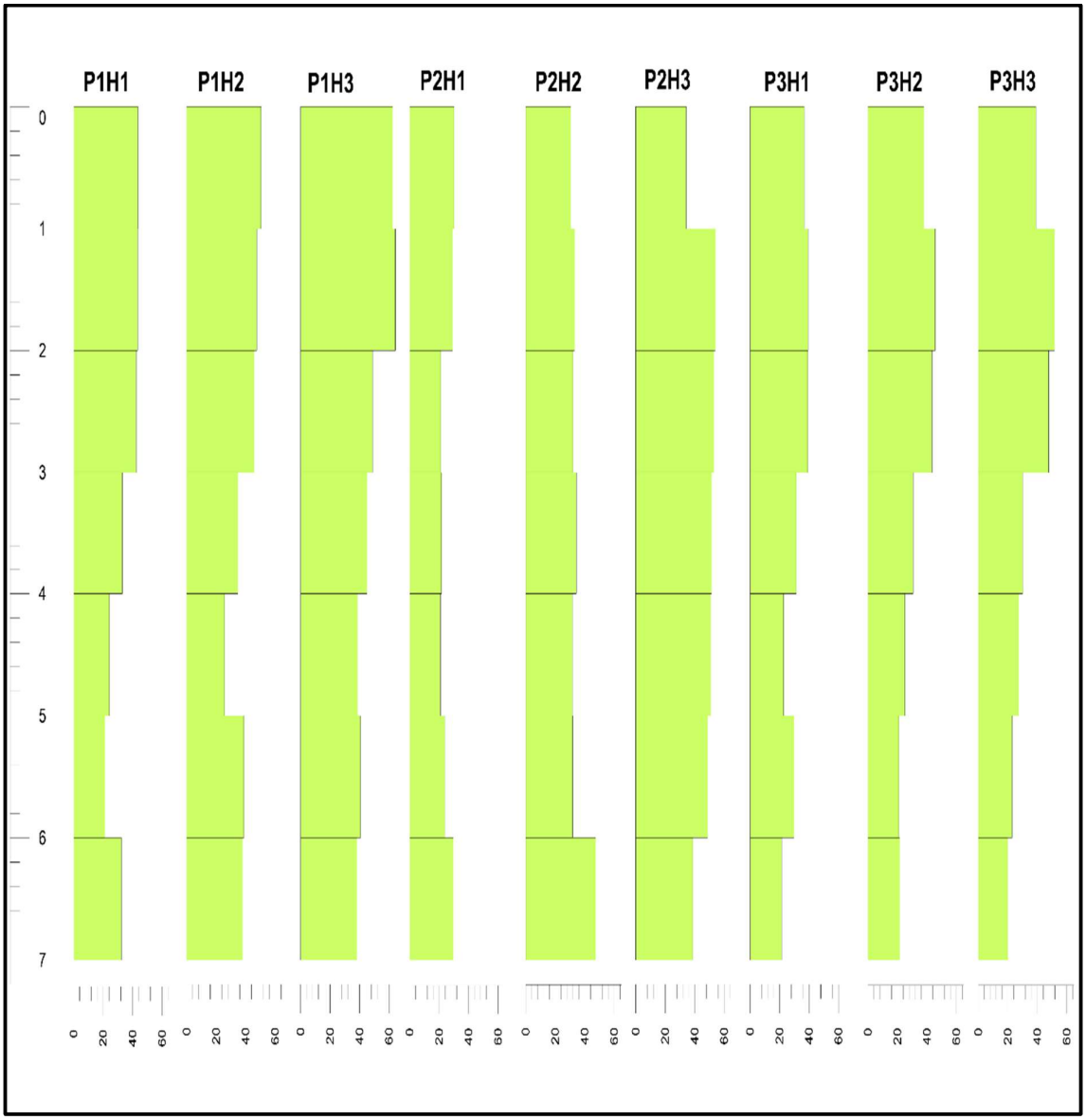

Figure 4.21b: Vertical distribution of Pb within Fumani Tailings Dam 2.

Lateral Distribution of Pb

The geochemical map of Pb indicated that the western section of the tailing dam was characterised by low values of lead which abruptly increased towards the eastern edge of the tailing dam, where the lead concentration was highest (Fig. 4.21c). The values appear to have divded the tailings dam into two parts, thus a low concentration zone in the western section and a high concentration zone in the eastern section of the dam.

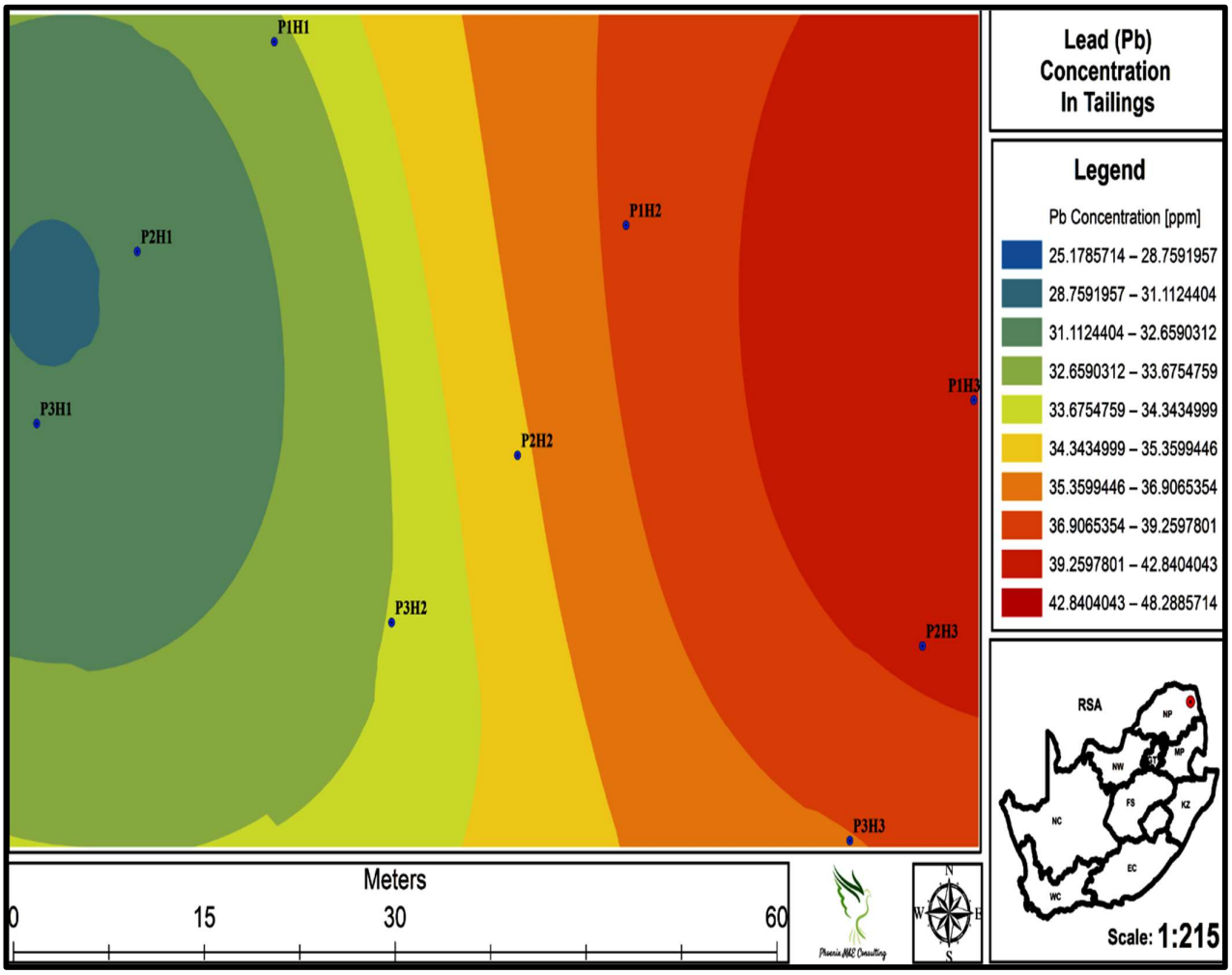

Figure 4.21c: Prediction map of Pb within Fumani Tailings Dam 2.

Zinc

Vertical Distribution of Zn

Zinc concentration within Fumani Tailings Dam 2 was characterised by a positively skewed distribution with a mean of 96,85 ppm (Fig. 4.22a). The distribution indicated that most of the recorded zinc values where high with a small proportion of low values. The observed zinc values ranged between 43.5 ppm to 146 ppm. Majority of the values were recorded between 83,46 and 123,45 ppm.

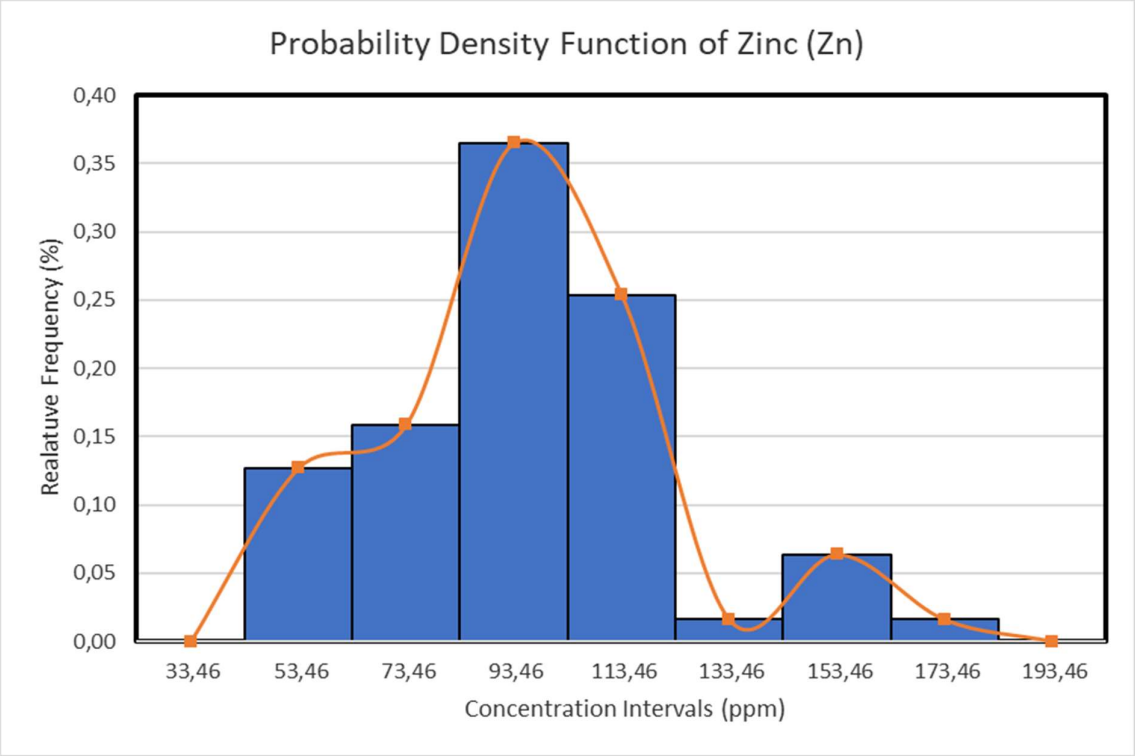

Figure 4.22a: Probability density function of zinc within Fumani Tailings Dam 2.

The Zinc distribution within Fumani Tailing Dam 1 was characterised by a threshold concentration of 136.4 ppm. This led to the identification of 5 anomalous values. These values were 145.38, 146.05, 152.60, 153.88 and 182.5. These values were recorded at boreholes P3H2S7, P1H2S2, P1H3S6, P2H2S2 and P2H1S5. The anomalous values occurred randomly with depth, suggesting that the Zn trend might be erratic within the Fumani Tailings Dam 2.

Further analysis of the vertical distribution of zinc was done using borehole logs (Fig. 4.22b). the borehole logs indicated that zinc concentration was erratic with depth within the Fumani Tailings Dam 2. Lowest values of Pb were observed on the third profile, with slightly higher values observed on the first and second profiles.

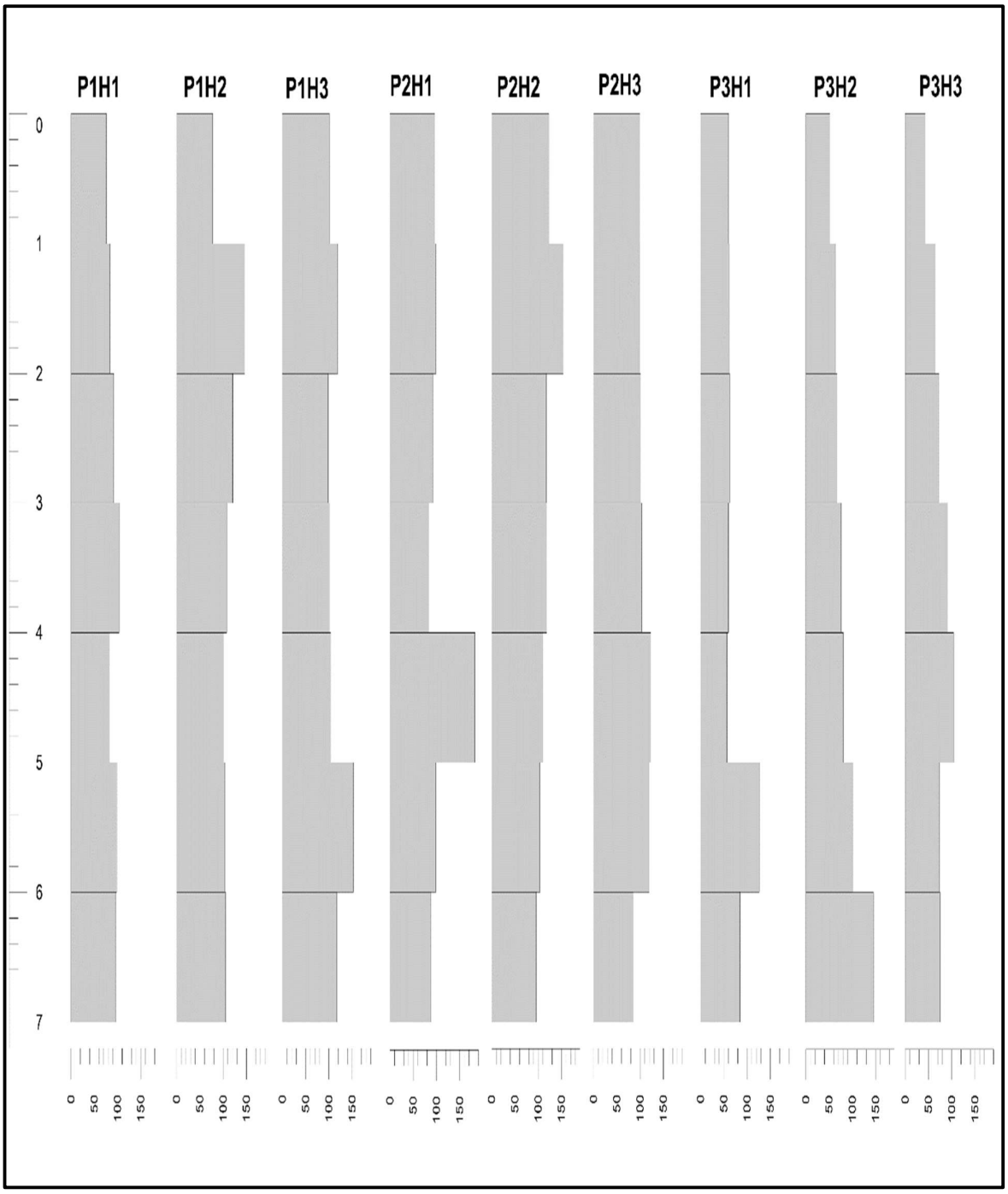

Figure 4.22b: Vertical distribution of Zn within Fumani Tailings Dam 2.

Latera Distribution of Zn

The geochemical map indicated that Zn values were lower at profile 3 (Fig. 4.22c), this profile was situated on the south-eastern direction on the tailings dam. The values seemed to be increasing as one moved towards the north-eastern direction, with exception to the centre of the tailings dam (P2H2) that had the highest value that was decreasing as one moved further from this point.

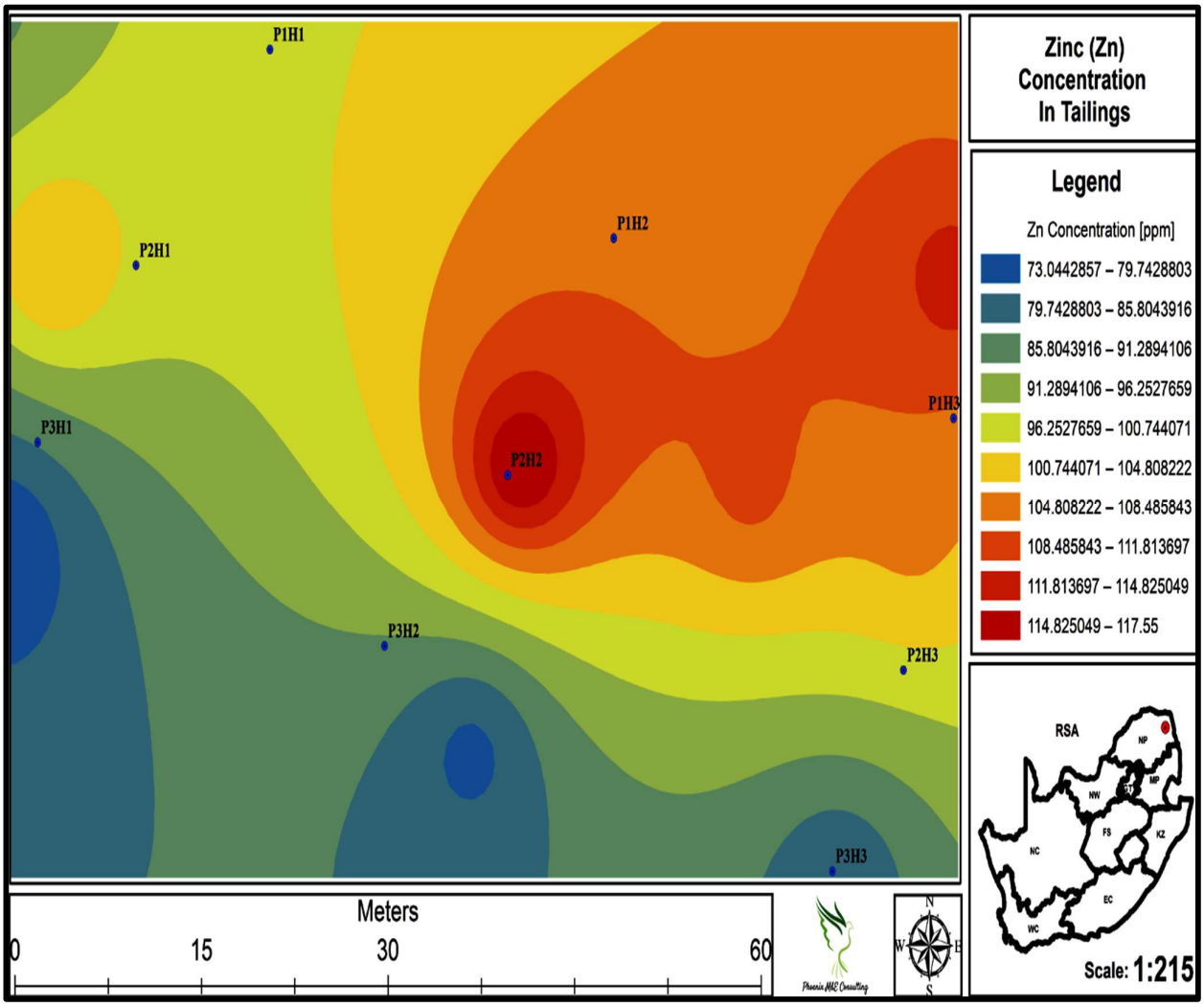

Figure 4.22c: Prediction map of Zn within Fumani Tailings Dam 2.

Copper

Vertical Distribution of Cu

Copper within Fumani Tailings Dam 2 was characterised by a normal distribution with a mean of 64,49 ppm (Fig. 4.23a). The distribution indicated that the proportion of high and low values within the data were equal. The copper concentration values ranged between 42.98 and 85 ppm. Most of the copper values recorded occurred within one standard deviation of the mean i.e., they occurred between 57 and 73 ppm.

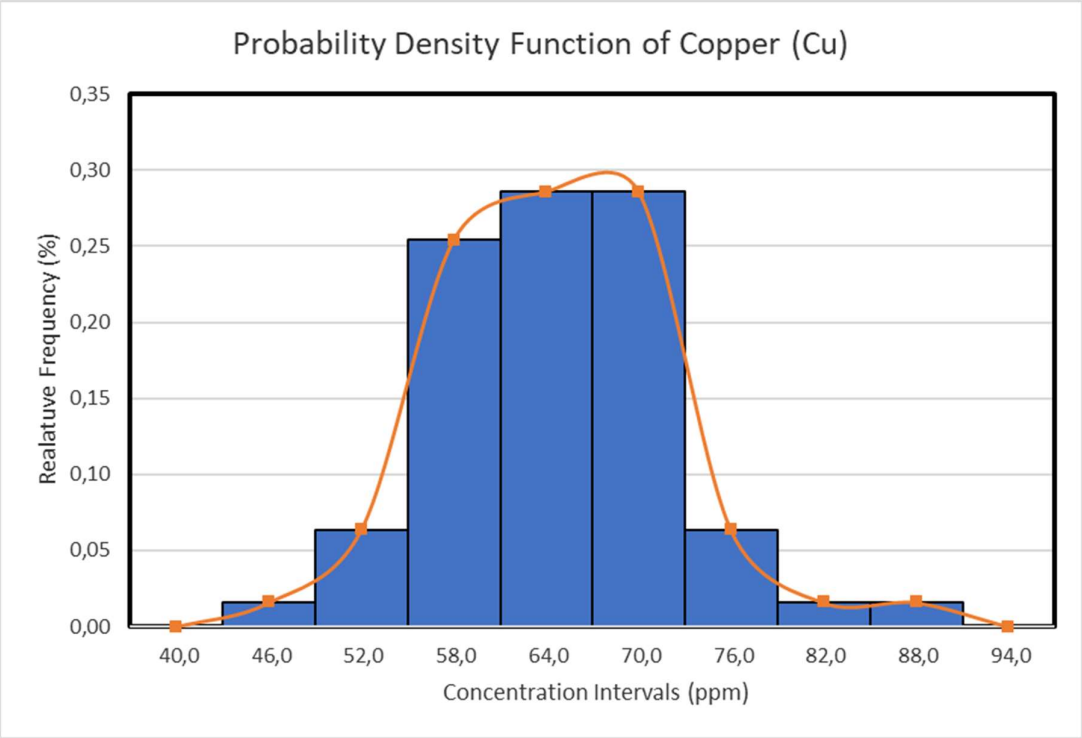

Figure 4.23a: Probability density function of copper within Fumani Tailings Dam 2.

The copper distribution within the Fumani Tailings Dam 2 was characterised by a threshold value 75.77 ppm. The threshold concentration led to the identification of 5 anomalous values. These values were 75.92 ppm (P2H2S5), 76,37 (P1H3S2), 77,47 (P2H1S5), 81,35 (P1H3S6) and 85 (P2H2S4). The anomalous values were found at random. This trend indicated that the vertical concentration of copper might have been erratic within the tailings dam.

Borehole logs indicated that Cu concentration was relatively uniform from the top to the bottom of the tailing dam (Fig. 4.23b). Three boreholes were the exception to this trend. Boreholes P1H3, P2H1 and P3H3, were characterised by a minute decrease in concentration between 3 to 5 m relative to the other boreholes at the same depth. The concentration of these boreholes increased again at 5 to 7 m to match the concentration of the top half of the tailing dam. The overall Cu distribution was rather erratic with depth.

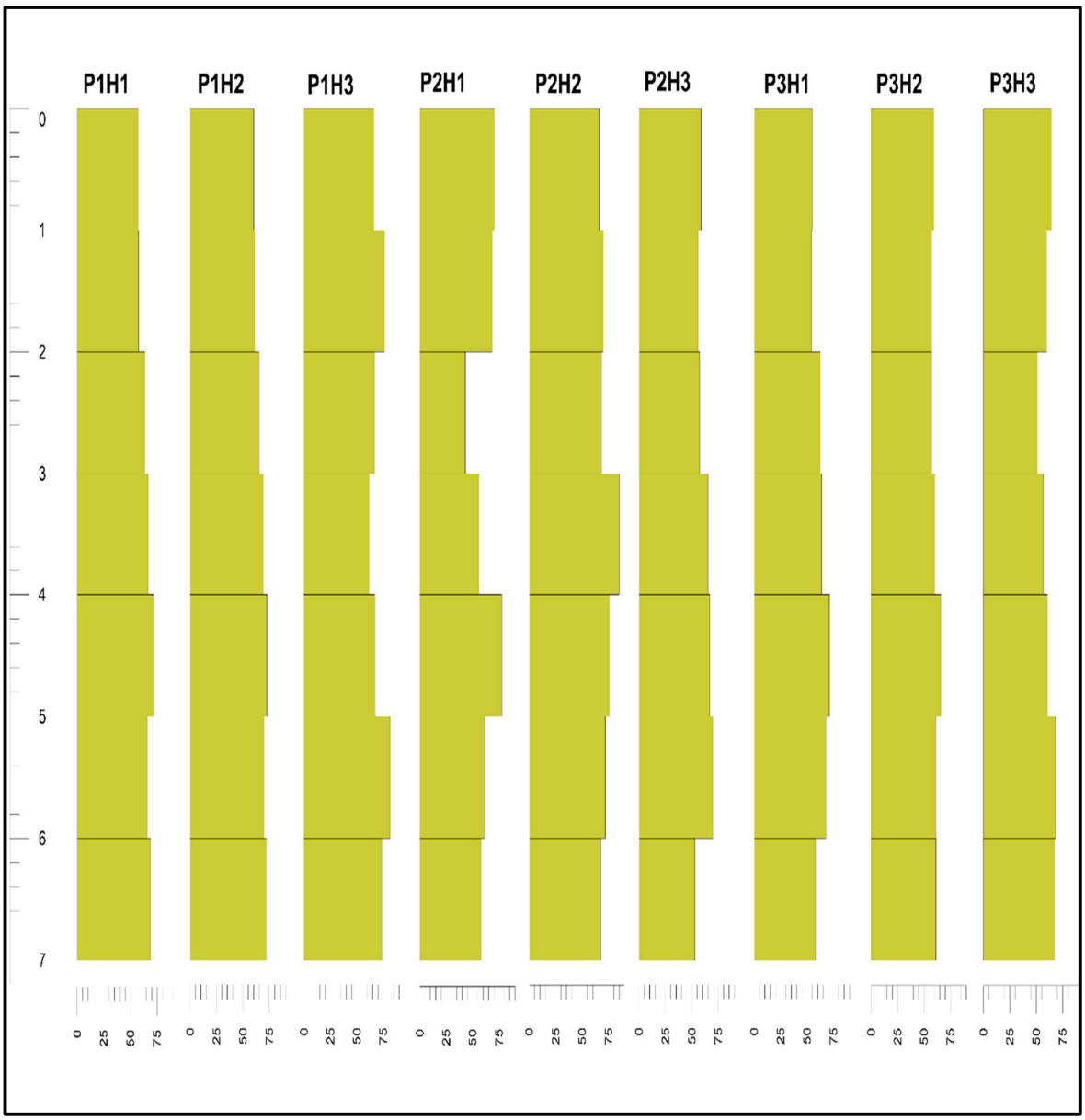

Figure 4.23b: Vertical distribution of Cu within Fumani Tailings Dam 2.

Lateral Distribution of Cu

The geochemical map revealed that Cu was highly concentrated within the north-eastern section of the tailings dam (Fig. 4.23c). This high concentration radiated outward in an omni directional manner. As it radiated outward the concentration gradually decreased until it reached its lowest observed concentration in the south-eastern section of the tailings dam.

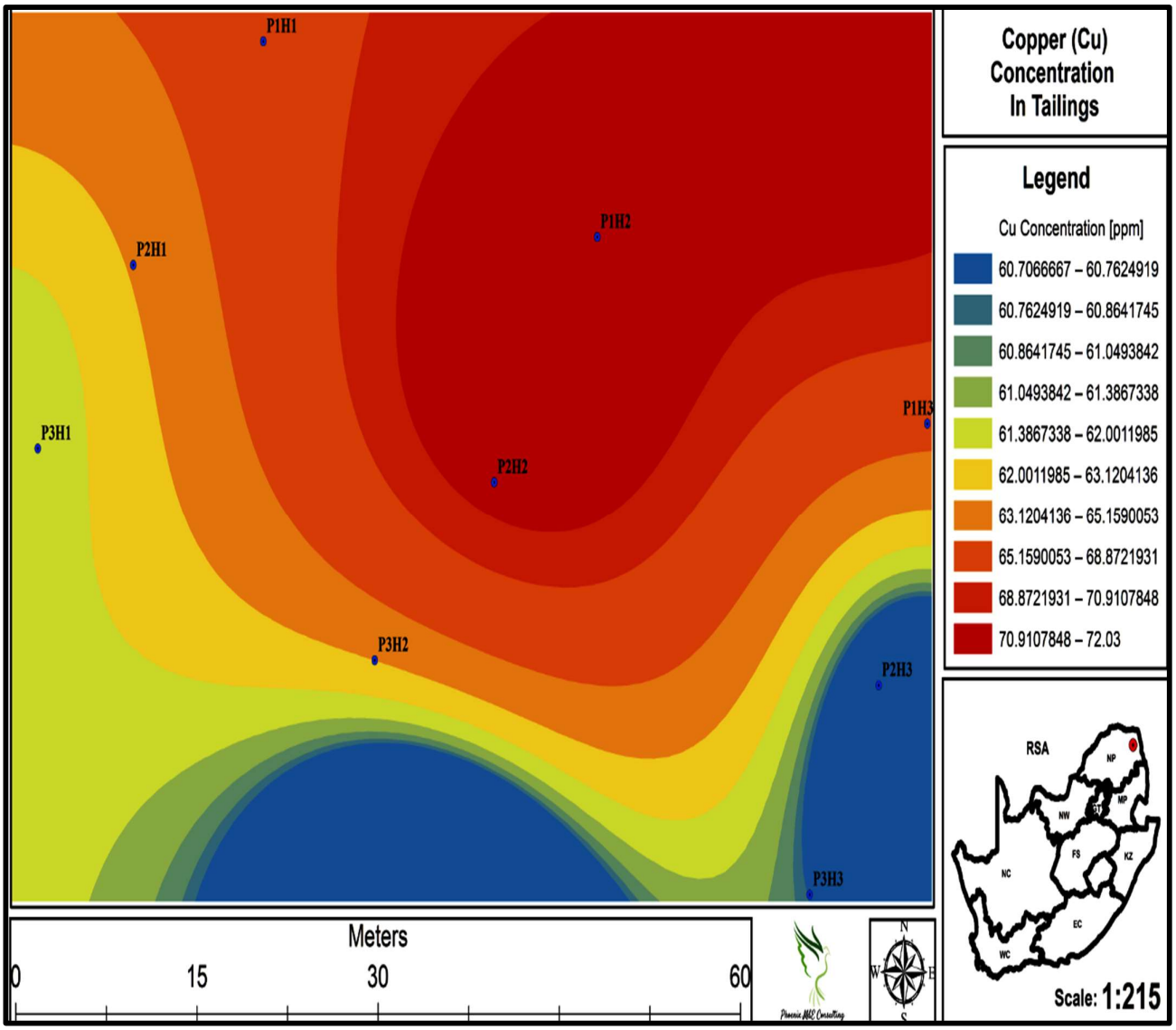

Figure 4.23c: Prediction map of Cu within Fumani Tailings Dam 2.

Arsenic

Vertical Distribution of As

Arsenic within Fumani Tailings Dam 2 was characterised by a positively skewed distribution with a mean of 4984,27 ppm (Fig. 4.24a). The distribution indicated that most recorded arsenic values were low with a small proportion of high values. Observed arsenic values ranged between 2851 to 8789,51 ppm. Most of the observed values were recorded between 3706 and 6275 ppm.

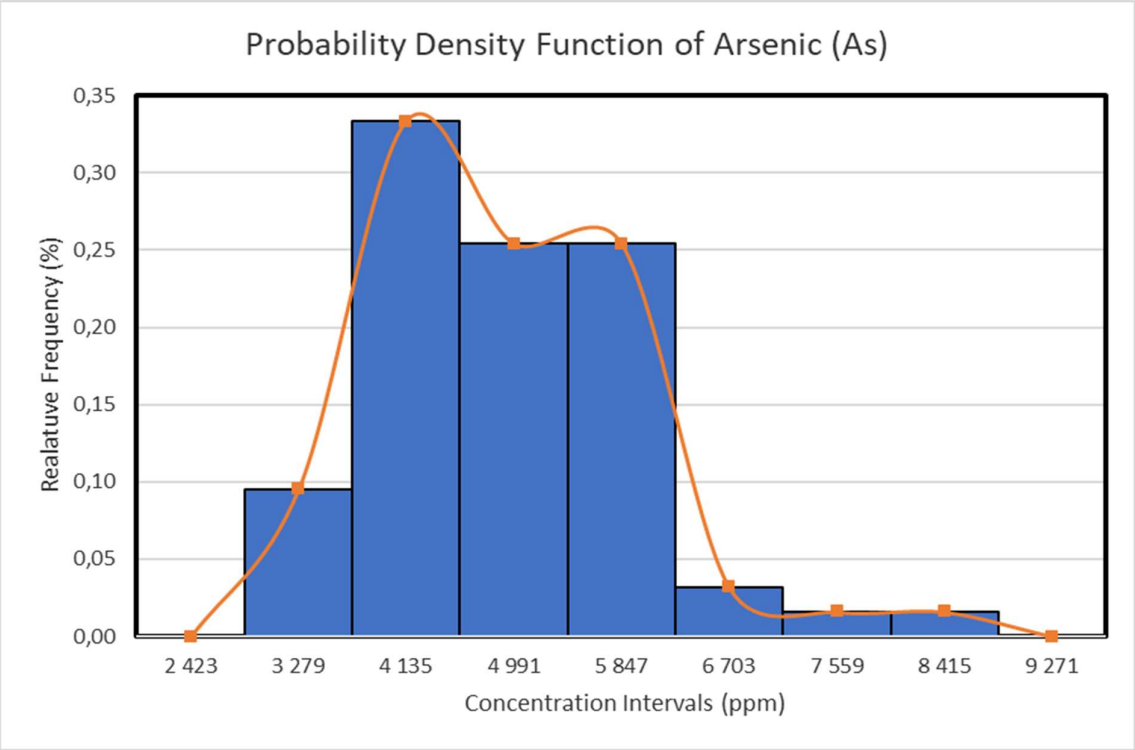

Figure 4.24a: Probability density function of arsenic within Fumani Tailings Dam 2.

Arsenic within tailing dam 1 was characterised by a threshold concentration value of 6631.98 ppm. This allowed the identification of two anomalous values. The values were 7426.84 ppm (P3H1S6) and 8789.51 ppm (P3H1S7). The values were recorded within the third profile blow the 6 meter depth mark. This trend suggested that arsenic concentration might have been higher towards the bottom of the tailings dam.

Further analysis of the vertical distribution of As was done through borehole logs (Fig. 4.24b). The boreholes indicated that arsenic concentration within the first meter of the tailings dam was low compared to concentrations at greater depth. The concentration at the 2 m increased slightly, it then remained constant throughout 2 to 3 m. At 4 m, the concentration increased again and remained relatively constant until the bottom of the tailings dam. This trend gave credence to the hypothesis that arsenic concentrations were higher at the bottom of the tailings dam. This trend was best observed in boreholes P1H1, P1H3, P2H3, P3H1 and P3H2. The overall arsenic trend seems to be increasing with depth.

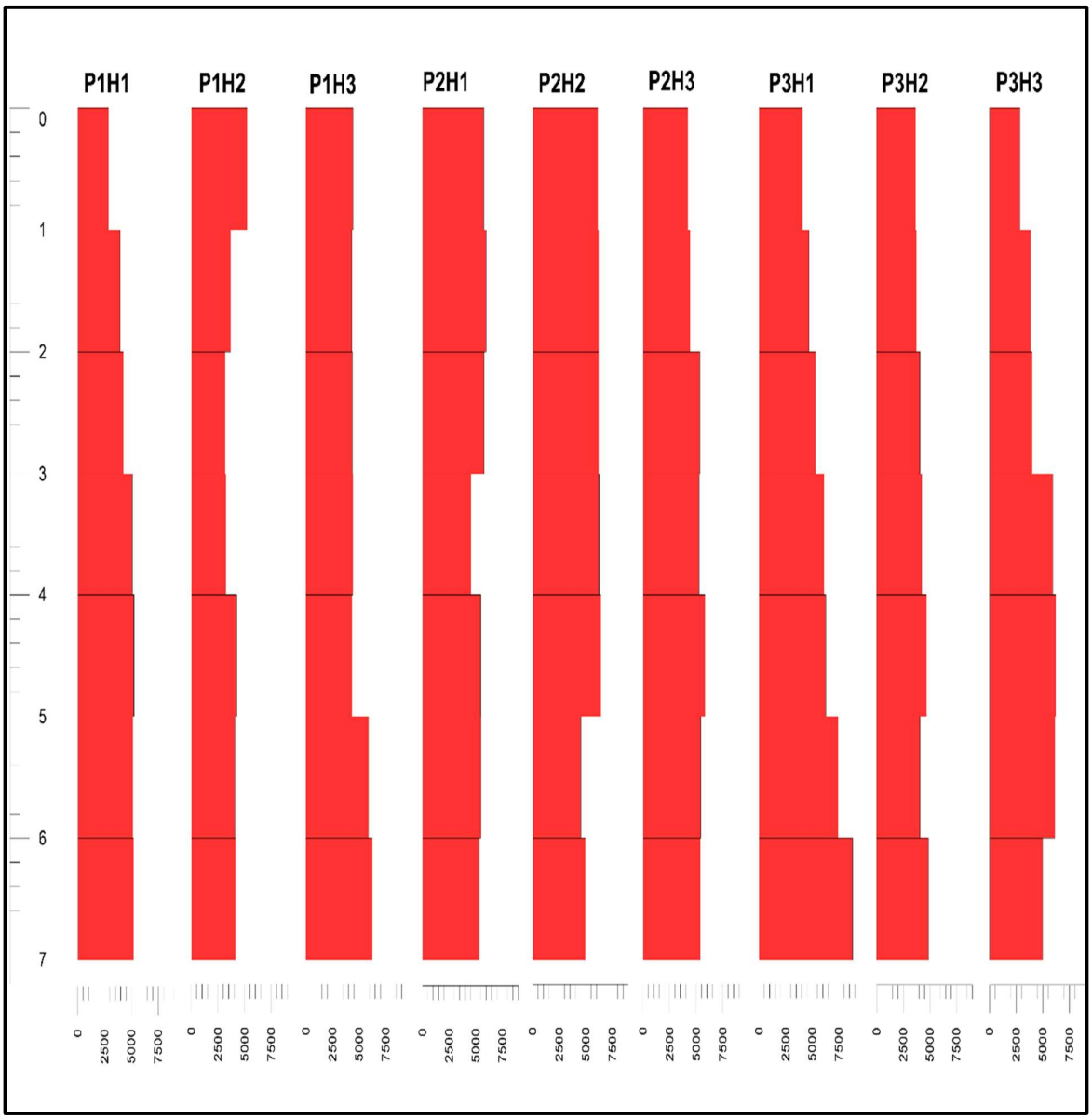

Figure 4.24b: Vertical distribution of As within Fumani Tailings Dam 2.

Lateral Distribution of As

The results of the model represented by the geochemical map indicated that arsenic values were high in the centre with a gradual decrease towards the north and south edge of the tailings dam (Fig. 4.24c). The highest values were observed at P3H1 and P2H2 which were both located in the western half of the tailing dam.

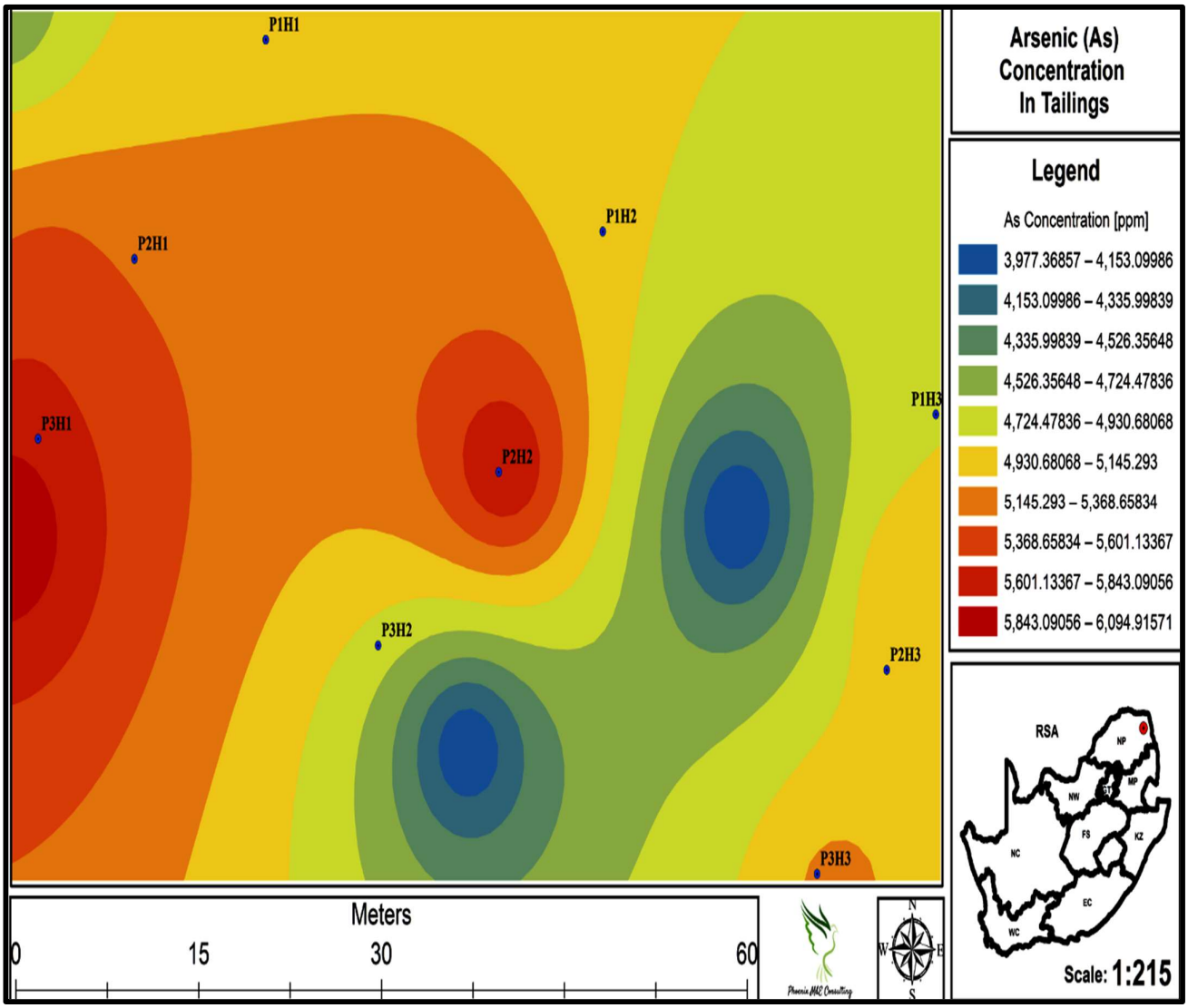

Figure 4.24c: Prediction map of As within Fumani Tailings Dam 2.

Cobalt

Vertical Distribution of Co

Cobalt concentration within Fumani Tailing Dam 2 was characterised by a negatively skewed distribution with a mean of 20,77 ppm (Fig. 4.25a). The distribution indicated that most cobalt values were high with a small proportion of small values. The recorded cobalt values ranged from 7.50 to 27.42 ppm. Majority of the values were recorded between 16.50 ppm and 25.50 ppm.

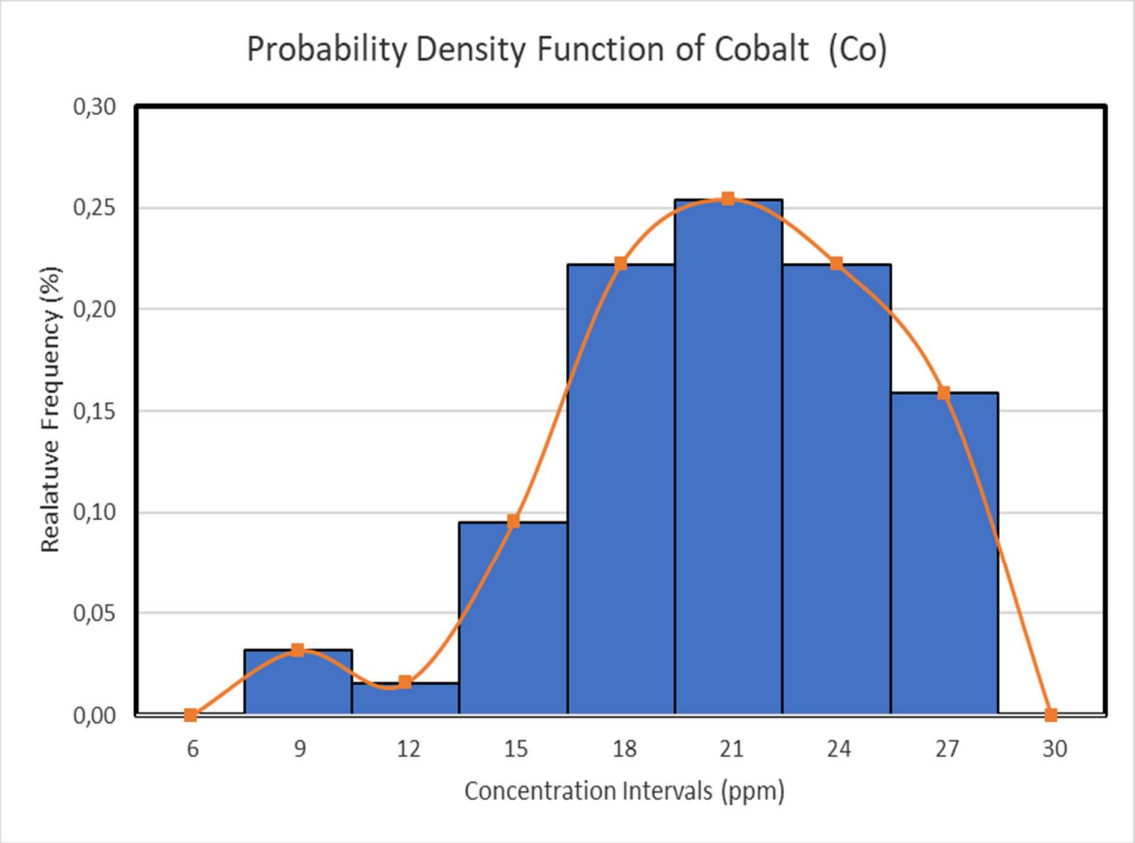

Figure 4.25a: Probability density function of cobalt within Fumani Tailings Dam 2.

Cobalt within the tailing dam had a threshold value of 27.42 ppm. There were no values greater than the recorded threshold vale, hence no Co anomalies within the Fumani Tailings Dam 2. The lack of anomalous values shed no light on the vertically distribution of Co within the Fumani Tailings Dam 2.

Further Co vertical analysis conducted through borehole logs (Fig. 4.25b) indicated that Co concentration was low within the first meter of the tailings dam compared to concentration at greater depth. The concentration at 1 to 2 m increased drastically and thereafter the concentration had a gradual increase in concentration with depth. This trend is best observed in boreholes P3H3. The overall highest values were observed in the first profile below 1 m. The general trend within the tailings dam was erratic with depth.

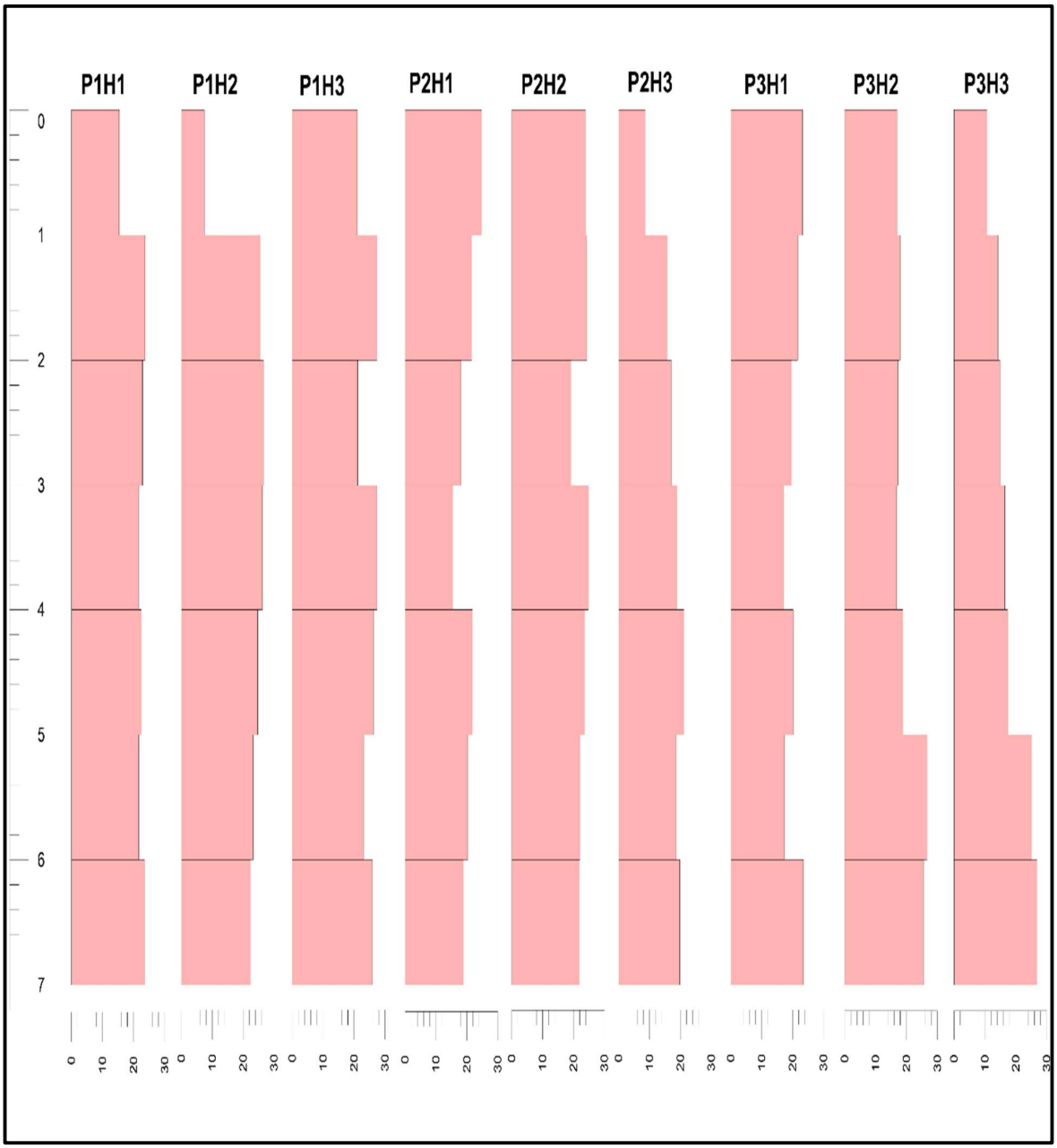

Figure 4.25b: Vertical distribution of Co within Fumani Tailings Dam 2.

Lateral Distribution of Co

The geochemical map indicated that Co had high concnetrations within the north-eastern section of the tailings dam (Fig. 4.25c). The high concentration gradually decreased towards the south and west edges of the tailing dam. The peak concentration within the southern edge of the tailing dam was low. On the other hand the peak concentration within the western edge of the tailing dam was intermediate.

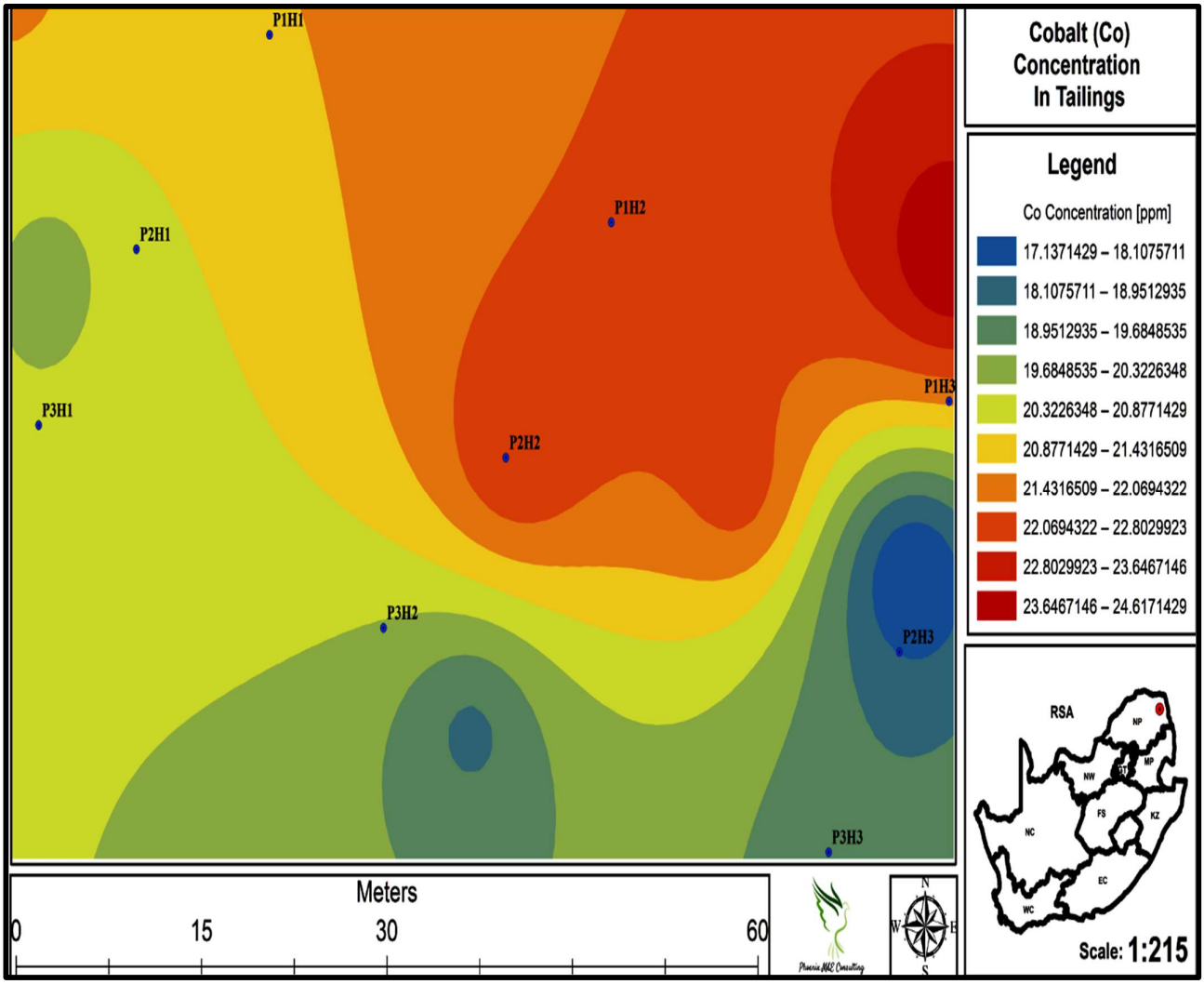

Figure 4.25c: Prediction map of Co within Fumani Tailings Dam 2.

Cadmium

Vertical Distribution of Cd

The vertical distribution of Cd was characterised by negatively skewed distribution with a mean concentration of 0,81 (Fig. 4.26a). The distribution indicated most cadmium values were high with a small proportion of low values. The values ranged from 0.8 to 1 ppm with most values occurring between 0,75 and 1 ppm.

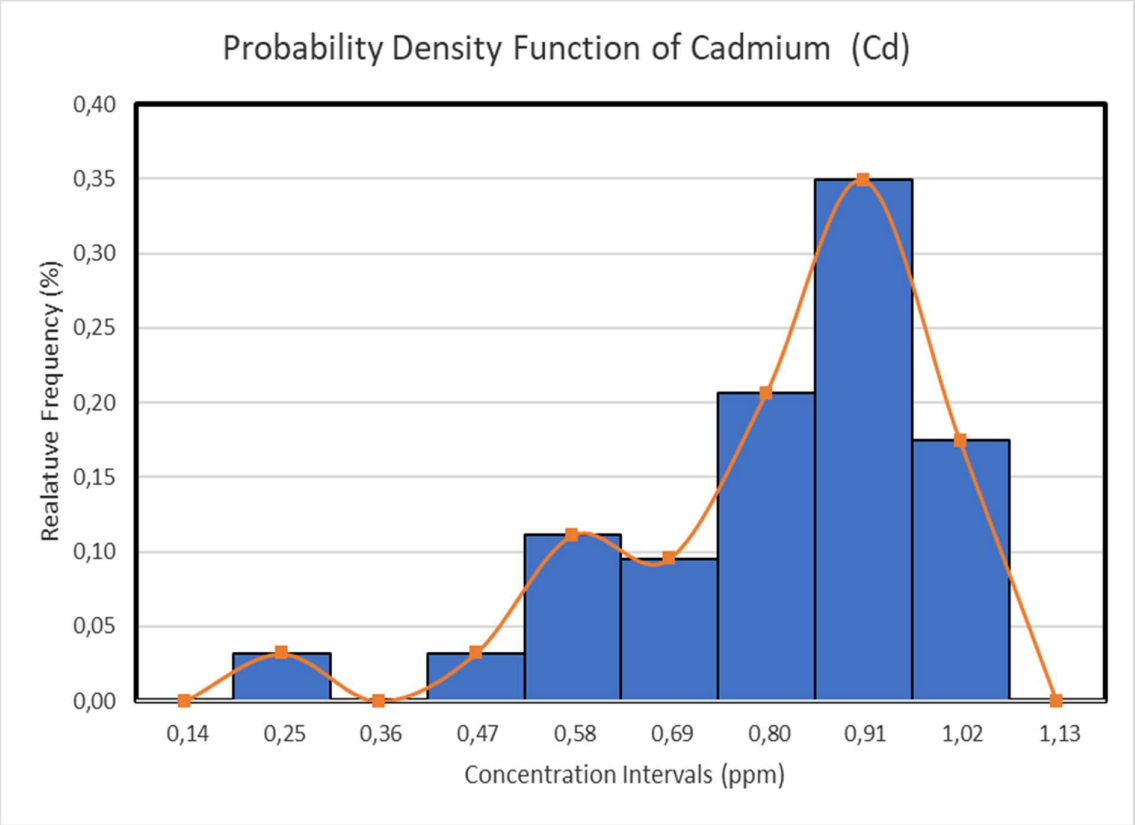

Figure 4.26a: Probability density function of cadmium within the Fumani Tailings Dam 2.

Cadmium within the Fumani Tailing Dam 2 was characterised by a threshold value of 1.06 ppm. at a threshold concentration of this magnitude, the cadmium distribution had no anomalous values. The lack of anomalous values did not provide any insight into the vertical distribution within the tailings.

The vertical distribution of cadmium was further analysed using borehole logs (Fig. 4.26b). The boreholes were characterised by a consistent level of Cd from the top to the bottom of the tailing dam. There were however areas that had slightly higher concentration. The concentration of cadmium at the 1 – 3 m as well as 3 to 5 m appeared to be higher compared to other depths.

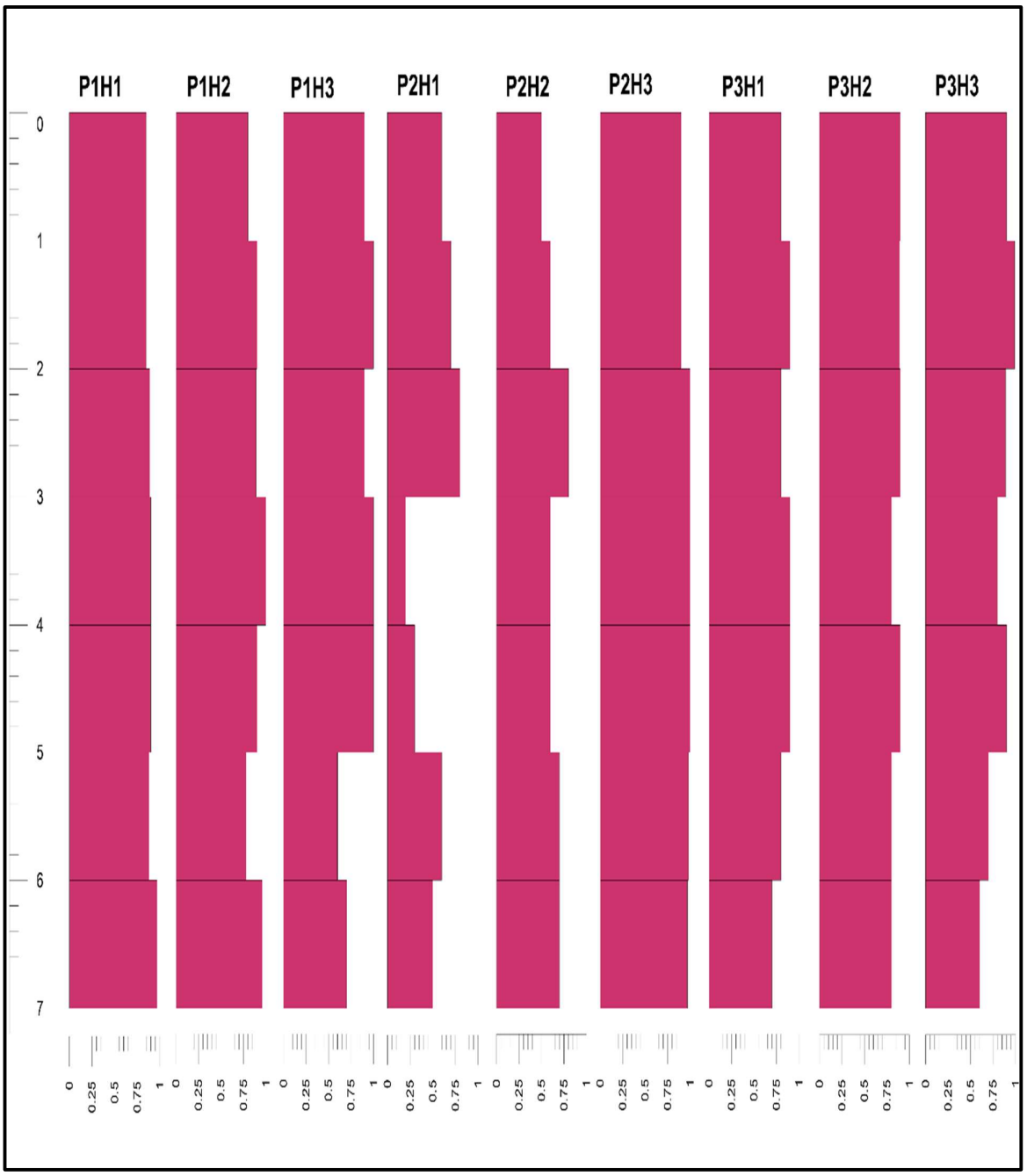

Figure 4.26b: Vertical distribution of cadmium within Fumani Tailing Dam 2.

Lateral Distribution of Cd

The geochemical map indicated that Fumani Tailing Dam 2 had three Cd concentration hotspots. The first hotspot was a high cadmium value located in the north-western edge of the tailing dam (Fig. 4.26c). The high concentration hot spot decreased in concentration towards the south-western section of the tailing dam. The second hotspot was a low cadmium value located in the centre of the tailing dam, this concentration expanded towards the north and south section of the tailing dam. As it expanded, it gradually increased in concentration peaking in the north and south with an intermediate level of cadmium concentration. The third hotspot was in the eastern edge of the tailings dam; it was characterised by a moderately high value that gradually decreased towards the north and south edges of the tailings dam.

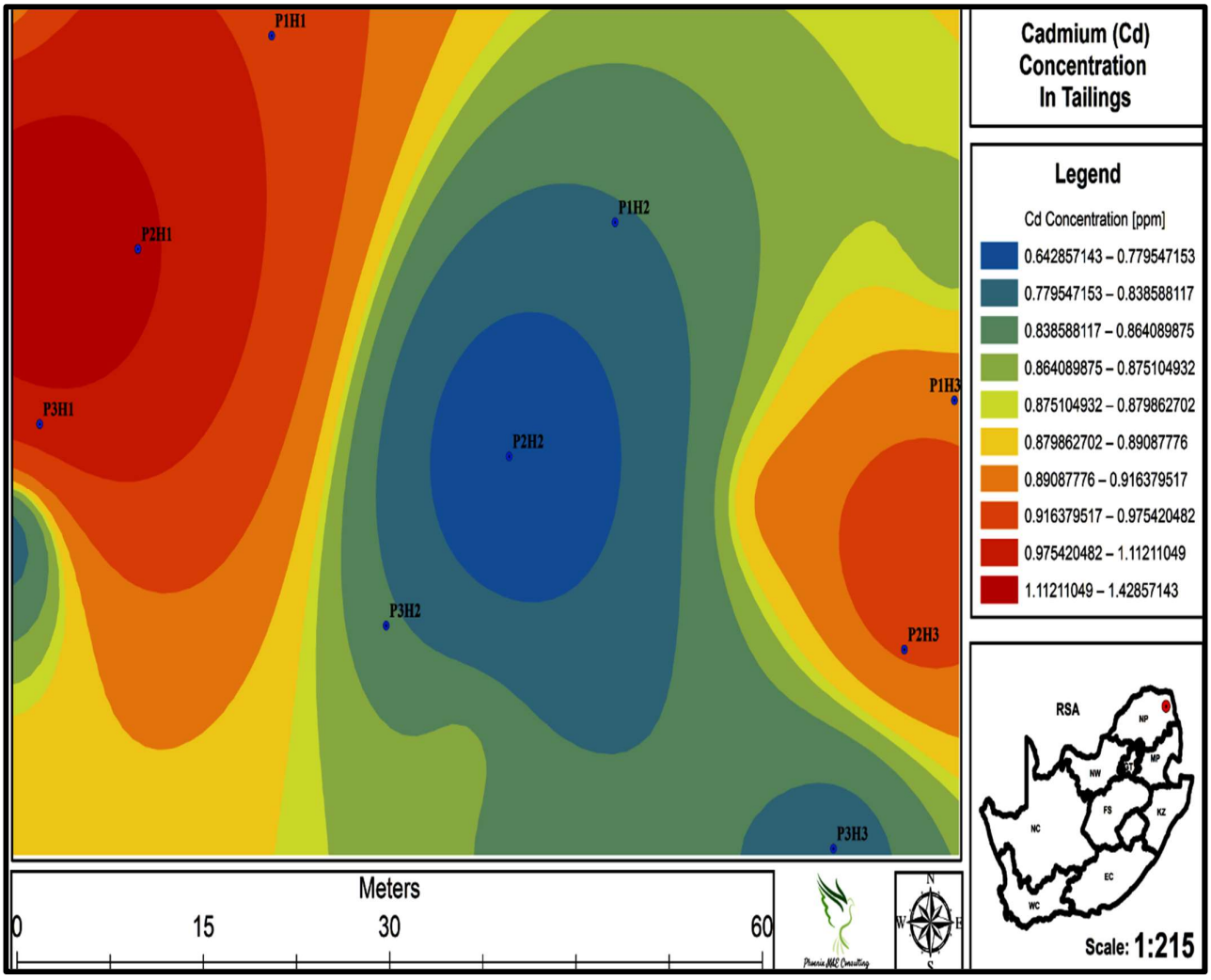

Figure 4.26c: Prediction map of Cd within Fumani Tailings Dam 2.

Chromium

Vertical Distribution of Cr

Chromium distribution within Fumani Tailings Dam 2 was characterised by a negatively skewed distribution with a mean of 72,14 ppm (Fig. 4.27a). The distribution indicated that most chromium values were high with a small proportion of low values. The values ranged from 23.90 to 115.32 ppm. Most of the values occurred between 62.90 and 115 ppm.

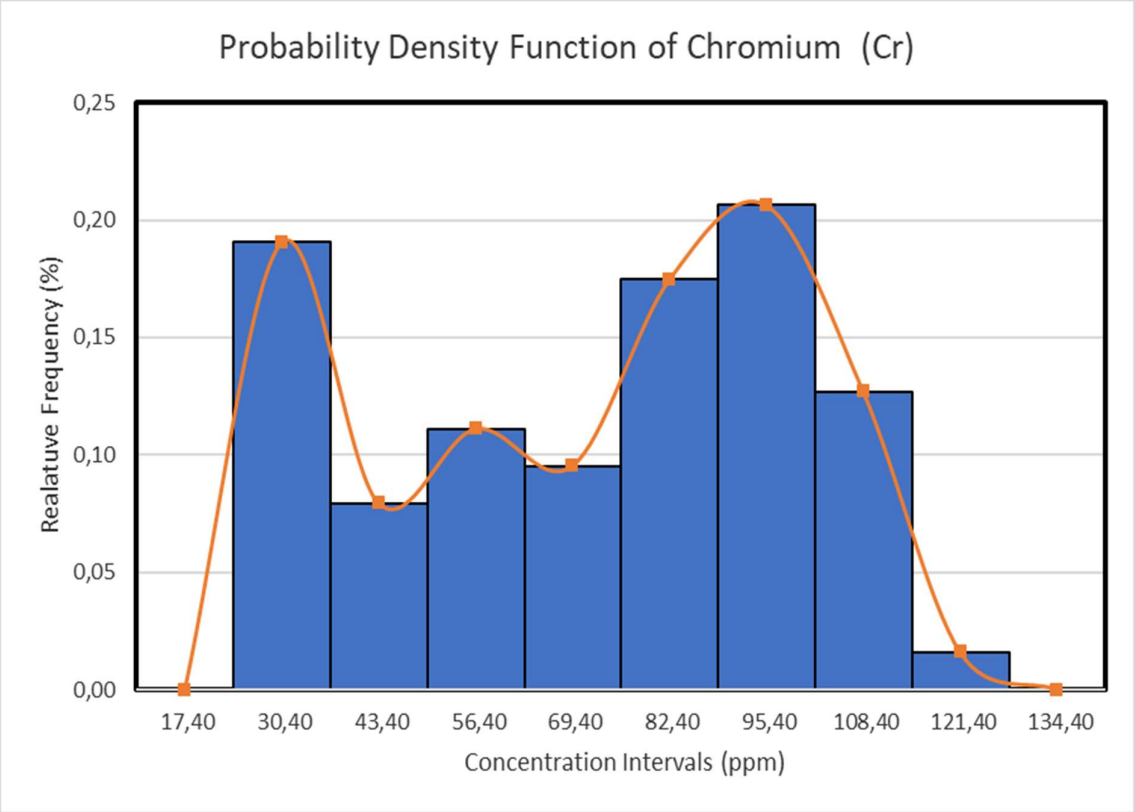

Figure 4.27a: Probability density function of chromium within Fumani Tailing Dam 2.

Chromium distribution within tailing dam 2 was characterised by threshold concentration value of 113.74 ppm. This allowed the identification of one anomalous value of 115.32 sampled from borehole P2H3S4. This did not present sufficient information to make inferences about the vertical distribution of chromium.

Further analysis of the vertical distribution of chromium through boreholes logs (Fig. 4.27b) revealed that the top and bottom of the tailings dam had similar concentrations. The first and last one meter of the tailings dam was characterised by high chromium concentration, with the space in-between characterised by alternating highs and low. The concentration between 1 to 3 m of depth appeared to be high with the concentration between 3 to 5 m exhibiting a sharp decrease in concentration. The concentration increased again at the 6-7 m to match the concentration observed within the first meter of the tailing dam.

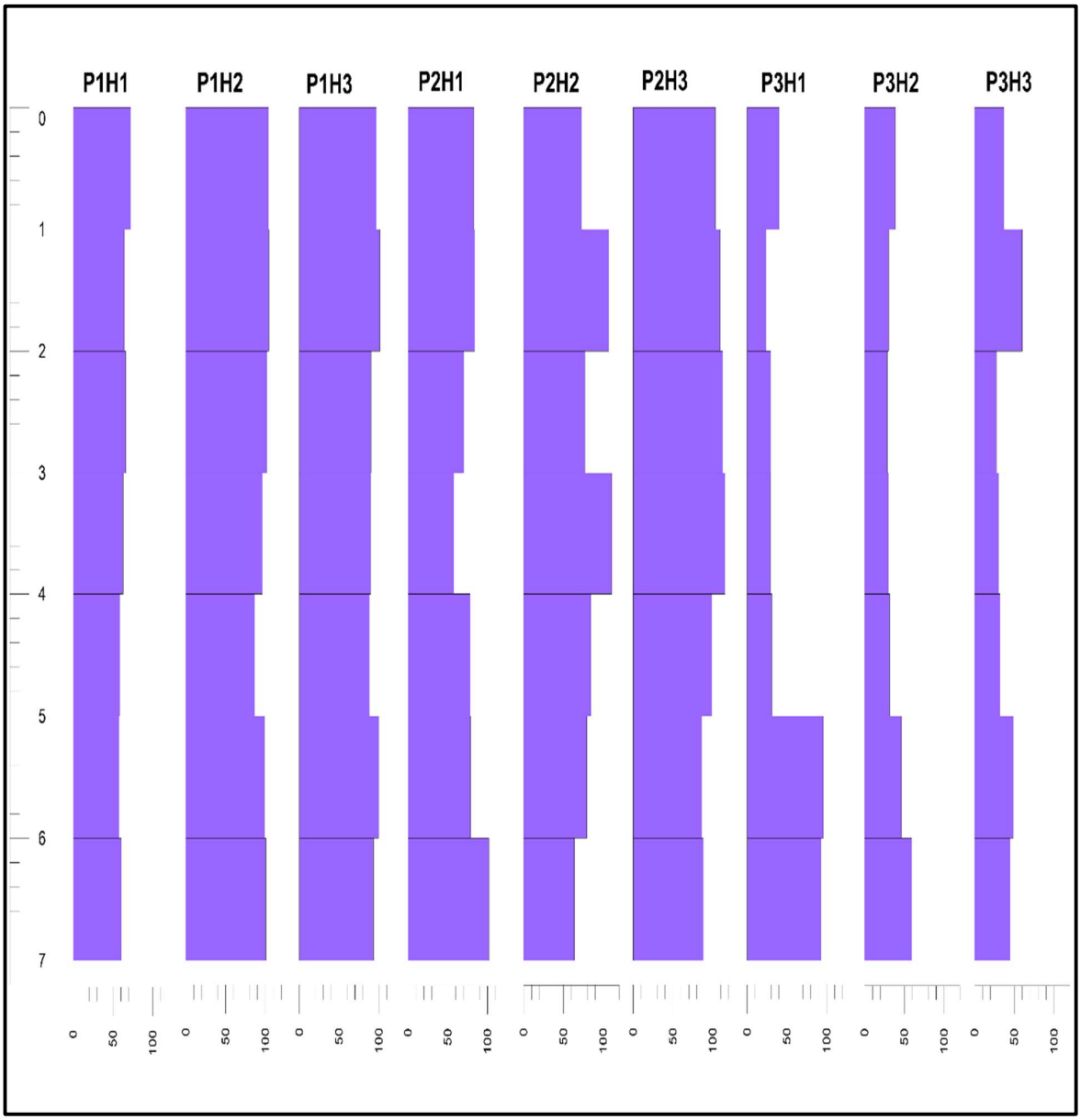

Figure 4.27b: Vertical distribution of Cr within Fumani Tailing Dam 2.

Lateral Distribution of Cr

The geochemical map of Cr within Fumani Tailings Dam 2 revealed highest Cr values within the north-eastern edge of the tailing dam. From there, the concentration gradually decreased in an omni directional manner reaching its low (Fig. 4.27c). west observed concentration in the south-western edge of the tailing dam. It appears the spatial correlation of chromium within the north-west to southeast direction was higher compared to that of the north-east to south-west direction. This hypothesis was made because chromium changed concentration at a less drastic rate in the northwest to southeast direction compared to the northeast to southwest direction.

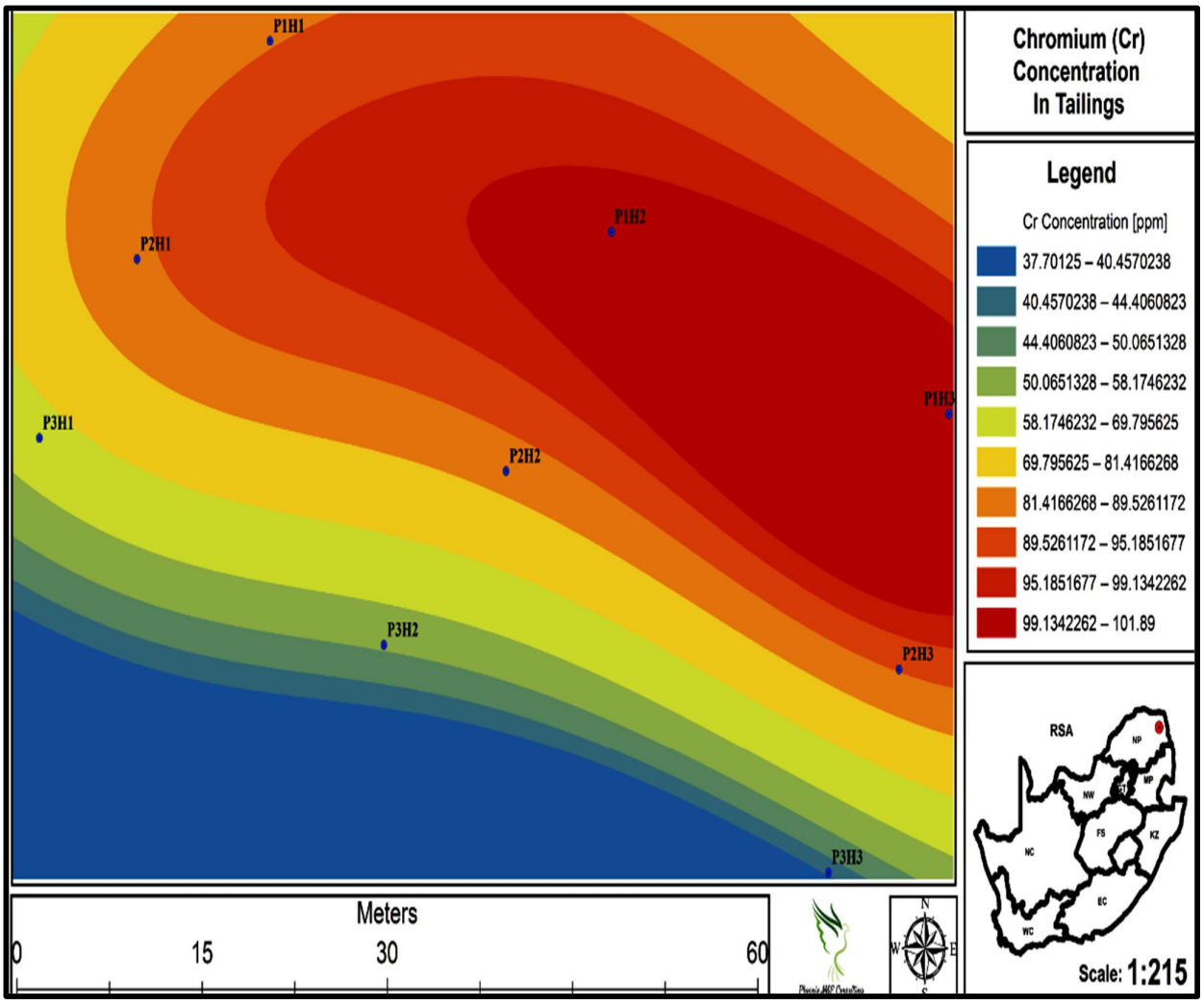

Figure 4.27c: Prediction map of Cr within Fumani Tailings Dam 2.

Nickel

Vertical Distribution of Ni

The vertical distribution of nickel within Fumani Tailings Dam 2 was characterised by a negatively skewed distribution with a mean of 93.25 ppm (Fig. 4.28a). The distribution indicated that most of the recorded nickel values were high values with a small proportion of low values. Recorded nickel values ranged from 8.17 to 148.20 ppm. Most of the recorded values occurred within 48,17 and 128.17.

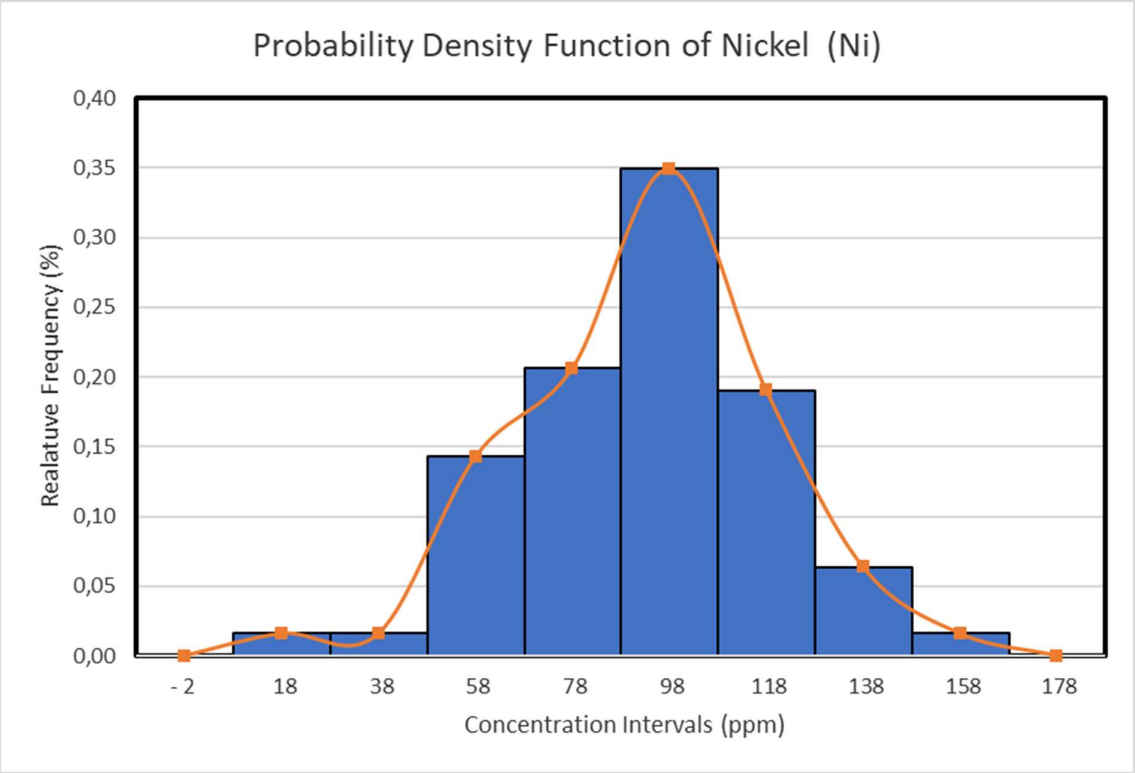

Figure 4.28a: Probability density function of nickel within Fumani Tailing Dam 2.

Nickel distribution within the Fumani Tailing Dam 2 was characterised by a threshold value of 132.06 ppm. At this threshold value, 3 anomalous values were identified. These values were 132.77 (P1H2S3), 136.8 (P2H2S1), and 148.2 (P2H2S2). The values were recorded from samples obtained within the first 3 m of the tailing dam, indicating that the vertical concentration of nickel may be higher at the top of the tailings dam.

The nickel concentrations within the first meter of the tailings dam was characterised by low values as indicated by the borehole logs with exception to P3H1 (Fig. 4.28b). From 1 to 2 m below the tailings dam, the concentration increased. Between 2 and 3 m depth, the concentration became erratic, with four of the nine boreholes experiencing an increase in nickel concentration and the remaining 5 experiencing a decrease in concentration. Thereafter, nickel concentration increased between 3 to 4 m, for the boreholes that had experienced a decrease in concentration between 2 to 3 m and remained constant for the borehole that had experienced an increase in concentration at the 2 to 3 m. Between the 5 to 7 m of depth nickel concentration decreased slightly compared to the concentration at depths above 5 m. In conclusion, the borehole logs revealed that nickel values occurred unpredictably with depth.

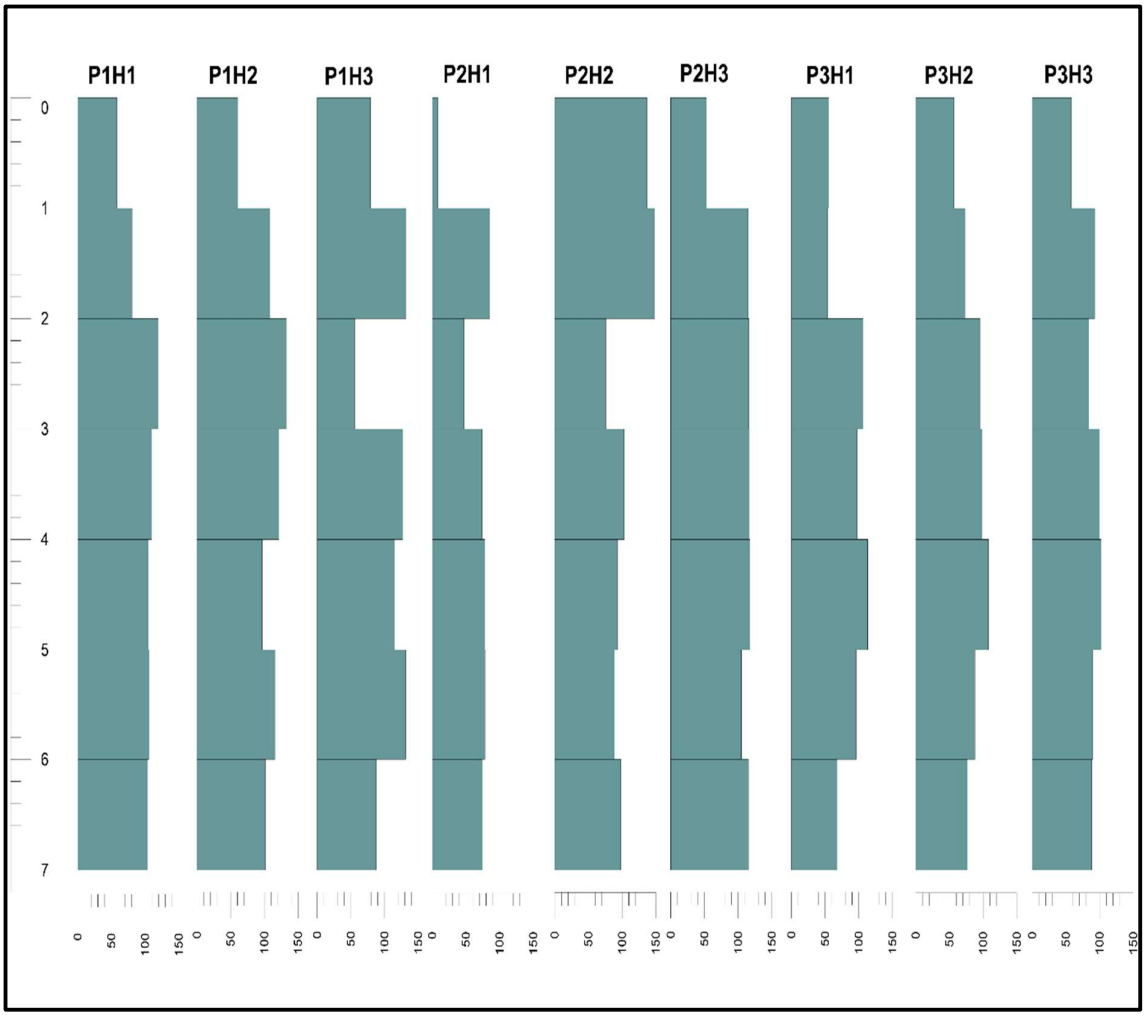

Figure 4.28b: Vertical Distribution of Ni within Fumani Tailing Dam 2.

Lateral Distribution of Ni

The Geochemical map produced for Ni within Fumani Tailings Dam 2 revealed high concentrations located in the center of the tailings dam (Fig. 4.28c). A gradual decrease in high concentration located within the eastern edge of the tailing dam was observed. These high concnetration gradually decreased towards the southwest section of the tailings dam where the lowest concnetration levels of nickel were observed.

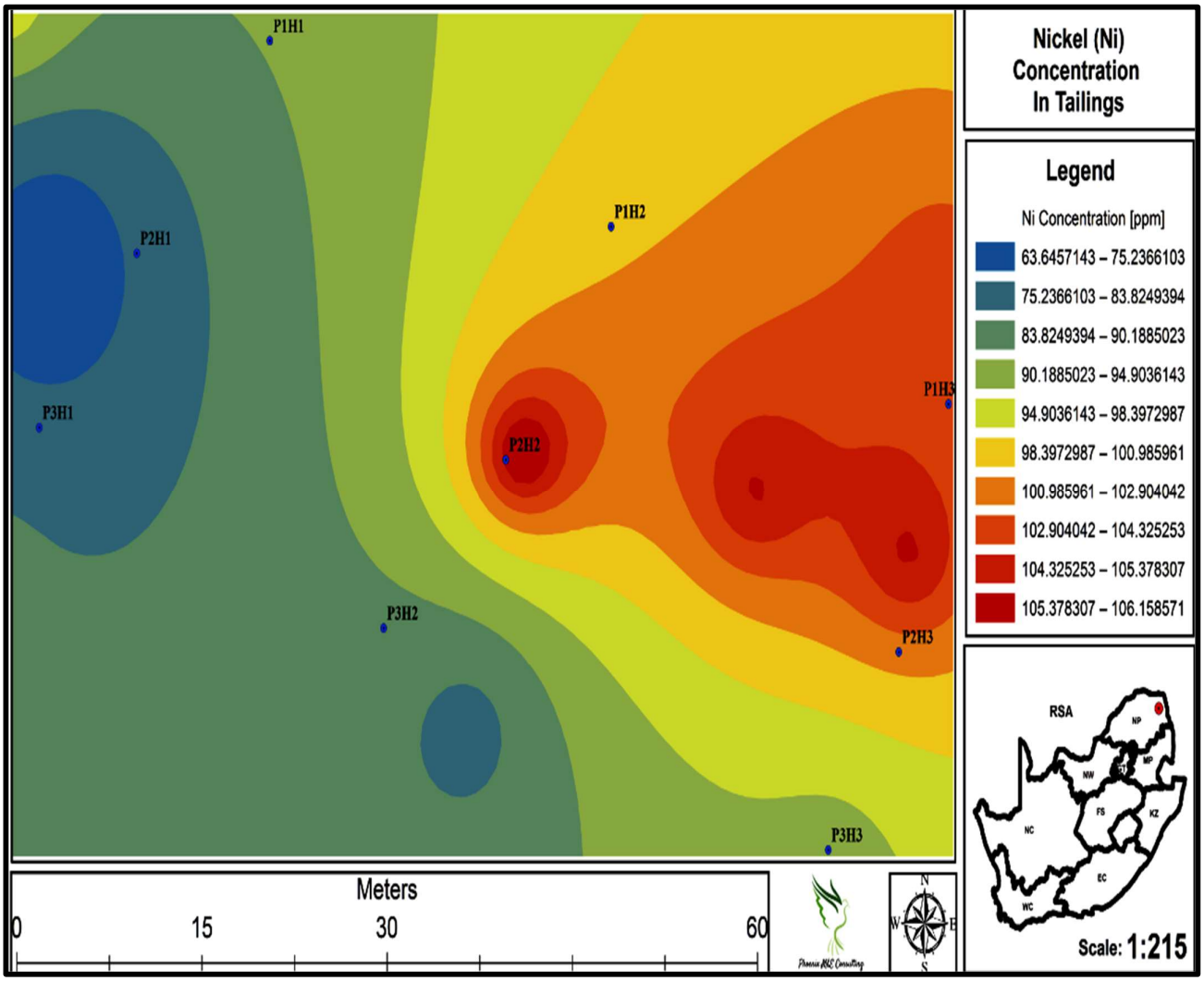

Figure 4.28c: Prediction map of Ni within Fumani Tailings Dam 2.

4.1.3 Pollution Status of Fumani Tailings Dams

The pollution status of the Fumani Tailings Dams 1 and 2 was determined using the Dutch guideline of concentrations in soil, single factor index method, and the soil screening values adapted from the South African government gazzete of the 2nd of May 2014. Several methods for determining the pollution status of the tailings dams were used in order to ascertain their status with a high degree of confidence. The denotations of T1 and T2 will be used to represent concentration of metals in Fumani Tailings Dams 1 and 2 respectively for all methods applied in the study.

4.1.3.1 Dutch Guideline of Standards

The mean and maximum values of metals within the Fumani Tailings Dams 1 and 2were compared to the Dutch guideline of concentrations in soil (Table 2.1). Using the mean obtained from the statistical summary of metals concentrations within the tailings dams (Table 4.1) as well as the Dutch guideline of concentrations in soil, a Table 4.4 was created. From Table 4.4, Pb, Zn, Cd and Cr fell within the A category on both tailings dams. Cu, Co and Ni fell within the B category on both tailings dams. Arsenic on the other hand highly exceeded the C category on both dams.

This simply means that the concentration recorded for Pb, Zn, Cd and Cr were not high enough to contaminate the tailings dams. Copper, Co and Ni concentrations were not high enough to contaminate the tailing dams, but high enough to warrant further investigation. Arsenic highly exceeded the C value of the Dutch guideline of concentrations in soil by 128 and 99.8 times in Fumani Tailings Dams 1 and 2 respectively, and therefore contaminates both tailings dams.

Table 4.4: Dutch Guideline of concentrations in soil combined with the mean of metals in the tailings dams (ppm)

	Pb	Zn	Cu	As	Co	Cd	Cr	Ni
A	50	200	50	20	20	1	100	50
B	150	500	100	30	50	5	250	100
C	600	3000	500	50	300	20	800	500
T1	20,22	101,95	60,49	6383,08	24,75	0,67	71,71	99,35
T2	36,39	96,85	64,48	4989,1	20,77	0,81	72,15	93,25

Using the maximum values of metals within the Fumani Tailings Dam 1 and 2 obtained from the statistical summary of metals concentrations within the tailings dams and the Dutch guideline of concentrations in soil, Table 4.5 was created. T1 and T2 denotes the maximum concentration of metals within the Fumani Tailings Dams 1 and 2 respectively.

Looking at Fumani Tailings Dam 1 maximum values in Table 4.5, Pb and Zn fall within the A category, Cu, Co, Cd and Cr fall within the B category, Ni falls within the C category while As highly exceeds the C category limits. This implies that the maximum Pb and Zn concentrations in Fumani Tailings Dam 1 apparently do not contaminate the tailings dam, with Cu, Co, Cd and Cr still within the allowable limits, however, further investigation is required. A site clean-up is required for Ni. Arsenic on the other had highly exceeds the C value and therefore contaminates the Fumani Tailings Dam 1 and requires clean up.

Looking at Fumani Tailings Dam 2 maximum values in Table 4.5, Zn and Cd fall within the A category, Pb, Cu, Co, and Cr fall within the B category, Ni falls within the C category whilst As highly exceeds the C category limits. This implies that the maximum Zn and Cd concentrations in Fumani Tailings Dam 2 apparently do not contaminate the tailings dam, with Pb, Cu, Co, and Cr still within the allowable limits, however, further investigation is required. A site clean-up is required for Ni. Arsenic on the other had highly exceeds the C value and therefore contaminates the Fumani Tailings Dam 2 and requires clean up.

Table 4.5: Dutch Guideline of concentrations in soil combined with the maximum values of metals in the tailings dams (ppm)

	Pb	**Zn**	**Cu**	**As**	**Co**	**Cd**	**Cr**	**Ni**
A	50	200	50	20	20	1	100	50
B	150	500	100	30	50	5	250	100
C	600	3000	500	50	300	20	800	500
T1	49,8	180,7	82,3	9732,6	43,7	1,1	107	147,9
T2	64,31	182,5	85	8789,51	27,42	1	115,32	148,2

Both tailings dams require a site clean-up for Ni and As since they contaminate the tailings dams. Arsenic is more than 100 times than the required limit in both tailings dams.

4.1.3.2 Single Factor Index Method (SFIM)

The SFIM incorporated the mean and maximum values of tailings and the Dutch Guideline of concentrations in soil to determine the quality index of the pollutant in the Fumani Tailings Dams 1 and 2. The Pollution Index (Pi) was calculated using the formula: Pi= Ci/Si, where Pi is the pollution index, Si is the Dutch Guideline of concentrations in soils and Ci is the value of the metal within the tailings dam. For this work, Si is the B class values of the Dutch Guideline of Standards. This is because investigation of contamination must be done in the B class as A class probably does not contaminate the tailings and C class contaminates the tailings.

Assessment standard states that:

Pi equals or less than 0.7 = tailings probably not contaminated

Pi between 0.7 and 1 = concentration within environmental quality standard

Pi between 1 and 2= concentration beyond environmental quality standard, light pollution

Pi between 2 and 3 = Moderate pollution

Pi greater than 3 = heavy pollution and requires clean up

The Dutch guideline of concentrations in soil (Table 2.1) together with the mean of metals within the Fumani Tailings Dams 1 and 2 obtained from Table 4.2 were combined to create Table 4.6 in order to determine the pollution status of the tailings dams using the SFIM.

From Table 4.1.6, Pb, Zn, Cu, Co, Cd and Cr had a Pi of less than 0.7 in both tailings dams. This means that these metals probably do not contaminate the tailings dams. Nickel had a Pi of 0.99 and 0.93 in T1 and T2 respectively. These values are still within the environmental quality standard as they do not cause any harm to the environment or human health, however monitoring must be done to ensure Ni concentration in both dams does not exceed.

Arsenic exceeds Pi of 3 by 71 and 55times in T1 and T2 respectively. This means that As highly contaminates both tailings dams and poses a high threat to human health as well as the environment. A clean-up of this metal is urgently required on both tailings dams.

Table 4.6: Environmental quality index of mean values of metals in the tailings dams (ppm)

	Pb	**Zn**	**Cu**	**As**	**Co**	**Cd**	**Cr**	**Ni**
Si	150	500	100	30	50	5	250	100
T1Ci	20,22	101,95	60,49	6383,08	24,75	0,67	71,71	99,35
T1Pi	0,13	0,2	0,6	212,77	0,5	0,134	0,29	0,99
T2Ci	36,39	96,85	64,48	4989,91	20,77	0,81	72,15	93,25
T2Pi	0,24	0,19	0,64	166,33	0,42	0,16	0,29	0,93

The Dutch guideline of concentrations (Table 2.1) together with the maximum value of metals within Fumani Tailings Dams 1 and 2 obtained from Table 4.2 were combined to create Table 4.7 to determine the pollution status of the tailings dams using the SFIM. From Table 4.6, Pb, Zn, Cd and Cr had a Pi of less than 0.7 in both tailings dams. Therefore, these metals apparently do not contaminate the tailings dams. Copper had a Pi that lied between 0.7 and 1in both tailings dams. This means that it is still within the environmental quality standard, and it does not cause any harm to the environment or human health. Cobalt Pi was less than 0.7 in T2 but was between 0.7 and 1 in T1. This means that Co probably does not contaminate both tailings dams.

Nickel had a Pi of 1.48 in both tailings dams, this means that the maximum concentration of Ni is a threat to the environment as well as human health and requires a clean-up in both dams. Arsenic exceeds the Pi of 3 by 108 and 98 times in tailings dams 1 and 2 respectively. This means that As highly contaminates both tailings dams and requires an urgent clean up.

Table 4.7: Environmental quality index of maximum values of metals in the tailings dams (ppm)

	Pb	Zn	Cu	As	Co	Cd	Cr	Ni
Si	150	500	100	30	50	5	250	100
T1Ci	49,8	180,7	82,3	9732,6	43,7	1,1	107	147,9
T1Pi	0,33	0,36	0,82	324,42	0,95	0,22	0,43	1,48
T2Ci	64,31	182,5	85	8789,51	27,42	1	115,32	148,2
T2Pi	0,43	0,37	0,85	292,98	0,55	0,2	0,46	1,48

Based on the SFIM, Ni slightly contaminates both the tailings dams on both mean and maximum concentration, however, it is still within the limits and does not cause any harm to the environment and human health. Arsenic on the other hand highly contaminates both the tailings Dams and requires a clean-up urgently.

4.1.3.3 South African Guideline of Standards

The soil screening value used for determining the pollution status of Tailings Dam 1 were adopted from the South African Government Gazette of 2014 and incorporated with the mean and maximum metal values to create Table 4.8.

From Table 4.8, it can be seen that Zn, Co and Cd do not require clean up in both tailings dams, they fall within the limits suitable for all land-use. The mean and maximum values of Pb, Cu and Ni exceeds the limit of land-uses protective of the water resources in both dams. The maximum and mean values of Cu in both dams highly exceed the limit of land-uses protective of water resources as well as that of the ecosystem and health. Arsenic and Cr values exceed all the required concentrations for all land-uses. It can be said with confidence that a clean-up for As and Cr is needed for both tailings dams. Since the tailings dams are located close to the river, it is important to monitor and clean up all values exceeding the limits of land-uses protective of water resources.

Table 4.8: Soil Screening values for different land-uses with mean and maximum values of metals in the tailings dams (ppm)

	All land-uses protective of the water resources (ppm)	Informal residential areas (ppm)	Standard residential areas (ppm)	Commercial industrial (ppm)	Protection of ecosystem and health (ppm)	Mean values of metals within tailings (ppm)		Maximum values of metals within tailings (ppm)
Pb	20	110	230	1900	100	T1	20.22	49.8
						T2	36.39	64.31
Zn	240	9200	19000	150000	240	T1	101.95	180.7
						T2	96.85	182.5
Cu	16	1100	2300	19000	16	T1	60.49	82.3
						T2	64.48	85
As	5.8	23	48	150	580	T1	6383.1	9732.6
						T2	4989.9	8789.5
Co	300	300	630	5000	22000	T1	24.75	43.7
						T2	20.77	27.42
Cd	7.5	15	32	260	37	T1	0.67	1.1
						T2	0.81	1
Cr	6.5	6.5	13	40	260	T1	71.71	107.00
						T2	72.15	115.32
Ni	91	620	1200	10 000	1 400	T1	99.35	147.9
						T2	93.25	148.2

Based on all three methods used to determine the pollution status of the Fumani Tailings Dams 1 and 2, it can be said with confidence that As heavily pollute the tailings dams and require an urgent clean-up as they poses a threat to human health as well as the environment. Nickel also slightly pollutes the tailings and requires a clean-up. Pb, Ni and Cr are above the limit for water resources and may contaminate the nearby river.

4.2 Soil

In order to assess the dispersion of metals from the Fumani Tailings Dams, it was crucial to assess the distribution of metals around the Fumani Tailings Dams in order to determine if the tailings dams pollute its surrounding area.

4.2.1 Distribution of Metals Around the Fumani Tailings Dams

4.2.1.1 Statistical Analysis and Calculations

The distribution of metals in soils within 5 km from the Fumani Tailings Dam in all four directions is listed in appendix C2, whilst the statistical analysis is displayed in Table 4.9. The data was obtained from XRF analysis, and the summary was derived from data using equations 4.1 to 4.5 to calculate the range, mean, variance, standard deviation and threshold.

Table 4.9: Statistical summary for XRF analytical data of metals in soil (ppm)

	Pb	Zn	Cu	As	Co	Cd	Cr	Ni
Maximum	16581,00	404,10	208,60	1779,70	50,90	0,10	1988,80	2296,90
Minimum	24,10	19,80	10,30	2,60	4,00	0,00	41,70	46,90
Range	16556,90	384,30	198,30	1777,10	46,90	0,10	1947,10	2250,00
Mean	464,67	74,87	75,74	49,87	18,68	0,02	399,15	422,23
Variance	4762637,71	2389,95	1636,85	54868,45	101,51	0,00	184919,31	266197,58
Standard Deviation	2182,35	48,89	40,46	234,24	10,08	0,04	430,02	515,94
Threshold	3738,19	148,20	136,43	401,23	33,79	0,08	1044,18	1196,15

From the statistical summary, it can be said that the data set around the Fumani Tailings Dam could either be spread out or have a few areas that are highly anomalous as the range and variance is quite huge for all the metals with exception to Cd. This indicates that some areas have very low values whilst other areas have very high values of the Metals. Cadmium values seem to be relatively constant throughout all the traverses with no extremely high values in other places. This equally means that the data is not spread out for Cd.

4.2.1.2 Correlation Matrix of Metals in Soil around Fumani Tailings Dams

The correlation relationship rule of thumb states that if the correlation coefficient is greater than $2/\sqrt{n}$, then the relationship exists between the two elements where n is the number of samples.

Since a total of 77 soil samples were collected around the Fumani Tailings Dams 1 and 2 , $2/\sqrt{77} = 0.228$, hence, for every r greater than 0.228 and less than -0.228, there is a relationship that exists between those two elements. Of the 28 correlation coefficients generated, only 15 relationships exist (Table 4.10). A fair to strong correlation exists between the following pairs respectively: 0.232 (Zn-As and Zn-Pb), 0.279 (Ni-Zn), 0.417 (Cr-Zn), 0.431 (Ni-Cu), 0.468 (As-Co and Co-Pb), 0.525 (Cr-Cu), 0.540 (Cu-Zn), 0.577 (Co-Zn), 0.683 (Ni-Co), 0.759 (Co-Cu), 0.769 (Cr-Co), 0.959 (Ni-Cr) and a perfect correlation of 1 exists between As and Pb.

Table 4.10: Correlation matrix of the Metals around the Fumani Tailings Dams

	Pb	Zn	Cu	As	Co	Cd	Cr	Ni
Pb	1							
Zn	0,232	1						
Cu	0,14	0,54	1					
As	1	0,232	0,14	1				
Co	0,468	0,577	0,759	0,468	1			
Cd	-0,098	-0,097	-0,094	-0,098	-0,196	1		
Cr	0,084	0,417	0,525	0,084	0,769	-0,143	1	
Ni	0,022	0,279	0,431	0,022	0,683	-0,15	0,959	1

4.2.1.3 Distribution of Metals around the Fumani Tailings Dams

The distribution of metals around the Fumani Tailings Dams was based on the XRF results of the metals around the tailings dams and represented through distribution graphs and prediction maps produced from ordinary kriging. T1, T2, T3 and T3 were used to denote Traverse 1, 2, 3 and 4 respectively.

Lead

The values of Pb around the Fumani Tailings Dams spread from 24.1 ppm to 16581 ppm, giving a range of 16556.9. The high range indicates values are more spread out with a high variability in the distribution. The high variability led to the use of a logarithmic scale in the creation of the bar graph (Fig. 4.29a) to also allow the smaller values to appear within the graph.

The threshold value of Pb was found to be 3738.19 ppm. Out of the 77 samples collected, only three anomalous values of 16581, 5389.6 and 8586.9 ppm were observed at sampling points T1S3, T1S4 and T1S5 respectively. All anomalous values were observed at T1.

The highest Pb values at T1 were the anomalous values, followed by 259.4 ppm located at T1S8, this indicates a huge difference between the anomalous values and the following highest value. This means that the anomalies could have been from the tailings dams as well as from a different source of Pb as there is a sharp change between the anomalous areas and the areas around it. The anomalous values of Pb were lower than those found within the tailings dams, confirming a new source of Pb. The lowest Pb value recorded at T1 was 80 ppm.

The highest Pb value in T2 was 346.3 ppm, recorded at T2S1. The second largest value recorded in T2 was 112.5 ppm recorded at T2S2, with the rest of the values occurring at less than 80 ppm. The lowest value of Pb recorded in T2 was 24.9 ppm located at T2S18.

The highest Pb value recorded in T3 was 519.4 ppm followed by 105.3 ppm located at T3S5 and T3S11 respectively. The remaining Pb values within this traverse were less than 94 ppm. The lowest Pb value recorded in T3 was 26.1 ppm.

The highest value of Pb recorded in T4 was 177.7 ppm followed by 111.4 ppm then 100.3 ppm recorded at T4S8, T4S6 and T4S2 respectively. The remaining Pb values within this traverse were less than 63 ppm. The lowest value of Pb recorded was 24.1 ppm which was the lowest value within the entire study area.

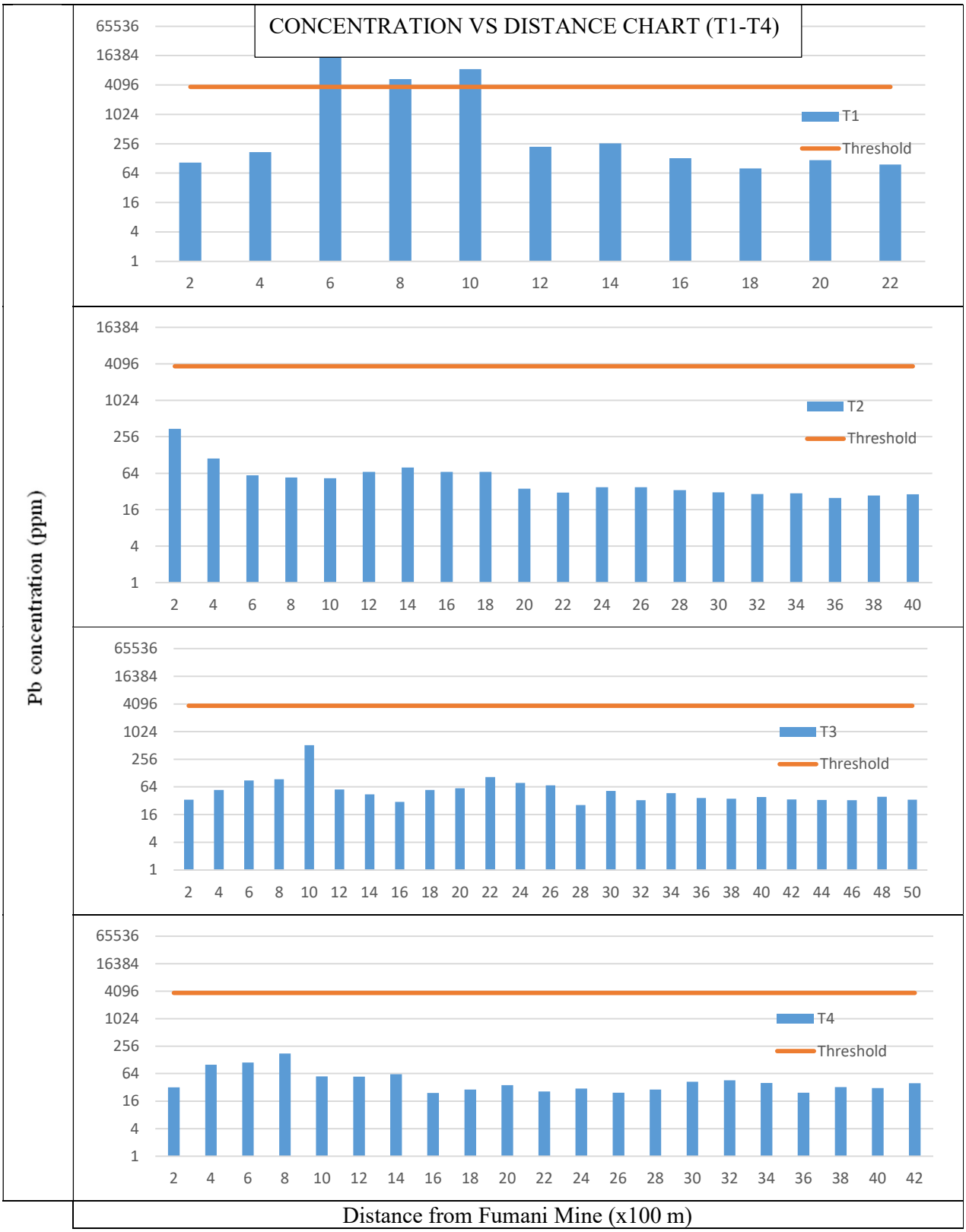

Figure 4.29a: Distribution of Pb (ppm) along the 4 traverses.

The geochemical map was used to analyse the lateral distribution of Pb around the Fumani Tailings Dams. The geochemical map indicates high Pb values at the eastern part of the map which is within the vicinity of the Fumani tailings dams. The concentration of Pb gradually decreased with increase in distance from the Fumani Tailings Dams (Fig. 4.29b).

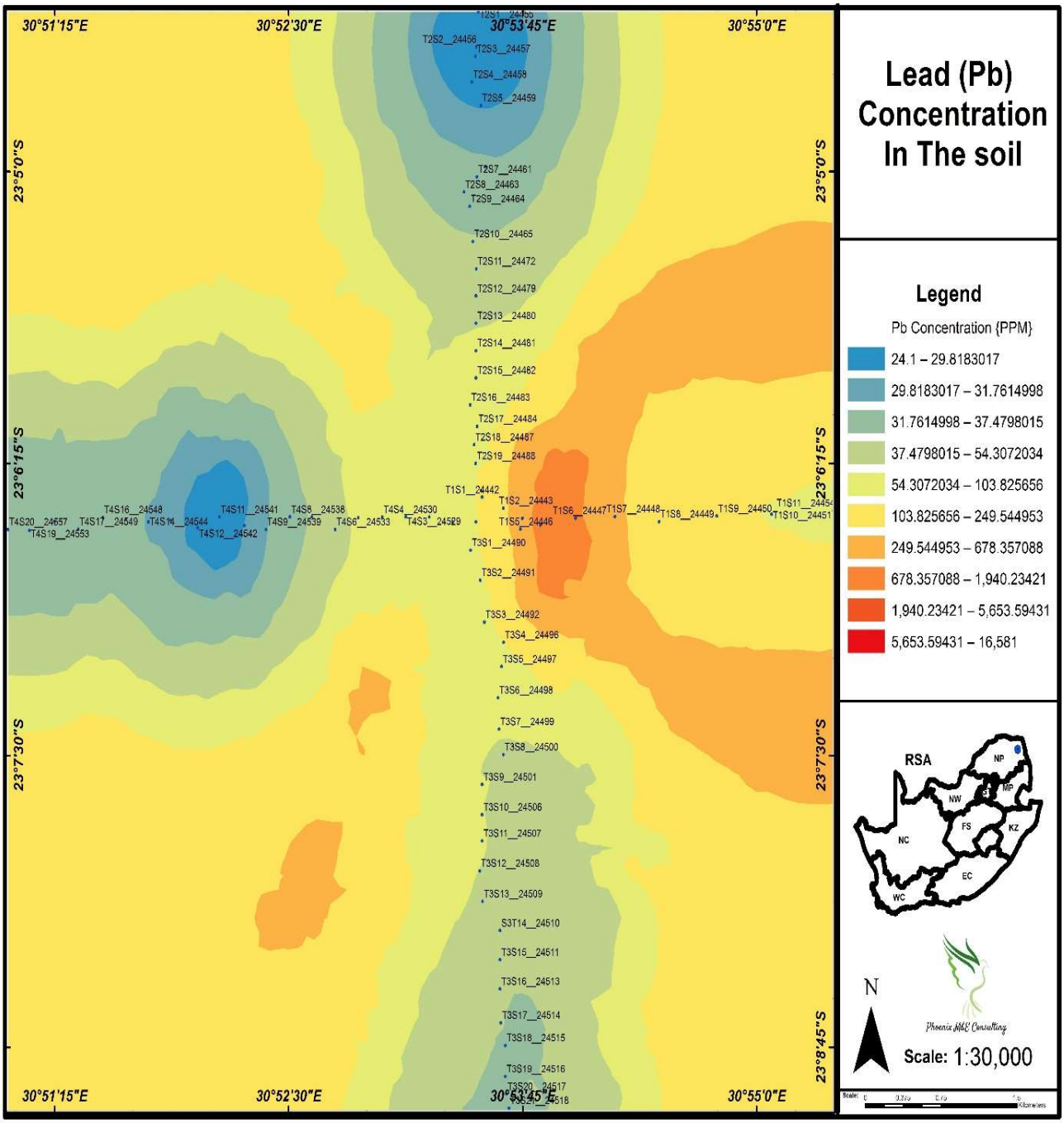

Figure 4.29b: Prediction map of Pb on soils around the Fumani Tailings Dams.

Distribution of Zn

The concentration of Zn around the Fumani Tailings Dams ranged from 19.8 ppm to 404.1 ppm giving a range of 384.3 giving a small variability hence the use of normal scale bar graphs. the lowest value was found at T4S16 about 3200 m away from the tailings dams. The highest value of Cu was found at T2S4 which was about 800 m away from the tailings dams.

The threshold value was found to be 148.2 ppm and all values above it was considered as anomalous (Fig. 4.30a). Out of all the 77 samples collected, only 2 samples were found to have anomalous values of Zn, one in t1 and the other one in T2. No anomalous values were observed in T3 and T4.

The values of Zn in T1 ranged from 63.4 ppm to 205.1 ppm at T1S12 and T1S4 respectively. The highest value in T1 was found to be the only anomalous value within this traverse. The general trend within T1 seems to not have been clearly defined.

The values of Zn in T2 ranged from 30.3 ppm to 404.1 ppm at T2S16 and T2S4 respectively. The highest value in this traverse was found to be the only anomalous value within T2, and the highest Zn value recorded in the entire study area. The Zn values seem to increase from T1S1 up until it reaches the highest value at T2S4, the values then suddenly dropped to 76 ppm in T2S5 and all values that followed were less than 100 ppm up to the end of the traverse. Indicating a sharp contact between the anomalous area and the surrounding area.

Zinc values in T3 ranged from 32.7 ppm to 110.6 ppm at T3S14 and T3S19 respectively. There were no anomalous values in this traverse. The general trend within this traverse seems to be erratic and follow no pattern.

The values of Zn in T4 ranged from 19.8 ppm to 102.8 ppm at T4S16 and T4S2 respectively. The lowest value recorded in T4 was the lowest value in the entire study area around the tailings dams. There was no anomalous value within this traverse. The general trend within T4 seems to be erratic and follow no pattern.

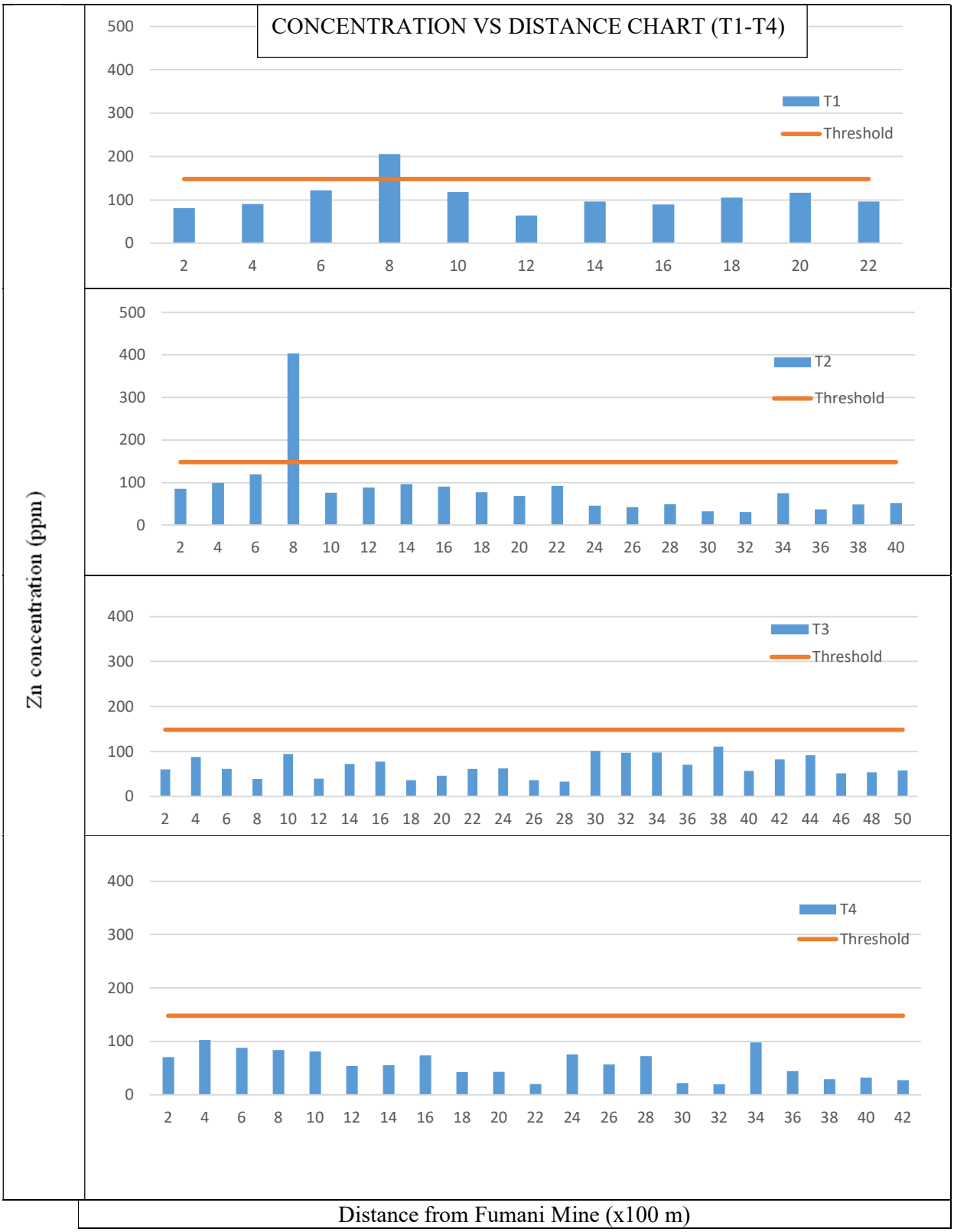

Figure 4.30a: Distribution of Zn (ppm) along the 4 traverses.

The prediction map confirms that the high Zn concentrations are located at T1 and T2 that lie on the northern and eastern part of the Tailings dams, with low Zn concentrations on the western and southern part of the Fumani Tailings Dams as indicated on the Zn bar graphs (Fig. 4.30b).

The northern part of the tailings dams indicates high Zn values from about T2S1 to T2S6. The concentrations then gradually decrease from T2S7 up to T2S20. The eastern part of the tailings dams seemed to have a relatively constant Zn Concentration with few slightly higher concentrations around T1S3-T1S6 and T1S10.

The western part from the tailings dams indicates Zn concentrations gradually decreasing with increase in distance from the tailings dams. The southern part of the tailings dams indicates a gradual decrease from the tailings dams with increasing distance from T3S1 to T3S13, the concentrations then start to gradually increase and decrease again. The general trend depicted from the map indicates higher concentrations closer to the tailings dams and lower concentrations with increase in distance from the Fumani Tailings Dams.

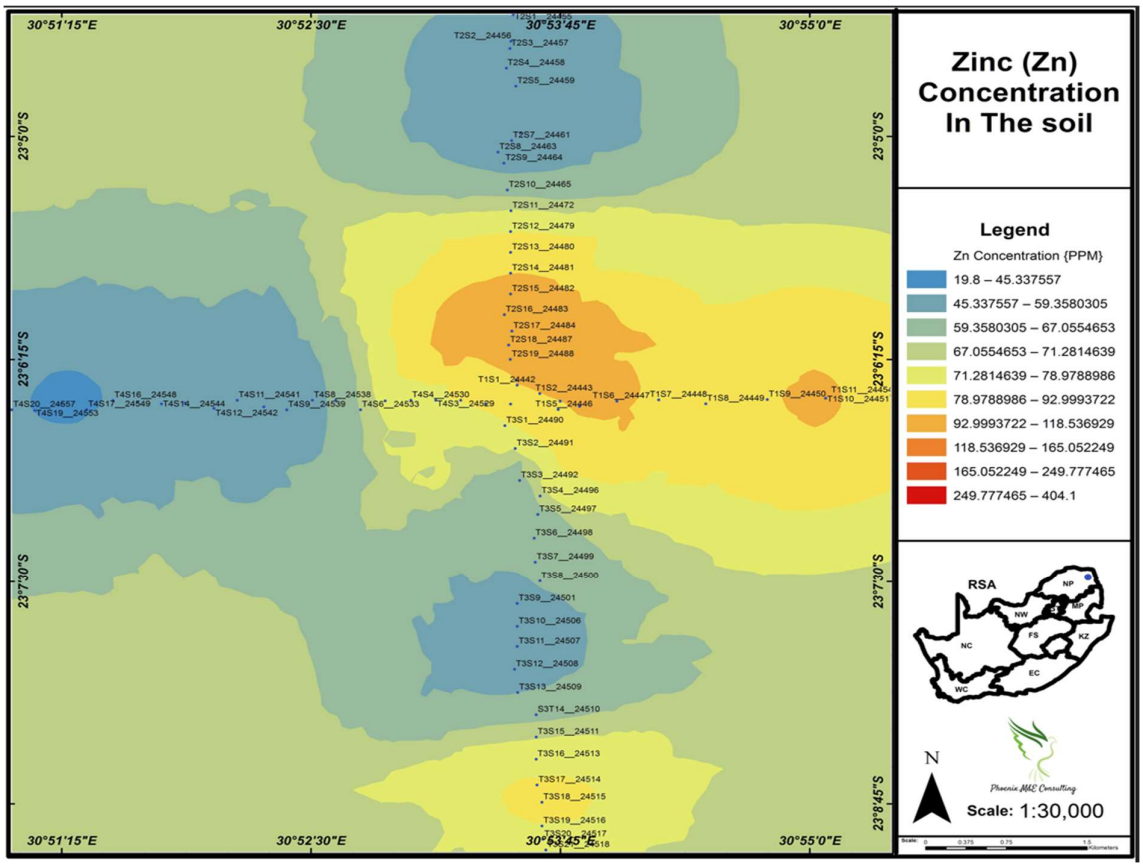

Figure 4.30b: Prediction map of Zn on soils around the Fumani Tailings Dams.

Distribution of Cu

The concentration of copper around the Fumani Tailings Dams ranged from 10.3 ppm to 208.6 ppm giving a range of 208.6 indicating a low variability hence the use of normal bar graphs. the lowest value was found at T3S13 about 2600 m away from the tailings dams. The highest value of Cu was found at T2S2 which was about 400 m away from the tailings dams.

The threshold value was found to be 136.43 ppm and all the values above it were considered anomalous (Fig. 4.31a). Out of all the 77 samples collected, only 6 samples were found to have anomalous values of Cu. The anomalous values and their locations were: 308.6 ppm at T2S2, 160.6 ppm at T2S4, 153.6 ppm at T1S7, 146.8 ppm at T4S2, 141.3 ppm at T1S2 and 140.8 ppm at T1S1.

The values of Cu in T1 ranged from 39.6 ppm to 153.6 ppm at T1S6 and T1S7 respectively. This indicates a sharp change in the values as they are relatively closer to each other. Three points were found to be anomalous in T1 with values of 153.6 ppm, 141.3 ppm and 140.8 ppm at sampling points T1S7, T1S2 and T1S1 respectively. The general trend within this traverse seems to not have been clearly defined.

The values of Cu in T2 ranged from 34.6 ppm to 208.6 ppm at T2S16 and T2S2 respectively. Only two values were anomalous within this traverse. The anomalous values were 208.6 ppm and 160.6 ppm located at T2S2 and T2S4 respectively. These points were relatively close to the tailings dams. The general trend in this traverse seems to consist of higher values closer to the tailings dams and decreases as one moves further from the tailings dams.

The values of Cu in T3 ranged from 10.3 ppm to 131 ppm at T3S13 and T3S8 respectively. The lowest value within the study area was located within this traverse. All values within this T3 were less than the threshold value hence no anomalous values within T3. The general trend within this traverse was the most erratic as compared to the other traverse.

The values of Cu in T4 ranged from 22.8 ppm to 146.8 ppm at T4S11 and T4S4 respectively with the highest value being the only anomalous value within this traverse. There was no defined general trend in this traverse.

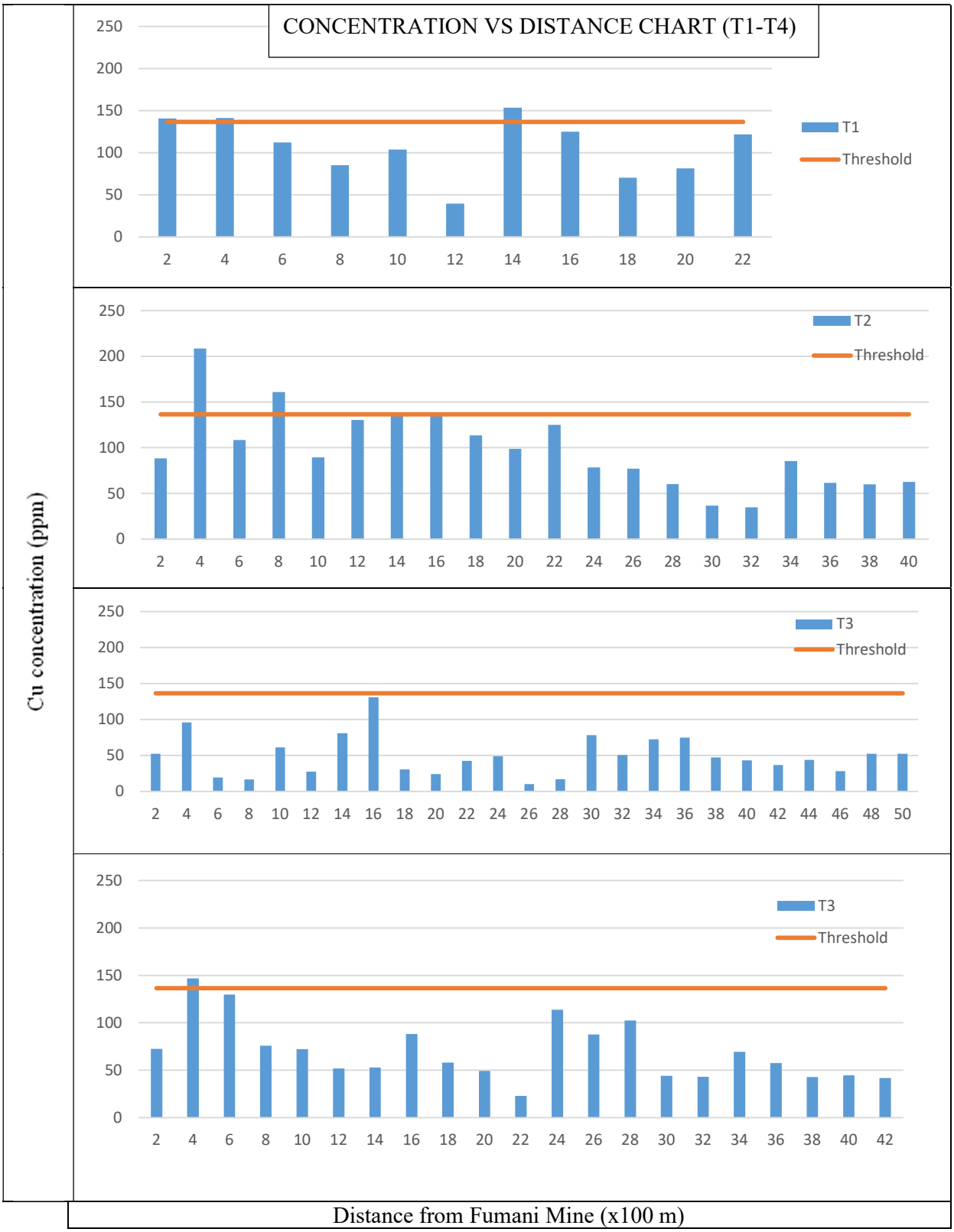

Figure 4.31a: Distribution of Cu (ppm) along the 4 traverses.

The prediction map of Cu on soils around the Fumani Tailings Dams indicated high Cu concentrations located at T1 and T2 (Fig. 4.31b), these traverses lie on the northern and eastern part of the tailings dams respectively. Low Cu concentrations were observed on the western and southern part of the Fumani Tailings Dams as indicated on the Cu bar graphs.

North of the tailings dams indicated high Cu values from about T2S2 to T2S7 (Fig. 4.31b). The concentrations then gradually decrease from T2S8 up to T2S18 and slowly increase to the end of T2. The eastern part of the tailings dams seemed to have a relatively constant Cu Concentration with slightly higher concentrations around T1S7 to T1S8.

The western part of the tailings dam indicated that Cu concentrations were gradually decreasing from T4S1 to T4S11 and slightly increased from around T4S12 to T4S15. where the concentration decreased again to the end of T4.

The southern part of the tailings dams indicated a gradual decrease of Cu with increasing distance from the tailings dams at T3S1 to T3S14, the concentrations then start to gradually increase and decrease again. The general trend depicted from the map indicates higher concentrations on the north to eastern side of the Fumani Tailings Dams. The concentration around the tailings dam was slightly high in relation to the rest of the study area.

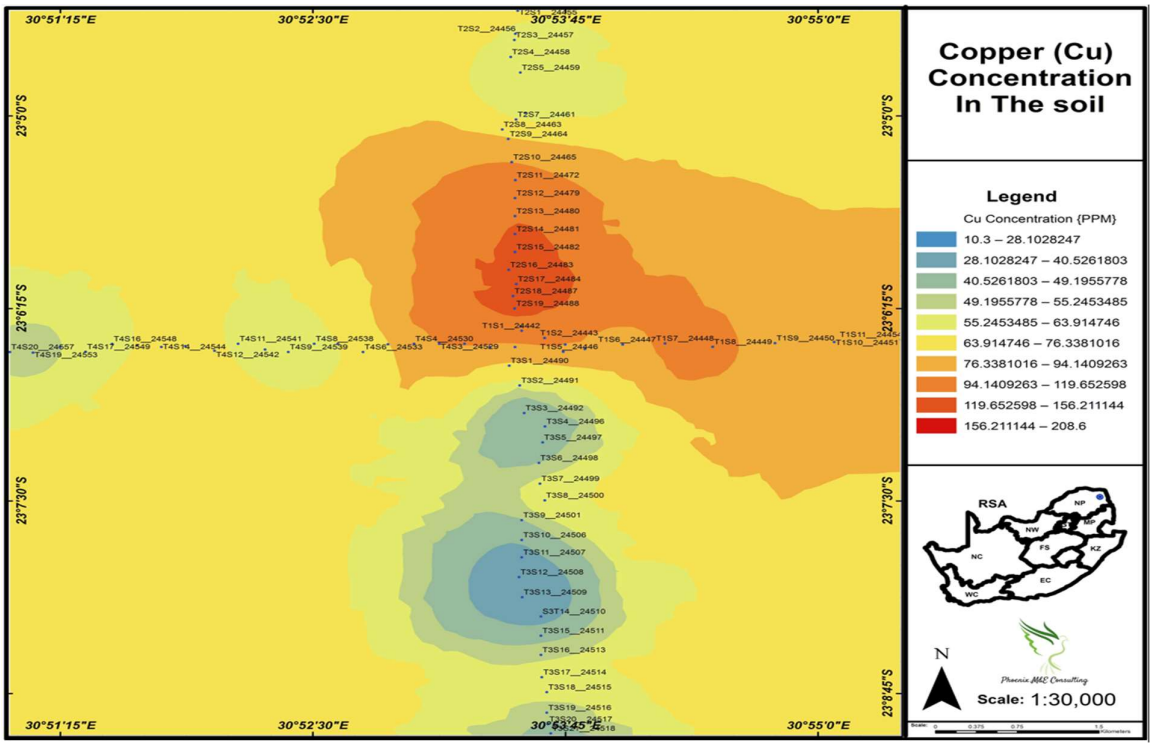

Figure 4.31b: Prediction map of Cu on soils around the Fumani Tailings Dams.

Distribution of As

The values of As around the Fumani Tailings Dams ranged from 2.6 ppm to 1779.7 ppm, giving a variance of 54868.45. The high variance indicated that the values were more spread out with a high variability in the distribution. The high variability led to the use of a logarithmic scale (Fig. 4.32a) to also allow the smaller values to appear within the graph.

The threshold value of As was found to be 401.23 ppm, with all values above it considered anomalous. Out of the 77 samples collected, only three anomalous values of 1779.7, 579.2 and 921.7 ppm were observed points T1S3, T1S4 and T1S5 respectively. All anomalous values were observed at T1 at 600, 800 and 1000 m away from the Fumani Tailings Dams.

The highest As values observed at T1 were the anomalous values, followed by 27.8 ppm located at T1S7, this indicates a huge difference between the anomalous values and the following highest value. This means that the anomalies could have been from a different source of Pb and not from the tailings dams as there is a sharp change and not a gradational one between the anomalous areas and the areas around it. The lowest Pb value recorded at T1 was 8.6 ppm.

The values of As in T2 ranged from 37.2 ppm to 2.7 ppm at T2S18 and T2S1 respectively. No values were anomalous within this traverse. The lowest value is 0.1 ppm more than the lowest value of As in the study area. The highest value of As in this traverse is 47.8 times less than the highest As value. The general trend in this traverse shows a decrease in As values as one moves further from the Fumani Tailings Dams.

The values of As in T3 ranged from 2.8 ppm to 55.7 ppm at T3S14 and T3S1 respectively. No values were anomalous within this traverse. The lowest value is 0.2 ppm more than the lowest value of As in the study area. The highest value of As in this traverse is 47.8 times less than the highest As value. The general trend in this traverse shows a decrease in As values as one moves further from the Fumani Tailings Dams.

The values of As in T4 ranged from 2.6 ppm to 19.1 ppm. The highest As value in this traverse was recorded at T4S4, whilst the lowest As values were recorded at three points namely: T4S8, T4S13 as well as T4S18. The lowest value within the study area was located within this traverse. No values were anomalous within in T4. The general trend in this traverse shows a decrease in As values as one moves further from the Fumani Tailings Dams.

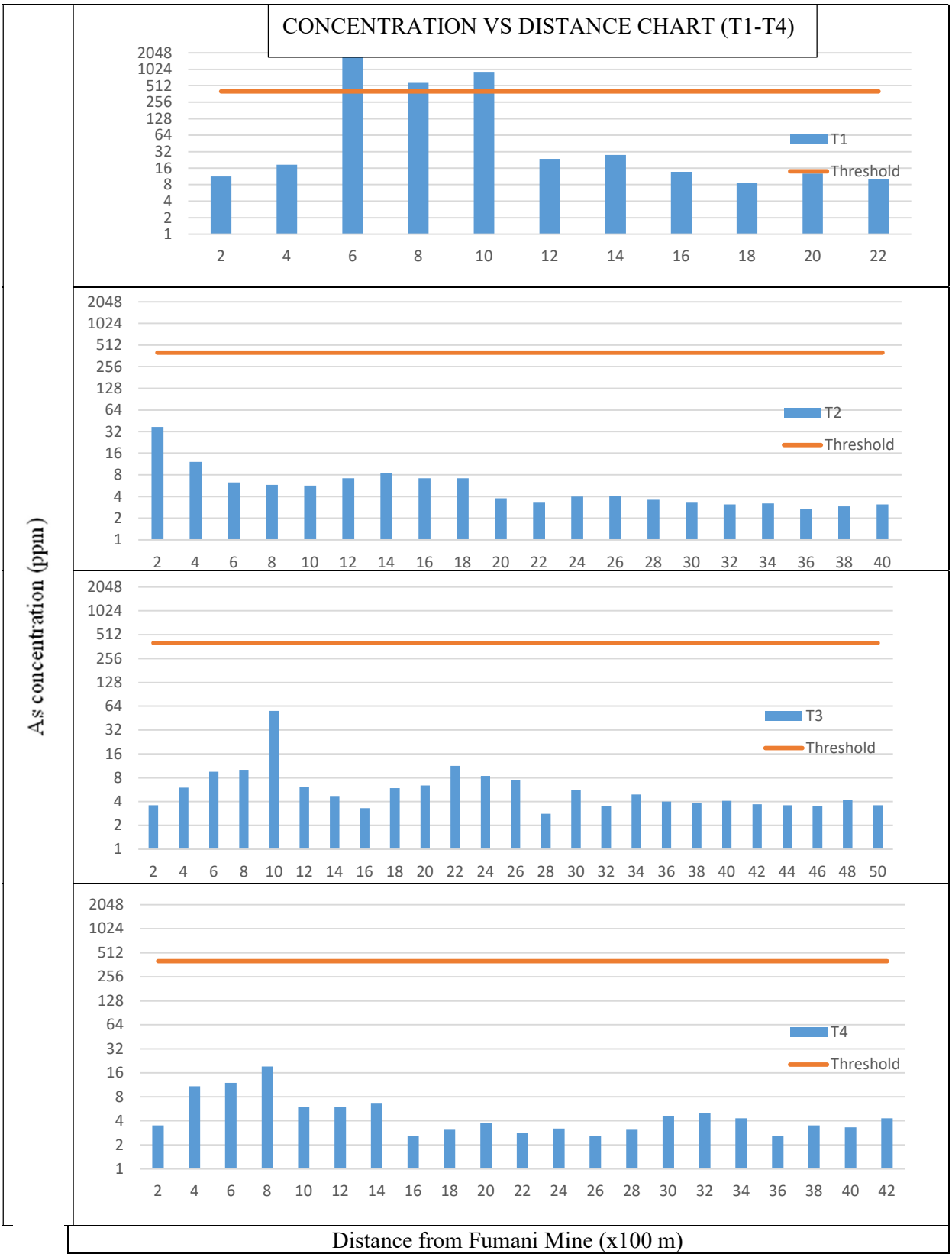

Figure 4.32a: Distribution of As (ppm) along the 4 traverses.

The geochemical map depicting lateral distribution of As in soil around the Fumani Tailings Dams was characterised by high concentrations in the close vicinity of the tailings dams, in the western part of the tailings dams. The concentration of As decreased with increase in depth from the Fumani tailings dams. Lower concentrations of As were observed along T2, T3 and T4 towards the end of these traverses.

The overall trend observed from this geochemical map is similar to that observed from the geochemical map of lateral distribution of lead in soils around the Fumani Tailings Dams.

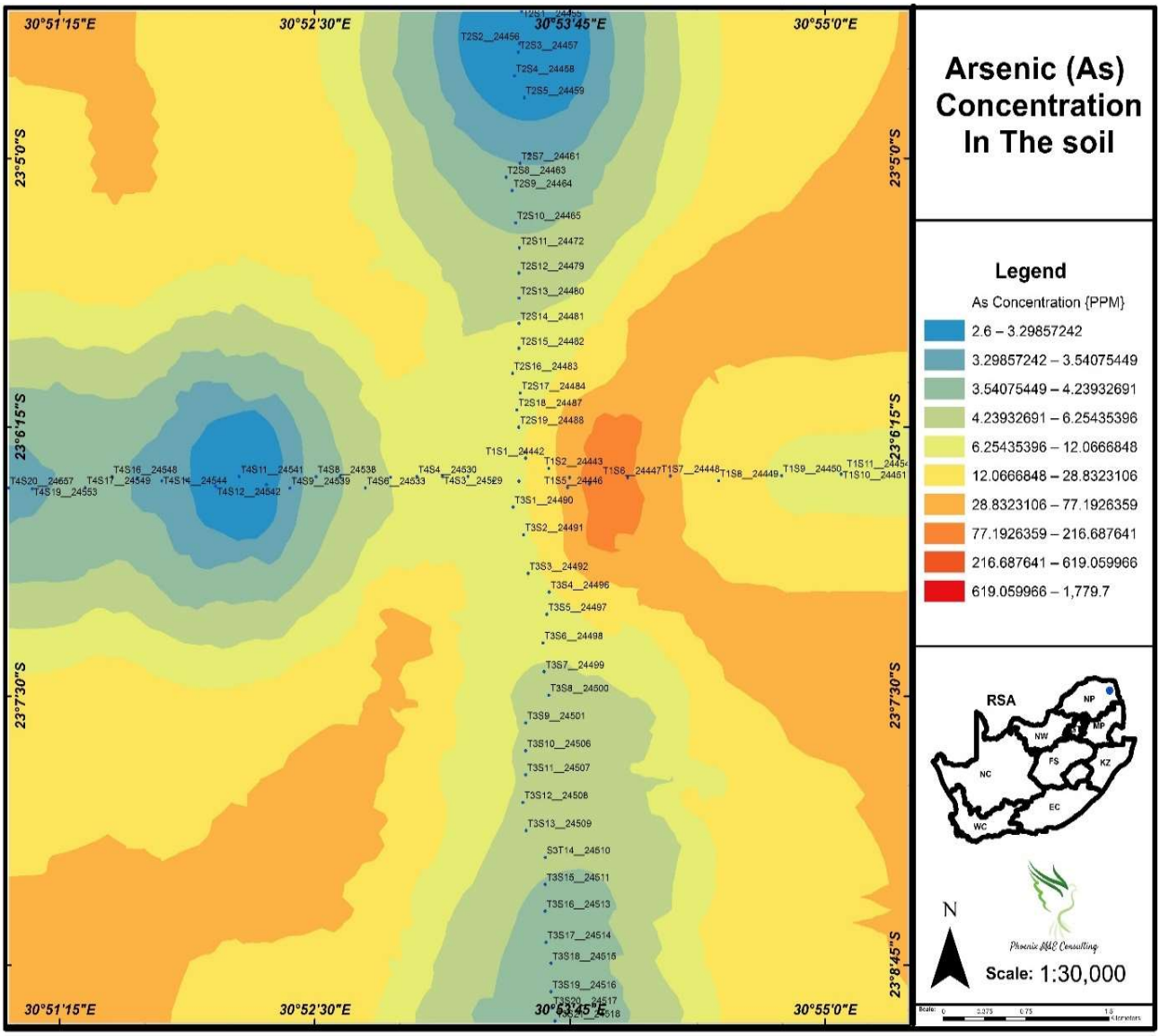

Figure 4.32b: Prediction map of As on soils around the Fumani Tailings Dams.

Distribution of Co

The concentration of Co around the Fumani Tailings Dams ranged from 4 ppm to 50.9 ppm giving a range of 46.9 ppm, the low range indicates that the data was not spread out hence the use of normal scale bar graphs. The lowest value was found at T3S13 about 2600 m away from the tailings dams. The highest value of Co was found at T2S3 which was about 600 m away from the tailings dams (Fig. 4.33a).

The threshold value was found to be 33.76 ppm and all values above it were considered anomalous (Fig. 4.33a). Out of all the 77 samples collected, only 5 samples were found to have anomalous values of Co, of which three were in T1, and two in T2.

The values of Co in T1 ranged from 12.6 ppm to 50.9 ppm at T1S6 and T1S3 respectively. The highest value obtained in T1 was the highest Co value in the entire study area. There three anomalous values found in this traverse were 50.9 ppm, 38.2 ppm and 36.9 ppm located at T1S3, T1S5 and T1S2 respectively. The general trend within T1 seems to be erratic and does not follow any pattern.

The values of Co in T2 ranged from 6.7 ppm to 37.6 ppm at T2S15 and T2S4 respectively. There were two anomalous values within T2 of 37.6 ppm and 34.3 ppm located at T2S4 and T2S3 respectively. These points were relatively close to tailings dams. The general trend in this traverse seems to consist of higher values closer to the tailings dams and decreases as one moves further from the tailings dams.

The values of Co in T3 ranged from 4 ppm to 30.2 ppm at T3S13 and T3S2 respectively. The lowest value within the study area was located within T3. There were no anomalous values in this traverse. The seems to be an erratic Co trend in T3 as the values follow no pattern.

The values of Co in T4 ranged from 7.3 ppm to 36.4 ppm at T4S11 and T4S3 respectively. Two anomalous values of 36.4 ppm and 34.4 ppm located at T4S3 and T4S2. Higher Co values were found from T4S1 to T4S4, with the rest of the Co values beingless than 22 ppm.

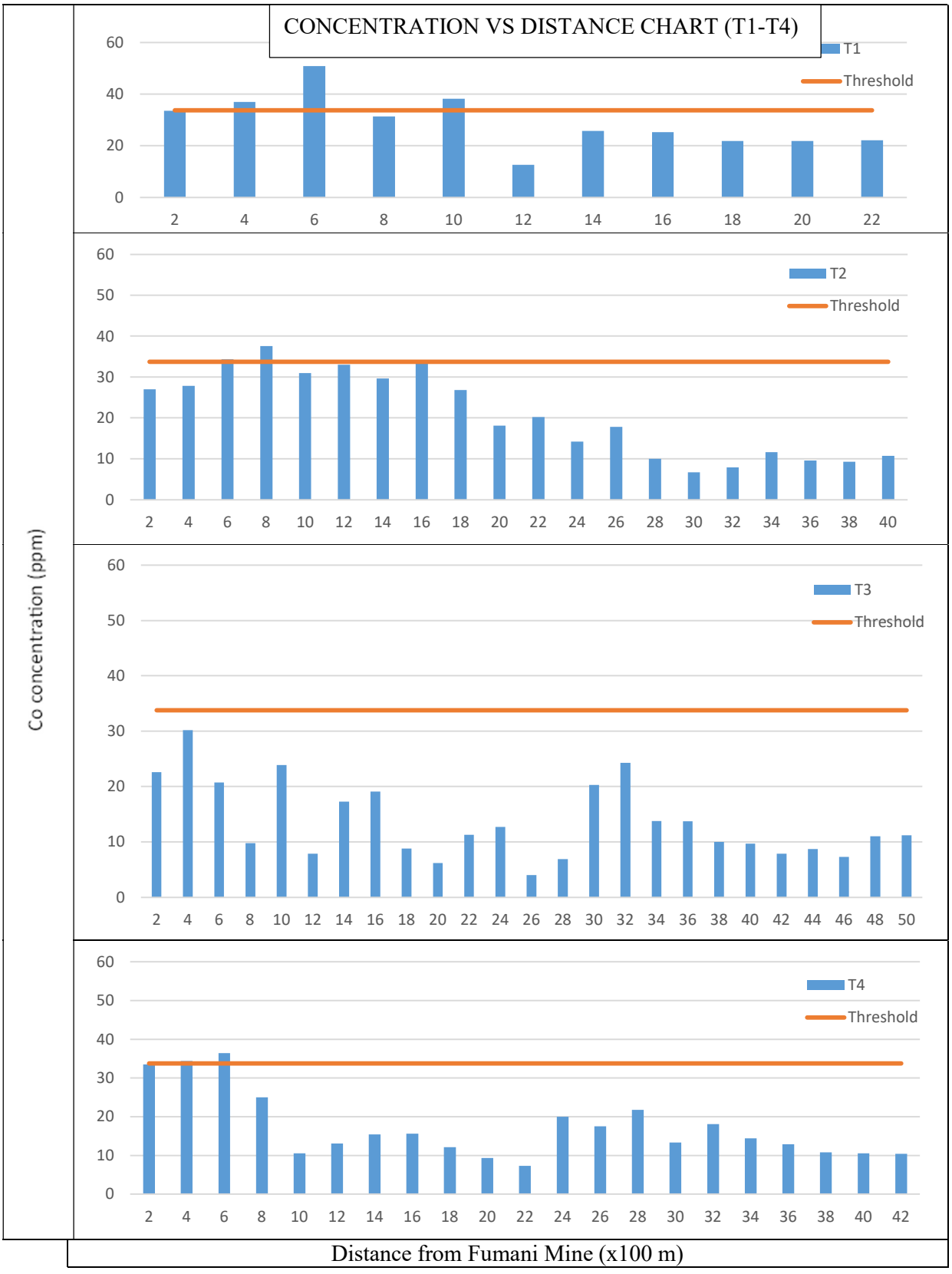

Figure 4.33a: Distribution of Co (ppm) along the 4 traverses.

The prediction map of Co on soils around the Fumani Tailings Dams indicated that high Co concentrations are located at the center of the map, with low Co concentrations as one moves further from the tailings dams (Fig. 4.33b).

The northern part of the tailings dams indicates high Co values closer to the tailings dams that decrease gradually as one moves further from them. The eastern part of the tailings dams seemed to have a relatively constant Co Concentration with slightly higher concentrations from around T1S1 to T1S6.

The western part from the tailings dams indicates Co concentrations gradually decreased from T4S1 to T4S1, and slightly increase from around T4S13 to T4S16, then decreased again to the end of T4.

The southern part of the tailings dams indicated a gradual decrease from the tailings dams with increasing distance from T3S1 to T3S14, the concentrations then started to gradually increase and decrease again. The general trend depicted from the map indicates higher concentrations on the center of the Fumani Tailings Dams, and it is similar to that observed on the geochemical map of Cu.

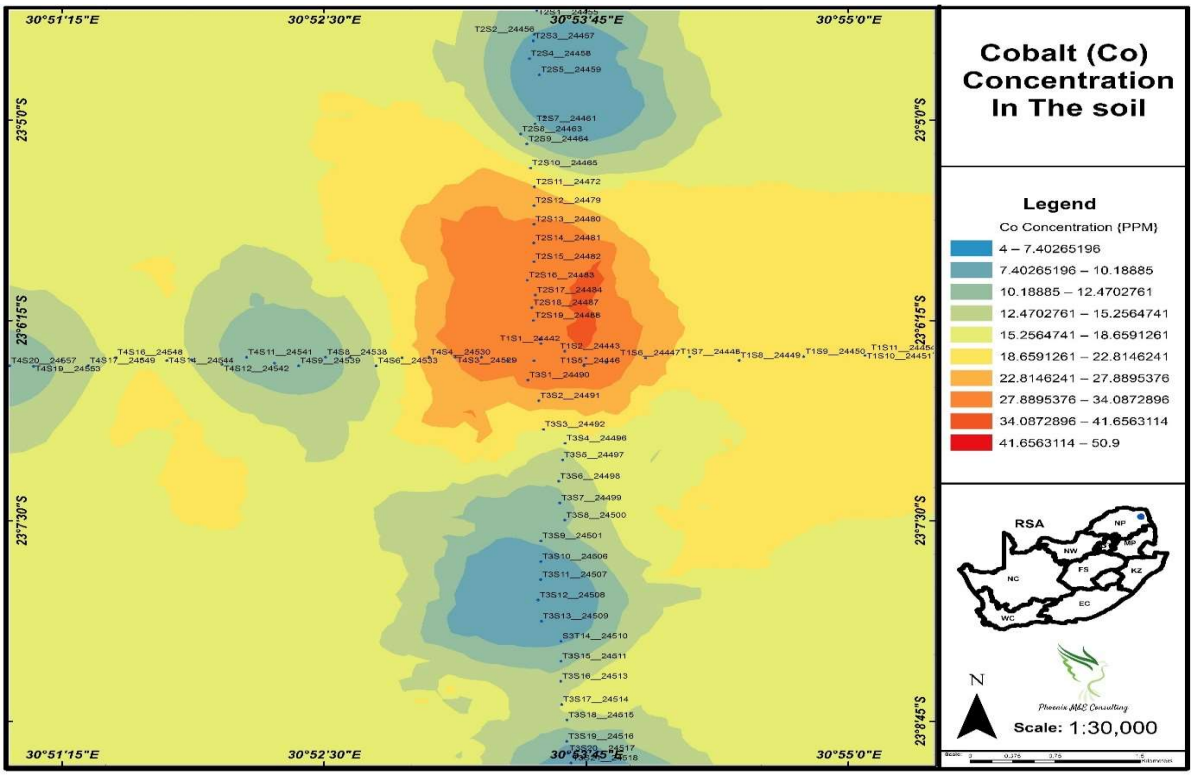

Figure 4.33b: Prediction map of Co on soils around the Fumani Tailings Dams.

Distribution of Cd

The concentration of Cd around the Fumani Tailings Dams ranged from 0 ppm to 0.1 ppm giving a range of 0.1. Out of the 77 samples collected, 16 samples had a value of 0.1 ppm, and the remaining 61 samples had a value of 0 ppm Cd.The threshold value was found to be 0.08 ppm and all values above it were considered anomalous (Fig. 4.34a). Out of all the 77 samples collected, 16 samples were found to have anomalous values of Cd. Traverse 1 had 2 anomalous value, T2 and T3 each had 5 anomalous values whilst T4 had 4 anomalous values. All the anomalous values had a value of 0.1 pp.

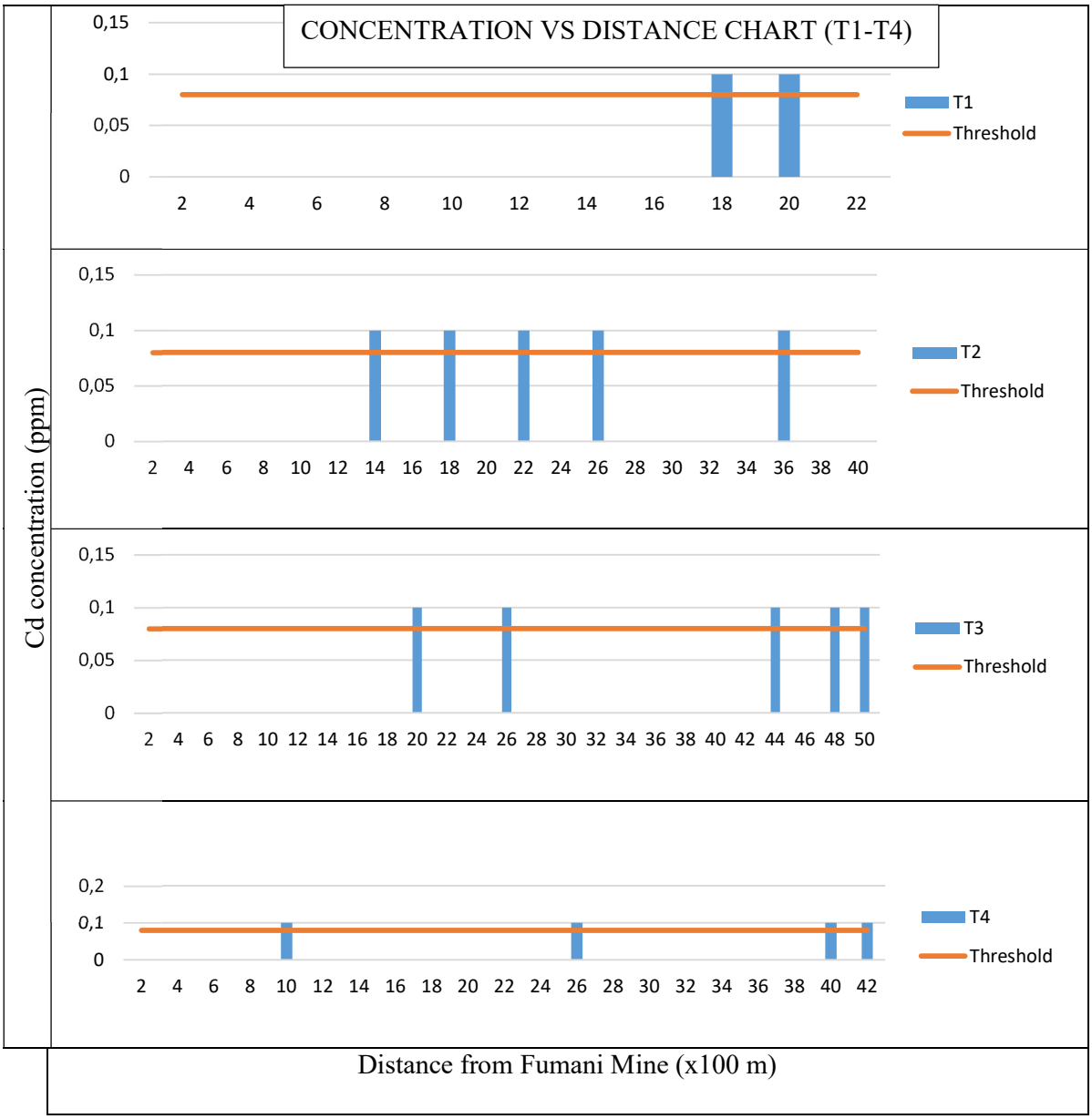

Figure 4.34: Distribution of Cd (ppm) along the 4 traverses.

No prediction map for Cd could be produced as the concentration is the same throughout.

Distribution of Cr

The concentration of Cr around the Fumani Tailings Dams ranged from 41.7 ppm to 1988.8 ppm giving a range of 1947.1 hence the use of normal scale bar graphs. the lowest value was found at T3S13 about 2600 m away from the tailings dams. The highest value of Cu was found at T2S3 which was about 600 m away from the tailings dams.

The threshold value was found to be 1044.18 ppm and all values above it were considered anomalous (Fig. 4.35a). Out of all the 77 samples collected, only 6 samples were found to have anomalous values of Cr, of which three were located in T2, one in T3 and two in T4.
The values of Cr in T1 ranged from 184.9 ppm to 1037.1 ppm at T1S6 and T1S2 respectively. There was no anomalous value fount in this traverse. Only the highest value in T2 is above 1000 ppm, with the remaining values all less than 800 ppm. The general trend within T1 seems to be erratic and does not follow any pattern.

The values of Cr in T2 ranged from 105.2 ppm to 1988.8 ppm at T2S14 and T2S3 respectively. The highest value recorded in this traverse was the highest Cr value recorded within the study area. three values were anomalous within T2. The anomalous values were 21988.8 ppm, 1587.4 ppm, and 1288.7 ppm located at T2S3, T2S5, and T2S6 respectively. These points were relatively close to tailings dams. The general trend in this traverse seems to consist of higher values closer to the tailings dams and decreases as one moves further from them.

The values of Cr in T3 ranged from 41.7 ppm to 1284.5 ppm at T3S13 and T3S1 respectively. The lowest value within the study area was located within T3. The highest value in this traverse was the only anomalous value in T3. Chromium values seem to be very high at the first two sampling points and decreased drastically from 994.8 ppm to 384.7 ppm. All the remaining Cr values within T3 were less than 384.7 ppm.

The values of Cr in T4 ranged from 100.2 ppm to 1474.4 ppm at T4S21 and T4S1 respectively. Two anomalous values of 1474.4 and 1395.8 pp were located within this traverse at T4S1 and T4S2. The general trend within this traverse seems to consist of higher values closer to the tailings dams and decreased as one moved further from them. The four values located close to the tailings dams had Cr values greater than 500 ppm whilst those 1000 m from the tailings dams and more had Cr values less than 400 ppm.

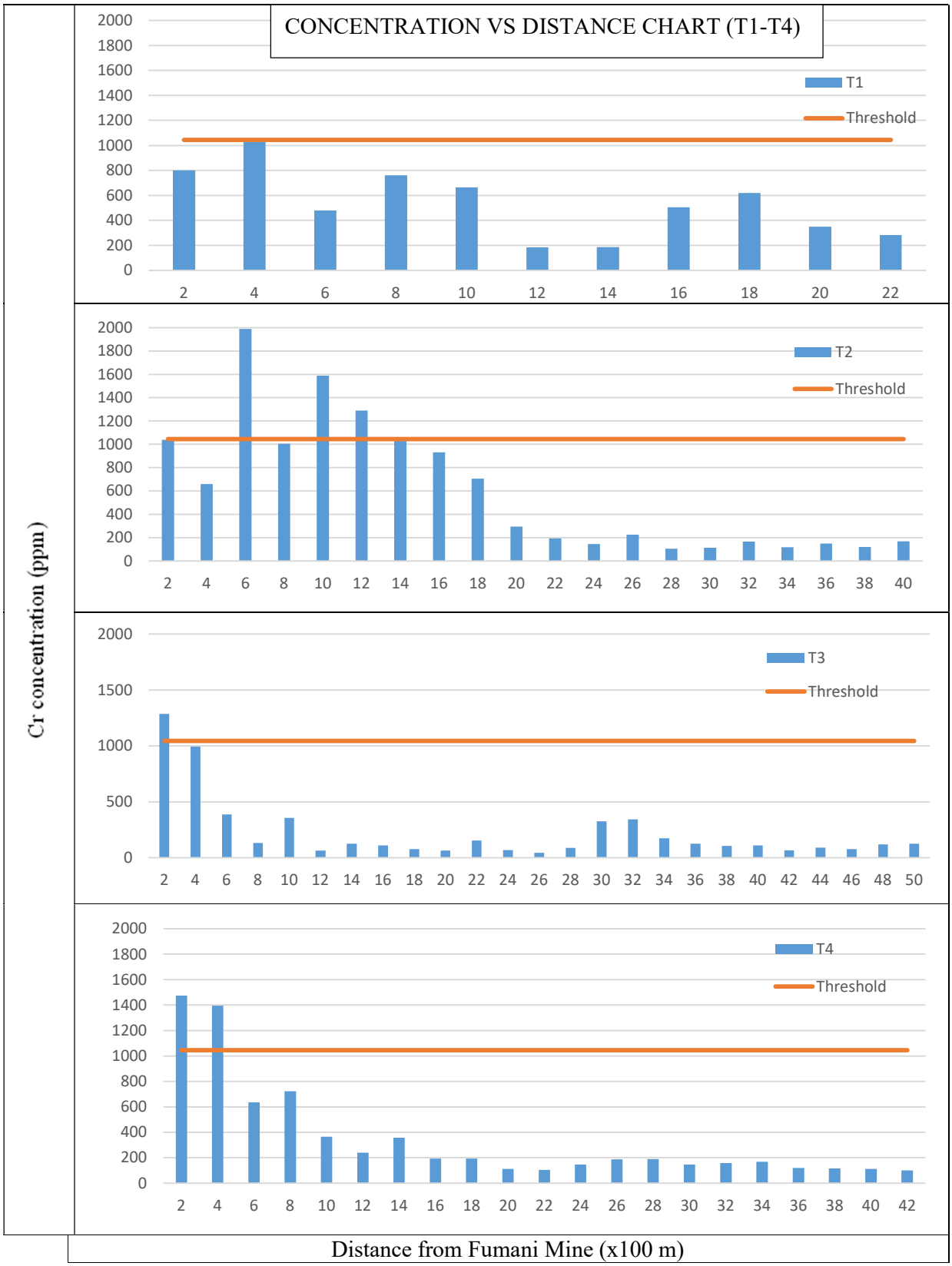

Figure 4.35a: Distribution of Cr (ppm) along the 4 traverses.

The prediction map of Cr on soils around the Fumani Tailings Dams was modelled using ordinary kriging method. The prediction map confirms that the high Cr concentrations are located at the center of the map, with low Cr concentrations as one moves further from the tailings dams (Fig. 4.35b).

The prediction map reviled lower concentrations along T3,T1 and T2 respectively. The remaining area had fairly high concentrations of Cr. Based on the prediction map, it can be said that the high values in the center of the tailings dams might be from the tailings dams as well as another source as the concentration is higher as compared to the concentration in the close vicinity of the tailings dams.

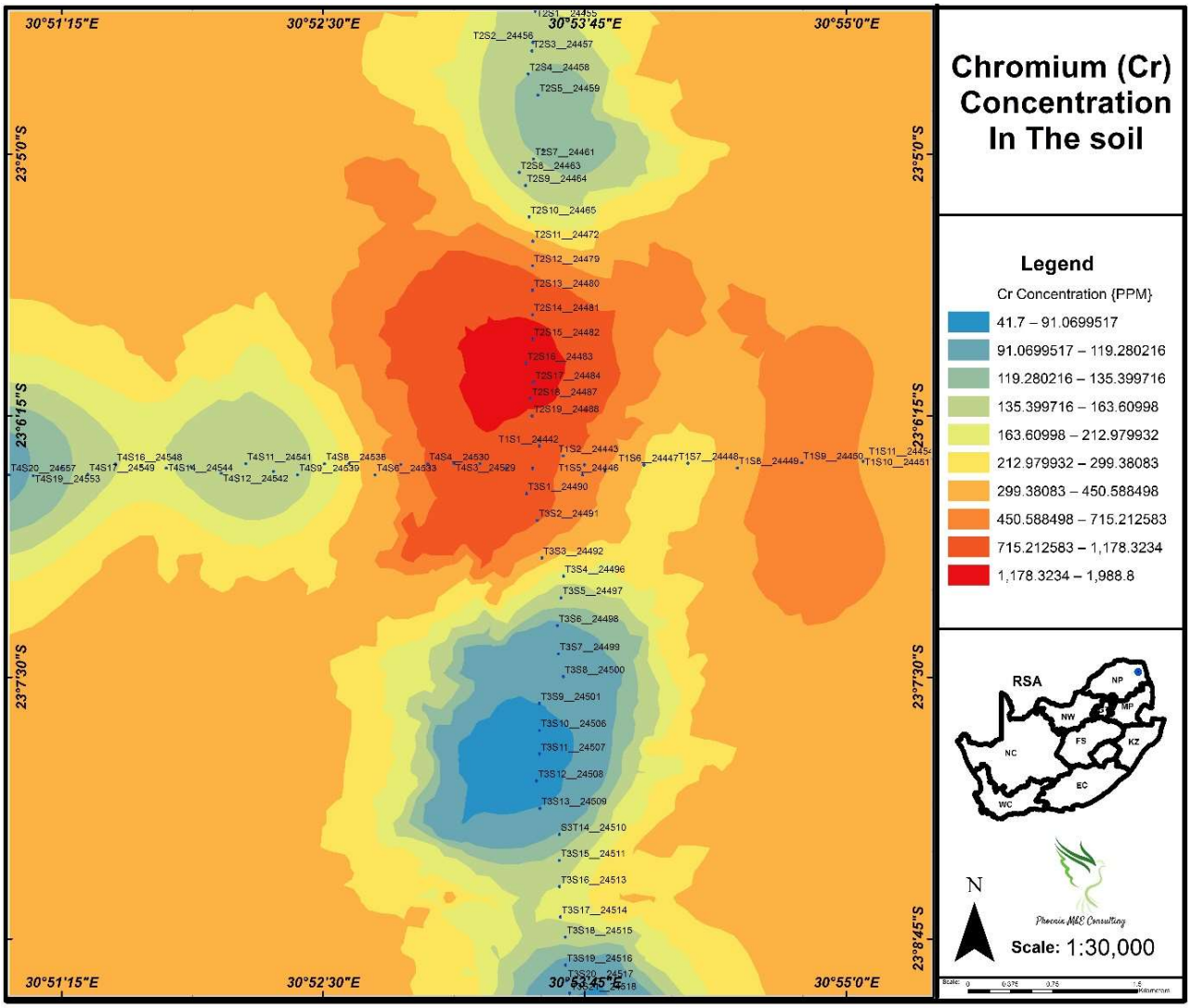

Figure 4.35b: Prediction map of Cr on soils around the Fumani Tailings Dams.

Distribution of Ni

The concentration of Ni around the Fumani Tailings Dams ranged from 46.9 ppm to 2296.9 ppm giving a range of 2250 and a variance of 266197.58 variability. The lowest value was found at T3S13 about 2600 m away from the tailings dams. The highest value of Cu was found at T2S2 which was about 400 m away from the tailings dams.

The threshold value was found to be 136.43 ppm and all values above it were considered anomalous (Fig. 4.36a). Out of all the 77 samples collected, only 6 samples were found to have anomalous values of Ni. Each traverse had one anomalous value, with exception to T2 which had 4 anomalous values.

The values of Ni in T1 ranged from 155.3 ppm to 1360.1 ppm at T1S7 and T1S2 respectively. One point which was the highest point in this traverse was found to be anomalous. The general trend within this traverse seems to not have been clearly defined.

The values of Ni in T2 ranged from 75 ppm to 2296.9 ppm at T2S16 and T2S3 respectively. Only 4 values were anomalous within T2. The anomalous values were 2296.9 ppm, 1637.3 ppm, 1600.2 ppm and 1385.8 ppm located at T2S3, T2S5, T2S1 and T2S6 respectively. These points were relatively close to tailings dams. The general trend in this traverse seems to consist of higher values closer to the tailings dams and decreases as one moves further from the tailings dams.

The values of Ni in T3 ranged from 46.9 ppm to 1962 ppm at T3S13 and T3S1 respectively. The lowest value within the study area was located within T3. The highest value in this traverse was the only anomalous value in T3. The general trend within this traverse seems to consist of higher values closer to the tailings dams and decreases as one moves further from the tailings dams.

The values of Ni in T4 ranged from 54.8 ppm to 2082.4 ppm at T4S21 and T4S1 respectively with the highest value being the only anomalous value within this traverse. The general trend within this traverse seems to consist of higher values closer to the tailings dams and decreases as one moves further from the tailings dams.

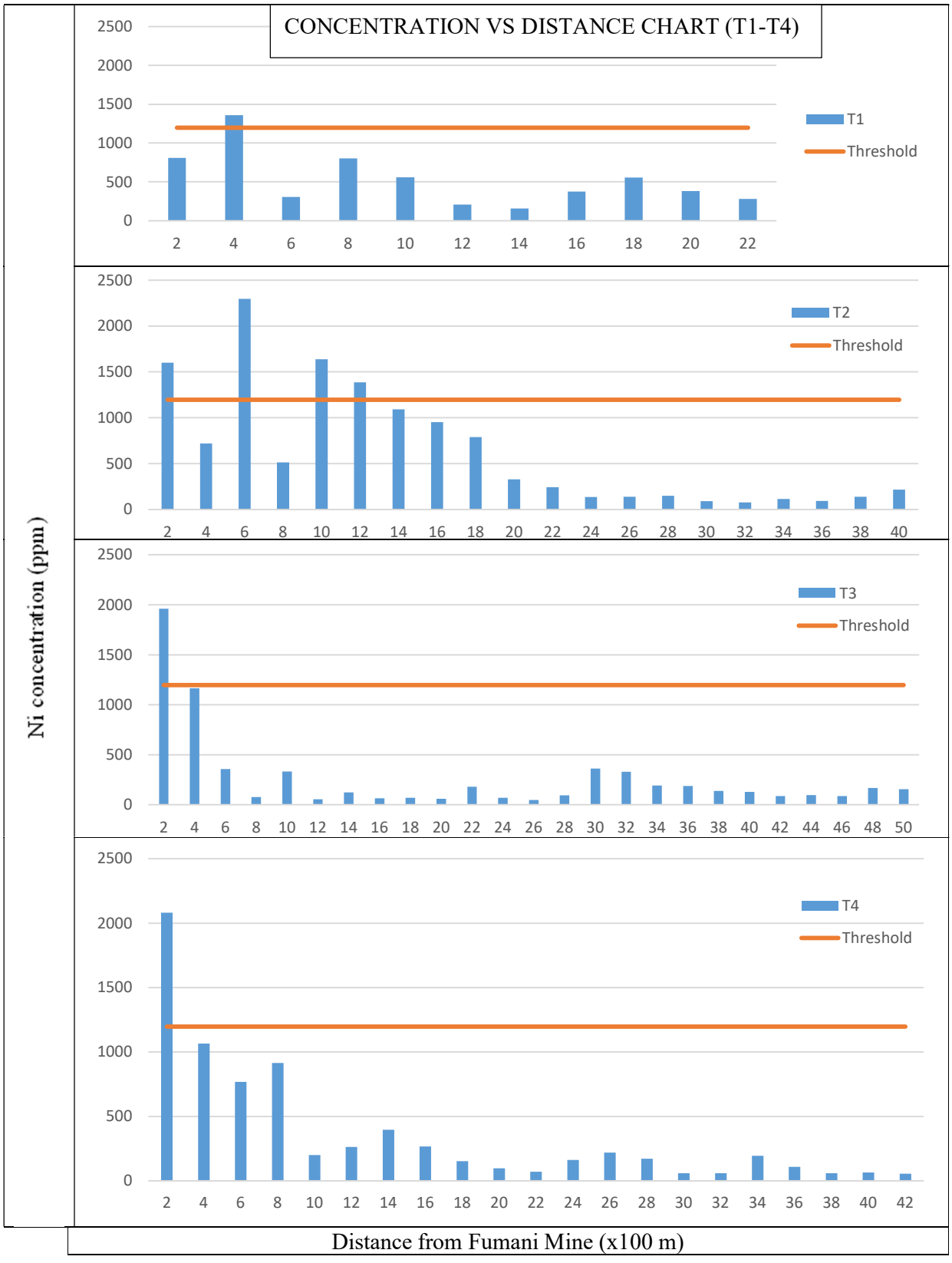

Figure 4.36a: Distribution of Ni (ppm) along the 4 traverses.

The prediction map of Ni on soils around the Fumani Tailings Dams was modelled using ordinary kriging method. The prediction map confirms that the high Ni concentrations are located at the center of the map, with low Ni concentrations as one moves further from the tailings dams (Fig. 4.36b).

The prediction map reviled lower concentrations along T3, T1 and T2 respectively. The remaining area had fairly high concentrations of Ni. Based on the prediction map, it can be said that the high values in the center of the tailings dams might be from the tailings dams as well as another source as the concentration is higher than the concentration in the close vicinity of the tailings dams. This trend is similar to the one observed in the prediction map of Cr in soils around the Fumani Tailings Dams.

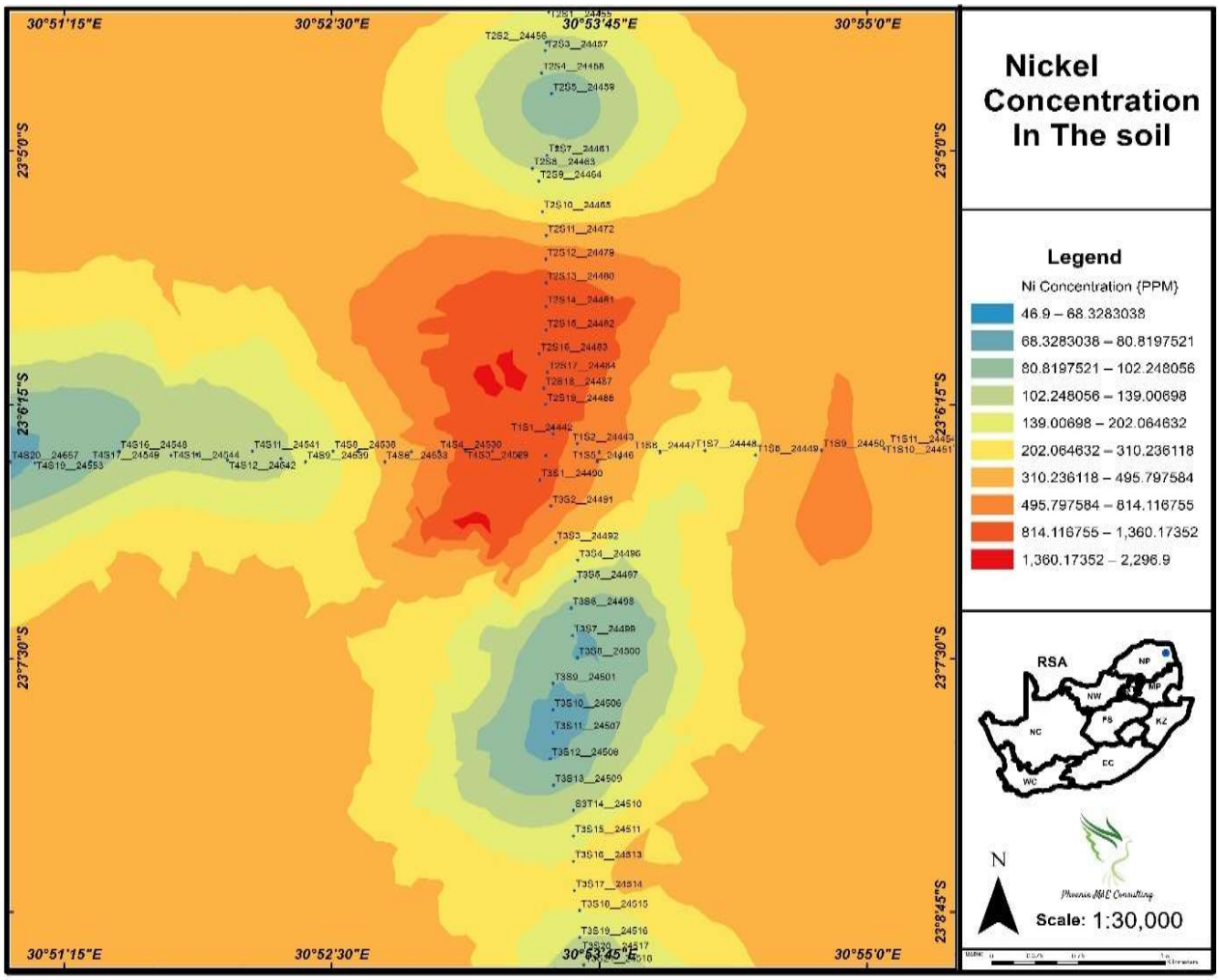

Figure 4.36b: Prediction map of Ni on soils around the Fumani Tailings Dams.

4.2.2 Pollution Status of soil surrounding Fumani Tailings Dams

The pollution status of soil around the Fumani Tailings Dams was determined using the Dutch guideline of standards, single factor index method as well as using the soil screening values adapted from the South African government gazette of 02 May 2014. It was important to use different methods to determine the pollution status of the soil with confidence.

4.2.2.1 Dutch Guideline of Standards

The range as well as the maximum values of metals were compared to the Dutch guideline of standards. T1 denotes the concentration of metals in soil around the Fumani Tailings Dams.

Using the range obtained from the statistical analysis of soil Table 4.9 and the Dutch guideline of Concentrations in soil, Table 4.11 was created. From Table 4.11, it is evident that the range of metals in the soil around the tailings falls in different categories of the Dutch guideline standards and do not follow a particular trend. The range of Cd was 0.10 ppm, placing it in the A category. Zn and Co fall in the B category. The range of Cu was 198.30 ppm which falls within the C category. The range of Pb (16556.90 ppm), As (1777.10 ppm), Cr (1947.10 ppm) and Ni (19954.10 ppm) highly exceeds the C category limit.

This simply means that Cd probably does not contaminate the soil. Zn and Co are still within the limits however; further investigation is required. Although Cu contaminates the soil, it is still within the Dutch guideline limit of the C category. Pb, As, Cr and Ni on the other hand highly exceeded the C value and therefore greatly contaminate the soil and require clean up.

Table 4.11: Dutch Guideline Standards combined with the range of metals in soil (ppm)

	Pb	Zn	Cu	As	Co	Cd	Cr	Ni
A	50	200	50	20	20	1	100	50
B	150	500	100	30	50	5	250	100
C	600	3000	500	50	300	20	800	500
Range	16556,9	384,3	198,3	1777,1	46,9	0,10	1947,1	2250,

Using the maximum concentrations of metals obtained from the statistical analysis Table of soil Table 4.10 and the Dutch guideline Table 4.12 was created. From Table 4.12, it can be seen that the maximum values of metals in the soil around the tailings dams falls in different categories of the Dutch guideline standards and do not follow a particular trend. The maximum value of Cd was 0.10 ppm, placing it in the A category. Zn had a maximum value of 404.1 ppm, placing it in the B category. Co and Cu had maximum values of 50.9 ppm and 208.6 ppm respectively which fall within the C category. The maximum values of Pb (16581.00 ppm), As (1779.70 ppm), Cr (1988.80 ppm) and Ni (2023.10 ppm) exceeds the C category limit.

This simply means that Cd probably does not contaminate the soil. Zn is still within the limits however; further investigation is required. Cu and Co contaminate the soil and therefore site requires clean-up. Pb, Cr and Ni on the other hand highly exceed the C value and therefore contaminate the soil and require a site clean-up.

Table 4.12: Dutch Guideline Standards with the maximum values of metals in soil (ppm)

	Pb	Zn	Cu	As	Co	Cd	Cr	Ni
A	50	200	50	20	20	1	100	50
B	150	500	100	30	50	5	250	100
C	600	3000	500	50	300	20	800	500
T1	16581,00	404,10	208,60	1779,70	50,90	0,10	1988,80	2296,90

4.2.2.2 Single Factor Index Method (SFIM)

The SFIM incorporated the mean and maximum values of soils around the Fumani Tailings Dams and the Dutch Guideline of concentrations in soil in order to determine the quality index of the pollutant around the Fumani Tailings Dams 1 and 2. The Pollution Index (Pi) was calculated using the formula: Pi= Ci/Si, where Pi is the pollution index, Si is the Dutch Guideline of concentrations in soils and Ci is the value of the metal within the tailings dam. For this work, Si is the B class values of the Dutch Guideline of Standards. This is because investigation of contamination must be done in the B class as A class probably does not contaminate the tailings and C class contaminates the tailings.

Assessment standard states that

Pi equals or less than 0.7 = tailings probably not contaminated

Pi between 0.7 and 1 = concentration within environmental quality standard

Pi between 1 and 2= concentration beyond environmental quality standard, light pollution

Pi between 2 and 3 = Moderate pollution

Pi greater than 3 = heavy pollution and requires clean up

The Dutch guideline of concentrations in soil (Table 2.1) together with the mean values of metals around the Fumani Tailings Dams 1 and 2 obtained from Table 4.9 were combined to create Table 4.13 in order to determine the pollution status of the area around the tailings dams using the SFIM.

From the Table 4.13 it is evident that the PI for Cd is less than 0.7. The PI for Zn and Co lie between 0.7 and 1. The PI for Cu was 1.983, which lies between 1 and 2. The PI for Pb, As, Cr and Ni greatly exceeds 3.

This means that Cd, Zn and Co do not contaminate the soils around the Fumani Tailings Dams. Cu slightly pollutes the soil around the tailings dams whilst Pb, As, Cr and Ni highly pollutes the soil around the tailings dam.

Table 4.13: Environmental quality index of the range of metals in soil around Fumani Tailings Dams (ppm)

	Pb	**Zn**	**Cu**	**As**	**Co**	**Cd**	**Cr**	**Ni**
Si	150	500	100	30	50	5	250	100
Ci	16556,9	384,3	198,3	1777,1	46,9	0.1	1947,1	2250
Pi	110,379	0,7686	1,983	59,2367	0,938	0,02	7,7884	22,5

The Dutch guideline of concentrations in soil (Table 2.1) together with the maximum values of metals around the Fumani Tailings Dams 1 and 2 obtained from Table 4.9 were combined to create Table 4.14 in order to determine the pollution status of the area around the tailings dams using the SFIM.

From the Table 4.14 it is evident that the PI for Cd is less than 0.7. The PI for Zn lies between 0.7 and 1. The PI for Co was 1.018 which lies between 1 and 2. The PI for Cu lies between 2 and 3. The PI for Pb, As, Cr and Ni greatly exceeds 3.

This means that Cd and Zn do not contaminate the soils around the Fumani Tailings Dams. Cu moderately pollutes the soil around the tailings dams whilst Pb, As, Cr and Ni highly pollutes the soil around the tailings dam.

Table 4.14: Environmental quality index of the maximum values of metals in soil around Fumani Tailings Dams (ppm)

	Pb	**Zn**	**Cu**	**As**	**Co**	**Cd**	**Cr**	**Ni**
Si	150	500	100	30	50	5	250	100
Ci	16581	404,1	208,6	1779,7	50,9	0.1	1988,8	2296,9
Pi	110,54	0,8082	2,086	59,3233	1,018	0,02	7,9552	22,969

4.2.2.3 South African Guideline of Standards

The soil screening value used for determining the pollution status of the Mtititi area around the Fumani Tailings Dams were adopted from the South African Government Gazette of 2014 and incorporated with the mean and maximum metal values to create Table 4.15.

From Table 4.15, the range and maximum values of Cd and Co do not exceed the concentrations of any land use. Zn and Cu range and Maximum values do not exceed any of the land uses with exception to land used for Protection of ecosystem and health the SSV for this land use is 240 ppm and 16 ppm respectively. The range and maximum values were found to be 384.2 ppm and 404.1 ppm for Zn and 198.3 and 208.6 for Cu respectively.
Pb, As and Cr highly exceed the standard soil values and require clean-up for all the land uses listed in Table 4.15.

Table 4.15: Soil Screening values for different land uses around the Fumani Tailings Dams

Metals and metalloids	Informal Residential areas	Standard residential areas	Commercial industrial	Protection of ecosystem and health	Range of metals within tailings dam1	Maximum values of metals within tailings dam1
Arsenic	23 ppm	48 ppm	150 ppm	580 ppm	1777.10 ppm	1779.70 ppm
Cadmium	15 ppm	32 ppm	260 ppm	37 ppm	0.10 ppm	0.10 ppm
Cobalt	300 ppm	630 ppm	5000 ppm	22000 ppm	46.90 ppm	50.90 ppm
Copper	1100 ppm	2300 ppm	19000 ppm	16 ppm	198.30 ppm	208.60 ppm
Lead	110 ppm	230 ppm	1900 ppm	100 ppm	16556.90 ppm	16581.00 ppm
Zinc	9200	19000 ppm	150000 ppm	240 ppm	384.20 ppm	404.10 ppm
Nickel	620 ppm	1200 ppm	10 000 ppm	1 400 ppm	2250.00 ppm	2296.90 ppm
Chromium	6.5 ppm	13 ppm	40 ppm	260 ppm	1947.10 ppm	1988.80 ppm

4.3 Economic Potential of Tailings Dams

4.3.1 Gold within the Fumani Tailings Dams 1 and 2

All tailings samples collected from Fumani Tailings Dams 1 and 2 were analysed using fire assaying techniques, and the results are analysed, presented and, interpreted.

4.3.1.1 Statistical Analysis and Calculations

Using the equations 4.1 to 4.5 together with the gold values obtained from fire assay analysis, Table 4.16 was created. Fumani Tailings Dam 1 is denoted by T1 whilst Fumani Tailings Dam 2 is denoted by T2. Table 4.16 indicated that gold within the Fumani Tailings Dams 1 and 2 ranged from 0.31 ppm to 2.79 ppm and from 0.36 ppm to 4.44 ppm respectively. The statistical analysis revealed an average concentration value of 1.34 ppm and 1.44 at Fumani Tailings Dams 1 and 2 respectively. The threshold value for Au within the tailings dams was found to be 2.22 and 2.34 within Fumani Tailings Dam 1 and 2 respectively.

Table 4.16: Statistical summary of gold values within the Fumani Tailings Dams 1 and 2 (ppm)

	Max	Min	Mean	Range	SD	Threshold
T1	2,79	0,31	1,34	2,48	0,54	2,22
T2	4,44	0,36	1,44	4,08	0,6	2,34

4.3.1.2 Correlation Matrix of Gold and other Metals within the Fumani Tailings Dams

Correlation was used in this study to determine the relationship between gold and other metals. The correlation coefficient was calculated using equation 4.6. Since the Fumani Tailings Dams 1 and 2 had 84 and 63 samples analysed for gold respectively, then the correlation coefficient should be greater than $2/\sqrt{84}$ and $2\sqrt{63}$ for a relationship to exist between gold and that metal. For Fumani Tailings Dams 1 and 2, r should be greater than 0.218 and 0.251 respectively.

Table 4.17: Correlation matrix of gold and heavy metals within the tailings dam

	T1	T2
	Au	Au
Au	1	1
Pb	-0,01492	-0,13169
Zn	0,056675	-0,00794
Cu	-0,09206	-0,07551
As	0,01037	0,034445
Co	0,029522	-0,28486
Cd	-0,11374	-0,23127
Cr	-0,07227	0,072814
Ni	0,166071	-0,27097

There is no relationship that existed between gold and any other metal within the Fumani Tailings Dams 1. A fair negative relationship of -0.285 (Au-Co) and -0.271 (Au-Ni) exists as indicated by the correlation matrix in Table 4.17. This could be due to the fact that most of the Au have been removed and only the small amount that could not be recovered through the carbon in pulp method remains in the tailings dams.

4.3.1.3 Vertical Distribution of Gold within the Fumani Tailings Dams

Fumani Tailings Dam 1

Geochemical assay data revealed that Au values within the Fumani Tailings Dams 1 ranged from 0.31 ppm to 2.79 ppm recorded at sampling points P3H1S6 and P1H1S7 respectively. The average gold value was found to be 1.34 ppm within the tailings dam. The threshold value was found to be 2.22 ppm, with 5 values greater than it. These values were identified at P1H1S4-S7, and P2H4S1 with values of 2.31 ppm (P1H1S6), 2.33 ppm (P2H4S1), 2.36 ppm (P1H1S4), 2.67 (P1H1S5) and 2.79 ppm (P1H1S7). Four of the 5 anomalous values were observed on the first borehole of profile 1. This indicates that high Au values may be located within P1.

Gold borehole logs provided a clearer picture of the distribution with depth within the Fumani Tailings Dam 1 (Fig. 4.37). The borehole logs revealed that, gold exhibits an erratic trend within the tailings dam 1 with depth.

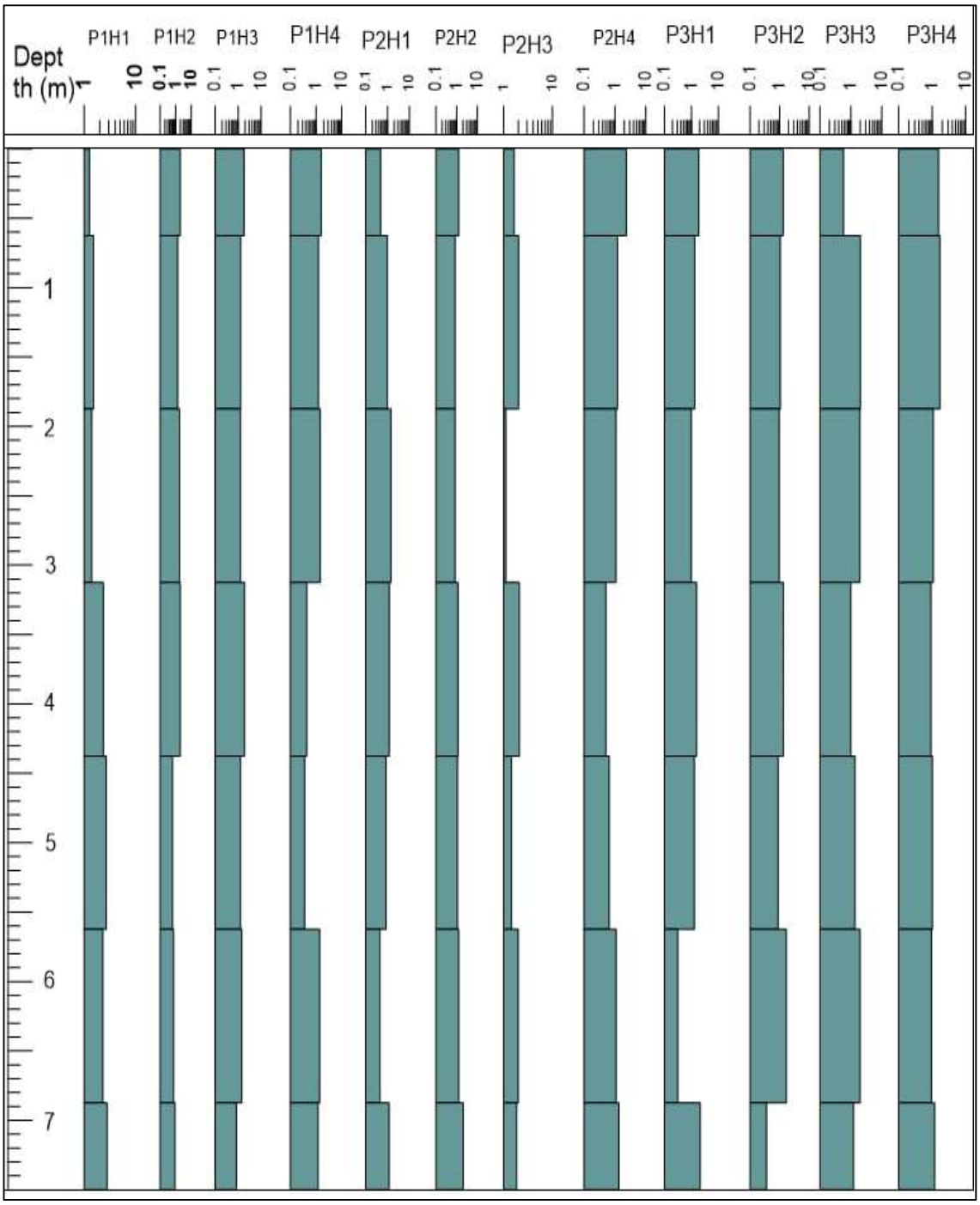

Figure 4.37: Vertical Distribution of Gold within Tailings Dam 1.

Fumani Tailings Dam 2

Geochemical assay data revealed that Au values within the Fumani Tailings Dams 2 ranged from 0.36 ppm to 4.44 ppm recorded at sampling points P2H3S6 and P2H3S1 respectively. The average gold value was found to be 1.44 ppm within the tailings dam. The threshold value was found to be 2.34 ppm, with only 1 value greater than it.

Vertical distribution of gold within the Fumani Tailings Dams 2 as represented by the borehole logs revealed an erratic distribution (Fig. 4.38).

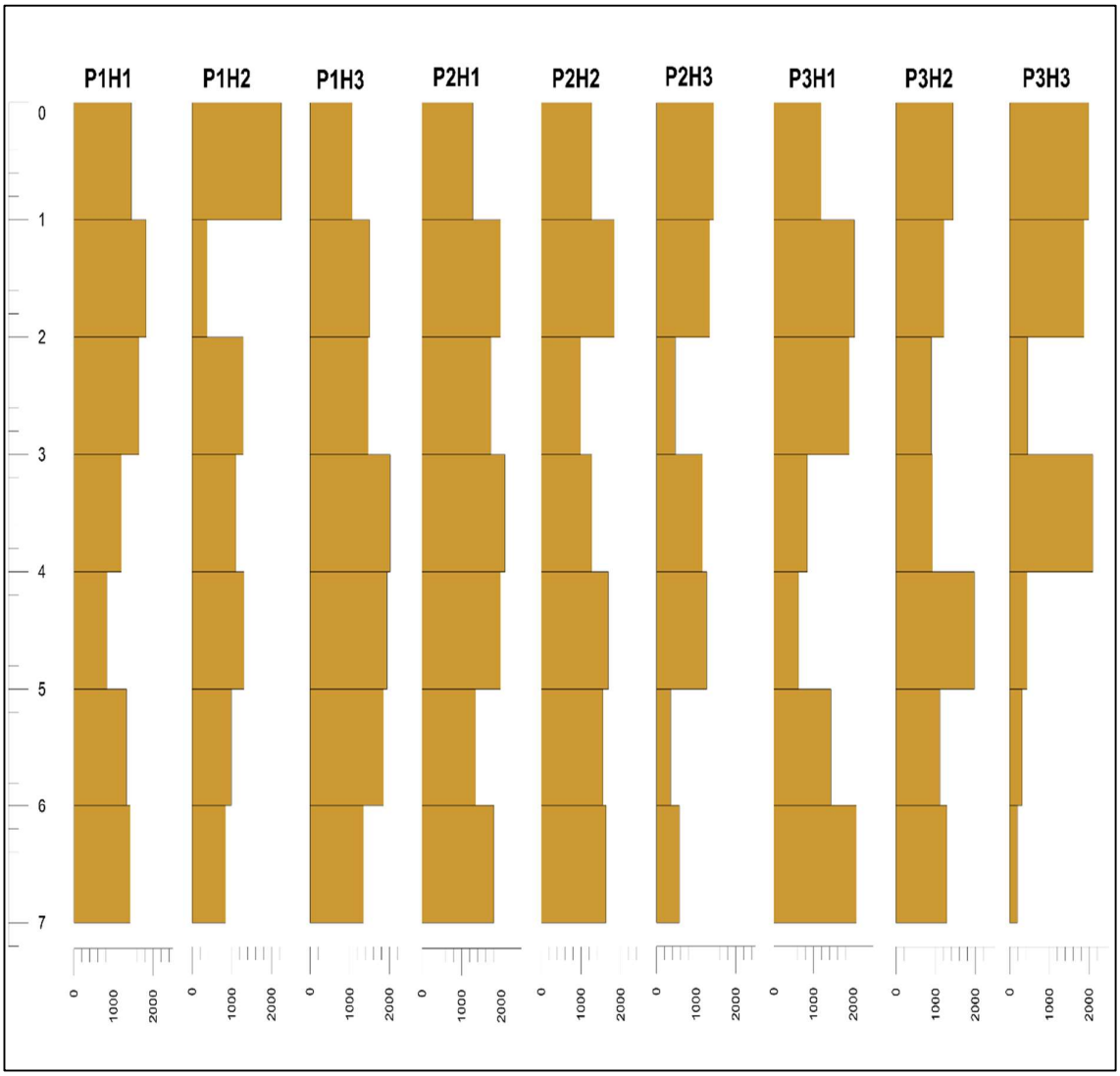

Figure 4.38: Vertical Distribution of Gold within Tailings Dam 2.

4.3.1.4 Tonnage and Concentration Estimation of Gold within the Fumani Tailings Dams

Using the volume and the bulk density of the Fumani Tailings Dams 1 and 2, it was possible to calculate the tonnage of the tailings as well as the concentration of gold within the Fumani Tailings Dams 1 and 2.

The Volume of the tailings in Fumani Tailings Dam 1 and 2 was 124 000 m^3 and 87000 m^3 respectively, both with a bulk density of 1.8 t/m^3 each (Corridor Mining Resources, 2010), The total tons of tailings within the dam were then calculated using the formular T=V x D and represented in Table 4.18, where; T= tonnage of tailings, V= volume of tailings and D= bulk density.

T= 124 000 m^3 x 1.8 t/m^3 = 223 200 tonnes of tailings within Fumani Tailings Dam 1.

T= 87 000 m^3 x 1.8 t/m^3 = 156 600 tonnes tailings within Fumani Tailings Dam 2.

The tonnes of the tailings within each tailings dam were used to calculate the concentration of gold within each tailings dam, using the formular P=T x C, where; P= Gold concentration, T= tonnage of tailings and C= mean value of gold in g/t.

P = 223 200 t x (1.34g/t ÷ 1000 kg) = 299.1 kg gold within the entire Fumani Tailings Dam 1.

P = 156 600 t x (1.44g/t ÷ 1000 kg) = 225.5 kg gold within the entire Fumani Tailings Dam 2.

Table 4.18: Gold concentration within the Fumani Tailings Dams 1 and 2

	Volume of the tailings (V)	Bulk density (D)	Tonnage of tailings (T)	Average Au values (C)	Gold concentration (P)
Tailings Dam 1	124 000 m^3	1.8 t/m^3	223 200 t	1.34 ppm = 0.00134 g/t	299.1 kg
Tailings Dam 2	87 000 m^3	1.8 t/m^3	156 600 t	1.44 ppm = 0.00144 g/t	225.5 kg

Based on the statistical calculations, it can be said that there is a total of 299.1 kg and 225.5 kg of gold within the Fumani Tailings Dam 1and 2 respectively.

4.3.2 Tailings as a Building Material

4.3.2.1 Mineralogical and Geotechnical Properties of Tailings

To determine the suitability of the Fumani tailings for brick production, it was crucial to classify the tailings to determine their mineralogical and geotechnical character. To archive this with great confidence, major oxide analysis, particle size distribution as well as the Atterberg tests were conducted. The tailings were then classified using the Unified Soil Classification System as well as the AASHTO Classification System.

Mineralogical Properties of Tailings

Clay is an important constituent in the process of brick making. To produce quality bricks from tailings, it is important to determine the distribution of the following major oxides: silica, alumina, iron oxide, lime, and magnesia. Table 4.19 indicates that silica was the most dominant oxide within Fumani Tailings Dams 1 and 2. The average silica percentage ranged from 59.26 to 76.07 within Fumani Tailings Dam 1, whilst its percentage ranged from 59.22 to 75.59 within Fumani Tailings Dam 2. In terms of distribution, silica was followed by iron oxide, then alumina. The order of magnitude of the occurrence of major oxides within Fumani Tailings Dams 1 and 2 was as follows: SiO_2> Al_2O_3> Fe_2O_3> MgO> K_2O> CaO> TiO_2> Na_2O> MnO> P_2O_5.

Table 4.19: Statistical Summary of the major oxides within the Fumani Tailings Dams 1 and 2

Sample name	SiO2 (%)	TiO2 (%)	Al2O3 (%)	Fe2O3 (%)	MnO (%)	MgO (%)	CaO (%)	Na2O (%)	K2O (%)	P2O5 (%)
Total T1	84	84	84	84	84	84	84	84	84	84
Total T2	63	63	63	63	63	63	63	63	63	63
Max T1	76,07	1,89	19,91	21,22	0,41	10,2	5,15	2,59	4,11	0,64
Max T2	75,59	1,59	18,11	23,01	0,44	10,38	5,22	2,88	4,01	0,66
Min T1	47,74	0,26	3,64	1,6	0,04	0,27	0,36	0	0,62	0,04
Min T2	47,33	0,23	3,59	1,6	0,03	0,26	0,33	0	0,63	0,04
Average T1	59,26	1,97	13,43	10,53	1,11	2,92	2,45	1,77	2,71	1,06
Average T2	59,22	1,97	13,44	10,51	1,12	2,94	2,45	1,78	2,7	1,05
Range T1	28,33	1,64	16,27	19,62	0,38	9,93	4,79	2,59	3,49	0,6
Range T2	28,26	1,36	14,52	21,41	0,41	10,12	4,89	2,88	3,38	0,62

The required quantities of major oxides for quality brick production have been summarised and listed in table form in Table 4.20 below.

Table 4.20: Required percentages of major oxides for quality brick production (Civilseek, 2022)

	SiO_2	Al_2O_3	Fe_2O_3	CaO	MgO
Required quantity (%)	50-60	20-30	4-6	1-4	4-5

Silica is responsible for the brick's durability, strength, hardness and its resistance to shrinkage. The most suitable soil for quality brick production should have 50-60% silica content. The average percentage of SiO_2 was found to be 59.26 and 59.22 within Fumani Tailings Dams 1 and 2 respectively. The SiO_2 content within both dams falls within the required range for good quality brick production.

Alumina acts as a cementing material in brick production. Alumina is also responsible for the plasticity of bricks. The most suitable soil for quality brick production should have 20-30% alumina content. The average Al_2O_3 was found to be 13.43 % and 13.44% within the Fumani Tailings Dams 1 and 2 respectively. This was less than the required amount for quality brick production. This means that the bricks might have a low plasticity, making it difficult to be molded into the desired shape.

Iron oxide is responsible for the colour of bricks, but most importantly, Fe_2O_3 acts as a flux, helping silica to fuse at lower temperatures. To produce good quality bricks, the amount of iron oxide should be between 4% and 6%. From Table 4.19, it is evident that the average Fe_2O_3 percentage was 10.53 and 10.51 within Fumani Tailings Dams 1 and 2 respectively. These values exceed the required amount, this may cause bricks to become too soft whilst burning, resulting in deformation. Bricks produced from these tailings are more likely to fail the dimension tolerance test.

Lime is responsible for making bricks harden faster during burning. The desired amount of CaO required for quality brick production is 1-4%. The average CaO percentage within the Fumani Tailings Dams 1 and 2 was 2.45 within both tailings dams. This was within the required range for strong and durable brick production.

Magnesia is responsible for the binding of particles together during burning. The required amount of MgO for quality brick production is between 4-5%. The average MgO percentage within Fumani Tailings Dams 1 and 2 was found to be 2.92 and 2.94 respectively. These were less than the required amount. A lower MgO content means that bricks produced from this material will have a decreased shrinkage limit.

Tailings on their own only satisfy the requirements for SiO_2 and Cao. The alumina and magnesia averages were lower than the required quantities for brick making. The Fe_2O_3 was above the required quantity. This means that tailings alone will not be able to produce quality bricks.

Geotechnical Properties of Tailings within the Fumani Tailings Dams

Particle Size Distribution

The data in table 4.21 indicates the total amount of tailings that passed through each sieve during geotechnical tests and represented as a whole number and in percentage.

Table 4.21: Sieve analysis results of Fumani Tailings Dams 1 and 2

Sieve diameter (mm)	Fumani Tailings Dam 1 % passing		Fumani Tailings Dam 2 % passing	
	A	B	C	D
4	100	100	100	100
2	100	100	100	100
1	99	99	98	99
0.5	99	99	96	99
0.25	96	96	96	98
0.125	76	76	81	89
0.075	73	74	80	76

The percentage of the material passing each sieve was decreasing with the decrease in sieve diameter. From Table 4.20 and figure 4.26, it can be seen that 100 % of the material pass through the 4- and 2-mm diameter sieves in all the samples. Since soil particles greater than 2 mm diameter are known as gravel, it can be said with confidence that no gravel was detected in all the samples. Particles that pass through the 0.075 mm diameter sieve are known as fine grained, with those that lie between the 0.075- and 2-mm diameter sieve known as sand. Since a percentage of 73,74, 80 and 76 from sample A, B, C and D pass though the 0.075 mm diameter sieve respectively, it can be said that that is the percentage of particles that can be

classified as fine particles within the tailings. This means that a total percentage of 27,26,20 and 24 are sand sized particles within sample A, B, C and D respectively. Because more than 50% 0f the material passed through the 0.075 mm diameter sieve, it can be said that the tailings are fine grained material. The sieve analysis results can also be represented using grain size distribution graphs (Fig. 4.39), where samples A and B represent material in Fumani Tailings Dam 1, and C and D represents material in Fumani Tailings Dam 2.

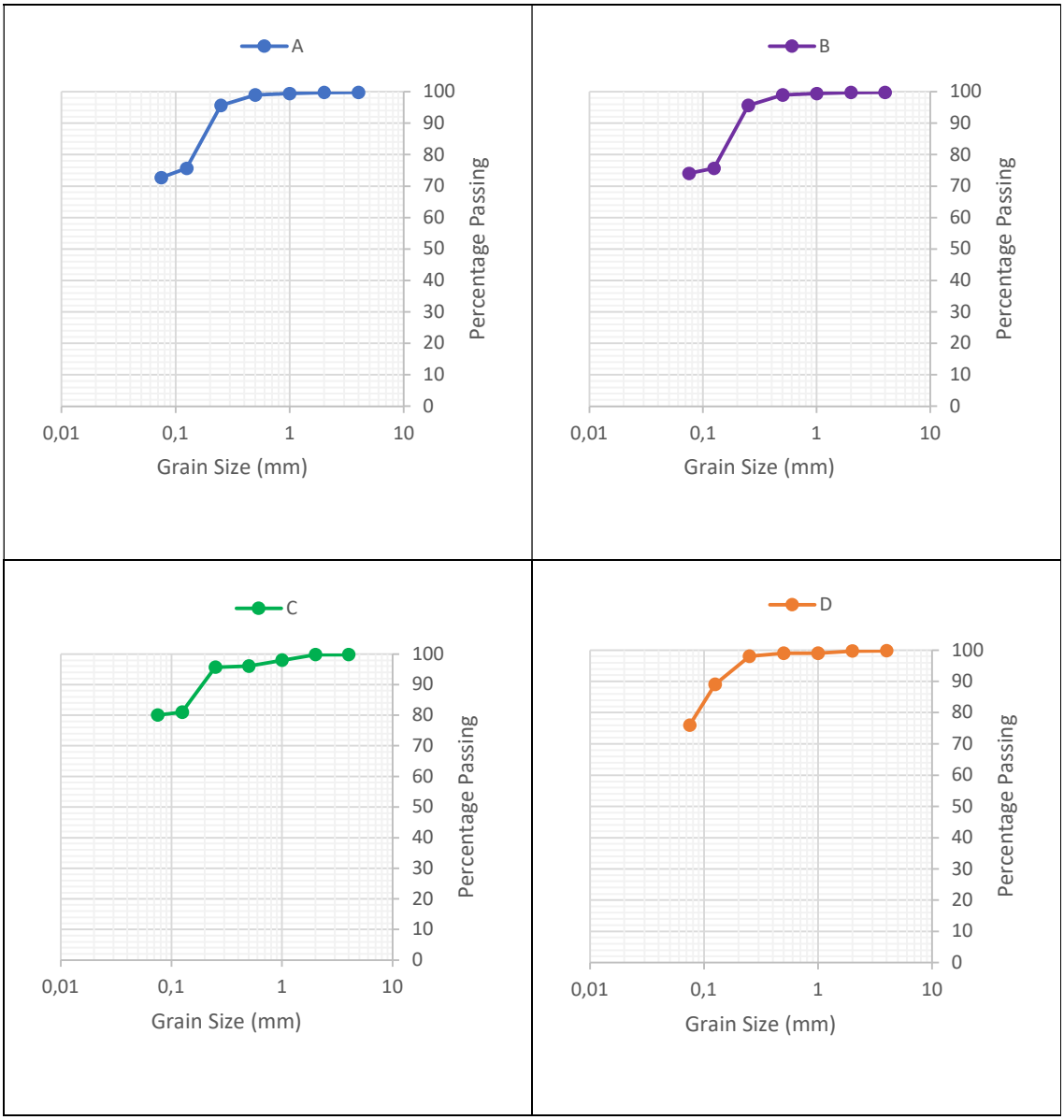

Figure 4.39: Grain size distribution graphs.

Atterberg Limits

Liquid Limit (LL)

The liquid limit of the Fumani Tailings Dams 1 and 2 is indicated in Table 4.22 below. The LL at Fumani Tailings Dam 1 was 25% and 26% at samples A and B respectively, whilst the LL at Fumani Tailings Dams 2 was 23% and 24% at samples C and D respectively. A liquid limit less than 30% is considered low. Since the LL in both Fumani Tailings Dams 1 and 2 is less than 30%, this indicates that the tailings have a low LL and consequently, have low soil compressibility. This also implies that it requires a less amount of water to be added into the tailings for it to flow as a liquid (The Construction Civil, 2022).

Table 4.22: Liquid Limit of Fumani Tailings Dams 1 and 2

	Sample ID	LL (%)	LL as a whole number
Fumani Tailings Dam 1	A	24.68	25
	B	26.01	26
Fumani Tailings Dam 2	C	23.29	23
	D	23.73	24

Plastic Limit (PL)

The plastic limit of the Fumani Tailings Dams 1 and 2 is indicated in Table 4.23 below. The PL at Fumani Tailings Dam 1 was 20% at both samples A and B, whilst the LL at Fumani Tailings Dams 2 was 19% and 20% at samples C and D respectively. A plastic limit less than 30% is considered low. Since the PL in both Fumani Tailings Dams 1 and 2 is less than 30%, this indicates that the tailings have a low PL and consequently (The Construction Civil, 2022).

Table 4.23: Plastic Limit of Fumani Tailings Dam 1 and 2

	Sample ID	PL (%)	PL as a whole number
Fumani Tailings Dam 1	A	20.21	20
	B	20.53	20
Fumani Tailings Dam 2	C	18.91	19
	D	19.98	20

Plasticity Index (PI)

The plasticity index of the Fumani Tailings Dams 1 and 2 (Fig. 4.40 and Table 4.24) is indicated below. The PI at Fumani Tailings Dam 1 was 5 and 6 at samples A and B respectively, whilst the PI at Fumani Tailings Dams 2 was 4 at both samples C and D. A plasticity index between 5-10 is considered low plasticity (Burmister, 1949). This means that the tailings within the Funani Tailings Dams 1 are of low plasticity in nature. The PI of tailings in Tailings Dams 2 was 4. A PI between 1-5 is considered as slight plasticity. This means that the tailings within the Fumani Tailings Dam 2 were slightly plastic.

Table 4.24: PI table of Fumani Tailings Dams 1 and 2 with descriptions

	A	B	C	D
PI	5	6	4	4
Description	Low plasticity	Low plasticity	Slight plasticity	Slight plasticity

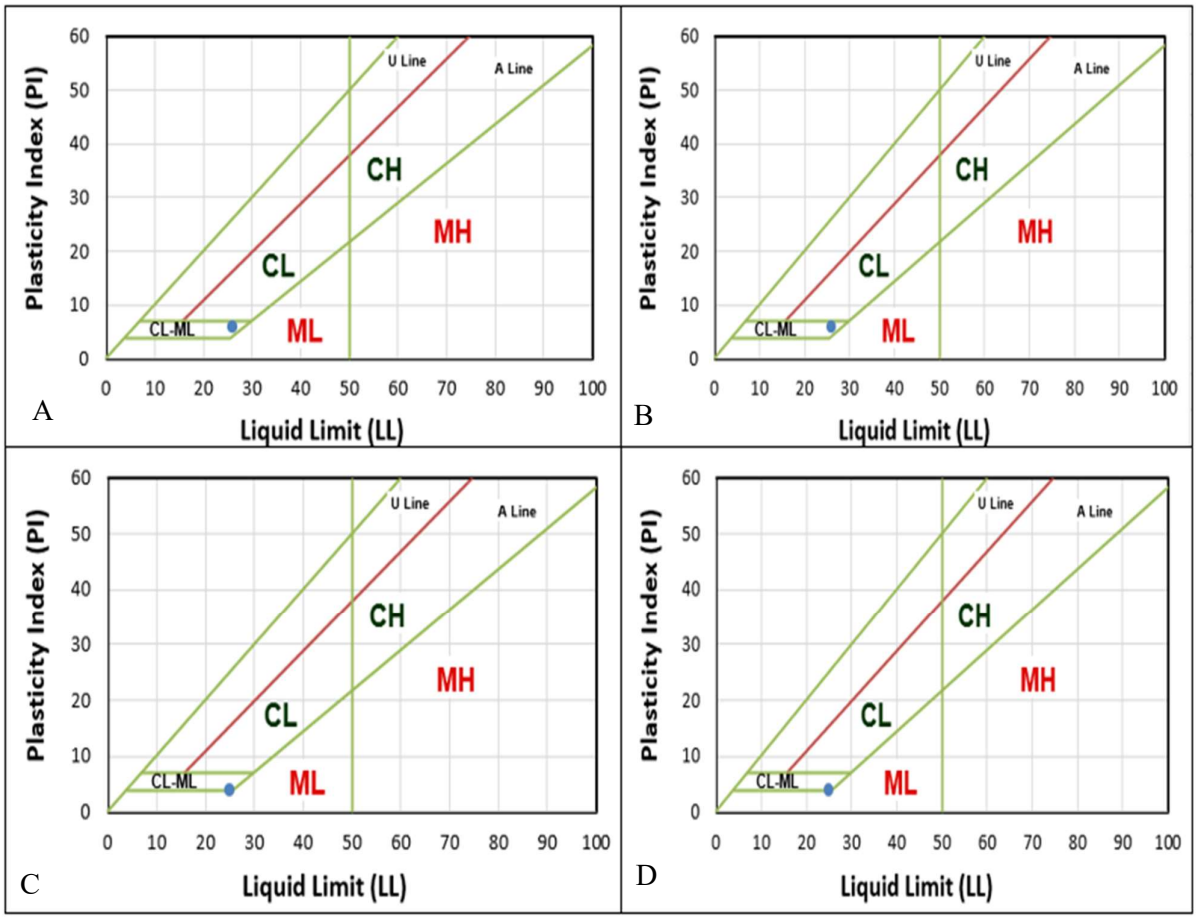

Figure 4.40: Casagrande Plasticity charts.

Tailings Classification

The Sieve analysis, Liquid limit, Plastic Limit as well as the Plasticity index will be used to classify tailings according to the USCS and the AASHTO classification system. Table 4.25 indicates the results obtained from the above-mentioned tests.

Table 4.25: Data required for tailings classification

	% Passing 0.075 mm sieve	LL (%)	PL (%)	PI	PI relative to A line (Fig. 4.42)
A	73	25	20	5	Above A line
B	74	26	20	6	Above A line
C	80	23	19	4	Above A line
D	76	24	20	4	Above A line

Unified Soil Classification system

The USCS states that if more than 50% of the material pass through the 0.075 mm sieve during the sieve analysis, then the material falls under fine grained soils. The percentage of material that passed through the 0.075 mm sieve was more than 50% in all samples, this means that the tailings in both Fumani Tailings Dams 1 and 2 is fine grained.

If the LL is less than 50%, then the material has a low compressibility, making it either clay or silt of low compressibility. Since the LL in all samples was less than 50%, this means that the tailings within the Fumani Tailings Dams 1 and 2 are either silt or clay with a low compressibility.

The plasticity index was between 1 and 5 in samples C and D, which falls within the slightly plastic category. The PI for sample A and B was 6, falling in the low plasticity category. This means that the tailings are either inorganic silts or inorganic clays of low plasticity denoted by ML and CL respectively.

When plotting the plasticity index graph, the point in all samples falls above the A line, in the ML and CL category, therefore, making the tailings silty clay. The USCS also states that if the LL is less than 30% with a PI between 4 and 7, the material falls within the mixed zone, where both CL and ML soils can be plotted, and generally known as silty clay.

The CL category consists of inorganic, sandy, silty, and lean clays of low compressibility, low to medium plasticity, and no or slow dilatancy. The ML category consists of inorganic silts, very fine sands, silty or clayey fine sands. The material in the ML group is slightly plastic to non-plastic, with a slow to rapid dilatancy.

AASHTO Classification System

AASHTO material classification system states that if more than 35% of the material pass through the 0.075 mm diameter sieve, then the material is known as silt or clay material and falls within the A-4 to A-7 group classification. Because more than 35% passed through the 0.075 mm sieve, the tailings within the Fumani Tailings Dams are either silt or clay.

The liquid limit of the tailings within the Fumani Tailings Dams 1 and 2 was found to be between 24 to 26%. AASHTO classifies material with a liquid limit less than 40% as either A-4 or A-6.

The plasticity index of the tailings within the Fumani Tailings Dams 1 and 2 was found to be less than 10. AASHTO classifies material with LL less than 40% and a PI less than 10% in the A-4 class.

Because the tailings are fine grained, the following equation will be used to calculate the group index; $GI = (F_{200} - 35)\ [\ 0.2+0.005(LL-40)] + 0.01\ (F_{200} -15)\ (PI – 10)$

Where GI is the group index, F_{200} is the percentage passing the 0.075 mm diameter sieve, LL is the liquid limit and PI is the plasticity index. The GI for Fumani Tailings Dams 1 and 2 was calculated and the results represented in Table 4.26.

Table 4.26: Group index of tailings within Fumani Tailings Dams 1 and 2

	A	B	C	D
GI	2.62 = 3	2.71 = 3	1.275 = 1	1.26 = 1

Based on the AASHTO Classification, the material within the Fumani Tailings Dams 1 and 2, is A-4(3) and A-4(1) respectively. Classifying the material within the Fumani tailings Dams 1 and 2 as silty soils that have a good to fair general rating as a subgrade.

4.3.2.2 Brick Tests Results

Clay Bricks

The Dimension tolerance test revealed that all the clay bricks that were produced with tailings had different dimensions. The bricks had rough rectangular faces, with distortions on their edges, making them damaged on their edges as well as their sides. Honey combing was observed on the surface of the bricks. Honeycombing can be caused by using material that is not cohesive whilst producing bricks. The bricks, therefore, were considered poor as they did not pass this test.

The bricks did not pass the water absorption, efflorescence as well as the compressive strength tests. All the clay bricks produced with tailings in them completely dissolved in the water and could not be tested.

The bricks were scratchable with a fingernail, leaving noticeable impressions on bricks. Dust could be blown off from the sample after scratching it. This meant that the bricks were considered poor and week.

All the bricks made with clay and tailings material broke into pieces when dropped from a 1 m height. This means that the bricks have a low impact value and are not suitable for construction.

It can therefore be said that all clay bricks made with different tailings to soil ratios of 10% to a 100% had failed all the brick tests and are therefore not suitable for construction.

Cement Bricks

The Dimension tolerance test revealed that all the cement bricks that were produced with tailings had different dimensions. The bricks had rough rectangular faces, with distortions on their edges, making them damaged on their edges as well as their sides. Honeycombing was observed on the surface of the bricks. This could be due to the particles not binding effectively due to low cohesion. The bricks, therefore, were considered poor.

The water absorption of the bricks was less than 15% in samples A,B, and C. Sample D had a water absorption of 15.1%, this was slightly above the required limit and therefore classified as a poor quality brick, whilst samples A, B and C were found to have passed the water absorption test.

According to ASTM C62, a good quality brick should have a compressive strength of 8.6 MPa or more. Samples A, C and D had a compressive strength of 3.5 MPa, whilst sample B had a compressive strength of 6.5 MPa. Since all the cement bricks had a compressive strength less than 8.6 MPa, the bricks produced were not of good quality and therefore could not be used for building.

All the cement bricks passed the hardness test. The bricks were not scratchable by the fingernail, no impression was left on the brick after scratching. These means that all bricks produced were hard.

The cement bricks did not break when dropped 1 m from the floor. This meant that the bricks had a high impact value.

The cement bricks produced were of poor quality and not suitable for building as they have failed the dimension tolerance and compressive strength tests.

CHAPTER 5: DISCUSSION, CONCLUSIONS AND RECOMMENDATIONS

5.1 Discussion

Borehole profile logs together with pH were used to characterise the Fumani Tailings Dams 1 and 2 into oxidation zone, transitional zone, and un-oxidised zone. This was done in order to determine the possibility of Acid Mine Generation from the tailings dams.

The findings from this study concur with those of previous studies that indicated that the tailings dams were most acidic at the first few meters from the surface (Nengovhela, 2016; Matshusa, 2013; Nemapate, 2017). Profile logs and pH logs both confirmed that the tailings dams were acidic at the surface to a depth of 2 m. The tailings dams were slightly acidic between 2 and 4 m. below the 4 m mark was the un-oxidised zone that was slightly neutral. Variations of the zones can be explained by the fact that the first upper 2 m depth is where oxygen and moisture are abundant for active chemical reactions to take place. Other factors that influence acid mine water generation are the hydrology of the dam and the rate of oxygen and water penetration through the dam. This to some extent may be influenced by the age of the dams.

Previous studies had also indicated that rehabilitation of dams using vegetation with deep roots can accelerate acid mine generation to deeper level beyond the 3 m mark (Nengovhela *et al*., 2006). The Fumani Tailings Dams, however, were not rehabilitated as they lie bare, subjected to wind erosion. The dams are thus prone to acid mine water generation.

Besides AMD, unrehabilitated tailings dams are known to release metals into the environment that can cause metal pollution. The metals can either be dispersed from the tailings dams to the environment through wind and water erosion. The data obtained from X-ray Spectrometry revealed that the order of magnitude of the occurrence of metals within Fumani Tailings Dams 1 and 2 was as follows: As> Zn> Ni> Cr> Cu> Pb> Co> Cd.

The data obtained from X-ray Fluorescence spectrometry was used together with the Dutch guideline of concentrations in soil, Singla Factor Index Method (SFIM) and the South African guideline of standards to assess the pollution status of the Fumani Tailings Dams 1 and 2 and their surroundings. Using the Dutch Guideline of Concentrations, it was found that the mean and maximum values of Pb, Zn, Cu, Co, Cd and Cr do not contaminate the Fumani Tailings

Dams, Ni falls in the C category whilst As exceeds the C category. This means that Ni and As contaminate the tailings dams and require site clean-up.

Using the SFIM, Pb, Zn, Cu, Co, Cd and Cr do not contaminate the tailings dams. Nickel values do not contaminate the tailings dams yet, however, it requires monitoring for it not to exceed these limits. Arsenic highly exceeds the Pi of 3 by over 50 times in both tailings dams, this means that As highly contaminate the tailings dams and requires site clean-up.

Using the South African Guideline of Standards, Zn, Co, and Cd do not contaminate the tailings dams and are within the required limits for all land uses. Pb, Cu and Ni exceeds the limits for water resources, As and Cr highly contaminates the tailings dams and require a site clean-up.

The pollution status of the area around the Fumani Tailings Dams was also determined using the Dutch Guideline of standards, SFIM and the South African Guideline of Standards.

Using the Dutch Guideline of Concentrations in soil surrounding the tailings, together with the mean and maximum metal concentration, the following could be deduced; Zn and Cd do not contaminate the surrounding area, Co and Cu are within the C values of the Dutch Guideline and therefore contaminate the soil, however, Pb, As, Cr and Ni highly exceed the C values and therefore require clean up.

Using the SFIM, the mean and maximum values of the metals, it was ascertained that Zn and Cd do not pollute the soil around the Fumani Tailings Dams. The maximum values for Cu and Co are beyond the environmental quality standard, with Co and Cu slightly and moderately contaminating the soil around the Fumani Tailings Dams respectively. Both mean and maximum values for Pb, As, Cr and Ni highly contaminate the soil.

Using the South African Guideline of Standards, Cd and Co do not contaminate the soil, Cu and Zn exceed the soil values above which they may pollute the ecosystem and affect human health. Ni pollutes the soil suitable for all land-use with exception to commercial and industrial use. Pb, As and Cr highly pollute the soil.

The methods used to determine the pollution status of the tailings dams and soil show that only Ni and As contaminate the tailings dams, whilst Pb, As, Cr, Co and Cu highly contaminate the soil. These high concentrations located on soils around the Fumani Tailings Dams, could be a

result of another source in addition to the possible metal dispersion by wind and water from the tailings dams.

Geochemical analysis of gold using fire assaying technique indicated values of gold within the Fumani Tailings Dams ranged from 0.31 ppm to 2.79 ppm at Fumani Tailings Dam 1 and from 0.36 ppm to 4.44 ppm in Fumani Tailings Dam 2. The average Values of gold within the Fumani Tailings Dams 1 and 2 was 1.34 ppm and 1.44 ppm respectively. Statistical calculations indicated that the total amount of gold within the Fumani Tailings Dams 1 and 2 was 299.1 kg and 225.5 kg respectively. These values prove to be high enough to warrant reprocessing of both tailings dams for gold. Pan African Resources, Sibanye still waters as well as South Deep are some of the companies currently reprocessing old gold tailings dams within South Africa. High gold prices, improved recovery techniques as well as rehabilitating benefits, make reprocessing tailings for gold a more lucrative business (Viljoen, 2009).

The geotechnical Studies were conducted on the Fumani Tailings Dams 1 and 2 in order to determine the characteristics and classification of tailings for engineering purposes, this was done in order to assess the suitability of tailings for brick production. The findings from this study concur with those from previous studies that indicated that tailings are silty, with low compressibility, plasticity and cohesion. The findings of this work were similar to those of other studies investigating the use of tailings as a construction material.

The Major oxides revealed that Tailings on their own only satisfy the requirements for SiO_2 and Cao. The alumina and magnesia averages were lower than the required quantities for brick making. The Fe_2O_3 was above the required quantity. This means that tailings alone have low plasticity, the bricks will be difficult to mold and shape. Bricks might also be deformed after burning; therefore, tailings alone will not be able to produce quality bricks.

Based on the Particle size distribution and Atterberg limits, the tailings were then classified using the USCS and the AASHTO classification Systems. Based on the USCS it can be said with confidence that the material in the tailings dams falls between the ML and CL class. The CL category consists of inorganic, sandy, silty, and lean clays of low compressibility, low to medium plasticity, and no or slow dilatancy. The ML category consists of inorganic silts, very fine sands, silty or clayey fine sands. The material in the ML group is slightly plastic to non-plastic, with a slow to rapid dilatancy. This alone is not suitable for brick production as the low

PI and LL results in low cohesion, this means that it will be difficult for the particles to bind together during brick production.

Based on AASHTO Classification system, the material within the Fumani Tailings Dams 1 and 2, falls within the A-4(3) and A-4(1) classes respectively. Classifying the material within the Fumani tailings Dams 1 and 2 as silty soils that have a good to fair general rating as a subgrade.

The tailings were then mixed with soil to produce clay bricks of different tailings to soil ratios. A total of 10 different soil to tailings were made and analysed, they all failed the brick test and were not suitable for engineering purposes. This was due to less alumina content that indicated a very low cohesion within the material.

Because the tailings on their own were not suitable for brick production, they were used as an additive in the creation of cement bricks. Cement bricks were then made using different tailings to cement mixture ratios. They underwent testing at the Soillab in Pretoria where they failed to meet the minimum requirement for bricks used in construction.

5.2 Conclusions

This study has satisfied its objectives. The values, distribution and dispersion of metals within the Fumani Tailings Dams 1 and 2 and their surrounding area has been clearly determined and assessed, along with their pollution statuses. The gold values within the tailings dams were ascertained to determine the possibilities of reprocessing. The suitability of tailings for brick production has been analysed and it was therefore concluded that :

- The oxidation zone at the Fumani Tailings Dams 1 and 2 was from the surface of the tailings dams to a depth of 2 m. The tailings were acidic at the first 2 m. tailings ranged from slightly acidic to slightly neutral from 2 m to 7 m. The tailings had an average acidic pH from the surface to a depth of 7m.
- This means that the tailings have the potential to cause acid mine generation if not rehabilitated.
- The lateral distribution of tailings was observed through compositing the concentrations within each borehole in the tailings dams to produce metal prediction maps through ordinary kriging.

- Metal values obtained from X-ray Fluorescence spectrometry revealed that Ni slightly contaminates the tailings dams, whilst As highly contaminates both tailings dams and requires an urgent site clean-up.
- There is therefore a high potential of metal pollution within the area around the Fumani Tailings Dams 1 and 2. This may cause negative impacts to the environment as well as human health through dust inhalation and food chain as the tailings are easily blown by wind into the environment.
- The soil surrounding the tailings dams had extremely high values of Pb, As, Cr, Co and Cu, since these values were low within the tailings dams but high within the soils around the tailings dams, they could be from a different source.
- This indicates that they may be high background values and not necessarily pollution from the tailings dams alone.
- There was no relationship between gold and the other metals, this was due to the fact that most of the gold has already been removed during mineral processing, the amount of gold within the tailings is that which could not be recovered during beneficiation.
- The average Values of gold within the Fumani Tailings Dams 1 and 2 was 1.34 ppm and 1.44 ppm respectively with the highest gold value at 4.44 ppm. Statistical calculations indicated that the total amount of gold within the Fumani Tailings Dams 1 and 2 as 299.1 kg and 225.5 kg respectively. These values prove to be high enough to warrant reprocessing of both the Fumani Tailings Dams 1 and 2 for gold.
- The materials within the Fumani tailings dams are poor for engineering purposes as they have a low alumina content, low LL and low PI. This means the tailings have low compressibility, low plastic, no cohesion and low dilatancy. These make it difficult for tailings materials to be molded into the required shape and for particles to bind. It can therefore be said that tailings on their own are not suitable for brick production.
- This was evident when the clay and cement bricks made from different tailings to soil ratios and different cement to tailings ratios failed the brick tests. The bricks, produced during this study are therefore not suitable for construction.

5.3 Recommendations

The following recommendations were made:

- The study recommends the reprocessing of gold within the Fumani Tailings Dams using mining methods that do not further contaminate the tailings and/or the environment, such as hydraulic mining.
- Before reprocessing the tailings dams, proper tailings management plans that are environmentally friendly, align to the government requirements and uses recent and improved technologies, must be done to ensure proper storage of tailings during and after reprocessing.
- Further studies on the use of tailings as additives to either ready mix concreate in addition to sand should be conducted.
- Further detailed exploration of gold on soils exhibiting high concentrations of Pb, As, Ni, Cr, Co and Cu, as the gold mineralisation within the Fumani mine were found within quartz veins with sulphide mineralisation, BIF, carbonate veins or sulphide replacement veins.

REFERENCES

Altaany, F.H. and Jassim, F.A. (2013). Image Interpolation Using Kriging Technique for Spatial Data. http://arxiv.org/pdf/1302.1294. Accessed: 22 February 2013.

Asati, A., Pichhode, M. and Nikhil, K. (2016). Effect of Heavy Metals on Plants: An Overview. International Journal of Application or Innovation in Engineering and Management, Vol. 5, No. 3, pp. 57-66.

Banfalvi, G. (2011). Heavy Metals, Trace Elements and their Cellular Effects. In: Banfalvi, G. Cellular (Ed.). Cellular Effects of Heavy Metals. Springer. pp. 3-28.

Blake, W. (2013). The Changing Faces of Tailings Retreatment. Modern Mining, pp. 58-63.

Brandal, G., Cloete, M. and Anhaeusser, C.R. (2006). Archaean Greenstone Belts. In: Johnson, M.R., Anhaeusser, C.R. and Thomas, R.J. (Eds.). The Geology of South Africa. Geological Society of South Africa, Johannesburg/Council for Geoscience, Pretoria, pp. 9-56.

Bullen, W.D., Wilson, M.G.C. and Vorster, C.J. (1995). The Metallogeny of the Pieterburg and Tzaneen areas. Council of Geoscience, Geological Survey of South Africa, pp. 6-44.

Burmister, D.M. (1949). Principles and Techniques of Soil Identification. Proceedings.

Calam, C. (2020). New Tailings Reprocessing Technology Has Environmental Benefits. Thermo Fisher, 10 June.

Chibuike, G.U. and Obaiora, S.C. (2014). Heavy Metal Polluted Soils: Effect on Plants and Bioremediation Methods. Applied and Environmental Soil Sciences, Vol. 2014, 12 pp.

Childs, C. (2004). Interpolating Surfaces in ArcGIS Spatial Analyst. https://support.esri.com/en/knowledgebase/GISDictionary/term/interpolation. Accessed: 23 November 2014.

Civilseek, (2022). Manufacturing of Bricks; Method, Process, Types. https://civilseek.com/manufacturing-of-bricks/. Accessed: 14 December 2022.

Collins, R.G. (1991). Louis Moore Gold Mine Co (Pty) Ltd: Information Circular. Council of Geoscience, Pretoria, STK Reference, 2970 (unpublished report).

Corridor Mining Resources (2010). Technical Review and Pre-Feasibility on the Treatment of Fumani FRD Material, document no. 080069-34-400-07-001, unpublished report, pp. 10.

Costa, L. and Silva, J. (2020). Strategies used to Control the Costs of Underground Ventilation in some Brazilian Mines. REM-International Engineering Journal, Vol. 74, No. 4, pp. 555-560.

Das, B.M. (2006). Principles of Geotechnical Engineering. Seventh edition, Global Publishing Programs, United States of America.

Dehghani, A., Mostad-Rahimi, M., Mojtahedzadeh, S.H. and Gharibi, K.K. (2009). Recovery of Gold from the Mouteh Gold Mine Tailings Dams. Journal of the Southern African Institute of Mining and Metallurgy, Vol. 109, pp. 417-421.

Department of Land Affairs and Forestry, (2006). National Spatial Planning Information, Shape Files, Pretoria, South Africa.

Evett. J. and Cheng. L. (2007). Soil and Foundation. Orentice Hall, pp. 9-29. ISBN 0132221381

Fleming, C. (2003). The Economic and Environmental Case for Recovering Cyanide from Gold Plant Tailings. Johannesburg, SGS MINERALS SERVICES.

Frimmel, H. (2019). The Witwatersrand Basin and Its Gold Deposits. In: K.A. and H.A. (Eds.). The Archaean Geology of the Kaapvaal Craton, Southern Africa. Geneva: Springer, Cham, pp. 255-275.

Gold Price, (2022). 20 Year Gold Price History in US Dollars per Ounce. https://goldprice.org/gold-price-charts/20-year-gold-price-history-in-us-dollars-per-ounce. Accessed: 09 March 2022.

Grim, E.R. and Kodama, H. (2013). Clay Minerals. https://www.britannica.com/EBchecked/topic/120723/clay-mineral. Accessed: 03 March 2017.

Groenheide, S. (2021). Tailings: Being Clear on the Opportunities and the Risks. Royal IHC.

Harvey, P.J., Handly, H.K. and Taylor M.P. (2015). Identification of the Sources of Metal (lead) Contaminations in Drinking Water in North-eastern Tasmania using Lead Isotopic

Compositions. Environmental Science and Pollution Research. doi: 10.1007/s11356-015-4349-2. (https//dxx.doi.org/10.1007%2Fs11356-015-4349-2).

Howell, N., Lavers, J., Paterson, D., Garrett, R. and Banati, R. (2012). Trace Metal Distribution in Feathers from Migratory, Pelagic Birds. http://www.ansto.gov.au/AboutANSTO/MedicalCenter/News/ACS01. Australia Nuclear Science and Technology Organisation. Accessed: 25 June 2015.

Hussain, A., Abbas, N. and Arshad, F. (2013). Effects of Diverse Doses of Lead (Pb) on Different Growth Attributes of Zea Mays L. Agricultural Sciences, Vol. 4, No. 5, pp. 262–265.

Intellidex, (2018). Financial Provisioning for Rehabilitation and Mine Closure: A Study of South African Platinum and Coal Mining Companies. https://www.

Jayakumar, K., Rajesh, M., Baskaran, L. and Vijayarengan, P. (2013). Changes in Nutritional Metabolism of Tomato (Lycopersicon Esculantum Mill.) Plants Exposed to Increasing Concentration of Cobalt Chloride. International Journal of Food Nutrition and Safety, Vol. 4 No. 2, pp. 62–69.

Johnson, M.R., Enhaeusser, C.R. and Thomas R.J. (2006). The Geology of South Africa. Council for Geoscience and Geological Society of South Africa, pp. 34-36.

Khobragade, K. (2020). Impact of Mining Activity on Environment: An Overview. International Journal of Scientific and Research Publications, Vol. 10, No. 5, pp. 784-789.

Kitco, (2020). Price of Gold in kg. https://www.kitco.com/golg-today-south-africa/index.html. Accessed: 05 April 2020.

Koumal, G. (1994). Method of Environmental Clean-up and Producing Building Material using Cu Mine Tailing Waste Material. US patent US5286427 A.

Lenntech, (2017). The Chemical Elements and Water. https://www.lenntech.com/periodic/elements/cu.htm#ixzz40KZlnyvT. Accessed: 22 February 2020.

Lombaard, A.F. (1956). Report on Klein Letaba Goldfields, North-eastern Transvaal: Klein Letaba Mining Co. STK 06560012 (unpublished report).

Loots, C. (2020). Gold Tailings Retreatment Offers an Environmental Solution. Mining weekly, 26 November.

Malatse, M. and Ndlovu, S. (2015). The Viability of using the Witwatersrand Gold Mine Tailings for Brickmaking. Journal of the Southern African Institute of Mining and Metallurgy, Vol. 115, No. 4, pp. 321-327.

Manivasagaperumal, R., Vijayarengan, P., Balamurugan, S. and Thiyagarajan, G. (2011). Effect of Copper on Growth, Dry Matter Yield and Nutrient Content of Vigna Radiata (L.) Wilczek. Journal of Phytology, Vol. 3, No. 3, pp.53-62.

Manoharan, C., Sutharsan, P. and Dhanapandian, S. (2012). Characteristicts of some Clay Material from Tamilnadu, India, and their Possible Ceramic uses. Ceramica, Vol. 58, pp. 412-418.

Maskell, D., Heath, A. and Walker, P. (2016). Appropriate Structural Unfired Earth Masonry Units. Construction Material, Vol. 169, No. 5, pp. 1-10.

Matandare, B., Mukurunge, T. and Bhila, T. (2019). Impacts of Mining Operations on Water Resources and Ecosystems: The Case of Letseng Diamonds in Lesotho. International Journal for Scientific Research and Development, Vol. 6, No. 12, pp. 634-640.

Matshusa, K., Ogola, J.S. and Maas, K. (2012). Dispersion of Metals at Louis Moore Gold Tailings Dam. Limpopo Province, South Africa. International Mine Water Association, 334 pp.

McCarthy, T.S. (2011). The Impact of Acid Mine Drainage in South Africa. South African Journal of Science, Vol. 107, No 5/6, pp.1-7.

McMillan, A. (2020). Mine Tailings and Their Environmental Legacy. The Sudbury Star, Accessed: 14 October 2020.

Mishra, G. (2017). Soil classification. https://theconstructor.org/geotechnical/soil-classification/3358/. Accessed: 20 February 2020.

Nemapate, N. (2017). Evaluation of Economic Potential of Gold Tailings Dams: Case Studies of the Klein Letaba and Louis Moore Tailings Dams, Limpopo Province, South Africa. A

Masters Dissertation Submitted to the Department of Mining and Environmental Geology, School of Environmental Sciences, University of Venda, in Fulfilment of the Master of Earth Sciences in Environmental Geology.

Nematshahi, N., Lahouti, M. and Ganjeali, A. (2012). Accumulation of Chromium and its Effect on Growth of (Allium cepa cv. Hybrid), European Journal of Experimental Biology, Vol. 2, No. 4, pp. 969–974.

Nengovhela, A.C., Yibas, B. and Ogola, J.S. (2006). Characterisation of Gold Tailings Dams of the Witwatersrand Basin with Reference to their Acid Mine Drainage Potential, Johannesburg, South Africa. Water SA, Vol. 23, No. 4, pp. 499-506.

Nielen, M.W.F. and Marvin, H.J.P. (2008). Challenges in Chemical Food Contaminants and Residue Analysis. In: Pico, Y. (Ed.). Food Contaminants and Residue Analysis. Elsevier. ISBN 0080931928. pp. 1-28.

Nummi, E. (2015). From Tailings to Treasure? A New Mother Lode. https://www.thermofisher.com/blog/mining/from-tailings-to-treasure-a-new-mother-lode/. Accessed: 22 February 2022.

Ogola, J.S., Mitullah, W.V. and Omulo, M.A. (2002). Impacts of Gold Mining on the Environment and Human Health: A Case Study in the Migori Gold Belt, Kenya. Environmental geochemistry and health 24. Kluwer Accademic Publishers. Netherlands. pp. 141-158.

Ogola J.S. (2010). Dispersion of Heavy Metals and their Potential Impacts on the Environment: A Case Study of Gold Tailings Dams in Giyani Greenstone Belt, Limpopo Province, South Africa. In: Wolkersdorfer and Freund (Eds.). Mine water innovative thinking. Sydney, Nova. Scottia, Canada. CBU press. pp. 591-592.

Ogola, J., Shavhani, T. and Mundalamo, R. (2018). Possibilities of Reprocessing Tailings Dams for Gold and other Minerals: A Case Study of South Africa. Journal of Environmental Science and Allied Research, Vol. 2017, No. 1, pp. 39-42.

Oladejo, O.F., Ogundele, L.T., Inuyomi, S.O., Olukotun, S.F., Fakunle, M.A. and Alabi, O.O. (2021). Heavy Metals Concentrations and Naturally Occurring Radionuclides in Soils Affected

by and Around a Solid Waste Dumpsite in Osogbo Metropolis, Nigeria. Environmental Monitoring and Assesment, Vol. 193, No. 11.

Pezzarossa, B., Gorini, F. and Petruzelli, G. (2011). Heavy Metals and Selenium Distribution and Bioavailability in Contaminated Sites: A Tool for Phytoremediation. In: Selim, H.M. (Ed.). Dynamics and Bioavailability of Heavy Metals in the Rootzone. CRC Press. pp. 93-128.

Pistilli, M. (2022). 12 Largest Producers of Gold by Country (Updated 2022). Investing News, 16 February.

Pretorius, A. I, Van Reenen, D. D. and Bartorn, J. M. (1988). BIF-hosted gold mineralization at the Fumani Mine, Surteherland Greenstone Belt, South Africa. South African Journal of Geology, Vol. 91, No. 4, pp. 429-438.

Qu, C., Ma, Z., Yang, J., Lie, Y., Bi, J. and Huang, L. (2014). Human Exposure Pathways of Heavy Metals in a Lead-Zinc Mining Area. In: Asrari, A. (Ed.). Heavy Metal Contamination of Water and Soil: Analysis, Assessment and Remediation Strategies. Apple Academic Press. pp. 129-156.

Rosner, T., Boer, R., Reynerke, R., Aucamp, P. and Vermaak, J. (2001). A Preliminary Assessment of Pollution Contained in the Saturated and Unsaturated Zone Beneath Reclaimed Gold-mine Residue Deposits. Report no.797/1/01. Pretoria. Water Research Commission.

Ramontja, T., Coetzee, H., Hobbs, P.J., Burgess, J.E., Thomas, A., Keet, M., Yibas, B., Van Tonder, D., Netili, F., Rust, U.A., Wade, P. and Maree, (2011). Mine Water Management in the Witwatersrand Gold Fields with Special Emphasis on Acid Mine Drainage Inter-Ministrial-Committee on Acid Mine Drainage. Pretoria. South Africa.

Rico, M., Benito, G., Salgueiro, A.R., Diez-Herrero, A. and Pereira, H.G. (2008). Reported Tailings Dam Failures: A Review of the European Incidents in the Worldwide Context. Journal of Hazardous Materials, Vol. 152, No 2. pp. 846-852.

Saeed, A. and Zhang, L. (2012). Production of Eco-friendly Bricks from Cu Mine Tailings through Geopolymerization. Construction and Building Materials. Vol. 29. pp. 323-331.

Saexplorer, (2016). Malamulele Climate. https://www.saexplorer.co.za/south-african/climate/malamulele-climate.asp. Accessed: 12 August 2016.

Sharma, M.R. and Raju, N.S. (2013). Correlation of Heavy Metal Contamination with Soil Properties of Industrial Areas of Mysore, Karnataka, India by Cluster Analysis. International Research Journal of Environment Sciences, Vol. 2, No. 10, pp.22-27.

Smit, C.A., van Reenen, D.D., McCourt, S., Huizenga, J.M., Belyanin, G. and Vafeas, N.A. (2019). Hypozonal Orogenic Gold Mineralization in the Giyani Goldfield, Northern Kaapvaal Craton/ Limpopo Complex. South African Journal of Geology, Vol. 122, No. 4, pp. 455-488.

Steenkamp, N.C. and Clark-Mostert, V. (2012). Inferred Historic Gold Mining Approaches, Giyani Greenstone Belt, South Africa. 9th International Mining History Congress. pp. 17-20.

Steyn, C.E., Van Der Watt, H.V.H. and Claassens, A.S. (1996). On the Permissible Nickel Concentration for South African Soils. South African Journal of Science, Vol. 92, pp. 359-363.

Tailings.info, (2017). Hydraulic Mining of Tailings. www.tailings.info/technical/hydraulic.htm. Accessed: 22 February 2020.

Test, T. (2008). ERGO to be Reborn. Mining Review Africa, 19 August.

The Construction Civil, (2022). Liquid Limit of Soil. https://www.theconstructioncivil.org/liquid-limit-of-soil/. Accessed: 14 December 2022.

Todorova, E., Avramov, I. and Georgakiev, I. (2017). Journal of Mining and Geological Sciences, Vol. 60, No. 2, pp. 10-16.

Turton, A. (2016). Greenfields Logic in a Brownfields Reality. Without Prejudice, 20 September.

Vallero, D.A. and Letcher, T.M. (2013). Unravelling Environmental Disasters. Elsevier. ISBN 9780123970268.

Vick, S.G. (1990). Planning, Design, and Analysis of Tailings dams. Vancouver, BiTech. ISBN. 0921095120.xi, 369 pp.

Viljoen, M. (2009). The Life, Death, Revival of the Central Rand Goldfield. World Gold Conference, The South African Institute of Mining and Metallurgy, South Africa, pp. 131-136.

Ward, J.H.W. and Wilson, M.G.C. (1998). Gold outside the Witwatersrand Basin. In: Wilson, M.G.C. and Anhaeusser, C.R. (Eds.). The Mineral Resources of South Africa, pp. 740.

Yang, Y., Zhu, S., Li, Q., Yang, B. and Chen, Y. (2011). Research on making fired bricks with gold tailings. International Conference on Computer Distributed Control and Intelligent Environmental Monitoring. Qingdao Shandong. China.

Zhang, L. (2013). Production of Bricks from Waste Materials – a review. Construction and Building Materials. Vol. 47, pp. 643-655.

Zongjie, L., Junrui, C., Zengguang, X., Yuan, Q. and Jing, C. (2019). A Comprehensive Review on Reasons for Tailings Dam Failures Based on Case History. Advances in Civil Engineering. Vol. 2019. 18 pages. https://doi.org/10.1155/2019/4159306. Accessed: 9 December 2019.

Appendices

APPENDIX A:

Fumani Tailings Dam1

A1: Borehole Profile Logs

P1H1

Depth		Physical Characteristics					Illustration
From	**To**	**Colour**	**Texture**	**Hardness**	**Moisture**	**Other**	
0	0,1	orange	gritty	mixture of hard and soft	dry	loose, dusty, with hard pebbles	
0,1	0,33	light orange	gritty	very hard	dry	gritty	
0,33	0,78	Grey	smooth	soft	moist	soft and sticky	
0,78	0,95	green	gritty	hard	dry	compacted, feels gritty	
0,95	1,35	dark grey and green	smooth	soft and hard	very moist	very sticky with hard pebbles	
1,35	7	light grey	smooth	soft	moist	easy to drill	

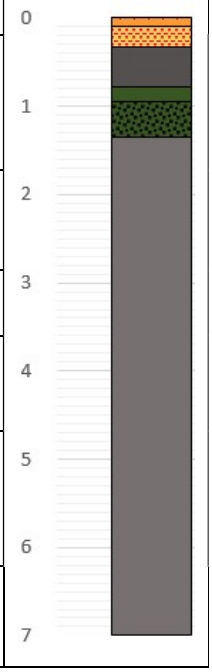

P1H2

Depth		Physical Characteristics					Illustration
From	**To**	**Colour**	**Texture**	**Hardness**	**Moisture**	**Other**	
0	0,82	orange	gritty	hard and soft	dry	loose and dusty with pebbles. difficult to collect	
0,82	0,91	green	smooth	soft	moist	sticky	
0,91	1,04	dark grey	gritty	hard and soft	wet	alternating layers of hard and soft. gritty material	
1,04	7	light grey	smooth	soft	moist and soft	sticky	

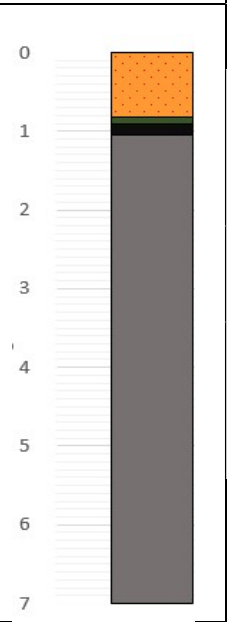

P1H3

Depth		Physical Characteristics					Illustration
From	**To**	**Colour**	**Texture**	**Hardness**	**Moisture**	**Other**	
0	0,35	orange	smooth	soft	dry	dusty and loose	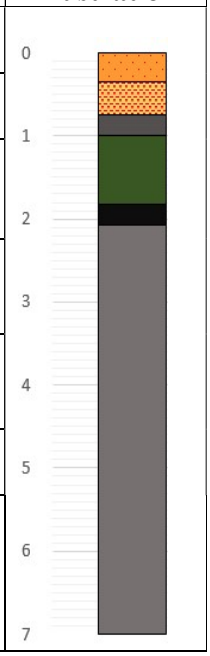
0,35	0,75	light orange	smooth	soft	dry	loose, pebbles	
0,75	1	grey	gritty	hard	dry	compacted, gritty	
1	1,82	green	gritty	hard	dry	compacted and gritty	
1,82	2,08	dark green	gritty	hard	dry	compacted	
2,08	7	light grey	smooth	soft	moist	sticky	

P1H4

Depth		Physical Characteristics					Illustration
From	**To**	**Colour**	**Texture**	**Hardness**	**Moisture**	**Other**	
0	0,35	orange	smooth	soft	dry	loose, dusty and oxidised	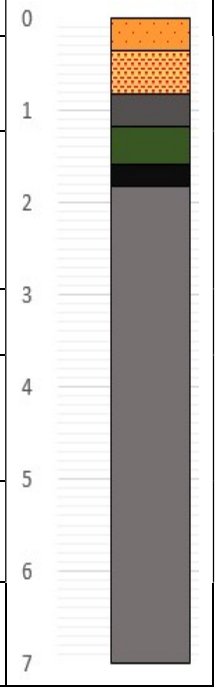
0,35	0,82	light orange	gritty	very hard	dry	difficult to penetrate layer with hand auger	
0,82	1,18	grey	smooth	soft	moist	easy to drill	
1,18	1,58	green	gritty	hard and soft	dry	hard and soft with a gritty feeling	
1,58	1,82	dark grey	smooth	soft	moist	sticky	
1,82	7	light grey	smooth	soft	moist	easy to drill	

P2H1

Depth		Physical Characteristics					Illustration
From	**To**	**Colour**	**Texture**	**Hardness**	**Moisture**	**Other**	
0	0,18	orange	smooth and gritty	soft and hard	dry	dusty and gritty	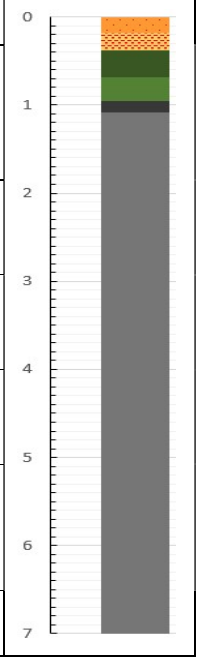
0,18	0,38	light orange	gritty	very hard	dry	gritty and compacted	
0,38	0,69	green	gritty	very hard	dry	compacted layer	
0,69	0,95	light green	gritty	very hard	dry	very compacted	
0,95	1,08	dark grey	smooth	soft	wet	sticky shinny green material	
1,08	7	light grey	smooth	soft	moist	easy to drill	

P2H2

Depth		Physical Characteristics					Illustration
From	**To**	**Colour**	**Texture**	**Hardness**	**Moisture**	**Other**	
0	0,23	orange	smooth and gritty	hard	dry	loose, oxidised dust with gritty feel	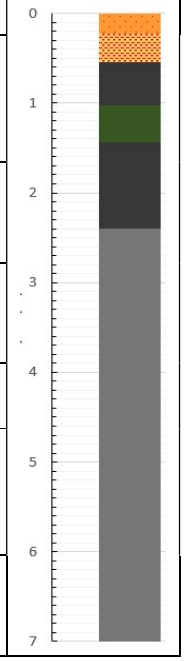
0,23	0,54	light orange	gritty	hard	dry	compacted, with hard pebbles	
0,54	1,03	dark grey	smooth	hard and soft	wet	contains shinny pebbles	
1,03	1,44	green	gritty	hard	dry	compacted	
1,44	2,4	dark grey	smooth	soft	wet	sticky with green shiny material	
2,4	7	light grey	smooth	soft	moist	easy to collect sample	

P2H3

Depth		Physical Characteristics					Illustration
From	**To**	**Colour**	**Texture**	**Hardness**	**Moisture**	**Other**	
0	0,28	orange	gritty	hard	dry	loose, dusty with hard flakes	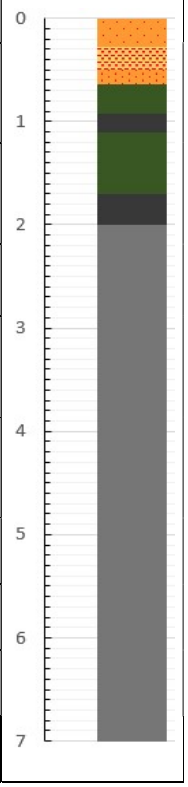
0,28	0,5	light orange	gritty	hard and soft	dry	layers of iron oxide	
0,5	0,64	orange	gritty	hard	dry	compacted	
0,64	0,92	green	gritty	hard	dry	with grey and blue pebbles	
0,92	1,1	dark grey	smooth	soft	moist	with grey and blue pebbles	
1,1	1,7	dark green	gritty	hard	dry	shinny	
1,7	1.88	dark grey	smooth	soft	moist	shinny	
1.88	2	dark green	smooth	soft	moist	shinny	
2	7	light grey	smooth	soft	moist	easy to drill	

P2H4

Depth		Physical Characteristics					Illustration
From	**To**	**Colour**	**Texture**	**Hardness**	**Moisture**	**Other**	
0	0,12	orange	smooth and gritty	soft and hard	dry	loose, oxidised with blue flakes	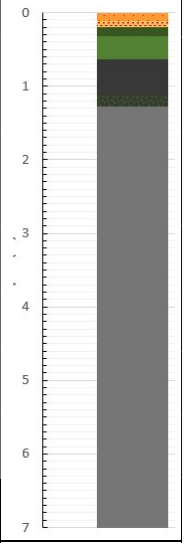
0,12	0,2	light orange	gritty	hard	dry	loose with blue and green pebbles,	
0,2	0,32	green	gritty	very hard	dry	compacted	
0,32	0,64	light grey	gritty	very hard	dry	compacted	
0,64	1,12	dark grey	smooth	soft	wet	sticky and shinny	
1,12	1,28	green	gritty	hard and soft	dry	blue pebbles	
1,28	7	light grey	smooth	soft	moist	easy to drill	

P3H1

Depth		Physical Characteristics					Illustration
From	**To**	**Colour**	**Texture**	**Hardness**	**Moisture**	**Other**	
0	0,08	orange	gritty and smooth	soft	dry	loose, flaky and dusty	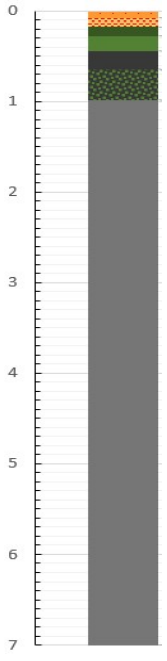
0,08	0,18	light orange	gritty and smooth	hard	dry	loose with hard pebbles, highly oxidised	
0,18	0,28	green	gritty	very hard	dry	compacted with grey and blue pebbles	
0,28	0,44	light green	gritty	very hard	dry	compacted	
0,44	0,64	dark grey	smooth	soft	wet	sticky and shinny	
0,64	0,98	green	gritty	very hard	dry	compacted	
0,98	7	grey	smooth	soft	moist	shinny particles	

P3H2

Depth		Physical Characteristics					Illustration
From	**To**	**Colour**	**Texture**	**Hardness**	**Moisture**	**Other**	
0	0,17	orange	smooth	soft and hard	dry	loose, flaky and dusty	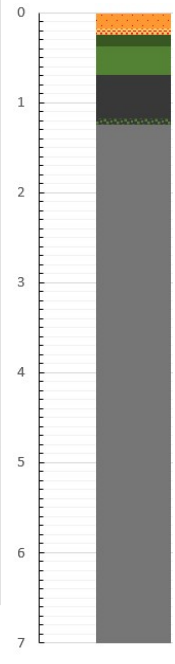
0,17	0,25	light orange	gritty	hard	dry	loose and oxidised. flakes and hard pebbles	
0,25	0,37	green	gritty	hard	dry	compacted. blue and green pebbles. shinny	
0,37	0,69	light green	gritty	hard	dry	compacted	
0,69	1,17	dark grey	smooth	soft	moist	sticky and shinny	
1,17	1,24	green	gritty	hard	dry	compacted	
1,24	7	grey	smooth	soft	moist	shinny particles	

P3H3

Depth		Physical Characteristics					Illustration
From	To	Colour	Texture	Hardness	Moisture	Other	
0	0,6	orange	smooth	soft and hard	dry and dusty	loose, flaky and dusty	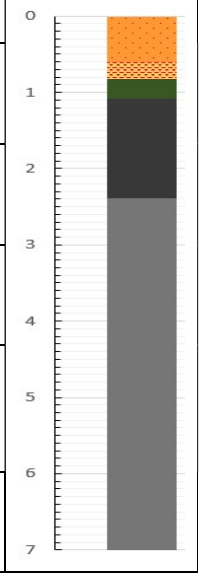
0,6	0,82	light orange	gritty	hard	dry	oxidised. flakes and hard pebbles	
0,82	1,08	green	gritty	hard	dry	hard compacted layer with soft layers	
1,08	2,39	dark grey	smooth and gritty	mixture	wet	moist and soft with green shiny particles	
2,39	7	grey	smooth	soft	moist	moist and soft with shiny particles	

P3H4

Depth		Physical characteristics					Illustration
From	To	Colour	Texture	Hardness	Moisture	Other	
0	0,21	orange	smooth	soft and hard	dry	loose, flaky and dusty	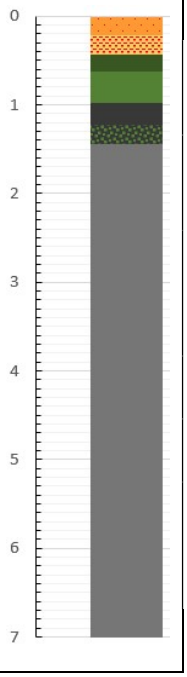
0,21	0,43	light orange	gritty	hard	dry	loose flakes and hard pebbles	
0,43	0,62	green	gritty	hard	dry	compacted. blue and green pebbles. shinny	
0,62	0,98	light green	gritty	hard	dry	very hard	
0,98	1,22	dark grey	smooth	soft	moist	easy to drill	
1,22	1,44	green	gritty	hard	dry	compacted. blue and green pebbles. shinny	
1,44	7	grey	smooth	soft	moist	soft and moist	

A2: Metals

Sample Id	Pb	Zn	Cu	As	Co	Cd	Cr	Ni
P1H1S1	17,5	134,8	49,3	7841,9	11,9	0,3	37,8	44,4
P1H1S2	18,2	111,8	80,4	7687,9	25,7	0,5	86,3	127,4
P1H1S3	16,9	121,4	49	7622,2	15,2	0,6	91,6	95,1
P1H1S4	25,7	103	67,9	7809,9	27,3	0,2	64,3	145,7
P1H1S5	18,5	99,2	50,2	8173,9	23,8	0,7	69,7	123,5
P1H1S6	14,6	160,7	79,9	4465,3	19,3	0,5	16,3	114,4
P1H1S7	17,9	134,3	42,6	8666,5	23,5	1	57,7	136,7
P1H2S1	27,9	113	74,3	7646,5	19,3	0,9	106,3	90,1
P1H2S2	14,4	111,7	29,4	4933,3	21,5	0,3	46,2	116,2
P1H2S3	16,8	104,1	36,7	8991,8	39,1	0,6	87,9	93,7
P1H2S4	49,8	97,5	70,5	7940,4	43,7	0,2	83,7	121,5
P1H2S5	29,5	113,2	67,3	8466,7	29,7	0,6	65,8	114,1
P1H2S6	18,1	131,1	66,2	7819,7	18,2	0,3	64,3	86,1
P1H2S7	48,8	150,3	39,1	5763,5	32,6	0,7	98,5	129,3
P1H3S1	29,1	112,6	71	7934,4	25	0,4	90,1	64,7
P1H3S2	29,8	92,7	68,6	7543,2	25,1	0,6	70,3	79,4
P1H3S3	28,5	95,6	66,8	7784,6	31,1	0,2	62,8	53
P1H3S4	20,9	91,6	42,7	7741	11	0,6	69,9	46,9
P1H3S5	16,4	82,5	54,8	5467,5	19,3	0,7	56,7	92,7
P1H3S6	37,3	180,7	76,9	7420,1	30,9	0,1	57,7	77,4
P1H3S7	24	99	61,8	7448,8	20,4	0,8	69,7	78,8
P1H4S1	16,5	83,1	53	2009,7	16,5	1	59,8	47,4
P1H4S2	14,8	118,7	59,4	1886	34,7	0,9	65,8	143,8
P1H4S3	11,5	97,7	47,9	1899	24,9	0,9	52,6	89,6
P1H4S4	12,6	84,2	59,4	5296,2	24,3	0,8	51	97,6
P1H4S5	15,3	110,4	65,3	5656,1	25,2	1	52,1	93,6
P1H4S6	12,8	19,5	62,4	2973,3	24,4	1	44,2	96,4
P1H4S7	13,9	114,8	61,2	5770,3	26,5	1,1	51,2	96,1
P2H1S1	20,3	80	58	6618,8	11,1	0,4	95,3	43,8
P2H1S2	16,7	80,8	62,5	7822,6	31,5	0,5	81,1	121,1
P2H1S3	14,1	79,4	56,5	9028,7	32,4	0	70	115,1
P2H1S4	17	101,4	60,8	8764,1	27,3	0,8	77,6	118,1
P2H1S5	14,7	96,5	60,7	9629,8	23,1	0,8	62,6	107,2
P2H1S6	17,9	100,3	60,7	9119,2	22,8	0,8	73,6	105,8
P2H1S7	25,9	144,4	60,9	9732,6	24,4	0,9	79,3	103,3
P2H2S1	18,7	114,7	55,9	8812,1	15,6	0,8	86,9	63,6
P2H2S2	12,3	126,1	60,6	5330	35	1	83,5	140,2
P2H2S3	13,6	102,2	64,5	6517,5	25,8	0,9	77,2	89,9
P2H2S4	12,2	57,4	64,4	6587,8	21,8	0,6	74,5	89,1
P2H2S5	13,1	67,8	63,4	5688,9	21,8	0,8	67,9	81,4
P2H2S6	16,9	74,7	66,9	4979	21,8	0,8	73	88

Sample ID	Pb	Zn	Cu	As	Co	Cd	Cr	Ni
P2H2S7	14,4	65	59,9	5277,8	22,3	0,8	80,2	91,3
P2H3S1	13,3	82,3	47,5	5125,5	18	1	86	84,7
P2H3S2	12,5	78,1	56,3	6503,9	28,7	1	43,7	116
P2H3S3	10,8	62,2	56,7	7118,3	24,4	0,8	65,5	101,5
P2H3S4	11,5	52,5	54,3	6962,3	23,5	0,8	75,7	99,2
P2H3S5	11,2	69,2	56,3	6174,8	24,1	0,9	69,1	84,2
P2H3S6	12	70,1	55	7114,5	22,8	0,9	74,1	87,5
P2H3S7	20,1	81,5	53,7	1988	25,2	0,1	45,2	88,7
P2H4S1	20,8	131,1	61,3	1849,6	30,1	1	52,3	101,4
P2H4S2	19,9	91,9	56,6	1819	26,2	0,7	57	83,8
P2H4S3	20,3	95,3	65,7	1965,7	31,7	0,9	54,2	101,7
P2H4S4	19,9	75,4	60,9	2130,3	26,9	0,8	46,3	102,2
P2H4S5	11,3	90,6	52,5	2059,1	31,3	0,8	42,5	106,2
P2H4S6	11,7	89,4	54,7	1940,8	26	0,9	37,3	103
P2H4S7	14,3	101,4	61,4	2070,2	27,1	0,9	56	107,5
P3H1S1	29,8	120,2	63,8	7147,5	33,1	0,6	70,5	147,9
P3H1S2	33	152,4	69,8	8097,6	28,8	0,8	106,5	147,6
P3H1S3	31,5	115,2	66,9	8062	18,9	0,6	69,6	74,6
P3H1S4	33,3	114,3	82,3	7920,6	24	0,6	107	99,6
P3H1S5	31,4	109,1	75,3	8161,7	23,4	0,7	83,6	92,1
P3H1S6	31,8	103,6	71,8	8400,6	22,1	0,7	79,2	88,4
P3H1S7	8,4	95,8	67,3	6325	21,9	0,7	63,7	97,9
P3H2S1	29,4	89,2	56,3	6513,8	12,9	0,6	93,5	65,2
P3H2S2	21	122,6	77,4	6054,2	28,6	0,7	94,7	144,1
P3H2S3	18,4	91,7	67	6604,9	25,1	0,7	79	105,5
P3H2S4	18,2	85	66,3	6714,6	25	0,6	83,2	115,6
P3H2S5	18,4	99,8	69,4	6790,5	25	0,6	73,2	109,5
P3H2S6	17,3	97	68,2	7255,1	26,1	0,6	75,9	116,7
P3H2S7	8,3	82,3	12,6	3065,3	15,9	0,6	60,5	83,3
P3H3S1	17,7	85,8	48,9	7671,6	24,6	0,5	85,7	111,8
P3H3S2	23,1	115,8	60,8	6858,1	22,4	0,5	78,9	141,8
P3H3S3	14,8	93,9	11,8	3642,1	16,3	0	75,2	79,5
P3H3S4	18,3	93,6	68,5	7479,7	25,7	0,6	78	111,3
P3H3S5	19,9	113	74,3	7646,5	23	0,9	106,3	90,1
P3H3S6	14,4	111,7	29,4	3933,3	21,5	0,3	46,2	116,2
P3H3S7	16,8	104,1	66,7	7191	25,1	0,6	87,9	93,7
P3H4S1	20,8	121,5	70,5	7940,4	36,7	0,7	86,7	135
P3H4S2	21,5	113,2	70,3	8466,7	29,7	0,6	85,8	94,1
P3H4S3	28,1	151,1	76,2	7819,7	26,2	0,6	84,3	86,1
P3H4S4	30	150,3	80,1	7763,5	32,6	0,7	98,5	129,3
P3H4S5	29,1	112,6	71	7934,4	25	0,6	90,1	84,7
P3H4S6	29,8	92,7	68,6	7543,2	25,1	0,7	80,3	79,4
P3H4S7	28,5	95,6	66,8	7784,6	21,1	0,8	81,8	83

A3: Major Oxides

Sample name	SiO2 (%)	TiO2 (%)	Al2O3 (%)	Fe2O3 (%)	MnO (%)	MgO (%)	CaO (%)	Na2O (%)	K2O (%)	P2O5 (%)
P1H1S1	52,28	1,291	17,11	13	0,347	2,0874	1,23	0,491	1,16	0,073
P1H1S2	49,82	1,616	13,48	15,3	0,297	3,6094	1,46	0,794	1,07	0,085
P1H1S3	50,41	0,558	6,18	21,22	0,154	3,1229	1,11	1,386	2,07	0,153
P1H1S4	53,28	1,248	9,93	12,92	0,147	4,1194	1,36	1,096	1,32	0,088
P1H1S5	50,29	0,778	9,2	15,96	0,176	4,2555	1,76	1,267	1,46	0,117
P1H1S6	59,69	1,018	13,64	5,11	0,078	1,2384	1,2	0,675	2,51	0,056
P1H1S7	54,18	1,871	15,31	10,75	0,181	1,0973	1,1	0,598	2,21	0,092
P1H2S1	52,55	1,234	15,18	11,21	0,21	1,6987	1,47	0,295	2,1	0,091
P1H2S2	56,7	1,805	15,35	9,71	0,182	2,2816	0,68	0,977	1,19	0,073
P1H2S3	55	1,321	14,65	9,74	0,224	1,5192	1,69	0,382	1,57	0,078
P1H2S4	53,62	1,52	15,5	9,87	0,226	0,9077	0,65	0,104	1,79	0,073
P1H2S5	66,48	0,884	14,04	4,78	0,109	1,4465	0,77	0,274	1,49	0,071
P1H2S6	66,94	0,927	13,68	4,15	0,079	1,3721	1,21	0,209	1,29	0,076
P1H2S7	66,17	1,194	15,05	4,31	0,067	0,7723	0,68	0,095	1,36	0,08
P1H3S1	68,3	1,218	12,58	5,22	0,141	0,5876	0,78	0,242	1,33	0,066
P1H3S2	76,07	0,907	11,25	3,6	0,067	0,3973	0,44	0,073	1,41	0,059
P1H3S3	71,16	0,562	12,89	3	0,037	0,5275	0,64	1,613	1,68	0,079
P1H3S4	65,2	1,003	14,59	4,39	0,11	0,7975	0,83	0,849	1,28	0,059
P1H3S5	62,87	1,246	15,56	8,17	0,124	0,5401	0,5	0,37	1,9	0,091
P1H3S6	59,87	1,393	17,8	6,32	0,085	0,6236	0,62	0,393	1,66	0,056
P1H3S7	57,29	1,746	16,45	9,09	0,143	0,8992	0,64	0,322	1,77	0,083
P1H4S1	54,83	1,696	19,44	8,12	0,135	0,6059	0,5	0,02	1,63	0,095
P1H4S2	50,69	1,656	19,91	11,23	0,154	0,6098	0,36	0	1,3	0,102
P1H4S3	48,06	1,894	17,96	14,1	0,239	0,8994	0,38	0,052	1,31	0,108
P1H4S4	49,95	1,623	17,04	13,11	0,276	1,2402	0,48	0,067	1,38	0,105
P1H4S5	49,22	1,462	15,9	14,37	0,306	2,3869	0,66	0,166	1,35	0,103
P1H4S6	49,52	1,213	14,22	13,23	0,314	5,0199	1,58	0,929	0,98	0,074
P1H4S7	52,1	1,175	9,32	16,83	0,244	2,6122	1,15	1,488	1,56	0,076
P2H1S1	51,92	1,112	11,46	14,57	0,283	5,8906	1,14	0,498	1,01	0,071
P2H1S2	59,69	0,264	4,63	16,98	0,202	2,7766	2,96	0,394	2,03	0,184
P2H1S3	56,9	0,258	3,64	19,06	0,29	2,6262	3,5	0	1,45	0,166
P2H1S4	47,74	0,33	4,11	19,12	0,199	2,8943	2,67	1,783	2,1	0,19
P2H1S5	54,03	0,346	5,1	19,09	0,277	3,6478	5,15	0,888	2,29	0,232
P2H1S6	59,64	0,871	12,52	10,45	0,147	2,4946	0,97	0,536	1,66	0,063
P2H1S7	72,62	0,584	13,62	3,34	0,048	0,6875	1,02	1,51	2,14	0,039
P2H2S1	58,54	1,33	16,06	7,64	0,121	0,9117	0,86	0,732	2,05	0,072
P2H2S2	57,1	1,702	16,35	8,56	0,111	0,823	0,95	0,783	2,13	0,075
P2H2S3	64,75	0,735	15,35	3,86	0,047	0,901	0,93	1,39	1,88	0,049
P2H2S4	65,17	0,495	15,97	2,48	0,04	1,2607	1,37	1,422	2,3	0,051
P2H2S5	66,06	0,8	13,57	4,43	0,064	1,6863	1,46	1,755	2,07	0,062
P2H2S6	57,8	0,753	16,9	5,15	0,06	1,4526	1,59	1,154	2,1	0,058

Sample name	SiO2 (%)	TiO2 (%)	Al2O3 (%)	Fe2O3 (%)	MnO (%)	MgO (%)	CaO (%)	Na2O (%)	K2O (%)	P2O5 (%)
P2H2S7	66,07	0,339	15,05	1,6	0,042	0,5973	0,83	1,359	4,11	0,057
P2H3S1	68,56	0,659	10,27	2,73	0,039	1,1401	1,36	1,799	1,5	0,042
P2H3S2	56,28	1,021	14,35	8,4	0,141	2,4515	1,61	1,039	2,01	0,1
P2H3S3	52,72	1,665	12,56	10,59	0,171	4,8018	3,82	2,309	1,4	0,11
P2H3S4	64,63	1,135	13,45	5,83	0,135	1,4842	1,46	0,829	2,05	0,078
P2H3S5	54,8	1,29	15,16	5,75	0,089	1,5255	1,87	0,823	1,72	0,098
P2H3S6	60,57	1,077	14,07	4,25	0,073	1,3851	1,68	1,279	1,84	0,093
P2H3S7	60,07	1,062	13,81	4,07	0,062	1,331	1,59	1,273	1,92	0,092
P2H4S1	65,95	0,712	14,65	3,31	0,061	0,845	1,47	1,98	2,07	0,078
P2H4S2	62,27	0,819	14,86	3,7	0,068	1,02	1,42	1,049	2,09	0,113
P2H4S3	64,2	0,943	13,2	3,12	0,056	1,1098	1,63	2,114	2,03	0,085
P2H4S4	55,22	1,228	13,38	4,63	0,076	1,3624	1,56	0,977	1,75	0,064
P2H4S5	58,94	1,353	14,97	4,81	0,075	1,5152	1,58	1,2	1,87	0,078
P2H4S6	50,82	1,155	9,81	11,94	0,265	10,1976	2,84	2,59	0,62	0,074
P2H4S7	51,8	1,329	14,39	12,55	0,272	3,918	1,21	0	0,92	0,067
P3H1S1	49,95	1,7	14,97	13,41	0,218	2,9012	2,22	0,815	0,84	0,072
P3H1S2	59,54	1,294	11,17	9,08	0,163	4,4535	1,98	0,86	0,77	0,061
P3H1S3	71,6	1,006	11,54	4,08	0,063	0,9459	0,45	0,04	1,22	0,06
P3H1S4	67,18	0,847	14,13	5,15	0,09	0,9038	0,91	1,107	1,13	0,048
P3H1S5	61,75	1,028	12,03	6,16	0,112	1,9131	1,11	0,764	1,12	0,052
P3H1S6	60,34	1,212	15,71	6,31	0,102	0,8817	1,24	0,649	1,33	0,066
P3H1S7	66,31	1,161	15,13	5,03	0,095	0,689	0,58	0,298	1,44	0,051
P3H2S1	69,75	1,083	12,29	3,86	0,084	0,8587	0,68	0,279	1,84	0,08
P3H2S2	68,86	0,688	9	2,95	0,047	0,4834	0,96	0,885	1,14	0,037
P3H2S3	56,5	1,391	17,13	8,3	0,169	0,6949	0,79	0,137	1,46	0,084
P3H2S4	58,53	1,506	16,62	7,3	0,126	0,9601	0,79	0,267	1,29	0,068
P3H2S5	57,62	1,819	16,34	8,87	0,159	0,762	0,69	0,315	1,5	0,073
P3H2S6	67,1	0,713	13,7	5,54	0,035	0,3507	0,55	0,696	3,11	0,063
P3H2S7	64,99	0,61	11,66	7,17	0,046	0,2667	0,36	0	3,76	0,071
P3H3S1	63,99	1,129	13,31	5,82	0,137	1,417	1,46	0,815	2,03	0,076
P3H3S2	64,14	1,032	15,16	5,43	0,08	0,6316	0,83	1,002	1,88	0,058
P3H3S3	67,05	1,157	15,55	4,71	0,058	0,3497	0,69	0,613	1,68	0,058
P3H3S4	66,58	1,185	15,56	4,46	0,057	0,3584	0,71	0,835	1,78	0,059
P3H3S5	71,93	0,823	12,97	4,4	0,048	0,3062	0,67	1,001	1,66	0,049
P3H3S6	54,24	0,357	5,46	19,64	0,343	3,3038	3,44	0,963	2,28	0,175
P3H3S7	50,78	0,35	5,22	20,02	0,41	3,25	3,89	1,08	2,33	0,64
P3H4S1	54,85	0,359	5,4	19,6	0,337	3,257	3,45	0,835	2,32	0,177
P3H4S2	50,71	0,407	5,34	20,12	0,312	3,2869	3,38	1,091	2,33	0,163
P3H4S3	54,77	0,372	4,82	19,65	0,271	3,2175	4,33	0,861	2,12	0,218
P3H4S4	50,48	0,39	5,25	20,12	0,31	3,225	3,39	1,068	2,33	0,164
P3H4S5	54,85	0,359	5,4	19,6	0,337	3,257	3,45	0,835	2,32	0,177
P3H4S6	54,44	0,374	4,94	19,62	0,305	3,1838	4,1	0	2,24	0,193
P3H4S7	50,41	0,558	6,18	21,22	0,154	3,1229	1,11	1,386	2,07	0,153

A4: Sieve Analysis Results

Sample A					
sieve size (g)	Mass of sieve (g)	Mass of sieve and material (g)	Mass of material (g)	cumulative passing (g)	percentage passing
4	388.5	389.58	1.02	505.45	100
2	326.98	328.2	1.21	505.26	100
1	295.88	298.5	2.92	503.55	99
0.5	290.32	295.56	5.33	501.14	99
0.25	246	267.75	22.01	484.46	96
0.125	236.35	369.93	123.42	383.05	76
0.075	263.86	386.03	138.46	368.01	73
Pan	527.02	743.69	232.1		
TMR			506.47		
Sample B					
sieve size (g)	Mass of sieve (g)	Mass of sieve and material (g)	Mass of material (g)	cumulative passing (g)	percentage passing
4	388.5	389.58	1.08	503.25	100
2	326.98	328.2	1.22	503.11	100
1	295.88	298.5	2.62	501.71	99
0.5	290.32	295.56	5.24	499.09	99
0.25	246	267.75	21.75	482.58	96
0.125	236.35	369.93	122.17	382.16	76
0.075	263.86	386.03	133.58	370.75	74
Pan	527.02	743.69	216.67		
TMR			504.33		

APPENDIX B:

Tailings Dam 2

B1: Borehole Profile Logs

P1H1

Depth		**Physical Characteristics**					**Illustration**
From	**To**	**Colour**	**Texture**	**Hardness**	**Moisture**	**Other**	
0	0,1	orange	smooth	very hard	dry	loose, flaky and dusty. Highly oxidised	
0,1	0,3	light orange	gritty	hard	dry	compacted oxidised layer with pebbles	
0,3	0,5	green	gritty	very hard	dry	compacted, very thin crust like layer	
0,5	1,2	grey dark	smooth	soft	wet	muddy and shinny	
1,2	7	grey	smooth	soft	moist	shinny	

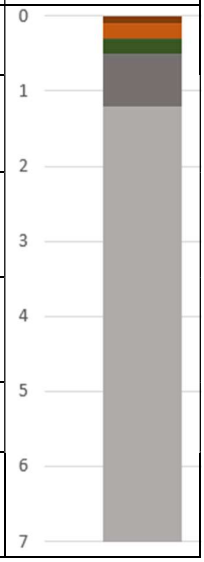

P1H2

Depth		**Physical characteristics**					**Illustration**
From	**To**	**Colour**	**Texture**	**Hardness**	**Moisture**	**Other**	
0	0,07	orange	mixture of smooth and gritty	mixture of very soft and hard	dry	dusty, highly oxidised with hard crust	
0,07	0,2	light orange	gritty	very hard	dry	difficult to penetrate with auger,	
0,2	0,6	green	gritty	hard	dry	compacted	
0,6	0,75	dark grey with green	smooth	soft	wet	muddy, mixed with green gritty material	
0,75	2,7	dark grey	smooth	soft	wet	muddy	
2,7	7	grey	smooth	soft	moist	shinny	

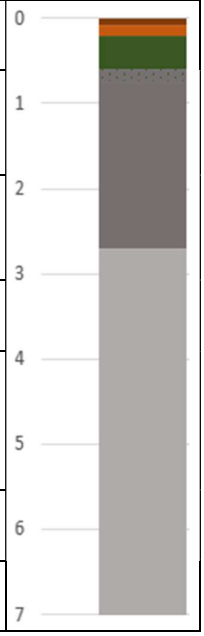

P1H3

Depth		Physical Characteristics					Illustration
From	**To**	**Colour**	**Texture**	**Hardness**	**Moisture**	**Other**	
0	0,12	orange	smooth and gritty	hard	dry	blue pebbles in material	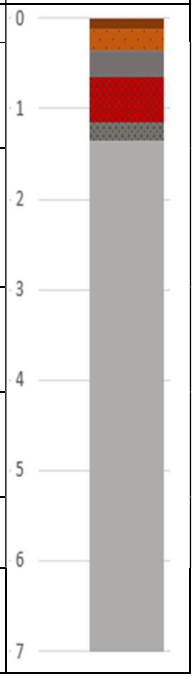
0,12	0,35	light orange and green	gritty	hard	moist and dry	sticky material mixed with pebbles	
0,35	0,66	grey	gritty	hard	dry	compacted and difficult to drill	
0,66	1,15	red with dark grey	gritty	hard	dry	gritty feel	
1,15	1,35	green and grey	smooth	soft	moist	muddy	
1,35	7	grey	smooth	soft	moist	easy to drill	

P2H1

Depth		Physical Characteristics					Illustration
From	**to**	**Colour**	**Texture**	**Hardness**	**Moisture**	**Other**	
0	0,15	orange with blue stains	gritty	hard	dusty	dry and dusty with hard flakes	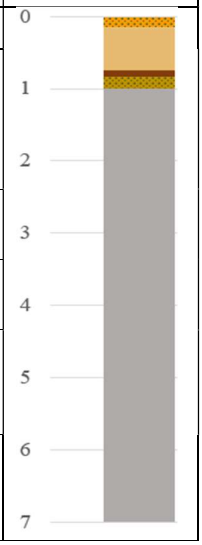
0,15	0,75	light orange	gritty	hard	dry	very hard layer	
0,75	0,83	red	gritty	hard	dry	very hard layer	
0,83	1	orange and green	smooth	soft	moist	soft and moist	
1	7	grey	smooth	soft	moist	soft and moist	

P2H2

Depth		Physical Characteristics					Illustration
From	**To**	**colour**	**Texture**	**Hardness**	**Moisture**	**Other**	
0	0,25	brownish orange	gritty	hard	dry	very hard and compacted	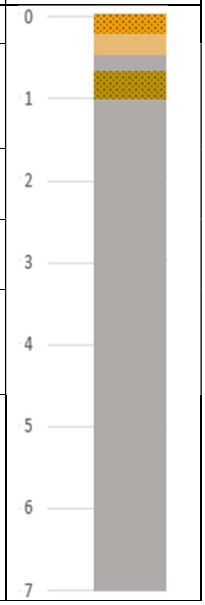
0,25	0,5	orange	gritty	hard	dry	very hard and compacted	
0,5	0,7	grey	smooth	soft	moist		
0,85	1,05	brown grey green	smooth	gritty and soft	wet	muddy with blue pebbles	
1,05	7	grey	smooth	soft	moist	soft	

P2H3

Depth		Physical Characteristics					Illustration
From	**To**	**Colour**	**Texture**	**Hardness**	**Moisture**	**Other**	
0	0,12	dark orange	gritty	hard	dry and dusty	blue hard pebbles	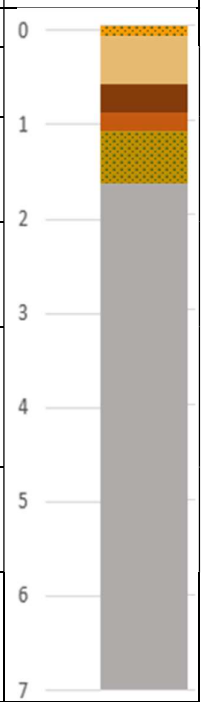
0,12	0,62	light orange highly oxidised	gritty	hard	dry and dusty		
0,62	0,92	red	gritty	very hard	dry	crust like and very difficult to drill	
0,92	1,12	brownish red layer	gritty	hard	moist with dry pebbles	gritty feel	
1,12	1,67	soft greenish grey, yellow	smooth	soft	wet	easy to drill	
1,67	7	grey	smooth	soft	muddy	easy to drill	

P3H1

Depth		Physical Characteristics					Illustration
From	**To**	**Colour**	**Texture**	**Hardness**	**Moisture**	**Other**	
0	0,12	orange	gritty	hard	very hard compacted layer	loose, dusty and flakey	
0,12	0,16	light orange	gritty	very hard	hard layer	hard iron oxide layers	
0,16	0,47	light orange plus blue grey	gritty	hard layer with soft moist	hard layer with moist soft	alternating hard and soft	
0,47	0,7	orange	gritty	hard	very hard compacted layer	compacted and difficult to penetrate	
0,7	0,91	grey with soft orange	gritty	soft	muddy	shinny	
0,91	1,4	dark grey	smooth	soft	muddy	shinny	
1,4	7	grey	smooth	soft	soft	shinny	

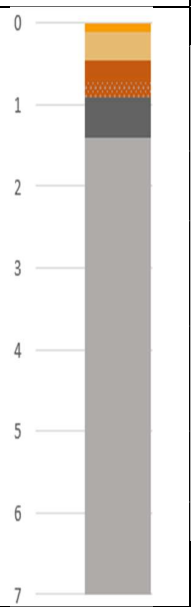

P3H2

Depth		Physical Characteristics					Illustration
From	**To**	**Colour**	**Texture**	**Hardness**	**Moisture**	**Other**	
0	0,14	orange	gritty	hard	dusty dry with hard pecks	loose and dusty	
0,14	0,2	light orange	gritty	hard	hard layer with bluish pebbles	compacted	
0,2	0,95	grey green	gritty	very hard	very hard layer containing pebbles	compacted	
0,95	1,15	greenish	gritty	soft	soft	loose	
1,15	1,34	orange	gritty	soft	soft and dry	shinny	
1,34	1,61	brownish red	gritty	hard	hard layer with bluish pebbles	shinny	
1,61	2,16	dark grey	smooth	soft	soft and muddy	shinny	
2,16	7	grey	smooth	soft	soft and moist	shinny	

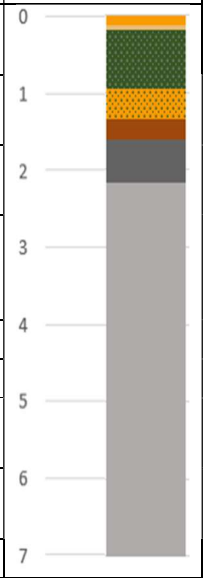

P3H3

Depth		Physical Characteristics					Illustration
From	**To**	**Colour**	**Texture**	**Hardness**	**Moisture**	**Other**	
0	0,15	orange	gritty	hard	dusty	thin layer	
0,15	0,37	light orange	gritty	hard	dry	compactyed with iron oxides	
0,37	0,87	orange brown	gritty	hard	dry	mixed with reddish soil	
0,87	0,92	redish orange compacted material	gritty	hard	dry	compacted	
0.92	1,3	green grey	gritty	Hard	moist	shinny	
1,3	1,39	grey	gritty	hard and soft	moist	shinny	
1,39	1,48	orange brown	gritty	soft	moist	mixed with muddy grey	
1,48	2,8	redish brown	gritty	soft	moist	mixed with muddy grey	
2,8	7	grey	smooth	soft	moist	shinny	

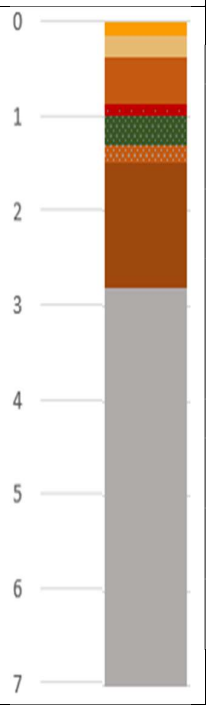

B2: Metals

Sample ID	Pb ppm	Zn ppm	Cu ppm	As ppm	Co ppm	Cd ppm	Cr ppm	Ni ppm
P1H1S1	43,6	75,85	57,35	2863,03	15,35	0,85	72,18	58,1
P1H1S2	43,5	83,78	57,61	3940,53	23,64	0,85	64,2	80,84
P1H1S3	42,46	91,6	63,86	4264,62	22,86	0,89	65,91	119,58
P1H1S4	33,04	103,55	66,52	5093,76	21,62	0,9	62,84	109,6
P1H1S5	24,15	82,74	71,86	5243,43	22,46	0,9	58,84	104,92
P1H1S6	21,18	98,6	65,88	5156,32	21,65	0,88	57,69	105,95
P1H1S7	32,45	96,4	68,76	5198,36	23,54	0,97	60,32	103,66
P1H2S1	50,4	77,1	60	5243,43	7,5	0,8	104,12	60,9
P1H2S2	47,55	146,05	61,24	3687	25,57	0,9	104,5	107,99
P1H2S3	45,8	120,53	65,05	3192,81	26,6	0,89	102,17	132,77
P1H2S4	34,8	107,8	69,3	3245,8	26,2	1	96,2	121,7
P1H2S5	25,6	101,2	72,6	4244,06	24,7	0,9	86,6	96,7
P1H2S6	38,8	103,8	69,87	4088,64	23,25	0,78	99,02	115,85
P1H2S7	37,9	104,99	72,31	4139,84	22,37	0,96	100,64	101,33
P1H3S1	62,4	101,2	66	4424	21	0,9	96,8	79,1
P1H3S2	64,31	118,84	76,37	4299,1	27,42	1	101,3	131,8
P1H3S3	48,9	98,3	66,7	4356,05	21,2	0,9	90,3	55,7
P1H3S4	45	101	61,8	4414	27,4	1	90,1	127
P1H3S5	38,7	104,1	67	4332	26,3	1	88,3	115,1
P1H3S6	40,61	152,6	81,35	5887,35	23,1	0,6	100,01	131,25
P1H3S7	38,1	116,75	73,66	6220,64	25,9	0,7	93,33	87,7
P2H1S1	30,07	95,99	70,68	5762,84	24,8	0,6	82,64	8,17
P2H1S2	29,2	98,81	68,55	5987,25	21,6	0,7	83,9	85,26
P2H1S3	21,08	92,64	42,98	5776,88	18,1	0,8	70,24	47,15
P2H1S4	21,5	83,88	55,76	4555,04	15,5	0,2	57,65	73,94
P2H1S5	20,9	182,5	77,47	5472,99	21,8	0,3	78,23	77,89
P2H1S6	23,9	98,6	61,26	5491,32	20,3	0,6	78,7	78,53
P2H1S7	29,6	87,4	57,98	5319,34	18,9	0,5	101,78	74,58
P2H2S1	30,5	123,18	65,93	6130,47	23,9	0,5	72,98	136,8
P2H2S2	33,1	153,88	70,11	6191,45	24,3	0,6	106,94	148,2
P2H2S3	32	117,58	68	6182,1	19,2	0,8	77,07	75,82
P2H2S4	34,4	118,1	85	6227,21	24,87	0,6	110,58	102,92
P2H2S5	31,7	110,54	75,92	6409,79	23,6	0,6	84,35	92,82
P2H2S6	31,8	103,75	71,92	4532,97	22,1	0,7	79,36	88,56
P2H2S7	47,48	95,82	67,33	4952,32	21,9	0,7	63,74	97,99
P2H3S1	34,27	99,6	58,61	4214,79	8,69	0,9	103,3	52,75
P2H3S2	54,15	99,2	55,84	4409,59	15,78	0,9	109,09	114,69
P2H3S3	53,01	101,05	57,23	5337,14	17,05	1	112,42	115,9
P2H3S4	51,34	103,28	65,07	5264,68	18,91	1	115,32	116,52
P2H3S5	50,92	122,48	66,83	5820,42	21,08	1	98,8	117,35

Sample ID	Pb ppm	Zn ppm	Cu ppm	As ppm	Co ppm	Cd ppm	Cr ppm	Ni ppm
P2H3S6	48,74	119,65	69,84	5416,97	18,64	0,98	86,2	104,7
P2H3S7	38,7	85,65	52,69	5364,94	19,81	0,97	88,1	115,4
P3H1S1	36,8	60,09	54,7	4072	23,2	0,8	40,23	55,3
P3H1S2	39,44	61,06	53,98	4688,25	21,71	0,9	23,9	53,69
P3H1S3	39,12	62,67	62,67	5283,43	19,66	0,8	29,64	106,39
P3H1S4	31,27	59,76	63,75	6121,51	17,03	0,9	29,48	97,51
P3H1S5	22,71	56,67	71,12	6282,87	20,22	0,9	31,08	113,15
P3H1S6	29,8	126,38	67,88	7426,84	17,3	0,8	95,65	96,1
P3H1S7	21,5	84,68	57,98	8789,51	23,5	0,7	92,86	67,9
P3H2S1	37,98	51,77	59,47	3663,03	16,94	0,9	38,55	56,67
P3H2S2	45,59	63,05	56,98	3743,56	17,96	0,89	30,42	73,27
P3H2S3	43,42	67,57	56,93	4067,16	17,29	0,9	28,59	95,24
P3H2S4	30,73	75,65	60,26	4226,1	16,73	0,8	29,93	98,71
P3H2S5	25,03	80,43	65,85	4688,84	18,79	0,9	31,56	107,77
P3H2S6	20,9	101,18	61,1	4068,78	26,72	0,8	46,35	87,98
P3H2S7	21,5	145,38	61,32	4866,54	25,54	0,8	59,35	76,54
P3H3S1	39,16	43,46	64,24	2850,89	10,69	0,9	36,86	58,04
P3H3S2	51,74	65,04	59,98	3853,42	14,2	0,99	59,98	92,85
P3H3S3	47,71	72,47	51,19	3995,98	14,91	0,89	27,53	84,1
P3H3S4	30,18	91,53	56,77	5942,06	16,43	0,8	30,38	99,9
P3H3S5	27,35	104,19	60,58	6198,81	17,37	0,9	32,04	102,4
P3H3S6	22,9	73,2	68,5	6144	25,2	0,7	48,95	89,64
P3H3S7	20	74,88	67,22	4984,27	26,9	0,6	44,62	88,32

B3: Major oxides

Sample name	SiO2 (%)	TiO2 (%)	Al2O3 (%)	Fe2O3 (%)	MnO (%)	MgO (%)	CaO (%)	Na2O (%)	K2O (%)	P2O5 (%)
P1H1S1	55	1,321	14,65	9,74	0,224	1,5192	1,69	0,382	1,57	0,078
P1H1S2	53,62	1,52	15,5	9,87	0,226	0,9077	0,65	0,104	1,79	0,073
P1H1S3	66,48	0,884	14,04	4,78	0,109	1,4465	0,77	0,274	1,49	0,071
P1H1S4	66,94	0,927	13,68	4,15	0,079	1,3721	1,21	0,209	1,29	0,076
P1H1S5	66,17	1,194	15,05	4,31	0,067	0,7723	0,68	0,095	1,36	0,08
P1H1S6	68,3	1,218	12,58	5,22	0,141	0,5876	0,78	0,242	1,33	0,066
P1H1S7	76,07	0,907	11,25	3,6	0,067	0,3973	0,44	0,073	1,41	0,059
P1H2S1	71,16	0,562	12,89	3	0,037	0,5275	0,64	1,613	1,68	0,079
P1H2S2	65,2	1,003	14,59	4,39	0,11	0,7975	0,83	0,849	1,28	0,059
P1H2S3	62,87	1,246	15,56	8,17	0,124	0,5401	0,5	0,37	1,9	0,091
P1H2S4	59,87	1,393	17,8	6,32	0,085	0,6236	0,62	0,393	1,66	0,056
P1H2S5	57,29	1,746	16,45	9,09	0,143	0,8992	0,64	0,322	1,77	0,083
P1H2S6	54,83	1,696	19,44	8,12	0,135	0,6059	0,5	0,02	1,63	0,095
P1H2S7	50,69	1,656	19,91	11,23	0,154	0,6098	0,36	0	1,3	0,102
P1H3S1	48,06	1,894	17,96	14,1	0,239	0,8994	0,38	0,052	1,31	0,108
P1H3S2	49,95	1,623	17,04	13,11	0,276	1,2402	0,48	0,067	1,38	0,105
P1H3S3	49,22	1,462	15,9	14,37	0,306	2,3869	0,66	0,166	1,35	0,103
P1H3S4	49,52	1,213	14,22	13,23	0,314	5,0199	1,58	0,929	0,98	0,074
P1H3S5	52,1	1,175	9,32	16,83	0,244	2,6122	1,15	1,488	1,56	0,076
P1H3S6	51,92	1,112	11,46	14,57	0,283	5,8906	1,14	0,498	1,01	0,071
P1H3S7	59,69	0,264	4,63	16,98	0,202	2,7766	2,96	0,394	2,03	0,184
P2H1S1	56,9	0,258	3,64	19,06	0,29	2,6262	3,5	0	1,45	0,166
P2H1S2	47,74	0,33	4,11	19,12	0,199	2,8943	2,67	1,783	2,1	0,19
P2H1S3	54,03	0,346	5,1	19,09	0,277	3,6478	5,15	0,888	2,29	0,232
P2H1S4	59,64	0,871	12,52	10,45	0,147	2,4946	0,97	0,536	1,66	0,063
P2H1S5	72,62	0,584	13,62	3,34	0,048	0,6875	1,02	1,51	2,14	0,039
P2H1S6	58,54	1,33	16,06	7,64	0,121	0,9117	0,86	0,732	2,05	0,072
P2H1S7	57,1	1,702	16,35	8,56	0,111	0,823	0,95	0,783	2,13	0,075
P2H2S1	64,75	0,735	15,35	3,86	0,047	0,901	0,93	1,39	1,88	0,049
P2H2S2	65,17	0,495	15,97	2,48	0,04	1,2607	1,37	1,422	2,3	0,051
P2H2S3	66,06	0,8	13,57	4,43	0,064	1,6863	1,46	1,755	2,07	0,062
P2H2S4	57,8	0,753	16,9	5,15	0,06	1,4526	1,59	1,154	2,1	0,058
P2H2S5	68,56	0,659	10,27	2,73	0,039	1,1401	1,36	1,799	1,5	0,042
P2H2S6	56,28	1,021	14,35	8,4	0,141	2,4515	1,61	1,039	2,01	0,1
P2H2S7	52,72	1,665	12,56	10,59	0,171	4,8018	3,82	2,309	1,4	0,11
P2H3S1	64,63	1,135	13,45	5,83	0,135	1,4842	1,46	0,829	2,05	0,078
P2H3S2	54,8	1,29	15,16	5,75	0,089	1,5255	1,87	0,823	1,72	0,098
P2H3S3	60,57	1,077	14,07	4,25	0,073	1,3851	1,68	1,279	1,84	0,093
P2H3S4	60,07	1,062	13,81	4,07	0,062	1,331	1,59	1,273	1,92	0,092
P2H3S5	65,95	0,712	14,65	3,31	0,061	0,845	1,47	1,98	2,07	0,078
P2H3S6	62,27	0,819	14,86	3,7	0,068	1,02	1,42	1,049	2,09	0,113
P2H3S7	64,2	0,943	13,2	3,12	0,056	1,1098	1,63	2,114	2,03	0,085
P3H1S1	55,22	1,228	13,38	4,63	0,076	1,3624	1,56	0,977	1,75	0,064
P3H1S2	58,94	1,353	14,97	4,81	0,075	1,5152	1,58	1,2	1,87	0,078

Sample name	SiO2 (%)	TiO2 (%)	Al2O3 (%)	Fe2O3 (%)	MnO (%)	MgO (%)	CaO (%)	Na2O (%)	K2O (%)	P2O5 (%)
P3H1S4	51,8	1,329	14,39	12,55	0,272	3,918	1,21	0	0,92	0,067
P3H1S5	49,95	1,7	14,97	13,41	0,218	2,9012	2,22	0,815	0,84	0,072
P3H1S6	59,54	1,294	11,17	9,08	0,163	4,4535	1,98	0,86	0,77	0,061
P3H1S7	71,6	1,006	11,54	4,08	0,063	0,9459	0,45	0,04	1,22	0,06
P3H2S1	67,18	0,847	14,13	5,15	0,09	0,9038	0,91	1,107	1,13	0,048
P3H2S2	61,75	1,028	12,03	6,16	0,112	1,9131	1,11	0,764	1,12	0,052
P3H2S3	60,34	1,212	15,71	6,31	0,102	0,8817	1,24	0,649	1,33	0,066
P3H2S4	66,31	1,161	15,13	5,03	0,095	0,689	0,58	0,298	1,44	0,051
P3H2S5	69,75	1,083	12,29	3,86	0,084	0,8587	0,68	0,279	1,84	0,08
P3H2S6	68,86	0,688	9	2,95	0,047	0,4834	0,96	0,885	1,14	0,037
P3H2S7	56,5	1,391	17,13	8,3	0,169	0,6949	0,79	0,137	1,46	0,084
P3H3S1	58,53	1,506	16,62	7,3	0,126	0,9601	0,79	0,267	1,29	0,068
P3H3S2	57,62	1,819	16,34	8,87	0,159	0,762	0,69	0,315	1,5	0,073
P3H3S3	67,1	0,713	13,7	5,54	0,035	0,3507	0,55	0,696	3,11	0,063
P3H3S4	64,99	0,61	11,66	7,17	0,046	0,2667	0,36	0	3,76	0,071
P3H3S5	63,99	1,129	13,31	5,82	0,137	1,417	1,46	0,815	2,03	0,076
P3H3S6	64,14	1,032	15,16	5,43	0,08	0,6316	0,83	1,002	1,88	0,058
P3H3S7	67,05	1,157	15,55	4,71	0,058	0,3497	0,69	0,613	1,68	0,058

B4: Sieve Analysis Results

Sample C					
sieve size (mm)	Mass of sieve (g)	Mass of sieve and material (g)	Mass of material (g)	cumulative passing (g)	percentage passing
4	388.92	390.05	1.13	504.78	100
2	327.12	328.5	1.38	504.53	100
1	295.89	307.8	11.91	494	98
0.5	290.35	310.06	19.71	486.2	96
0.25	246	270.68	24.68	481.23	95
0.125	236.82	330.97	94.15	411.76	81
0.075	264.17	366.94	102.77	403.14	80
Pan	527.7		250.18		
TMR			505.91		
Sample D					
	Mass of sieve (g)	Mass of sieve and material (g)	Mass of material (g)	cumulative passing (g)	percentage passing
4	388.78	389.48	0.7	514.86	100
2	326.91	328.02	1.11	514.45	100
1	295.24	298.11	2.87	512.69	99
0.5	290.21	294.14	3.93	511.63	99
0.25	245.72	258.57	12.85	502.71	98
0.125	236.15	294.71	58.56	457	89
0.075	263.56	384.97	121.41	394.15	76
Pan	527.2	841.33	314.13		
TMR			515.56		

APPENDIX C:

Soil

C1: Metals in soils

Sample ID	Pb (ppm)	Zn (ppm)	Cu (ppm)	As (ppm)	Co (ppm)	Cd (ppm)	Cr (ppm)	Ni (ppm)
T1S1	105,7	80,4	140,8	11,3	33,5	0	798,9	810,3
T1S2	173	90,5	141,3	18,6	36,9	0	1037,1	1360,1
T1S3	16581	122	112,3	1779,7	50,9	0	480	305,8
T1S4	5396,6	205,1	85,1	579,2	31,3	0	761,6	799,7
T1S5	8586,9	118,4	103,7	921,7	38,2	0	665,5	559,9
T1S6	220,7	63,4	39,6	23,7	12,6	0	184,9	206,7
T1S7	259,4	95,8	153,6	27,8	25,8	0	186,9	155,3
T1S8	128,9	88,9	124,7	13,8	25,2	0	505,1	376,5
T1S9	80	105,3	70,1	8,6	21,8	0,1	620,8	557,3
T1S10	118,1	116,3	81,5	12,7	21,8	0,1	350,4	382,7
T1S11	95,1	96	121,7	10,2	22,1	0	282,9	280,3
T2S1	28,6	52	62,7	3,1	10,7	0	168,2	217
T2S2	27,4	48,2	59,8	2,9	9,3	0	120,6	138
T2S3	24,9	36,9	61,6	2,7	9,6	0,1	149,9	94,2
T2S4	29,6	74,8	85,6	3,2	11,6	0	118,1	114,3
T2S5	29	30,3	34,6	3,1	7,9	0	165,5	75
T2S6	31	32,4	36,8	3,3	6,7	0	114,2	89,3
T2S7	33,4	48,7	60,4	3,6	10	0	105,2	150,1
T2S8	37,6	42,3	77	4,1	17,8	0,1	225,9	140,1
T2S9	37,5	45,9	78,4	4	14,2	0	146,8	136,9
T2S10	30,6	92,1	124,9	3,3	20,2	0,1	193,4	241,3
T2S11	35,7	69,1	98,8	3,8	18,1	0	293,7	328,7
T2S12	67,4	77	113,4	7,2	26,8	0,1	705,2	789,1
T2S13	67,2	90,6	135	7,2	33,5	0	930,2	952,9
T2S14	79	96,7	135,6	8,5	29,6	0,1	1027,6	1090,3
T2S15	67,4	88,3	130,4	7,2	33	0	1288,7	1385,8
T2S16	52,6	76	89,4	5,7	31	0	1587,4	1637,3
T2S17	54	404,1	160,6	5,8	37,6	0	1005,8	513
T2S18	58,8	119,3	108,5	6,3	34,3	0	1988,8	2296,9
T2S19	112,5	99,4	208,6	12,1	27,8	0	659,5	720
T2S20	346,3	85,3	88,3	37,2	27	0	1040	1600,2
T3S1	33,9	60	52,5	3,6	22,6	0	1284,5	1962
T3S2	55,6	88,1	95,7	6	30,2	0	994,2	1164,1
T3S3	88,1	61,2	19,5	9,5	20,7	0	384,7	357,2
T3S4	93,7	39	16,8	10,1	9,8	0	132,5	76,9
T3S5	519,4	94,2	61,3	55,7	23,9	0	356,8	331,9
T3S6	56,6	39,3	27,6	6,1	7,9	0	62,5	55,4
T3S7	44,2	72,5	81	4,7	17,3	0	125,2	123,4
T3S8	30,6	77,4	131	3,3	19,1	0	108,4	63,5

Sample ID	Pb (ppm)	Zn (ppm)	Cu (ppm)	As (ppm)	Co (ppm)	Cd (ppm)	Cr (ppm)	Ni (ppm)
T3S9	55,1	36,5	30,6	5,9	8,8	0	74,7	70,1
T3S10	59,8	45,9	24,1	6,4	6,2	0,1	62,8	59,5
T3S11	105,3	61	42,4	11,3	11,3	0	153,3	179,1
T3S12	77,9	62,5	49,2	8,4	12,7	0	68,3	71,9
T3S13	70	36,3	10,3	7,5	4	0,1	41,7	46,9
T3S14	26,1	32,7	17,2	2,8	6,9	0	89,1	94,1
T3S15	52,4	101,4	78,3	5,6	20,3	0	326,5	360,7
T3S16	33,1	97,2	50,8	3,5	24,3	0	342,2	329,5
T3S17	47,4	97,9	72,6	4,9	13,8	0	173,8	193,2
T3S18	37,1	70,5	74,7	4	13,7	0	125,9	188,1
T3S19	35,5	110,6	47,1	3,8	10	0	103,8	137,8
T3S20	38,6	57	43,2	4,1	9,7	0	108,5	127,8
T3S21	34,3	82,3	36,7	3,7	7,9	0	65,8	86,6
T3S22	33,3	91,9	43,9	3,6	8,7	0,1	90,2	97
T3S23	32,9	51,3	28,3	3,5	7,3	0	75,3	86,9
T3S24	39,3	54	52,2	4,2	11	0,1	119,9	168,7
T3S25	33,8	57,8	52,3	3,6	11,2	0,1	124,3	155,6
T4S1	32,3	70,4	72,3	3,5	33,5	0	1474,4	2082,4
T4S2	100,3	102,8	146,8	10,8	34,4	0	1395,8	1066,4
T4S3	111,4	88,1	130	12	36,4	0	636,3	768,7
T4S4	177,7	83,8	75,7	19,1	25	0	722,9	914,5
T4S5	55,9	81,3	72,2	6	10,5	0,1	365,8	199,3
T4S6	55,6	54,3	51,9	6	13,1	0	239,1	262,2
T4S7	62,2	55,4	53,1	6,7	15,4	0	358,6	395,1
T4S8	24,1	73,8	88,1	2,6	15,6	0	191,8	266
T4S9	28,6	43,1	58,1	3,1	12,1	0	191,8	151,1
T4S10	35,7	43,2	49,3	3,8	9,3	0	110,5	95,4
T4S11	26,1	20	22,8	2,8	7,3	0	102,7	69,6
T4S12	30,2	75,7	113,8	3,2	20	0	146,8	161,3
T4S13	24,3	56,7	87,7	2,6	17,5	0,1	187,5	218,8
T4S14	28,6	72,7	102,4	3,1	21,8	0	188,3	171,9
T4S15	42,6	22,4	44,1	4,6	13,3	0	146,5	59,4
T4S16	46,1	19,8	43	5	18,1	0	158,5	57,9
T4S17	40,2	98	69,5	4,3	14,4	0	166,9	193,2
T4S18	24,5	44,5	57,7	2,6	12,9	0	119,6	108,7
T4S19	32,4	29,5	42,8	3,5	10,8	0	116,5	57,7
T4S20	31,2	32,1	44,6	3,3	10,5	0,1	110,4	64,7
T4S21	39,8	27,4	41,9	4,3	10,4	0,1	100,2	54,8

APPENDIX D:

Bricks

D1: Clay Bricks

Brick	Brick ID	Tailings (%)
	J	10
	I	20
	H	30
	G	40
	F	50

	E	60
	D	70
	C	80
	B	90
	A	100

D2: Cement Bricks

Cement bricks	Brick ID	Tailings ratio	Tailings %
	A	1:1	50
	B	1:2	33.33
	C	0.5:2	20
	D	2:1	66.66